This TR supersedes MTC-TDR-64-1
AD 432 034 dated 18 Dec 1963

AD 601689

AD NO. ____
DDC FILE COPY

ETR-TR-65-7

THE ACCURACY OF ETR INSTRUMENTATION

C.S. Cummings, Ph. D., R.H. Ackerson, Ph. D.,
A.S. Baron, et al, RCA MTP

DDC
JUL 1 1965
TISIA

MAY 1965

NOCFSTI

SYSTEMS ANALYSIS DIVISION
DIRECTORATE FOR DATA PROCESSING
DEPUTY FOR RANGE OPERATIONS
AIR FORCE EASTERN TEST RANGE
AIR FORCE SYSTEMS COMMAND
PATRICK AIR FORCE BASE, FLORIDA

Best
Available
Copy

Qualified users may obtain copies of this report from the Defense Documentation Center.

Defense Documentation Center release to Clearinghouse for Federal Scientific and Technical Information of the United States Department of Commerce is authorized.

When U. S. Government drawings, specification, or other data are used for any purpose other than a definitely related Government procurement operation, the Government thereby incurs no responsibility nor any obligation whatsoever, and the fact that the Government may have formulated, furnished, or in any way supplied the said drawing, specification or other data, is not to be regarded by implication or otherwise, or in any manner licensing the holder or any other person or corporation, or conveying any rights or permission to manufacture, use, or sell any patented invention that may in any way be related thereto.

Do not return this copy. Retain or destroy.

THE ACCURACY OF ETR INSTRUMENTATION

C. S. Cummings, Ph. D., R. H. Ackerson,
Ph. D., A. S. Baron, et al, RCA MTP

FOREWORD

Technical Report No. ETR-TR-65-7 was prepared under subcontract No. 65-5300-01 by Systems Analysis, RCA Service Company, Missile Test Project, Patrick Air Force Base, Florida. RCA Service Company is subcontractor to the ETR Range Contractor, Pan American World Airways, Guided Missile Range Division, Patrick Air Force Base, Florida.

The sponsoring agency is Systems Analysis Division, Directorate for Data Processing, Deputy for Range Operations, AFETR, Patrick Air Force Base, Florida.

Contributors to this edition of "The Accuracy of ETR Instrumentation" are the following:

CONTRIBUTORS TO PART I

R. H. Ackerson, Ph. D.
V. Chew
C. S. Cummings, Ph. D.
P. S. Dubbeldam, Ph. D.
J. A. Greene
M. A. King
P. N. Somerville, Ph. D.

CONTRIBUTORS TO PART II

A. S. Baron
W. N. Beall
R. A. Brown
H. C. Cox
W. L. Elenburg
J. E. French
D. E. Forrest
J. A. Greene
A. E. Hoffmann-Heyden
W. F. Kennedy
V. B. Kovac
N. L. Lindemann
J. P. Lushene
R. C. Manring
J. J. O'Connor
J. A. Paddock
D. H. Parks*
P. C. Ray
L. B. Rice, Ph. D.
V. C. Rupert
H. D. Yenzer

*Special acknowledgement to D. H. Parks, RCA Mathematical Services for his contribution to the discussion of the GLAD Program.

C. S. Cummings, Technical Editor.

This technical report has been reviewed and approved.

Asa P. Whitmire
Colonel, USAF
Director, Data Processing

ABSTRACT

The annual summary statements of the accuracy of Eastern Test Range Tracking Instrumentation are presented in this report. The statements are based on studies conducted by RCA Systems Analysis. The report also provides brief system descriptions and a detailed discussion of the definition of errors encountered in tracking system evaluations, methods and techniques used to estimate errors, error sources, specific ETR methodologies including data analysis flow diagrams and a discussion of the variance - covariance error propagation required to determine the accuracy of reduced position, velocity and acceleration data. Work on the determination of instrumentation accuracy is a continuing project and revisions and refinements to the estimates of accuracy are issued periodically as additional information is made available.

TABLE OF CONTENTS

	Page
FOREWORD	ii
ABSTRACT	iii
GENERAL INTRODUCTION	xiv
1.0 Preface to the Report	xiv
2.0 Objective and Scope of the Report	xxi
3.0 ETR Tracking Systems	xxii
3.1 Optical Systems	xxii
3.2 Electronic Systems	xxiii
3.3 Acoustic Systems	xxvi

PART I

GENERAL METHODOLOGIES OF ERROR ANALYSIS AND ACCURACY DETERMINATION

CHAPTER 1 INTRODUCTION	1-1
CHAPTER 2 DEFINITION AND DISCUSSION OF ERRORS	2-1
2.1 Classical Point of View	2-1
2.2 Engineering Point of View	2-6
2.3 Total Error	2-14
2.4 Accuracy and Precision	2-16
CHAPTER 3 METHODS USED TO ESTIMATE ERROR VARIANCE	3-1
3.1 Methods Using a Standard	3-1
3.1.1 "Best Estimate of Trajectory" (BET)	3-1
3.1.1.1 The GLAD Program	3-2
3.1.2 Inertial Guidance Data as Reference	3-6a
3.1.2.1 Comparisons in a Common Coordinate System	3-6a
3.1.2.2 Comparisons in Tracking System Parameters	3-6b
3.1.2.3 Noise Estimation During Powered Flight	3-6b
3.1.2.4 Data Analysis with Inertial Guidance	3-6c
3.1.3 A Significantly More Accurate Instrumentation System	3-7

	Page
3.2 Least Squares Methods	3-8
3.2.1 Regression Analysis	3-9
3.2.2 Analysis of Variance	3-11
3.2.3 Equations of Motion Curve Fitting	3-14
3.2.4 Residual Analysis	3-15
3.3 A Multi-Instrument Technique (Grubbs' Method)	3-17
3.4 Variate Difference Technique	3-23
3.5 Analytical Investigation - Error Models	3-26
3.6 Confidence, Tolerance and Prediction Regions	3-33
3.6.1 One-Dimensional Case	3-33
3.6.2 Two-Dimensional Case	3-41
3.6.3 Three Dimensional Case	3-46
CHAPTER 4 TECHNIQUES FOR DETERMINING VELOCITY AND ACCELERATION ACCURACIES	4-1
4.1 Correlated Data	4-3
4.1.1 Free Fall Data Analysis	4-3
4.1.2 Powered Flight Data Analysis	4-6
4.2 Uncorrelated Data	4-7
CHAPTER 5 ERROR PROPAGATION	5-1
5.1 Error Propagation in the Just-Determined Case	5-4
5.1.1 Propagation of Errors in Position	5-12
5.1.2 Propagation of Errors in Velocity and Acceleration Data	5-17
5.1.2.1 Propagation of Errors in Velocity Data	5-17
5.1.2.2 Propagation of Errors in Acceleration Data	5-19
5.1.3 Coordinate Transformation of Error Expressions	5-20
5.2 Error Propagation in the Over-Determined Case	5-22
5.2.1 General Principles	5-22
5.2.2 The Variance-Covariance Matrices of Measurement Errors	5-27

Page

PART II

SYSTEM DESCRIPTIONS, ERROR SOURCES AND ACCURACIES

1.0 INTRODUCTION	1-1
2.0 SUMMARY OF ETR TRACKING INSTRUMENTATION ACCURACIES	2-1
3.0 OPTICAL INSTRUMENTATION	3-1
3.1 Procedure for Estimating System Accuracies and Performance	3-1
3.1.1 Data Flow	3-1
3.1.2 Methodology for Estimating System Accuracies	3-3
3.1.3 Methodology of Analysis of System Performance	3-9
3.2 FIXED CAMERA	3-15
3.2.1 System Description	3-15
3.2.2 Error Sources	3-19
3.2.3 System Accuracies	3-22
3.2.3.1 Accuracy Estimates	3-22
3.2.3.2 Performance Data	3-24
3.3 CINE-THEODOLITE	3-27
3.3.1 System Description	3-27
3.3.2 Error Sources	3-30
3.3.3 System Accuracies	3-31
3.3.3.1 Accuracy Estimates	3-33
3.3.3.2 Performance Data	3-34
3.4 BALLISTIC CAMERA	3-37
3.4.1 System Description	3-37
3.4.1.1 Conventional Ballistic Camera System	3-38
3.4.1.2 Modified Ballistic Camera System	3-42
3.4.2 Error Sources	3-43

	Page
3.4.3 System Accuracies	3-46
3.4.3.1 Accuracy Estimates	3-47
4.0 PULSED RADARS - LAND BASED	4-1
4.1 Procedure for Estimating System Accuracies	4-1
4.1.1 Introduction	4-1
4.1.2 Method of Error Determination	4-1
4.1.2.1 Flow Diagrams	4-2
4.1.2.2 Test Conditions in Support of Accuracy Evaluation	4-2
4.1.2.3 Mathematical Model for Treatment of Error Data	4-5
4.2 Error Sources	4-7
4.2.1 Pulsed Radar Error Model	4-7
4.2.2 Error Breakdown by Frequencies	4-11
4.3 C-BAND RADARS	4-12
4.3.1 System Description	4-12
4.3.1.1 General	4-12
4.3.1.2 AN/FPS-16 and AN/MPS-25 Radars	4-14
4.3.1.3 AN/FPQ-6 and AN/TPQ-18 Radars	4-15
4.3.2 System Accuracies	4-16
4.4 S-BAND RADARS (MOD II)	4-22
4.4.1 System Description	4-22
4.4.2 System Accuracies	4-23
4.5 X-BAND RADARS (MOD IV)	4-24
4.5.1 System Description	4-24
4.5.2 System Accuracies	4-25
4.6 UHF DOWNRANGE RADAR (TRINIDAD)	4-26
4.6.1 System Description	4-26
4.6.2 System Accuracies	4-28

	Page
5.0 PULSED RADARS - SHIPBORNE	5-1
5.1 ADVANCED RANGE INSTRUMENTATION SHIPS (ARIS)	5-1
5.1.1 System Description	5-1
5.1.2 Error Sources	5-3
5.1.3 Error Model	5-5
5.1.4 Methodology for Estimating System Accuracies	5-9
5.1.5 System Accuracies	5-10
5.2 TWIN FALLS VICTORY	5-11
5.2.1 System Description	5-11
5.2.2 System Accuracy Determination	5-11
6.0 CW RADARS	6-1
6.1 Procedure for Estimating System Accuracies	6-1
6.2 MISTRAM	6-4
6.2.1 System Description	6-4
6.2.1.1 MISTRAM I	6-4
6.2.1.2 MISTRAM II	6-6
6.2.1.3 Measurement Techniques	6-6
6.2.1.4 Characteristics and Specifications	6-7
6.2.2 Error Sources	6-10
6.2.2.1 MISTRAM Error Models	6-10
6.2.2.2 Survey Error Estimation	6-13
6.2.3 System Accuracies	6-14
6.2.3.1 Accuracy Estimates	6-14
6.2.3.2 Data Characteristics - MINUTEMAN	6-23
6.2.3.3 Data Characteristics - TITAN	6-32
6.2.3.4 Data Characteristics - SATURN	6-39
6.3 GLOTRAC	6-46
6.3.1 System Description	6-46

	Page
6.3.2 Error Sources	6-52
6.3.3 System Accuracies	6-55
6.3.3.1 Accuracy Estimates	6-55
6.3.3.2 Data Characteristics	6-55
6.4 AZUSA MARK II	6-62
6.4.1 System Description	6-62
6.4.1.1 General	6-62
6.4.1.2 Measurement Techniques	6-62
6.4.1.3 Characteristics and Specifications	6-67
6.4.2 Error Sources	6-68
6.4.3 System Accuracies	6-70
6.4.3.1 Accuracy Estimates	6-71
6.4.3.2 Data Characteristics	6-71
6.5 UDOP	6-77
6.5.1 System Description	6-77
6.5.2 Error Sources	6-83
6.5.3 System Accuracies	6-85
6.5.3.1 Accuracy Estimates	6-86
7.0 IMPACT SYSTEMS	7-1
7.1 IMPACT PREDICTION, LOCATION AND DETERMINATION	7-1
7.1.1 Procedure for Estimating System Accuracies	7-1
7.1.2 System Description	7-3
7.1.3 Error Sources	7-6
7.1.4 System Accuracies	7-6
7.2 MILS	7-12
7.2.1 Procedures for Estimating System Accuracies	7-12
7.2.1.1 Definition of Terms	7-12
7.2.1.2 Computation of Confidence Ellipses, MILS/BOA	7-13

	Page
7.2.1.3 Estimation of BOA Accuracy in the Antigua Target Array	7-15
7.2.1.4 Method of Obtaining Pooled Accuracies - MILS/BOA and Target Array Systems	7-22
7.2.2 System Description	7-26
7.2.2.1 Target Array, MILS	7-28
7.2.2.1.1 Target Array Solution, Missile Tests	7-30
7.2.2.2 BOA, MILS	7-33
7.2.2.2.1 BOA Solution, Missile Tests	7-38
7.2.2.2.2 Pre- and Post-Test Calibrations, BOA Surveyed Areas	7-38
7.2.3 Error Sources	7-41
7.2.3.1 BOA Sources of Error	7-41
7.2.3.1.1 BOA System Random Error Sources	7-41
7.2.3.1.2 BOA Systematic Errors	7-44
7.2.3.2 MILS Target Array Error Sources	7-45
7.2.3.2.1 Target Array Random Errors	7-45
7.2.3.2.2 Target Array Systematic Errors	7-47
7.2.4 System Accuracies	7-48
8.0 NAVIGATION SYSTEMS	8-1
8.1 INTRODUCTION	8-1
8.2 LORAC	8-3
8.2.1 System Description	8-3
8.2.2 Error Sources	8-10
8.2.3 System Accuracies	8-15
8.2.3.1 "A" Network	8-15
8.2.3.2 "B" Network	8-17
8.3 INDEPENDENT SHIP NAVIGATION AND STABILIZATION SYSTEMS	8-18
8.3.1 Sextant	8-19
8.3.1.1 System Description	8-19
8.3.1.2 Error Sources	8-19

	Page
8.3.2 Electromagnetic Log	8-19
8.3.2.1 System Description	8-19
8.3.2.2 Error Sources	8-21
8.3.3 N7C	8-22
8.3.4 MK 19 Gyro - Compass	8-22
8.3.4.1 System Description	8-22
8.3.4.2 Error Sources	8-24
8.3.5 MK-I SINS	8-24
8.3.5.1 System Description	8-25
8.3.5.2 Error Sources	8-25
8.3.6 MK-IV SINS	8-26
8.3.6.1 System Description	8-26
8.3.6.2 Error Sources	8-27
8.3.7 Star Tracker	8-27
8.3.7.1 System Description	8-27
8.3.7.2 Error Sources	8-30
8.3.8 SONAR Benchmarking Equipment	8-30
8.3.8.1 System Description	8-30
8.3.8.2 Error Sources	8-31
8.3.9 Methods of Accuracy Determination	8-31
8.3.9.1 Calibration	8-31
8.3.9.2 Error Model	8-36
8.3.9.3 Accuracy Determination	8-38
8.3.10 Calibration Experiments	8-39
8.3.11 System Accuracies	8-40
9.0 SIGNATURE SYSTEMS	9-1
9.1 Procedure for Determining System Accuracies	9-1
9.1.1 Introduction	9-1
9.1.2 Radar Equation	9-2
9.1.3 Calibration	9-5
9.1.4 Accuracy Determination	9-17

	Page
9.2 Advanced Range Instrumentation Ships (ARIS)	9-20
9.2.1 System Description	9-20
9.2.2 Error Sources	9-21
9.2.3 System Accuracies	9-23
10.0 SURVEY	10-1
10.1 Terminology	10-1
10.2 Accuracies	10-3
10.2.1 Deflection of the Vertical	10-4
10.2.2 Geoid Heights	10-8
10.2.3 Mean Sea Level Planes	10-11
10.2.4 Survey Accuracies	10-12
APPENDIX I	A-I-1
REFERENCES	R-1
DISTRIBUTION	D-1

GENERAL INTRODUCTION

1.0 PREFACE TO THE REPORT

This report presents the annual summary statements of the accuracy of Eastern Test Range tracking instrumentation. These statements are made on the basis of studies conducted by RCA Systems Analysis.

The format of this edition of the Accuracy Report represents a substantial change from previous editions. The report is divided into two major parts: Part I, General Methodologies, and Part II, System Descriptions, Error Sources and Accuracies. The material presented in Part I is essentially the same as that contained in last year's report. A major revision and expansion of Part I is in preparation and scheduled for publication by December 1965. Part II, however, is completely revised. Three entirely new sections have been added: Shiphorne Pulse Radar, Navigation Systems and Signature Systems. This is in recognition of the vital role now being played by these systems at the Eastern Test Range. To avoid the expense of complete retyping, the format of last year's report has been retained in Part I, even though it is at variance with the revised format of Part II. It is hoped that this will not be a source of confusion to the user.

Material in Part II for each system is based on the common themes: procedure for estimating system accuracies, system description, error sources, and system accuracies. As a result of numerous questions and inquiries from users of the report during the past year, the system descriptions and accuracy determination discussions have been expanded to give more thorough treatment of the basic information required for proper understanding and application of the accuracy data. More detailed

discussion of error sources, error models and calibration has been included, even where complementary accuracy data are not available, in anticipation of the availability in 1965 of such data resulting from powerful new tools such as calibration missiles and satellites, a number of extensive evaluation programs and continuing application of the sophisticated reduction and analysis techniques currently in use at the Eastern Test Range.

With regard to the Eastern Test Range tracking instrumentation itself, many important milestones occurred in 1964 and early 1965. We are mainly concerned in this document with events that contributed directly to improved accuracy performance, although we should not overlook events that improve tracking coverage or equipment reliability, since these factors can have a positive, if indirect, effect on the accuracy with which a mission was supported. Many of the accuracy improvement factors enumerated below are a direct result of the "closed loop" nature of the Systems Analysis effort in which deficiencies and potential solutions revealed by the data and performance analysis effort are input to a formal recommendation procedure, initiated in early 1964, for action by the various cognizant agencies at the ETR. Also, the Systems Analysis Monthly Accuracy Bulletin, inaugurated in October 1964 has proved to be a significant tool in improving overall accuracy by providing Data Reduction personnel with latest values of basic accuracy data on a timely basis for use as a source of "a priori" values in the GLAD program, the most powertul of the new data processing and analysis tools currently in use at the Eastern Test Range. Referring to the individual systems, the following are some of the most significant events that occurred during the period represented by this report:

Error Model Best Estimate of Trajectory (GLAD Program)

1. The first GLAD-BET data reduction using MISTRAM, GLOTRAC, UDOP and AZUSA (Saturn);
2. The use of point-of-track corrections;
3. The ability to constrain rate biases between two separate data spans;
4. The use of inertial guidance data to detect discontinuities;
5. The ability to apply orbital constraints in free fall;
6. The determination of improved a priori estimates of error for all tracking system parameters.

GLOTRAC

1. First orbital data obtained (Centaur and Titan III);
2. Pretoria van installed and now in service on limited commitment;
3. The Western Test Range Complex (Point Arguello, Yuma and Nellis AFB) installed and now in service on limited commitment;
4. The first use of GLOTRAC range sum data (using San Salvador and Bermuda transmitters);
5. Improved Bermuda survey;
6. A number of successful GLAD reductions resulting in operational acceptance in early 1965 of the Segment 1 Complex at the Eastern Test Range;
7. Improved handover techniques;
8. Improved timing (time tones need no longer be used at ETR);
9. The establishment at Cape Kennedy of the GLOTRAC Global Support Center;
10. Detection and correction of an apparent error in Pretoria survey;
11. Utilization of smoothed radar data in the GLAD reduction;

12. Detection and correction of an antenna pointing error at Bermuda, resulting in significantly improved coverage and accuracy of reduced data;
13. Use of the Cape van to recover otherwise useless data in a test where the AZUSA error word failed;
14. Installation of improved acquisition circuitry in the GLOTRAC vans;
15. Installation of true phase lock detectors in the GLOTRAC vans, facilitating data handling and reduction;
16. Improvement of GLOTRAC antenna pointing characteristics, resulting in acquisition of more data and improved accuracy;
17. Use of tunnel diodes for microwave preamps. This improved threshold at MARK II AZUSA and reliability at other stations.

MISTRAM

1. The operational acceptance of MISTRAM I and II;
2. A new Eleuthera survey reduced the uncertainty of the location of Eleuthera relative to the Cape and removed a large apparent bias in the MISTRAM II data;
3. Improved handover techniques shortened data losses at handover;
4. Change from a 13 point, 2nd degree rate filter to a 23 point 3rd degree filter on MINUTEMAN data reduced the error due to lack of fit at staging;
5. The use of GLAD for the reduction of MISTRAM data, in place of the previous "non-redundant" program, resulted in improved Flight Test Data Report accuracy by reducing the effect of bias errors;
6. Antenna pointing problems were isolated and corrected, reducing the duration of losses at missile events;
7. Use of UDOP data in MISTRAM GLAD, where needed, assured continuous coverage across dropouts;

8. Improved real-time accuracy and performance of both MISTRAM I and MISTRAM II resulted from numerous hardware modifications and Cape Computer programming; (baseline intermixing, internal baseline comparisons, memory over 2 second dropout, memory over 2 second handover, etc.).

UDOP

1. The first use of ODOP (i.e. "Offset transponder UDOP" using an active uprange complex and passive downrange complex);
2. Much improved downrange digitizer performance;
3. The use of an increased bias offset frequency to accomodate higher data rates;
4. Improved editing and data reduction methods;
5. Correction of an error in the Pluto survey;
6. The use of MISTRAM data to bridge UDOP handover.

Pulse Radar

1. In the course of 1964, the AN/FPQ-6 radar at Antigua (No. 91.18), and the AN/TPQ-18 radars at MILA (No. 19.18), Grand Turk (No. 7.18), and Ascension (No. 12.18) were accepted for operational ETR support. In continuation of the acceptance tests, the radars were subjected to accuracy evaluations for updating of their initially demonstrated capabilities.
2. An improvement program is underway for the Trinidad UHF radar (No. 40.43), involving a variety of hardware modifications and incorporation of a 1260 computer and data handling interface equipment for the purposes of improving tracking performance, calibration, systems checkouts, data quality and data analysis.
3. In the interest of improved radar angle zero setting, methods were developed and introduced which employ an isolated target in the far field rather than the boresight

tower for initial antenna collimation.

4. Engineering changes in the MIPIR data logic achieved exact data/time tagging to compensate for the 4101 processer delay of 35 msec.
5. The MIPIR angle commutation frequency was raised to minimize chances for periodic angle noise during track of the wobbulated Gemini spacecraft beacon pattern.
6. Analysis of MIPIR radar accuracy in the course of systems activation demonstrated essentially consistent capability from radar-to-radar. The addition, and regular operational use, of MIPIR radars to the ETR C-band chain contributed to accuracy and reliability of trajectory coverages, increased data quality being achieved by inclusion of multiple radar data in GLAD solutions.
7. Techniques for automatic beacon sharing were introduced and contribute to the collection of redundant data for use in GLAD/BET data processing.
8. Investigations of the effects of superimposed beacon returns from multiple beacon spacecraft systems indicated that data degradation will be primarily in the noise domain and can be alleviated by appropriate filtering.
9. In the interest of improved coverage reliability, the DIRAM logic circuitry was modified to prevent loss of track in cases when the radar was initially designated at ranges coinciding with the interference region.

Ships

1. During 1964 extensive efforts were continued toward trouble shooting the equipment aboard the General H. H. Arnold and General H. S. Vandenberg. Also, during this year, a limited metric evaluation of the General H. H. Arnold was accomplished. Following this evaluation the General H. H. Arnold

was assigned to the Western Test Range for mission support. Toward the end of 1964 an extensive evaluation of both Metric and Signature capabilities of the General H. S. Vandenberg was in progress.

2. Preliminary analysis of the Vandenberg evaluation data indicate accuracies approximately a factor of two better than those reported herein for the Arnold. This improvement has resulted in part from correction of discrepancies revealed in analysis of the data in the areas of shipboard operating and maintenance procedures, data conversion and real time programming. Examples include: the discovery of sub-standard servo performance; the correction and improvement of navigation programming; the discovery of the cause of an apparent 0.1 second time shift in the data; and the discovery of C-band angle error signal phase shift and attenuation. The Vandenberg evaluation followed major equipment modifications. It is now equipped with a MK-IV SINS for navigation and a UHF radar in place of the former MK-I SINS and X-band radar.
3. Signature accuracy has been improved from about 10 db uncertainty at the beginning of the program to better than 3 db for all channels.

Suggestions are solicited from users of this report relative to format, scope, contents or additions that would improve its general usefulness as a source document on the accuracy of Range Tracking Instrumentation. Also, although every effort has been made to detect and eliminate errors, some undoubtedly remain. It will be appreciated if any such will be called to our attention so that they may be removed from a future printing or edition.

2.0 OBJECTIVE AND SCOPE OF THE REPORT

The report serves two major purposes:

1. To provide standards of performance against which to measure the future performance of tracking systems.
2. To provide standards of performance for use in determining the capability of the tracking systems to support the requirements of proposed missions.

In order to assure correct interpretation and use of the accuracy data, it is important to know exactly how they were obtained, including both the assumptions made and the methodologies used. Hence, the report provides a detailed discussion of the definitions of errors encountered in tracking system evaluations, methods and techniques used to estimate errors, specific ETR methodologies including data analysis flow diagrams and a discussion of the variance-covariance error propagation required to determine the accuracy of reduced position and acceleration data.

It is extremely important for the user of this report to recognize that no single number can be given to represent the accuracy of any tracking system, nor is there any pat answer to the apparently reasonable question: "Is system A better (i.e. more accurate) than system B?" This question usually has meaning only when asked with regard to a particular point on a particular trajectory for a particular missile. This is a consequence of the important influence of geometry and missile characteristics on the accuracy of trajectory data.

The evaluation of instrumentation systems is a continuing project and revisions and refinements to the estimates of system accuracy will be issued periodically as additional information becomes available.

3.0 ETR TRACKING SYSTEMS

There are four primary types of ballistic missile and space vehicle trajectory measuring systems in general use at the Eastern Test Range: Camera Systems, Pulse Radar Systems, CW (Continuous Wave) Systems and Underwater Sound Systems (MILS). These systems fall logically into three broad categories: optical, electronic and acoustic.

The optical systems are used to obtain precise information on the vehicle in the early stages of the trajectory where the electronic systems have difficulty in operating for reasons such as multipath, glint, missile antenna configuration and flame effects. Inherent in the operation of the optical systems are the limitations imposed by weather conditions, exhaust smoke, etc.

The electronic systems possess advantages over the optical systems in that they are all-weather systems and they may be used in real time. Such real time data are used for purposes of determining range safety impact prediction, nose cone recovery information, orbital element insertion parameters and acquisition information for downrange instrumentation.

The acoustic systems are used to obtain precise information on the impact point of the missile. They are also used in a secondary role to obtain position location of tracking ships.

3.1 Optical Systems

Basically, the Range uses three types of metric optical instrumentation systems: the Askania Cine-Theodolite, the CZR Fixed Camera and the Ballistic Camera. Cine-Theodolites are tracking cameras used to measure horizontal and vertical angles

(azimuth and elevation) of a line of sight and require exterior sighting telescopes to track along the flight path of a missile. The CZR Cameras are fixed cameras, supported on 3-axis gimbal mounts, capable of being oriented to cover the desired field of view. Each individual camera in a network gives the direction of a ray in space from the camera to the missile.

Ballistic Cameras, like the CZR Cameras, are fixed in orientation but utilize a glass plate to photograph the path of a missile or aircraft carrying a flashing light at night. The Ballistic Cameras are oriented by photographing the stars and are capable of extreme accuracy.

The cameras are essentially triangulation instruments and are used in arrays of two or more cameras to obtain the spatial position of the object being tracked. In the reduction of the optical data the concept of Intersection Photogrammetry is applied to the solution of the photogrammetric problem (the reconstruction of configurations in object space by means of image space data). This philosophy requires both the independent and precise orientation of each camera to be used in the photogrammetric net and the determination of the most probable solution to the photogrammetric problem by means of a least squares adjustment. The same concept may be applied to the problem of missile position determination (triangulation) and missile attitude determination.

3.2 Electronic Systems

Of the electronic systems, the CW Systems provide the most accurate trajectory information while the Pulse Radar Systems are used to supplement this information by supplying the necessary backup and support (because of their favorable downrange geometry) in trajectory areas not covered by the CW Systems.

Pulse Radars which operate on S-band (Mod II Radars), C-band (FPS-16, TPQ-18, and FPQ-6 Radars), X-band (Mod IV High Resolution Trackers) and UHF frequencies (Trinidad Radar System) are utilized at ETR for metric data and other specialized test objectives such as present position displays, target reflectivity measurements, surveillance, etc. The FPQ-6 and TPQ-18 Radars at the present time provide the major portion of ETR Pulse Radar metric data. These are high precision radars with large parabolic reflectors. Each radar gives the azimuth, elevation and range of the missile in flight.

The CW Systems are either of the Doppler (range sum) or interferometer (range difference) type. UDOP is an ultra high frequency CW Doppler system which measures the total Doppler shift in the frequency of a signal transmitted from the ground, received at the missile, doubled, retransmitted and received at various ground stations. The measurements in terms of accumulated cycle counts are converted to range sums from the transmitter to the missile to the receiver. The range sum data from four or more UDOP sites are reduced by means of a least squares adjustment to obtain the spatial position of the missile. The data must be initialized by some external means.

Other CW Systems are represented by GLOTRAC, MISTRAM I and II and AZUSA.

GLOTRAC is an integrated, high precision tracking system. It employs strong geometry*, simple field equipment and new concepts in data reduction. Each GLOTRAC station measures either

*By "strong geometry" we mean that the station locations, relative to the trajectory, are such as to maximize the contribution of their data to the trajectory determination.

a range sum or range difference. This quantity is derived by phase comparing a received 5000 mc signal with a local, highly stable, reference signal. GLOTRAC may either share the AZUSA transponder or may employ its own specially designed unit.

MISTRAM I (Missile Trajectory Measuring System) is a high precision CW interferometric tracker located at Valkaria, Florida and is composed of five sites arranged in an L shaped configuration . The central transmitting-receiving site is located at the vertex and is designated as site zero. One leg of the L configuration lies approximately parallel to the east-west direction. Each leg has two receiving sites: one at a distance of 10,000 feet and the other at a distance of 100,000 feet from the central site. Range is measured from the central site; range differences are measured between each site and the central site yielding a set of five measurements. MISTRAM II, located at Eleuthera Island, is essentially the same as MISTRAM I but has only two baselines, one 156,000 feet in length and the other 87,000 feet in length, yielding three measurements: range and two range differences.

AZUSA MARK II, located at the Cape, is a high precision CW interferometric tracker yielding four direction cosines and two range measurements.

AZUSA angle data are obtained by measuring the phase difference of signals received at two spaced antennas. Dividing the measurement of the phase difference by the antenna spacing yields a number equal to the cosine of the angle formed by the baseline and the line joining the antenna and source. The measured quantity is thus related to the direction cosine of a directed line in space. Two such baselines, bisecting and mutually perpendicular, comprise the angle tracking system. The slant

range is obtained by making phase difference measurements between modulated signals transmitted and received at the ground station.

3.3 Acoustic Systems

The MILS target array (Pentagon) and MILS Broad Ocean Area (BOA) systems are underwater acoustic systems which are utilized at ETR to obtain precise information concerning the location of missile nose cone and tankage splashes on the surface of the ocean or bomb explosions at various depths. The arrival times of an underwater sound source at an adequate number of known positions in the ocean provide data that may be reduced to locate and time the origin of the source. The method used at ETR for reducing sound arrival time data is known as "hyperbolic triangulation."

PART I

GENERAL METHODOLOGIES OF ERROR ANALYSIS
AND
ACCURACY DETERMINATION

CHAPTER 1

INTRODUCTION

Part I of this report discusses the mathematical and conceptual background basic to the analysis of instrumentation errors and accuracy performance. The definitions of error, effects of sampling and the distinction between accuracy and precision are treated first and should be clearly understood. This is followed by discussion of various techniques used to estimate error variance and the extremely important concept of the error model. This latter concept has acquired considerable practical application during the past year as an integral part of the most sophisticated of the data reduction routines now in use at ETR. Having developed the methods for estimating error variance, the important distinctions among confidence, tolerance and prediction regions are drawn. Finally, since the errors inherent to the tracking system itself are frequently, at least to some users, of less interest than the effect of these errors on the trajectory data, the basic concepts of error propagation (geometric dilution of precision or GDOP) are presented.

CHAPTER 2
DEFINITION AND DISCUSSION OF ERRORS

The error ϵ in any measurement x of a particular quantity (e.g., range, elevation angle, etc.) is defined as the difference between x and the true value μ (unknown and unknowable) of the magnitude of this quantity. Thus, $\epsilon = (x - \mu)$. Statisticians and engineers frequently differ in the manner in which they regard and classify these measurement errors. The following pages discuss both points of view.

2.1 CLASSICAL POINT OF VIEW

Classically, statisticians have grouped errors into two types - random and systematic.* Random errors are individually unpredictable. They are usually thought of as errors resulting from the sum of a number of uncontrollable variables, each of whose effects is ordinarily individually small. As an exception we have "accidental" errors, whose effects may of course be considerable. Such "accidental" errors, due to causes such as momentary data dropout, equipment malfunction (e.g., digitizer error, etc.) may be detected and removed by editing of the data due to their gross nature.

The systematic error of a measurement process refers to its tendency to measure something other than what was intended. If the mean of n measurements made with a specific instru-

*The use of the word "systematic" is rather unfortunate, as it seems to imply, incorrectly, that such an error is intrinsically due to the particular instrument system. A better word might be "non-random" or "bias", but "systematic" is practically exclusively used in the literature.

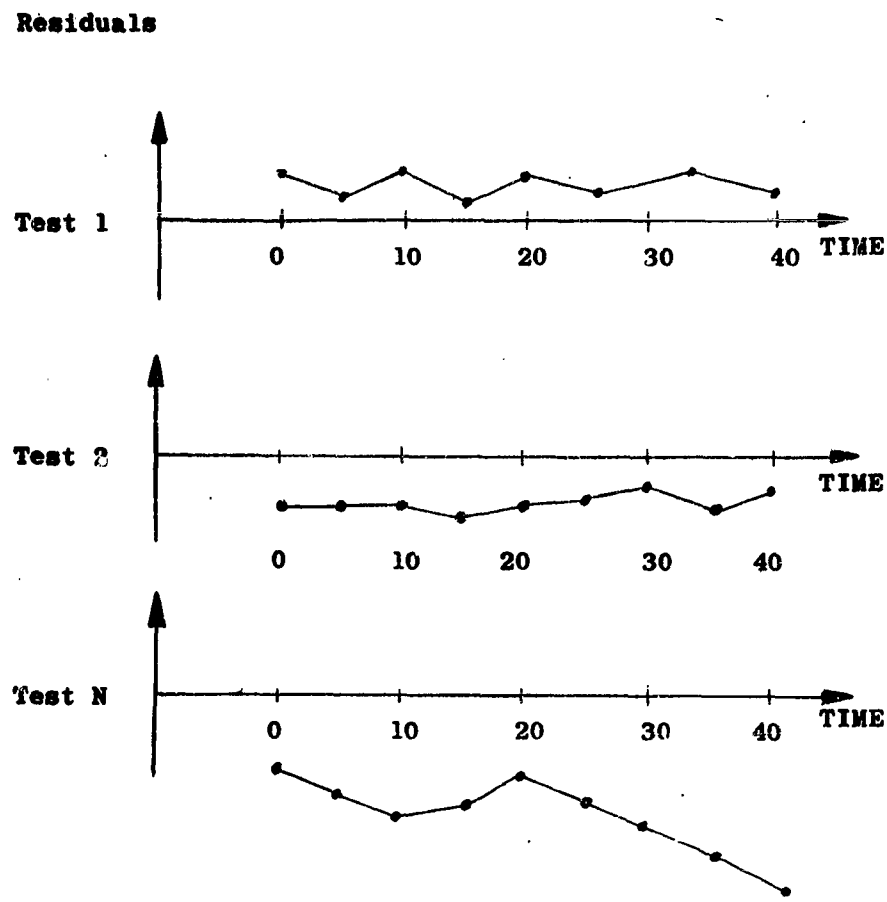
ment, under the same or similar conditions, tends to a quantity μ' as n increases indefinitely, while the true value is μ, the difference $(\mu' - \mu)$ is the systematic error or bias of the particular instrument. If the limit μ' does not exist, we cannot properly call x a measurement [Eisenhart, 1963]. We can, in general, assign a cause to these errors and can therefore remove them by calibration, at least in principle.

Systematic errors will usually consist of constant and time varying components. Zero-set errors, for instance, may cause a constant bias in the entire test*; on the other hand, variations in atmospheric conditions, effects of which are at best only partially removed, will introduce a bias which will vary from one time point to the next. As another example, radar beacon internal delay fluctuations will cause a varying systematic error in range measurements.

In actual practice, it is often difficult to distinguish between random and systematic errors. Errors such as zero-set errors, which are constant throughout any particular test, may vary from test to test; and for purposes of predicting expected performance of a tracking system on some future test, these errors must be considered random. Figure 2.1-1 shows typical between test and within test variation of errors, the variation during a test being due to a constant bias or a time dependent systematic error and/or random error.

*The resultant error in cartesian coordinate data can of course be time variant.

2.1 CLASSICAL POINT OF VIEW (CONT'D)



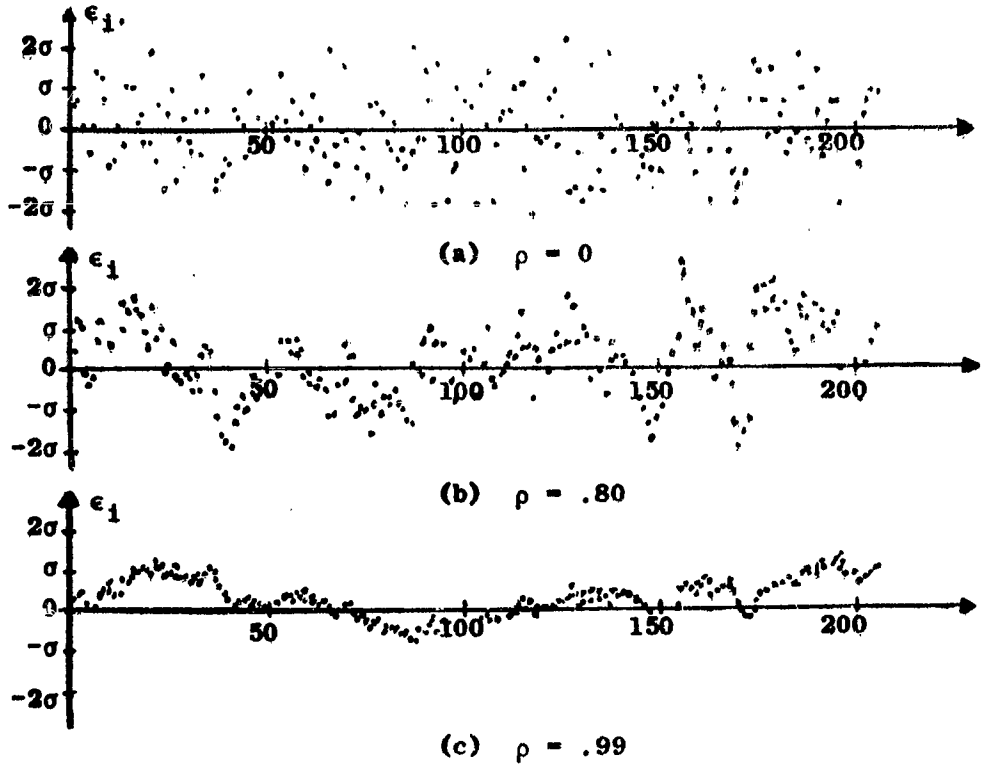
BETWEEN AND WITHIN TEST VARIATION OF ERRORS

FIGURE 2.1-1

The errors $\epsilon_1, \epsilon_2 \ldots, \epsilon_n$ in a time series of measurements are often correlated among themselves, especially if the measurements are from an electronic tracking system and closely spaced in time. Figure 2.1-2 shows three artificial series generated by the following Markov process (i.e., autoregressive model of order unity):

$$\epsilon_i = \sqrt{1 - \rho^2} \quad (\rho\epsilon_{i-1} + \delta_i). \qquad (2.1\text{-}1)$$

In equation 2.1-1, δ_i is a random normal deviate (i.e., δ_i is an observation from a normal distribution with zero mean and variance σ^2; also, δ_i and δ_j are uncorrelated). "It is readily shown that the correlation between the i-th and the (i + k)-th elements in any of the series is ρ^k and that the variance of any of the series is equal to σ^2 and hence is independent of ρ. It follows that all three series are of equal accuracy in the sense that they all have the same variance " [Brown, 1960]. This last statement is correct since all three series have zero expectations, from equation 2.1-1.



EFFECTS OF CORRELATION AMONG ERRORS

FIGURE 2.1-2

2.1 CLASSICAL POINT OF VIEW (CONT'D)

The three parts of Figure 2.1-2 correspond to $\rho = 0$, 0.80, and 0.99 respectively, where $\rho = 0$ implies serially independent errors. The figure illustrates the fact that "observations affected by errors having an appreciable degree of serial correlation may well be deceptively smooth, leading one to erroneous conclusions concerning the accuracy of the observations" [Brown, 1960]. It is also evident that serial correlation will induce oscillations in the data.

Serially correlated errors, oscillations in the data, may also have been produced by filtering, either digital or by the operation of the tracking systems, or by some factor or factors external to the tracking system, such as refraction effects or missile motion about the center of gravity. The errors in measurement which are attributed to this oscillatory effect have in the past been referred to as systematic or random error depending on the individual point of view. It is systematic in the sense that if the true serial correlations were known, and the oscillatory nature of the series is indeed the result of this correlation, then, knowing the true correlations, one could "remove it"; if not removed, the "oscillatory" effect remains in the data and should be treated as a random error for error propagation purposes.

2.2 ENGINEERING POINT OF VIEW

Borrowing from a terminology due largely to communications engineering, errors of measurement are described in terms of their frequency content. Total error is considered to be partially "noise" and partially bias. The bias error may be a constant value (zero frequency) or may

vary as a function of some parameter (time or slant range for instance) and therefore possess low frequency characteristics. Bias errors can be removed from the data when sufficient knowledge about them is available. From the engineering point of view a measurement is regarded as being composed of some true value (the "message") plus "noise". The "noise" which represents the deviations from the true values, can be regarded as being composed of a sum of sinusoidal functions, with random amplitudes and phases given by some probability distribution function. Error is thus described in terms of its frequency content.

Spectral analysis techniques are usually employed in the analysis of the frequency content of errors. We assume that these errors ϵ_t are a realization from an ensemble of random functions, usually referred to as a random or stochastic process. Further, for mathematical simplicity, we assume the process to be temporally homogeneous or stationary, by which we mean that its statistical properties do not vary with time. Finally, we assume that ϵ_t has no time trend or has been "detrended", so that its expected value is zero for all t. We write:

$$E(\epsilon_t) = 0 \qquad (2.2\text{-}1)$$

where E stands for "expected value of".

Because of the above equation, the auto-covariance function $R(\tau)$ of ϵ_t of lag τ is defined as

$$R(\tau) = E(\epsilon_t \epsilon_{t+\tau}) = \lim_{T \to \infty} \frac{1}{T} \int_{-\frac{T}{2}}^{\frac{T}{2}} \epsilon_t \epsilon_{t+\tau} \, dt. \qquad (2.2\text{-}2)$$

2.2 ENGINEERING POINT OF VIEW (CONT'D)

The variance of ϵ_t is obtained by setting $\tau = 0$ in equation (2.2-2). Thus:

$$R(0) = E(\epsilon_t^2) = \text{var}(\epsilon_t) = \lim_{T \to \infty} \frac{1}{T} \int_{-\frac{T}{2}}^{\frac{T}{2}} \epsilon_t^2 \, dt. \quad (2.2\text{-}3)$$

The spectral density function $f(\omega)$, if ϵ_t is considered as a continuous function of time, is defined as the Fourier transform of the auto-covariance function. Thus

$$f(\omega) = \frac{1}{2\pi} \int_{-\infty}^{\infty} e^{-i\omega\tau} R(\tau) \, d\tau \quad (2.2\text{-}4)$$

where $i = \sqrt{-1}$. Conversely, one may define $R(\tau)$ in terms of $f(\omega)$. Inverting equation (2.2-4), we obtain

$$R(\tau) = \int_{-\infty}^{\infty} e^{i\omega\tau} f(\omega) \, d\omega. \quad (2.2\text{-}5)$$

Therefore, knowledge of $R(\tau)$ gives $f(\omega)$ and vice-versa.

If the total area under the spectral density curve is unity, then the area between $\omega = \omega_1$ and $\omega = \omega_2$ may be interpreted as that part of the total variation or power of the process which is explained by oscillations having angular frequencies in the range (ω_1, ω_2). Thus, the curve can be thought of as allotting the total "power" of the process to oscillations of various frequencies, just as the probability density function of a random variable distributes the total probability of unity to the various intervals of values that the random variable may assume.

2.2 ENGINEERING POINT OF VIEW (CONT'D)

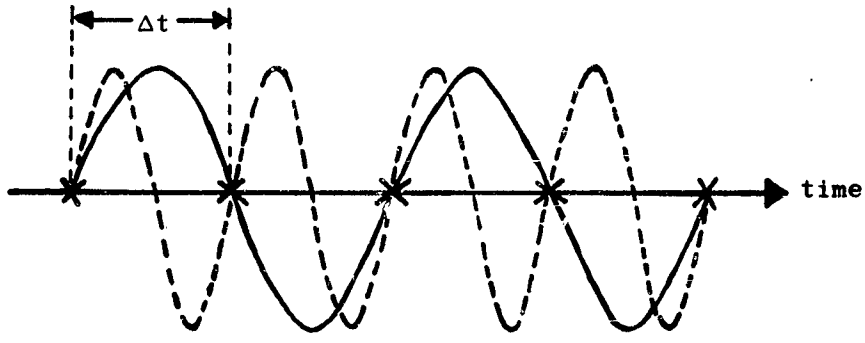
If the series is random, $R(\tau) = 0$ for all non-zero values of τ, since the observations are then independent, and the spectral density curve is a horizontal line. The process is called "white noise" because of its resemblance to the optical spectrum of white light, which is flat over the visible frequency range.

In practical applications, the spectral density function cannot be obtained from equation (2.2-4), since this requires knowledge of the auto-covariance function $R(\tau)$ for all values of τ ($-\infty$ to $+\infty$), while the sample data span is finite. The span length determines the frequency below which no contributions can be estimated. A span of length t seconds allows us to directly estimate the contribution to error from frequencies above and including $L = 1/t$ cycle per second. (Actually more than half the contribution to error for frequencies from $1/2.26t$ to $1/t$ can be estimated directly.)

Also, in practice, the original data, if continuously recorded, are digitized for processing. The sampling rate determines the frequency above which no contributions to error can be estimated directly. This frequency (denoted by f_N) is called the Nyquist frequency. If the function is sampled at intervals of Δt, then $1/(2\Delta t)$ cycles per second is the Nyquist frequency. For example, if the data are sampled at the rate of ten times per second, $\Delta t = 0.1$ seconds and $f_N = 1/0.2 = 5$ cps.

2.2 ENGINEERING POINT OF VIEW (CONT'D)

Following the terminology of fractional factorial design of experiments, wherein certain factorial effects are mutually confounded or aliased, Tukey [Tukey, 1959] refers to this effect of sampling continuous data as "aliasing", shown in Figure 2.2-1. The crosses refer to the sampled data. It is clear that the sampling has resulted in a certain loss of information, since the data cannot distinguish between the two curves.



EFFECTS OF SAMPLING

FIGURE 2.2-1

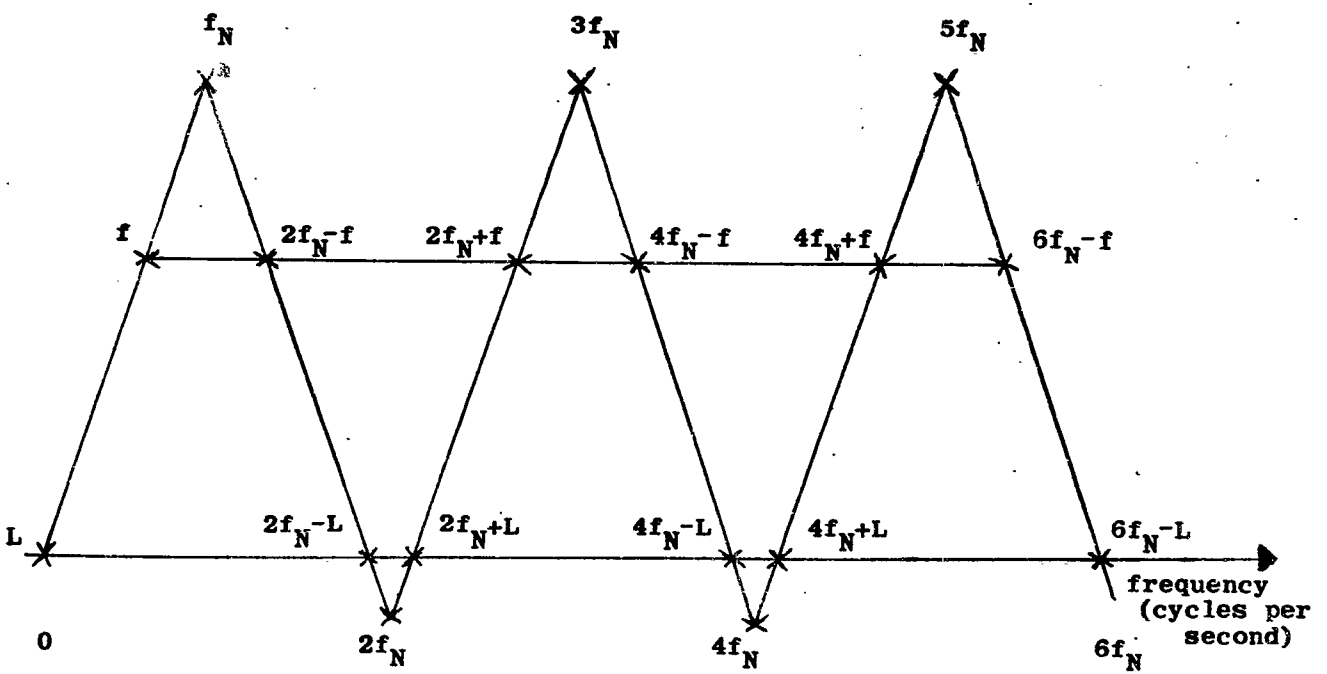
In general, any frequency of ω (radians per second) is aliased with $2\omega_N \pm \omega$, $4\omega_N \pm \omega$, $6\omega_N \pm \omega$, etc., so that if $f^*(\omega)$ is the spectral density of the continuous data, then the spectral density $f(\omega)$ of the sampled trace is given by

$$f(\omega) = \sum_{k=0}^{\infty} \left\{ f^* (2k\omega_N + \omega) + f^*(2k\omega_N - \omega) \right\} \qquad (2.2\text{-}6)$$

where the Nyquist frequency ω_N (radians per second) may be expressed in cycles per second, f_N, by dividing ω_N by 2π.

The folding effect is illustrated in Figure 2.2-2 in terms of frequencies in units of cycles per second. If we mark off a horizontal frequency scale, "crease" the spectrum at all multiples of the Nyquist frequency and "pleat" or "fold" it like an accordion as in Figure 2.2-2, then the horizontal line passing through f passes through the set of frequencies which are aliased together. The contribution from all of these frequencies is the "observed" contribution from f.

Figure 2.2-3 shows the smoothed spectral density curve of (Radar 3.16 minus AZUSA) residuals from 90 to 140 seconds of data, sampled at the rate of 10 points per second. Here, $t = 50$ seconds and $\Delta t = 0.1$ seconds, so that the lowest directly estimable frequency is $L = 1/t = .02$ cps and the highest or Nyquist frequency is $f_N = 1/(2\Delta t) = 5$ cps. Most of the power is seen to lie in the band 0 to 0.6 cps. Methods for estimating the ordinates of the spectral curve, and their smoothing, are discussed in [Press and Tukey, 1956, Appendix A (The Numerical Determination of Power Spectra).]



ALIASING OF FREQUENCIES

FIGURE 2.2-2

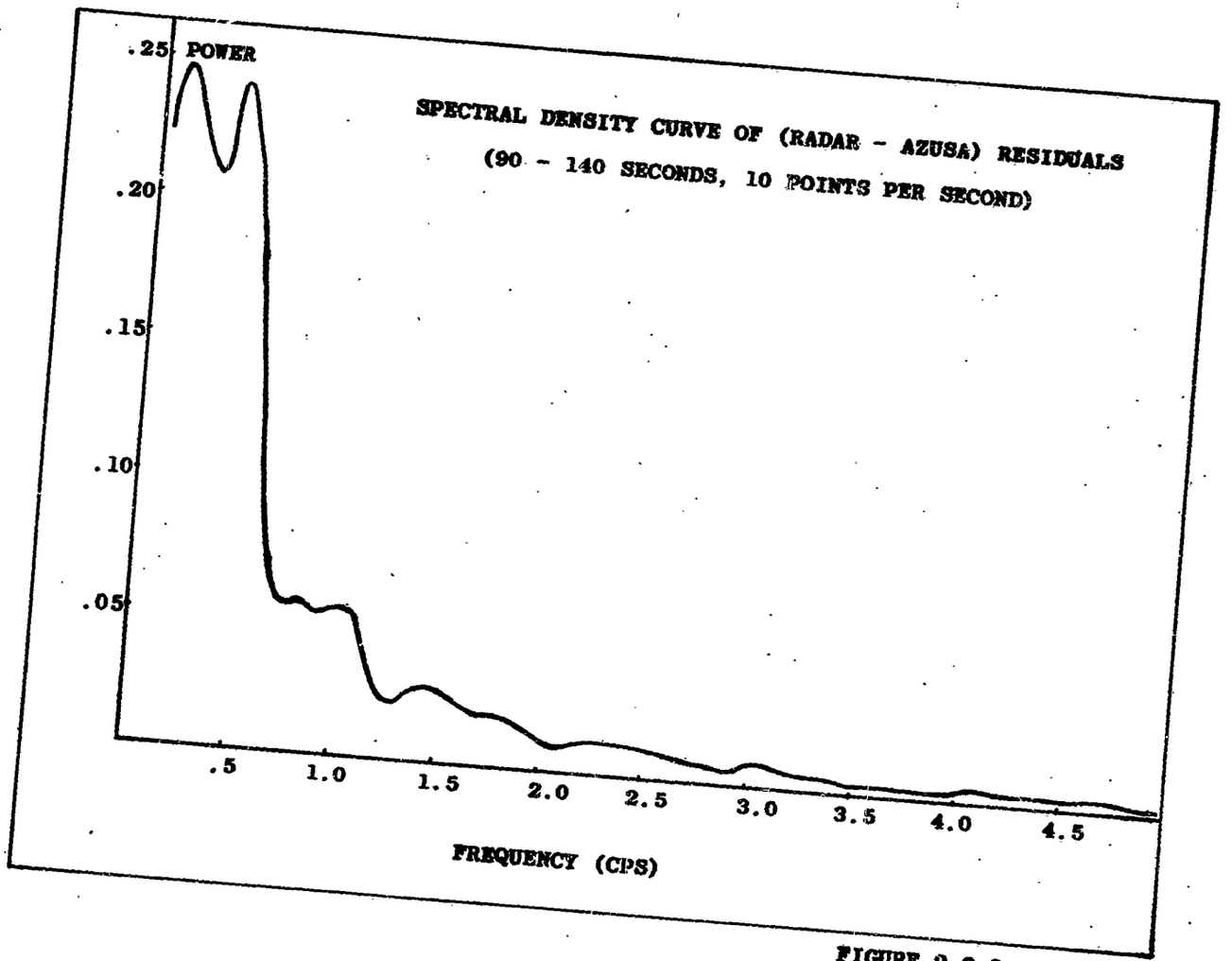

.25 POWER
.20
.15
.10
.05
SPECTRAL DENSITY CURVE OF (RADAR - AZUSA) RESIDUALS
(90 - 140 SECONDS, 10 POINTS PER SECOND)
.5
1.0
1.5
2.0
2.5
3.0
3.5
4.0
4.5
FREQUENCY (CPS)

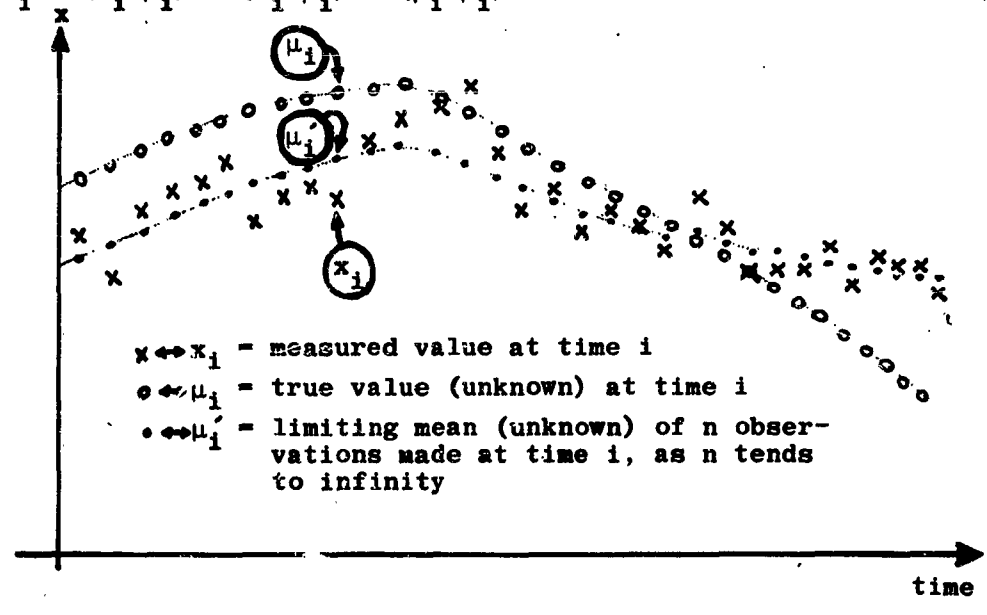
FIGURE 2.2-3

2.3 TOTAL ERROR

The total error ϵ_i in the observation x_i made at time i can be partitioned into random and systematic components as shown in equation (2.3-1) and illustrated in Figure 2.3-1.

$(\mu_i' - \mu_i)$ = systematic error $(x_i - \mu_i')$ = random error

$$\epsilon_i = (x_i - \mu_i) = (x_i - \mu_i') + (\mu_i' - \mu_i) = \text{total error} \quad (2.3\text{-}1)$$



RELATION BETWEEN TOTAL ERROR, RANDOM ERROR, AND SYSTEMATIC ERROR

FIGURE 2.3-1

As before, μ_i is the true value and μ_i' is the mean of the population from which x_i has conceptually been taken. The deviation of x_i from its mean μ_i' is a random component, while the difference $(\mu_i' - \mu_i)$ represents the systematic error or bias at time i. Assuming, quite realistically,

that these two parts are statistically independent, the total error variance is given by

$$\sigma_T^2 = \sigma_R^2 + S^2 \qquad (2.3\text{-}2)$$

where σ_T^2 stands for the total error variance and σ_R^2 and S^2 for the contribution to the total error variance due to the random and systematic errors respectively. Quite often, the systematic error is made up of a constant bias and a time varying bias (drift) and the random error of high frequency noise and low frequency noise (oscillating correlated error). Equation (2.3-2) may be written as

$$\sigma_{T_t}^2 = \sigma_{R_H}^2 + \sigma_{R_L}^2 + S_B^2 + \left[S_B(t)\right]^2 \qquad (2.3\text{-}3)$$

If there is no data noise a "smooth" data curve results but it will not be the true smooth curve because of the bias S_B and $S_B(t)$. Methods for estimating these components will be discussed in the next chapter.

If error components are reported in frequency bands, the total error variance is the sum of the error components in the various frequency bands.

Total error variance σ_T^2 is estimated by $\Sigma(x_i-\mu_i)^2/n$ if the true values μ_i are known and if the errors are uncorrelated. Inasmuch as the true coordinate values are seldom available, it is almost always necessary to use as a standard another tracking system which is an order of magnitude more accurate for the coordinates being compared. The standard may be some "Best Estimate of Trajectory", in which case an

estimate of the accuracy of the "BET" is available from the least squares solution, and must be combined with the root mean square of the differences between the coordinate measurements and the BET.

It must be emphasized that when a particular tracking system is used in arriving at a BET, then the coordinate values from that system and BET will be correlated. Thus, if x_t and $\hat{\mu}_t$ are the x-coordinate measurements of the given system and the BET, respectively, at time t,

$$\text{Var}(x_t) = \text{Var}(x_t - \hat{\mu}_t) - \text{Var}(\hat{\mu}_t) + 2\,\text{Cov}(x_t, \hat{\mu}_t) \quad (2.3\text{-}4)$$

If x_t and $\hat{\mu}_t$ are independent, then the covariance term will be zero. This may be the case if the particular system is not used in arriving at the BET.

2.4 ACCURACY AND PRECISION

Eisenhart, [Eisenhart, 1963] distinguishes between precision and accuracy as follows: "The precision of a measurement process refers to, and is determined by, the degree of mutual agreement characteristic of independent measurements of a single quantity yielded by repeated applications of the process under specified conditions; and its accuracy refers to, and is determined by, the degree of agreement of such measurements with the true value of the magnitude of the quantity concerned. In brief, "accuracy" has to do with closeness to the truth; "precision", only with closeness together."

In terminology of the previous section precision (or more correctly, imprecision) is specified by the random error variance while accuracy (or inaccuracy) is described

by the total error variance. An instrument is precise if σ_R is small; it is accurate if σ_T is small. It is clear from equation (2.3-2) that an accurate instrument is necessarily precise but not vice-versa. An instrument will be precise but not accurate if σ_R is small but S is large.

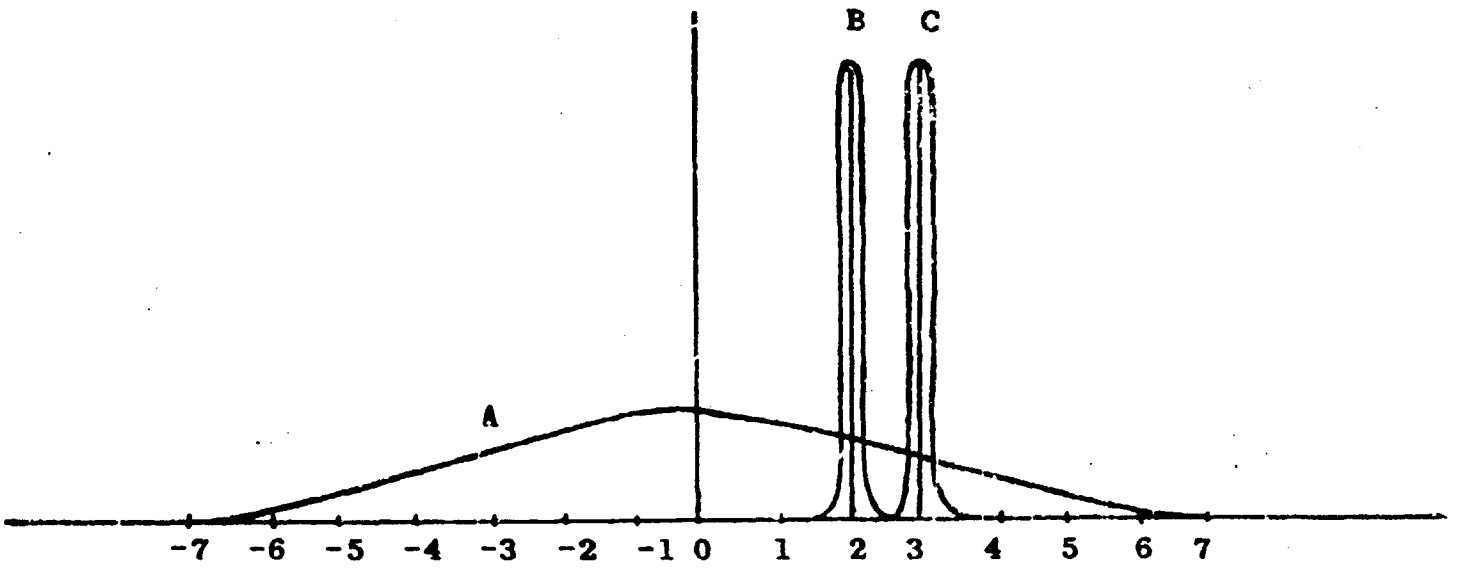
In practice, the comparison of the accuracies of two instruments may be quite difficult. If the two instruments have equal precisions, the one with the smaller bias will obviously be the more accurate; similarly, if the biases are equal or both negligible, the instrument with the higher precision may be said to have higher accuracy. The difficulty in the comparison arises when the two instruments have unequal precisions and biases.

Consider three instruments A, B and C whose properties are shown in Figure 2.4-1, where for simplicity we have assumed a normal distribution for each instrument, although any common distribution will serve the discussion just as well. By shifting the origin, if necessary, we can set the true value to be equal to zero. Following equation (2.3-2), we may define total error variance as the sum of the random error variance and the square of the bias. This gives total error variances of 6.25, 4.01 and 9.01 for A, B and C respectively. On this basis, instrument B may be said to be more accurate than A, so that an instrument with a small bias but a high precision can be more accurate than an unbiased instrument with low precision.

A: Bias = 0, $\sigma_R = 2.5$, $\sigma_T^2 = 6.25$;

B: Bias = 2, $\sigma_R = 0.1$, $\sigma_T^2 = 4.01$;

C: Bias = 3, $\sigma_R = 0.1$, $\sigma_T^2 = 9.01$.



COMPARISON OF ACCURACIES OF THREE MEASURING INSTRUMENTS

FIGURE 2.4-1

The conclusion that B is more accurate than A is also intuitively satisfactory. From the graphs, we see that we are 95% confident that instrument B will give an observation within $2 \pm 2(0.1)$, i.e., between 1.8 and 2.2, so that there is a probability of 2.5% that the error will exceed 2.2 units. On the other hand, with instrument A, the 95% tolerance limits for the errors are $0 \pm 2(2.5)$, i.e., between -5 and +5. There is thus a 5.0% probability of an error (in either direction) in excess of 5 units.

The use of total error as a criterion for accuracy is not too satisfactory when applied to the comparison between instruments A and C. On this basis, we have to conclude that A is more accurate. The graph, however, shows that with C the 95% tolerance limits for errors are $3 \pm 2(0.1)$ or between 2.8 and 3.2, compared to between -5 and +5 for instrument A. From this type of consideration, many people would select instrument C over A, "for in practical life it is often far better to always be quite close to the true value than to deviate all over the place in individual cases but strictly correct on the average" [Eisenhart, 1963]. Tolerance limits for errors should therefore be considered also in comparing accuracies.

It should be noted, however, that a high imprecision can be remedied by taking the mean of n observations, while biases are unaffected by averaging. Averages of $n = 9$ or more observations from instrument A will be seen to be more accurate than similar averages from B or C. With $n = 9$, random error standard deviations for A, B and C will then be $2.5/\sqrt{9}$, $0.1/\sqrt{9}$, and $0.1/\sqrt{9}$, with 95%

tolerance limits given by (-1.67, 1.67), (1.93, 2.07), and (2.93, 3.07), respectively. The superiority of A is even more apparent if n is larger. For example, if n = 25, the standard deviations of A and B are 2.5/5 = 0.5 and 0.1/5 = 0.02 and the 95% tolerarce limits for errors are (-1, 1) and (1.96, 2.04), respectively.

CHAPTER 3
METHODS USED TO ESTIMATE ERROR VARIANCE

3.1 METHODS USING A STANDARD

If a perfect standard is available, it is simple to estimate the accuracy of a second system. The variance of the discrepancies between the two systems is a measure of the accuracy of the second system. The difficulty arises when no perfect standard exists. Three different standards are used at the Eastern Test Range, namely Best Estimate of Trajectory, inertial guidance data, and a significantly more accurate instrumentation system.

3.1.1 "BEST ESTIMATE OF TRAJECTORY" (BET)

When several instrumentation systems track the same object, the results from the individual systems may be combined in some manner to give a single estimate of the trajectory. An approach which exploits the redundancy of data from several instrumentation systems is being utilized at the Eastern Test Range. This method has been called the "Best Estimate of Trajectory Utilizing Instrument Error Models." The procedure is concerned with estimating the systematic errors in an assumed error model, using these to unbias the data and then adjusting the unbiased data. Analysis has indicated that overlapping measurements from widely separated instruments over long time intervals are required for the optimum determination of the error model coefficients. If conditions of overlap and geometry are poor, the solution for the error model coefficients will often result in near indeterminacy.

3.1.1.1 The GLAD Program*

The GLAD (GLOTRAC Adjustment) computer program was originally conceived as a tool for the treatment of GLOTRAC data only. However, due to the program's mathematical generality and operational flexibility, it has also proved to be of great value in the reduction of data from other tracking systems. In addition, increased use has been made of the program as a general error analysis tool by planning and systems analysis personnel, and modifications have been made which allow its use in satisfying Best Estimate of Trajectory reduction requirements.

The mathematical derivation of the tracking system minimum variance solution which is the basis of the GLAD program may be found in [Lasman, 1962], [Brown, 1958] and [Arabadjis, 1961].

GLAD is a lineal descendant of earlier minimum variance computer programs developed by the Range for use in photogrammetric and Best Estimate of Trajectory reductions. The development of the routine has greatly enhanced the Range's capability for reducing data from multiple tracking systems, for analyzing system errors and for evaluating proposed tracking systems. GLAD is basically a transformation routine. When operated in the reduction mode (with actual observed data), the observations are transformed, subject to the minimum variance constraint, from the natural coordinates of the tracking systems (azimuth, elevation, range, range sum, range difference, direction cosines) into earth-fixed, rectangular Cartesian coordinates. If

*This discussion of GLAD is taken from a paper "What is the GLAD Program" by D. H. Parks, RCA Mathematical Services, presented at the Sixth Joint AFETR-Range User Data Conference, 8-9 April 1965.

systematic errors are assumed in the tracking data, they may be separated out into physically meaningful components (such as zero-set errors, timing errors, errors in tracker locations). As a by-product of the transformation of the observations into trajectory components and systematic error components, estimates of variance associated with the transformations are provided.

The estimates of variance in the transformations may be computed without having the actual observations available. This mode of operating the routine is called the GDOP (Geometric Dilution of Precision) mode. The magnitude of the GDOP's is solely a function of the assumed trajectory, assumed tracker combination, assumed random observational errors and assumed a priori knowledge of the systematic error components. The GDOP mode may thus be used to evaluate hypothetical tracking systems operating under hypothetical conditions.

Using the notation of the computer program description, the GLAD program is designed to solve iteratively, for the survey corrections (ΔS), the error model coefficient corrections (ΔP) and the trajectory coordinate corrections (ΔX), the set of linearized condition equations

(1) $(EM) = (BMS)(\Delta S) + (BMP)(\Delta P) + (BMX)(BXF)(\Delta X) + V_M$

(2) $(ES) = (\Delta S) + V_S$

(3) $(EP) = (\Delta P) + V_P$

(4) $(EX) = (\Delta X) + V_X$

Here,

$(EM) = (m') - (m)$

$(ES) = (S) - (S')$

$(EP) = (P) - (P')$

$(EX) = (X) - (X')$

where

(m") is the set of tracker observations

(m) is the evaluation of the measurement model using the current approximations

(S') is the a priori set of survey values

(S) is the current set of survey approximations

(P') is the a priori set of error model coefficients

(P) is the current set of error model coefficient approximations

(X') is the a priori set of trajectory coordinates

(X) is the current set of trajectory coordinate approximations

A typical measurement model is that for range:

(5) $(m) = a_4 m' + a_1 + a_2 t + a_3 m'$

where

$m' = r = (x^2 + y^2 + z^2)^{\frac{1}{2}}$

a_1, a_2, a_3, a_4 are error model coefficients to be estimated. Continuing with equations (1), (2), (3),

(BMS) is the matrix containing partials of the measurement model with respect to survey coordinates.

(BMP) is the matrix containing partials of the measurement model with respect to error model coefficients.

(BMX) is the matrix containing partials of the measurement model with respect to the master system trajectory coordinates.

$$(BMX) = \frac{\partial m}{\partial X_{local}} \frac{\partial X_{local}}{\partial X_{master}} = - (BMS)R$$

(BXF) = I, a unit matrix during powered flight

$$(BXF) = \frac{\partial X_{master}}{\partial FREE} \text{ during free fall}$$

(BXF) is determined by numerically perturbing the set of approximate initial conditions (FREE) used in the free fall integration. Two free fall intervals are allowed in GLAD.

The GLAD solution is that which minimizes the quantity.

$$(6) \quad s^2 = V_M^T W_M V_M + V_S^T W_S V_S + V_P^T W_P V_P + V_X^T W_X V_X$$

where

$$W_M = var^{-1}(m^\circ)$$

$$W_S = var^{-1}(S^\circ)$$

$$W_P = var^{-1}(P^\circ)$$

$$W_X = var^{-1}(X^\circ)$$

One great advantage shown by GLAD over previous minimum variance programs is in the number of options available to reduction personnel. These include

(a) Choice of 3, 6 or 9 trajectory parameters to be estimated - position, position and velocity or position, velocity and acceleration.

(b) Choice of adjustable or non-adjustable survey coordinates. Either or both origins involved in a range sum or range difference may be estimated. The survey adjustments in several instruments may be constrained to be equal.

(c) Choice of up to 7 adjustable or non-adjustable (enforced) error model coefficients for each measurement

source. Coefficients from different sources may be constrained to be equal.

(d) Choice of using random error estimates from tape or from cards or a combination of both.

(e) A varied choice of iteration conditions. The number of inner iterations (at each time point) for each outer iteration (over the whole trajectory for bias adjustment) is selective by station constants. Thus, if an adjustment of only trajectory points without bias adjustment is desired, only one outer iteration with several inner iterations would be called for. On the other hand, if enormous biases are known to be in the data (as in GLOTRAC range sums and range differences), it would be desirable to do no inner iterations during the first outer iteration. This would adjust the biases to agree with the trajectory being used as an initial approximation. Succeeding outer iterations, of course, would require inner iterations.

(f) The GDOP option. This allows variance transformation without the adjustment of observations.

GLAD is programmed in five links. The functions of each link are as follows:

Link 1 - This is the initialization link. Its primary function is to process the station constants and set up coordinate transformations. Link 1 is entered only once.

Link 2 - This is the data editing link. Results of previous computations (such as partial derivatives from the free-fall subroutine and the latest trajectory approximations) are merged here for entry into Link 3.

Link 3 - This is the main body of the program. The inner iterations and the partial derivative computations used in the bias adjustment are done here.

Link 4 - The bias adjustment is made in this link. This includes the maximum 50 x 50 matrix inversion.

Link 5 - In this link the data are processed for reading out.

The flow of data through the links is controlled by the station constants. If only one outer iteration were called for, the flow would be (Link 1→ Link 2→ Link 3→ link 5). If two outer iterations were called for, the flow would be (Link 1→ Link 2→ Link 3→ Link 4→ Link 2→ link 3→ link 5). Link 4 is always bypassed on the final outer iteration. It is possible, through the station constants, to compute the biases at intermittent times (up to 6 times) during the outer iterations. In this case the flow could oscillate between link 3 and link 4 during an outer iteration.

Analytically, GLAD would appear to offer a solution for most of the Range's calibration and planning problems. Numerically, however, when the problems reach the computer the results are not always pleasing. Major pitfalls include the following:

a. Poor convergence. This is a common numerical occurrence when station geometry is poor. A partial cure is increased precision in the computer.

b. Indeterminacy. This is usually indicated by negative values on the diagonal of the bias covariance matrix and correlation estimates with absolute values greater than unity. Poorly conditioned matrices made it

impossible to separate the Bermuda range error from the Bermuda survey error. After eliminating the survey error from the adjustment, the solution became determinant and the correlation matrix became reasonable.

c. Poor weighting. This has resulted in numerous complaints concerning published data, especially velocities, in which the noise content of the GLAD output was worse than in the best of the systems used as input. If weighting were based upon the true observation noise, this would not be possible. Steps are being taken to ensure that this does not occur on future tests.

The GLAD program has, since its first utilization for the reduction of GLOTRAC data, shown itself to be amenable to a wide variety of additional tasks. It has become a primary tool for Range planning and is being increasingly relied upon in meeting MISTRAM and Best Estimate of Trajectory reduction requirements. Modifications to the program now being planned will widen GLAD's capabilities even more and ensure a greatly increased utilization of the program in the future.

3.1.2 Data Analysis with Inertial Guidance Data as the Reference

3.1.2.1 Comparisons in a Common Coordinate System

When a number of instruments track the same object much information about the individual instruments may be obtained by pairwise data comparisons in a common coordinate system. When an independent reference standard is available, pairwise comparisons with the standard yield information about the individual instruments, and may also yield valuable information about the standard.

Inertial guidance data are an independent source of information about the tracked object. Further, since they are practically free of random effects and provide an essentially smooth trajectory, they are ideally suited as a reference standard for the detection of noise, oscillatory effects, ambiguities and other discontinuities in the tracking instrumentation data.

Inertial guidance data are subject to long term drift or bias errors which increase with time, and therefore cannot be used as a standard for estimating bias or drift in other systems, except possibly early in flight.

Multiple comparisons of inertial guidance data with tracking system data affording redundant coverage made in a common coordinate system result in the isolation of the particular system data which are anomalous. Any discrepancy in the reference standard data would of course be common to all sets of comparison data while a discrepancy occurring in only one set of data would be attributable to the tracking system data used in that comparison.

3.1.2.2 Comparisons in Tracking System Parameters

Comparisons of inertial guidance data with external tracking data in the coordinates of the external tracking system observations allow for the isolation of the particular tracking system parameter(s) giving rise to the data discrepancies.

Using additional information from function recordings, operator's logs, descriptions of mathematical processing techniques, data handling procedures, etc., data inconsistencies may be attributed to various causes, such as tracking system hardware or ancillary equipment malfunctions and data processing problems.

3.1.2.3 Inertial Guidance Data as Standard for Noise Estimation During Powered Flight

"Noise" estimates (i.e., excluding "drift" or "bias" errors) of individual tracking system data are made for powered flight data by dividing the data differences into intervals of T seconds (usually 20 seconds) in order to minimize the contribution of guidance data errors which are considered to lie essentially below .05 cycles per second. The standard deviation about the mean of the difference between the inertial guidance data and the tracking data is computed for each interval. While this computation provides "noise" estimates of tracking system rate or velocity data, it does not provide realistic estimates of the position data "noise" for the more precise tracking systems. The trend in the position difference data resulting largely from guidance system drift contributes heavily to the variance estimate. For such position data, a standard error estimate computed from the residuals about a linear curve fit to the 20 second intervals of data differences sufficies as an estimate of the position data "noise."

These separate estimates for a given tracking system may be "pooled" or averaged over a period of time where the standard deviations are expected to be homogeneous (i.e., during sustainer or during booster stage). Intervals where discontinuities or other factors affect the standard deviation unduly are usually eliminated from the "pooling."

3.1.2.4 Data Analysis with Inertial Guidance

The analysis of tracking system data using inertial guidance position and velocity data is accomplished by comparisons of tracking system data and inertial guidance data in both a common Cartesian coordinate system and the tracking system coordinates.

All differences are tabulated and plotted. Means and standard deviations about the mean are computed. Orthogonal polynomials may also be fitted to the difference data and the standard deviations of orthogonal polynomials residuals computed.

Plots and difference data are analyzed for data discrepancies. When discrepancies are noted, they are pointed out in the tracking system report for that specific test along with causative factors if known. If cause of the discrepancy is unknown, it is marked for further investigation by all concerned groups (i.e., Data Analysis, Data Processing, Engineering, etc). The tracking system test report may also present estimates of tracking system rate and velocity data "noise" from the difference data.

3.1.3. A SIGNIFICANTLY MORE ACCURATE INSTRUMENTATION SYSTEM

If one knows that a given system is significantly more accurate than a second system, then an estimate of the error of the second system can be made from the discrepancies between the two. We can estimate the "bias," the "noise" and the "total error" of the second system. The total error is computed by taking the root mean square of the discrepancies between the two systems while the "noise" is estimated by the usual standard deviation about the mean of the residuals and the "bias" by the mean of the residuals.

If an estimate of the accuracy of the standard can be obtained it should be taken into consideration when estimating the variance of the system under investigation. In actual practice the reference system is apt to be only slightly more accurate than the system under investigation. Moreover, a reference system might be significantly more accurate under certain conditions of geometry but less accurate under other conditions. It becomes imperative under these circumstances to account for the error in the reference standard.

3.2 LEAST SQUARES METHODS

Suppose that we have a set of observations $y_1, \ldots, y_n$, which are subject to the following m constraints:

$$f_j (y_1, \ldots, y_n; \gamma_1, \ldots, \gamma_p) = 0, \; j = 1, \ldots, m. \quad (3.2\text{-}1)$$

In equations (3.2-1), the γ's are unknown parameters, to be estimated from the data. The above condition equations are given by geometrical and/or physical considerations of the system. For example, in photogrammetry, if $y_1, \ldots, y_n$ are the image coordinates from n/2 cameras, we have m = n and the number of parameters is p = 3, the cartesian coordinates X, Y, and Z of the object. The relationships that exist between the object and the image coordinates can be derived from the geometry of the camera system and are given in [Brown, 1957].

If m is greater than p, as is usually the case, we have an overdetermined situation. If the observations are ideal (i.e., free from measurement errors), we can choose any p of the m equations in (3.2.1) and solve for the p unknown parameters. In practice, the observations contain errors and we resort to least squares methods. If ϵ_i is the (unknown) error in y_i, we can write

$$y_i = \mu_i + \epsilon_i, \quad i = 1, 2, \ldots, n, \quad (3.2\text{-}2)$$

where μ_i is the true but unknown value that y_i is supposed to estimate. In its utmost generality, the method of least squares consists of choosing (subject to equations 3.2-1) those values of the parameters which will minimize the quadratic form $\underline{\epsilon}^T V^{-1} \underline{\epsilon}$, where $\underline{\epsilon}$ is the column vector of

errors and V^{-1} is the inverse of the variance-covariance or dispersion matrix of the errors. If the errors are uncorrelated, the matrix V will be diagonal and the above quadratic form reduces to the usual weighted sum of squares of errors. If in addition the errors are also homoscedastic (i.e., have equal variances), the quadratic form reduces to the ordinary sum of squares of the errors.

If the condition equations are non-linear functions, an iterative procedure for the minimization is usually adopted. Equations (3.2-2) are substituted into equations (3.2-1), which are then approximated by their first-order Taylor series expansions about $\mu_i = y_i$ and guessed values of the parameters. Computational details are given in [Brown, 1957].

The sections that follow are particular applications of this general least squares method of data adjustment.

3.2.1 REGRESSION ANALYSIS

In regression analysis, the dependent variable or response y is expressible as a function of say k independent variables or factors $x_1, \ldots, x_k$ in the form

$$y_i = f(x_{i1}, \ldots, x_{ik}; \gamma_1, \ldots, \gamma_p) + \epsilon_i; \; i = 1,2, \ldots,n, \tag{3.2-3}$$

where ϵ_i is the (unknown) error in y_i, the x's being assumed to be measured essentially without error. The γ's are unknown parameters. The errors are assumed to be normally, independently, and homoscedastically distributed with zero mean and variance σ^2.

3.2.2 REGRESSION ANALYSIS (CONT'D)

If the functional form of f is unknown or non-linear in the parameters, equation (3.2-3) is usually approximated by a model as follows, which is linear in the parameters:

$$y_i = \gamma_1 x_{i1} + \ldots + \gamma_p x_{ip} + \epsilon_i, \; i = 1, \ldots, n \qquad (3.2\text{-}4)$$

Equation (3.2-4) includes as particular cases the polynomial regression of y on one or more independent variables, with $x_{ij} = x_i^j$ in the case of regression on a single variable x. Also, the first x-variable is usually a "dummy" variable, with all its values equal to unity, in which case the first parameter γ_1 in (3.2-4) represents the intercept or height of the response function at the origin. If c_j is the least squares estimate of γ_j, and taking equation (3.2-4) as the mathematical model, the error ϵ_i is estimated by the residual $e_i = y_i - (c_1 x_{i1} + \ldots + c_p x_{ip})$ and the minimum-variance unbiased estimate of σ^2 is

$$s^2 = \sum_{i=1}^{i=n} e_i^2 \Big/ \epsilon(n-p). \qquad (3.2\text{-}5)$$

The difference between the total number n of residuals and the number p of parameters estimated in the model is called the number of degrees of freedom of s^2.

In ETR applications, the dependent variable y usually consists of difference data, e.g., MISTRAM minus ballistic camera data which have been reduced so as to be comparable. The independent variables are the flight or trajectory variables. For examples, from physical considerations, Relf [Relf, 1963] postulates the following regression model for ΔR, the difference in range measurements between MISTRAM and ballistic camera:

$$\Delta R = a_o + a_1 \dot{R} + a_2 R + a_3(\csc E_o) + e \qquad (3.2\text{-}6)$$

where E_o is the elevation angle with respect to the central receiver of the MISTRAM system. The independent variables in equation (3.2-6) are not essentially error-free, so that this assumption of regression analysis is violated.

Methods for testing hypotheses or constructing confidence intervals for the regression coefficients or the predicted values are discussed in the statistical texts, e.g., [Hader and Grandage, 1958]. It should be noted that if the errors are not independent, equation (3.2-5) is not a valid estimate of σ^2 and the usual techniques for drawing inferences about the regression coefficients are not applicable [Chew, 1964a]. Errors from a time series, for example, are apt to be correlated.

3.2.2 ANALYSIS OF VARIANCE

When data are collected from several sources, e.g., from several runs, flights, tests, aircraft, missiles, etc., the analysis of variance provides a convenient technique for partitioning the total variation in the data (as measured by the sum of squares of the observations) into components ascribable to the various sources of variation. The simplest situation is where the data can be categorized into one of several more or less homogeneous groups, according to a single criterion. Here, there are only two sources of variation -- a between-group and within-group variation. For example, flight data from a particualr type of missile and radar can be grouped according to tests, and a common problem then is to partition the total variability of the

data into the between-test and the within-test components.

Data as described above are said to constitute a one-way classification, while the design of the experiment giving rise to such data is called the completely randomized design. Historically, the experimental treatments (fertilizers, varieties, etc.) were allotted to the field plots in a completely random fashion, with or without equal replications of each treatment. The mathematical model for such a design is

$$y_{ij} = \mu + \gamma_i + \epsilon_{ij}, \quad j = 1, \ldots, n_i; \quad i = 1, \ldots, p \qquad (3.2\text{-}7)$$

where p is the number of groups, n_i is the number of observations in the i-th group, y_{ij} is the j-th observation in the i-th group, μ is the mean of the population from which the p groups form a sample, γ_i is the deviation from μ of the true mean of the i-th group, and ϵ_{ij} is the random contribution to y_{ij}.

Two different assumptions may be made concerning the γ's. In the fixed effects model, the γ's are unknown but fixed numbers. By introducing dummy variable x_i, where x_i takes the value unity if the observation comes from the i-th group and zero otherwise, and replacing the double subscripts by a single subscript by serially indexing the observations in some systematic manner, it is possible to write equation (3.2-7) in the regression form of equation (3.2-4). This is shown in detail in [Chew, 1958 , Appendix A].

3.2.2 ANALYSIS OF VARIANCE (CONT'D)

In the random effects model, the γ's are regarded as random variables with mean zero and variance σ_b^2. It is this between-group variance that is of primary interest and not the values of the γ's per se. The method for estimating σ_b^2 and the within-group variance σ^2 is suggested by the following analysis of variance table. The mean squares D and E are random variables with expected values given in the last column [Kempthorne, 1952, page 105]. Therefore, E estimates σ^2 while σ_b^2 is estimated by (D-E)/k. The quantity B is usually obtained by the difference (C-A).

TABLE 3.2-1

ANALYSIS OF VARIANCE

(ONE-WAY CLASSIFICATION - RANDOM MODEL)

SOURCES OF VARIATION	DEGREES OF FREEDOM	SUMS OF SQUARES	MEAN SQUARES	EXPECTED VALUES OF MEAN SQUARES
Between Groups	p-1	$A=\sum_i n_i(\bar{y}_i-\bar{\bar{y}})^2$	D=A/(p-1)	$\sigma^2+k\sigma_b^2$
Within Groups	n-p	$B=\sum_{ij}\sum(y_{ij}-\bar{y}_i)^2$	E=B/(n-p)	σ^2
Total	n-1	$C=\sum_{ij}\sum(y_{ij}-\bar{\bar{y}})^2$		

$$\bar{y}_i = (\sum_j y_{ij})/n_i; \quad \bar{\bar{y}} = (\sum_i n_i\bar{y}_i)/n = (\sum_{ij}\sum y_{ij})/n$$

$$k = (n^2-\sum_i n_i^2)/[n(p-1)].$$

3.2.2 ANALYSIS OF VARIANCE (CONT'D)

If errors are not independent, the above estimating procedure is not valid. While errors from different groups may reasonably be assumed to be uncorrelated, errors within a group are quite often correlated, especially if the measurements in a group are in the nature of a time series. This is the case, for example, if the different groups correspond to different tests.

When there are several sources of variability, the experiment should be designed so as to yield the desired information at the lowest possible cost. For a discussion of other experimental designs for the estimation of variance components, see [Chew, 1958].

3.2.3 EQUATIONS OF MOTION CURVE FITTING

A method for estimating the random high plus low frequency components of error which is utilized exclusively for the analysis of free fall data consists of fitting the equations of motion of the free fall ballistic missile to the data by the method of least squares and estimating the standard deviation from the residuals. For short spans of the order of 20 seconds and altitudes essentially outside the atmosphere, a Taylor series expansion of the two-body equations of motion truncated at the fourth degree is used. For data spans inside the atmosphere and/or larger than 20 seconds, the more exact equations of motion including drag and second and fourth zonal harmonics of the gravitational potential are used. For MISTRAM and GLOTRAC data-fitting, additional zonal, tesseral, and sectorial grativational terms are being added to the computer programs.

3.2.4 RESIDUAL ANALYSIS

In equation (3.2-8), the total error ϵ_i in the observation y_i can be decomposed into three components --- bias β_i, low frequency random component γ_i, and high frequency random component η_i. Thus

$$\epsilon_i = \beta_i + \gamma_i + \eta_i. \qquad (3.2\text{-}8)$$

The total variance of ϵ_i can be partitioned correspondingly to give

$$\sigma_T^2 = B^2 + \sigma_{R_L}^2 + \sigma_{R_H}^2. \qquad (3.2\text{-}9)$$

Suppose now that $e_1, \ldots, e_n$ are a set of n residuals, usually though not necessarily from a series of measurements in time, obtained from any one of the methods previously discussed. The problem is the estimation of the various variance components in equation (3.2-9).

In general, the problem is complicated by the fact that the residuals e_i and e_j do not estimate the total errors ϵ_i and ϵ_j equally precisely. For example, in photogrammetry, the residuals e_i and e_j might have come from a least squares adjustment of data from m_i and m_j cameras, respectively. Therefore, the total error should be estimated from a <u>weighted</u> sum of squares of residuals. Thus

$$s_T^2 = \sum_{i=1}^{i=n} (w_i e_i^2)/n \qquad (3.2\text{-}10)$$

where w_i is the weight to be attached to e_i.

We derive estimates of the other variance components in equation (3.2-9) from the following mathematical identity.

$$\frac{\Sigma w_i e_i^2}{n} = \frac{\Sigma(\sqrt{w_i} e_i - \bar{e})^2}{n} + \bar{e}^2 \qquad (3.2\text{-}11)$$

where

$$\bar{e} = (\Sigma \sqrt{w_i} e_i)/n \qquad (3.2\text{-}12)$$

is the weighted mean of the residuals. It is an estimate of the average bias and its square $\bar{e}^2$ estimates the contribution of the bias error to the total error variance. Subtracting $\bar{e}^2$ from s_T^2 gives an estimate of $(\sigma_{R_H}^2 + \sigma_{R_L}^2)$. If there is a separate estimate of $\sigma_{R_H}^2$ (e.g., from variate difference), it can be subtracted from the estimate of $(\sigma_{R_H}^2 + \sigma_{R_L}^2)$ to give an estimate of $\sigma_{R_L}^2$.

3.3 A MULTI-INSTRUMENT TECHNIQUE (GRUBBS' METHOD)

A method for estimating the precision of instruments was proposed by Grubbs, [Grubbs, 1948] which makes use of paired comparisons between several instruments. With three instruments, the method is a follows:

Let a_i, b_i, and c_i be three simultaneous readings of some measurement (e.g., range) at time i given by three instruments A, B, and C respectively. Denote their precisions by σ_A^2, σ_B^2, and σ_C^2. These are the quantities to be estimated from the following differences:

$$\begin{aligned} u_i &= a_i - b_i \\ v_i &= a_i - c_i \\ w_i &= b_i - c_i \end{aligned} \qquad (3.3\text{-}1)$$

If $\bar{u}$ is the arithmetic mean of the u's, the sample variance of the u's, denoted by s_u^2, is defined by the equation

$$s_u^2 = \sum_{i=1}^{i=n} (u_i - \bar{u})^2/(n - 1) \qquad (3.3\text{-}2)$$

where n is the number of time points. Defining s_v^2 and s_w^2 in a similar manner, we obtain estimates of the instrumental precisions as follows:

$$\begin{aligned} s_A^2 &= (s_u^2 + s_v^2 - s_w^2)/2 \\ s_B^2 &= (s_u^2 + s_w^2 - s_v^2)/2 \\ s_C^2 &= (s_v^2 + s_w^2 - s_u^2)/2 \end{aligned} \qquad (3.3\text{-}3)$$

3.3 A MULTI-INSTRUMENT TECHNIQUE (GRUBBS' METHOD) (CONT'D)

The variances of the estimates (3.3-3) are given in the Grubbs reference.

The validity of the method depends on several assumptions. First, we postulate the following mathematical model for the observations:

$$\begin{aligned} a_i &= \mu_i + \tau_i + \alpha_i \\ b_i &= \mu_i + \tau_i + \beta_i \quad (i = 1,2,\ldots,n) \\ c_i &= \mu_i + \tau_i + \gamma_i \end{aligned} \qquad (3.3\text{-}4)$$

In the above equation, μ_i is the true (but unknown) value that the three instruments are trying to estimate, which may, for example, be the true range of a missile from a common origin.

The term τ_i in equation (3.3-4) is the common bias peculiar to the i-th time point. It may be caused, for example, by random fluctuations in the atmosphere or in the frequency standard. This bias term will thus change with time in an un-specified fashion, but as long as it is the same (or at least essentially so) for all three instruments, the presence of this common effect will not invalidate the method, since the term will drop out on subtraction.

Finally, we assume that the errors (the α's, β's, and γ's) are independent random variables with zero means and variances σ_A^2, σ_B^2, and σ_C^2. The independence assumption refers not only to errors from the same instrument but also to errors from different instruments.

3.3 A MULTI-INSTRUMENT TECHNIQUE (GRUBBS' METHOD) (CONT'D)

With the assumptions on the previous page, it is easy to derive the estimates of σ_A^2, σ_B^2, and σ_C^2 given by equation (3.3-3). Substituting equation (3.3-4) in (3.3-1), we have

$$u_i = (\alpha_i - \beta_i),\ v_i = (\alpha_i - \gamma_i),\ \text{and}\ w_i = (\beta_i - \gamma_i) \qquad (3.3\text{-}5)$$

with variances given by

$$\sigma_u^2 = (\sigma_A^2 + \sigma_B^2),\ \sigma_v^2 = (\sigma_A^2 + \sigma_C^2),\ \text{and}\ \sigma_w^2 = (\sigma_B^2 + \sigma_C^2). \qquad (3.3\text{-}6)$$

Solving (3.3-6) for σ_A^2, σ_B^2, and σ_C^2 we obtain

$$\sigma_A^2 = (\sigma_u^2 + \sigma_v^2 - \sigma_w^2)/2;\quad \sigma_B^2 = (\sigma_u^2 + \sigma_w^2 - \sigma_v^2)/2 \text{ and}$$

$$\sigma_C^2 = (\sigma_v^2 + \sigma_w^2 - \sigma_u^2)/2 \qquad (3.3\text{-}7)$$

Replacement of each unknown variance σ^2 in equation (3.3-7) by its unbiased estimate s^2 immediately gives equation (3.3-3).

Grubbs' method should not be used indiscriminately. Besides the assumptions made concerning the mathematical model (equation 3.3-4), it is also assumed that a_i, b_i, and c_i are direct observations made at the same time point. If some of the values of a_i, b_i, and c_i have been obtained by interpolation, the variances given by equation (3.3-6) are incorrect. The effects of interpolation have not been studied.

3.3 A MULTI-INSTRUMENT TECHNIQUE (GRUBBS' METHOD) (CONT'D)

The assumption of a common bias term should also be borne in mind. If the bias is well approximated by say a linear trend but with different coefficients, we will have $a_i = \mu_i + (\lambda_A + \nu_A t_i) + \alpha_i$ and $b_i = \mu_i + (\lambda_B + \nu_B t_i) + \beta_i$, so that $u_i = a_i - b_i = (\lambda_A - \lambda_B) + (\nu_A - \nu_B)t_i + (\alpha_i - \beta_i)$ will have an expectation which is time-dependent, so that formula (3.3-2) is not a valid estimate of σ_u^2. If this assumption of common bias is satisfied, it is seen from equation (3.3-5) that u_i, v_i, and w_i have zero expectations. One check that can be made, therefore, is to test the significance of the deviations of $\bar{u}$, $\bar{v}$, and $\bar{w}$ from their zero expectations. If they do, in fact, have zero expectations, the variance of u may instead be estimated by

$$s_u^2 = \sum_{i=1}^{n} u_i^2/n. \qquad (3.3\text{-}8)$$

The assumption of independent errors is also open to criticism. It is well known that errors from a time series are quite often autocorrelated, expecially if the sampling rate is rather high. If this is the case, the u's, v's and w's will also be autocorrelated and the estimates of their variances, represented by equation (3.3-2), are not valid.

Even if errors from the same instrument are not correlated, we still require errors from different instruments to be independent. We shall indicate the effect of cross-correlation. Let ρ_{AB} be the correlation coefficient between corresponding errors from instruments A and B, and similarly for ρ_{AC} and ρ_{BC}. It is easy to show that instead of equation

(3.3-7), we shall now have

$$(\sigma_u^2 + \sigma_v^2 - \sigma_w^2)/2 = \sigma_A^2 - (\rho_{AB}\sigma_A\sigma_B + \rho_{AC}\sigma_A\sigma_C - \rho_{BC}\sigma_B\sigma_C) \qquad (3.3\text{-}9)$$

and similarly for the other two equations in (3.3-7). Equation (3.3-9) shows that $(s_u^2 + s_v^2 - s_w^2)/2$ is no longer a valid estimate of σ_A^2.

Furthermore, depending on the numerical values of the correlation coefficients, the expression $(s_u^2 + s_v^2 - s_w^2)/2$ can have a negative mean value. Thus, if $\rho_{BC} = 0$ and $\rho_{AB} = \rho_{AC} = \rho$, say, and the variances σ_A^2, σ_B^2, and σ_C^2 are equal (or essentially equal), the above estimating expression has expectation

$$\sigma_A^2(1 - 2\rho) \qquad (3.3\text{-}10)$$

which is negative for $\rho > 0.5$, thereby causing a tendency for estimates to be negative. Even if $(1 - 2\rho)$ is positive, there will be a rather high probability of negative estimates, if $(1 - 2\rho)$ is close to zero.

The tendency to give negative estimates of variance, which are necessarily positive, is a very unsatisfactory feature of Grubbs' method. Even with independent errors, such estimates will arise frequently, if the precisions of the instruments are of different orders of magnitude. For example, if $\sigma_A^2 = 1$, $\sigma_B^2 = 5$, and $\sigma_C^2 = 10$, we have that $\sigma_u^2 = 6$, $\sigma_v^2 = 11$, and $\sigma_w^2 = 15$. With good and reasonable

estimates given by say $s_u^2 = 5.5$, $s_v^2 = 10.1$, and $s_w^2 = 15.8$, the estimate of σ_A^2 given by $(s_u^2 + s_v^2 - s_w^2)/2$ is negative.

If errors are independent and instrumental precisions are comparable, negative estimates will seldom arise, though still possible, for then s_u^2, s_v^2, and s_w^2 will also be of comparable magnitudes, and there will be a high probability that the sum of the first two will exceed the third estimate.

In [Thompson, 1963] the problem of negative estimates of variance is solved for the simple case of two instruments and where, in equation (3.3-4), $\tau_i = 0$ and μ_i is a random variable with some mean μ. While the last restriction is reasonable in the situation considered by Thompson, where μ_i is the mean of the i-th batch, it is obviously not realistic in ETR applications.

3.4 VARIATE DIFFERENCE TECHNIQUE

One of the techniques most frequently used to estimate the random error variance in a set of trajectory observations from a given system is that of variate differences. The method is based on two assumptions, namely, that errors are statistically independent and that for short spans of data the true trajectory can be adequately represented by a polynomial of low degree. Successive differencing will eliminate this polynomial, together with any bias or low frequency errors, and hence will allow the estimation of the random error variance of the system.

Define the forward p-th difference of x_i, x_{i+1}, ..., x_{i+p} as usual by

$$\Delta_i^p = \binom{p}{0} x_i - \binom{p}{1} x_{i+1} + \binom{p}{2} x_{i+2} - \ldots + (-1)^p \binom{p}{p} x_{i+p} \qquad (3.4\text{-}1)$$

where

$$\binom{p}{k} = (p!)/\left[(k!)\,(p-k)!\right]$$

From a sample x_1, x_2, ..., x_n, the random error variance is estimated by

$$s^2 = \sum_{i=1}^{n-p} (\Delta_i^p)^2 / \left[(n-p)\binom{2p}{p}\right] \qquad (3.4\text{-}2)$$

In using p-th differences, it is assumed that a (p-1)-th degree polynomial will adequately represent the true trajectory. This assumption can be statistically tested. We call p the order of the variate differences.

It is well known that the error variance estimated from equation (3.4-2) is biased if the errors are autocorrelated.

3.4 VARIATE DIFFERENCE TECHNIQUE (CONT'D)

To overcome this difficulty, we can take every second or every third value only. Thus, if we originally have $n = 2m$ observations, we can apply formula (3.4-2) to $x_2, x_4, \ldots, x_{2m}$. We say that the lag here is two. If the lag is three, we apply the equation to the observations $x_3, x_6, \ldots, x_{3m}$, and similarly with higher lags. The lag should be high enough so that successive data points are uncorrelated; however, the time span covered by the new (p+1) successive observations, from which p-th differences are obtained, is now much longer and there is the danger that over this longer time span, a (p-1)-th degree polynomial may not be sufficient to represent the true trajectory, in which case the p-th differences will not contain noise only. A more satisfactory solution is to estimate the stochastic process that generates the errors and to apply a correction factor to formula (3.4-2) so as to make it unbiased. This is done in [Chew, 1964a] for autoregressive and moving-average error models.

It is useful and instructive to examine the frequency content of the estimate obtained from the variate difference technique. Let ΔT be the time interval between successive data points. The Nyquist frequency is thus $1/(2\Delta T)$ cycles per second. The variate difference technique (of order 4, 5 and 6 say) effectively examines the contributions to error of the frequencies between $.75/(2\Delta T)$ and $1/(2\Delta T)$ (and of course frequencies which are aliased with those in the intervals.) The estimate of the total error is approximately that which would result from having sampled the spectrum only in the interval $.75/(2\Delta T)$ to $1/(2\Delta T)$, and assumed the contribution was typical of the spectrum below $1/(2\Delta T)$. From this it is seen that

we may estimate the component of the variance in the interval .75/(2ΔT) to 1/2ΔT) by dividing the variance obtained using the variate difference method by four.

When lagged variate differences are used, the technique is still selective, but the spectrum is "sampled" in different intervals. For a lag of 2, the interval sampled is that between .75/(4ΔT) and 1.00/(4ΔT). For a lag of 4, the interval sampled is .75/(8ΔT) to 1.00/(8ΔT) (and its aliased intervals). For a lag L, the interval sampled is .75/(2LΔT) to 1.00/(2LΔT), plus the aliased intervals relative to the Nyquist frequency 1/(2LΔT). Because of aliasing, selective "sampled" portions of the frequency spectrum, for each lag, include contributions from intervals above its Nyquist frequency. Figure 3.4-1 illustrates the variate difference frequency response for a 4th order, lag L response function.

VARIATE DIFFERENCE FREQUENCY RESPONSE
4^{th} ORDER, LAG L RESPONSE FUNCTION

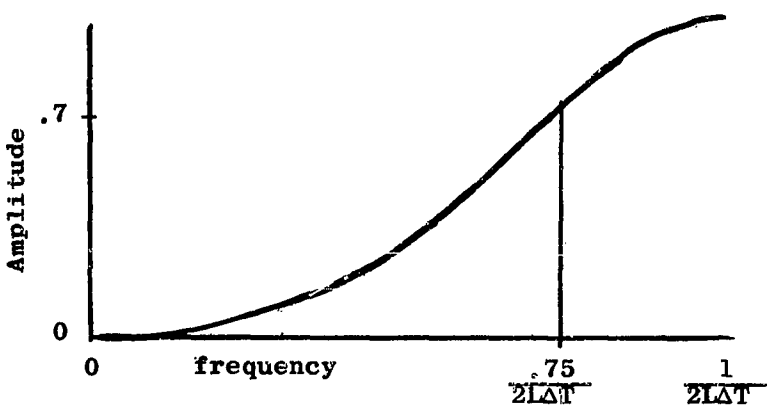


Figure 3.4-1

3.5 ANALYTICAL INVESTIGATION - ERROR MODELS

The first step in error analysis is to determine the system error models which describe amounts and sources of measurement errors. The errors to be accounted for in the model are partially systematic (i.e., they can be described by functional relations) and partially random (i.e., they can be described in statistical terms only since there is no functional expression available that relates the effect to cause or the complexity of the cause is beyond our full comprehension and ability to express it).

The terms in an error model should reflect the physical factors influencing the behavior of the data produced by the system under investigation. A mathematical model is first formulated which describes a tracking system in terms of the basic physical measurements such as counts per unit time, voltages, phase delay, etc. Based on this mathematical model, an error model is then determined which considers the system's error budget specifications and the ETR error parameters such as uncertainty of geodetic location, non-homogeneity of the propagation medium, etc., and on target - dependent factors depending on how each source of error would affect the measured data.

This general error model is next expressed as a test or calibration model which includes only those descriptive terms which can either be measured or be predicted from theoretical estimates based on the system's characteristics and operating parameters, and which are of significance in terms of the granularity (bit size) of the data. This model may not be linear, in which case it is rewritten in a linear approximation of the model.

3.5 ANALYTICAL INVESTIGATION - ERROR MODELS (CONT'D)

Sensitivity tests are made on the model by varying each of the terms independently within their expected ranges in order to determine the effect on the data. The size of the error terms used for sensitivity testing may be (a) estimated from operational data, or (b) predicted from considering the target, trajectory and system's operating characteristics. This analysis should also give an estimate of the truncation error induced by linearizing the model.

The statistical design of experiments and calibrations is based on the linear model and the results of the sensitivity tests. Dynamic simulation and static calibration tests are used to isolate errors and their behavior which would otherwise be confounded in a composite test. The results of the designed experiment are analyzed for the most significant terms. Individual models are also formulated for those systematic errors (terms in the general model) which can be expressed in a functional or graphical form of measurable source parameters. As the sources of error are identified the system is studied to determine if the errors are amenable to calibration, system modifications, or corrections in data processing.

The errors which evade description in functional form are analyzed for their frequency content and serial correlation in order to determine the most effective smoothing filters to be applied to the data. These errors are also examined for trends and patterns which persist or reoccur. Such patterns of errors indicate a possible systematic error source which needs to be investigated.

3.5 ANALYTICAL INVESTIGATION - ERROR MODELS (CONT'D)

Possible sources of systematic (bias) errors to be accounted for in an error model result from:

(a) inaccurate zero setting, initialization or calibration

(b) ambiguities (loss of count of the number of cycles in the range sum or range difference measurement)

(c) errors in range and range rate proportional to time resulting from uncertainty in the speed of light

(d) timing errors

(e) survey errors

(f) geodetic errors

(g) residual refraction errors

As an example of an error model formulation, an error model is derived in the following steps for a C-W type ranging system.

The first step is to develop the functional relationship between the derived range measurement R and the observed quantities. This may be expressed as:

$$R = \left(\frac{c}{4\pi f}\right) \phi$$

where

R = range (the path length between points a and b)

c = speed of light

f = frequency of the electromagnetic wave

ϕ = phase shift of a signal (wavelength λ) traveling the round trip from a to b and back to a

3.5 ANALYTICAL INVESTIGATION - ERROR MODELS (CONT'D)

The second step consists of differentiating the functional relationship derived in Step I with respect to each of the parameters:

$$dR = \left(\frac{c}{4\pi f}\right) d\phi + \left(\frac{\phi}{4\pi f}\right) dc - \left(\frac{c\phi}{4\pi f^2}\right) df$$

The third and fourth steps consist of dividing each side of this equation by the original function and adding:

$$\frac{dR}{R} = \frac{\left(\frac{c}{4\pi f}\right) d\phi}{\left(\frac{c}{4\pi f}\right) \phi} + \frac{\left(\frac{\phi}{4\pi f}\right) dc}{\left(\frac{\phi}{4\pi f}\right) c} - \frac{\left(\frac{c\phi}{4\pi f}\right) \frac{df}{f}}{\left(\frac{c\phi}{4\pi f}\right)}$$

$$= \frac{d\phi}{\phi} + \frac{dc}{c} - \frac{df}{f}$$

Replacing R by the expression $R = \frac{c\phi}{4\pi f}$, the differentials by finite increments Δc, Δf, and $\Delta\phi$, and re-arranging terms the following expression for ΔR is obtained:

$$\Delta R = R \left(\frac{\Delta c}{c} - \frac{\Delta f}{f}\right) + \left(\frac{c}{4\pi f}\right) \Delta\phi$$

This equation defines how errors in the speed of light, in the transmitted frequency, and in the measured phase delay affect the value of range that is finally determined by the system.

The uncertainty, $\Delta\phi$, in the phase delay occurs because the measured phase delay does not represent that caused by the true slant range. Residual errors in the zero-set, drift of the zero-set, and residual refraction errors combine to produce the uncertainty, $\Delta\phi$. The residual refraction error

can be approximated functionally as the product of a constant and some function of the elevation angle. The functional form of $\Delta\phi$ can, therefore, be written as follows:

$$\Delta\phi = \Delta S + kg\ (E)$$

where ΔS is the uncertainty in the zero-set.

Finally, there might occur an error in the measured phase delay because of an error in timing since phase delay and time are directly related:

$$\phi = 2\pi ft$$

$$\Delta\phi_{timing} = (2\pi f)\ \Delta t$$

The error in range caused by this timing error, ΔR_{timing}, is equal to the product of the range-rate and the uncertainty in time:

$$\Delta R_{timing} = R\Delta t_i$$

where Δt_i = the uncertainty in internal timing.

When comparing the C-W system with a reference system (standard) a discrepancy in range may occur because of the synchronization between the C-W system timing and the reference system timing. This part of the discrepancy in range would have the form:

$$R_{CW} - R_{STANDARD} = \dot{R}_{TRUE}\ \Delta t_s$$

where Δt_s represents the error in synchronization.

3.5 ANALYTICAL INVESTIGATION - ERROR MODELS (CONT'D)

The following equation summarizes the uncertainty in range produced by the five primary sources of systematic error: timing, refraction, speed of light, frequency instability, and zero-set:

$$\Delta R = (\Delta t_i + \Delta t_s)\,\dot{R} + k'g(E) + \left(\frac{\Delta c}{c} - \frac{\Delta f}{f}\right) R + \Delta s_R$$

where $k' = \frac{c}{4\pi f k}$, Δs_R is the constant bias in range, $\Delta s_R = \frac{c}{4\pi f}\,\Delta S$.

A term ϵ representing the residual or random error must also be added to the above expression to complete the general error model.

Some estimate of the functional form of the residual refraction errors must be made before the equation can be used as a regression equation. The functional relationship that is desired is one which describes the residual errors in range after the refraction correction has been made to the range data. The distribution of these residuals depends upon the nature of the methodology utilized to compute the refraction corrections. If the method of correction were accurate enough to account for all known physical causes of systematic errors in refraction corrections, the residual errors should, in principle, be random. The subject of precise refraction corrections, however, is complex and as yet unsettled. Depending upon the corrections made to the data, the functional form of the residual refraction errors in range might be expressed as the cosecant of the elevation angle measured with respect to the ground receiver. The error model equation may then be written as:

$$\Delta R = \alpha_o + \alpha_1 \dot{R} + \alpha_2 R + \alpha_3 \csc E + \epsilon$$

where ΔR = the difference between the measured range and the true range and the coefficients α_o, α_1, α_2, and α_3 represent the systematic errors described previously and ϵ the random or residual errors.

The following notation is used for the regression equation:

$$\Delta R = a_o + a_1\dot{R} + a_2 R + a_3 \csc E + e$$

where ΔR = the regression estimate of error in range and a_o, a_1, a_2, a_3, and e are estimates of the systematic and random errors.

3.6 CONFIDENCE, TOLERANCE AND PREDICTION REGIONS

The use of accuracy data frequently involves the concepts of confidence, tolerance and prediction regions. Because of the importance of a clear understanding of these concepts to the proper interpretation and use of the data, the following detailed discussion is included as an essential part of the Accuracy Report Methodologies.

3.6.1 ONE - DIMENSIONAL CASE

We define a tolerance interval for a random variable x, in general, as an interval (a,b) which has $100\gamma\%$ probability of containing at least $100\alpha\%$ of the individual values in the population. For example, if $\gamma = .95$ and $\alpha = .99$, we are 95% confident that at least 99% of the individual values will be within the interval (a,b). The value of γ is called the confidence coefficient, while the limits a and b are called tolerance limits. The limits may correspond, for example, to minimum and maximum diameters respectively of circular disks which can be tolerated in some manufacturing process. Before accepting a consignment of such disks, we would like to be almost certain (i.e., γ close to one) that a high percentage (α close to unity) of the items will be acceptable.

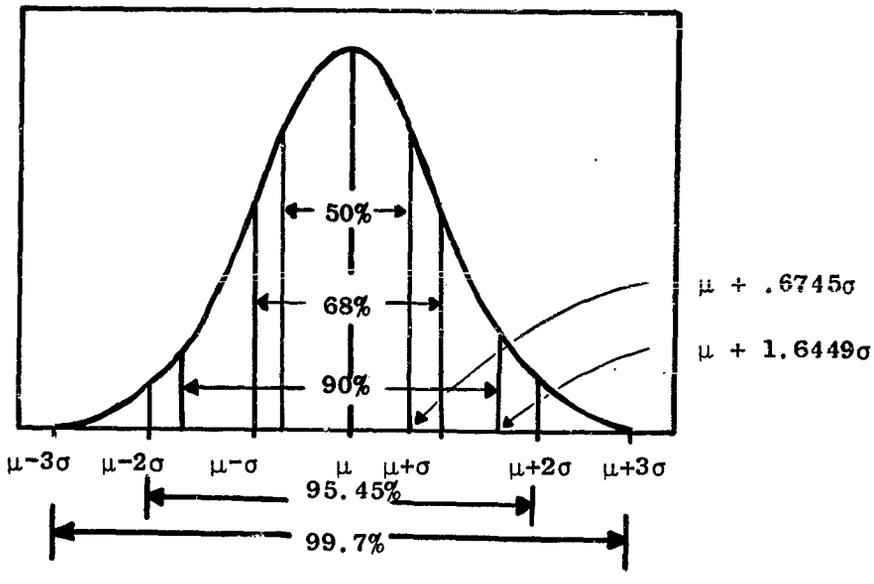
Suppose now that x is a random variable which follows the normal (or Gaussian) distribution with mean μ and standard deviation σ, where μ and σ are temporarily assumed to be known. We can calculate tolerance intervals, of the form $\mu \pm K\sigma$, corresponding to $\gamma = 1$ (i.e., absolute certainty). Values of K corresponding to various values of α are given in Table 3.6.1-1 and illustrated in Figure 3.6.1-1. Values

of K for other values of α may be obtained from tables of the normal distribution, which will be found in any text book on statistical methods.

Table 3.6.1-1 Areas (100α%) Under the Normal Curve Between $\mu \pm K\sigma$

K	α
0.6745	0.5000
0.7979	0.5751
1.0000	0.6827
1.6449	0.9000
2.0000	0.9545
3.0000	0.9973

Figure 3.6.1-1 Areas Under the Normal Probability Curve



The quantity 0.6745σ is called the probable error (PE) of x. It has the property that an observation is just as likely to fall inside as to fall outside the interval $(\mu \pm PE)$. The value of 0.7979σ is called the mean error (ME) of x. It is the mean value of $|x - \mu|$, the absolute difference between x and μ, so that more accurately, the ME should be called the mean absolute error. The value of 1.6449σ is called the map accuracy standard (MAS) of x and is used mainly in connection with location elevations. The number 3σ is sometimes called the "near-certainty" error. The relationships among the various errors are summarized in Table 3.6.1-2.

Table 3.6.1-2 Relations Among Standard, Probable, and Mean Errors

$1\ \sigma = 1.4826\ PE = 1.2533\ ME$
$1\ PE = 0.6745\ \sigma = 0.8453\ ME$
$1\ ME = 0.7979\ \sigma = 1.1830\ PE$

We can also construct an interval, which may be called a prediction interval [Bowker and Lieberman, 1961, page 253], such that it has a pre-assigned probability of enclosing the next observation. Since it is certain ($\gamma = 1$) that 90% of the individual values lie between $\mu \pm 1.6449\sigma$, the probability is 90% that the next observation will fall between $\mu \pm 1.6449\sigma$, and similarly for other multiples of σ. Prediction and tolerance intervals coincide in this case.

3.6.1 ONE - DIMENSIONAL CASE (CONT'D)

If, as is usually the case, the population parameters μ and σ are unknown, they will have to be estimated from a sample $x_1, x_2, \ldots, x_n$ of n observations. Assuming that the n observations are unbiased, uncorrelated, and equally precise, which will be the case if the observations are conceptually a random sample from the same population, the population mean μ and standard deviation σ are estimated by $\bar{x}$ and s, respectively, where

$$\bar{x} = \sum_{i=1}^{n} x_i/n \text{ and } s = \sqrt{\sum_{i=1}^{n} (x - \bar{x})^2 /(n - 1)}. \qquad (3.6.1\text{-}1)$$

Using the sample mean $\bar{x}$ and standard deviation s, we can construct three kinds of intervals, namely, a confidence interval for the true (but unknown) values of the parameters μ and σ of the population, a tolerance interval for the individual values in the population, and a prediction interval for the next observation.

The $100\gamma\%$ confidence interval for μ, say, has a probability of $100\gamma\%$ of containing (or enclosing) the true value of μ. In practice, we will have only one sample of n observations, but in terms of repeated sampling, we can interpret a confidence interval as follows. If we construct a $100\gamma\%$ confidence interval for μ from each of a large number of samples N, with n_i observations in the i-th sample, then approximately $100\gamma\%$ of the N confidence intervals so constructed will in fact include μ; if N is infinite, the proportion of intervals enclosing μ will be exactly γ.

3.6.1 ONE - DIMENSIONAL CASE (CONT'D)

The confidence interval for μ is of the form

$$\bar{x} \pm t\, s/\sqrt{n} \qquad (3.6.1\text{-}2)$$

where t (which follows "Student's" t - distribution) depends on the confidence coefficient γ and on the so-called degrees of freedom ν, which in this context is equal to $(n - 1)$. Values of t for $\gamma = .95$ and .99 are given in Table 3.6.1-3 for selected values of $\nu = n - 1$. More extensive tables are given in the literature, e.g., [Bowker and Lieberman 1961]. For example, from a sample of $n = 20$ observations, the 95% confidence interval for μ is $\bar{x} \pm (2.093)\, s/\sqrt{20}$ or $\bar{x} \pm 0.468s$.

For n greater than about 40, the normal distribution will give a good approximation to the t - distribution. (It can be shown that the t - distribution tends to the normal distribution as $n \to \infty$.) If σ is known, we use it in place of s in equation (3.6.1-2) and take $\nu = \infty$ in getting the t - value, which is equivalent to using the normal distribution table.

Table 3.6.1-3 95% and 99% Points of the t - distribution

Degrees of Freedom (ν)	Confidence Coefficient (γ) 0.95	0.99
10	2.228	3.169
19	2.093	2.861
20	2.086	2.845
30	2.042	2.750
40	2.021	2.704
50	2.009	2.678
60	2.000	2.660
100	1.984	2.626
200	1.972	2.601
∞	1.960	2.576

We can similarly construct a confidence interval for σ, of the form $(k_1 s, k_2 s)$, using the Chi-Square distribution [Bowker and Lieberman, 1961, page 219]. We can also construct a joint confidence region for μ and σ simultaneously [Mood and Graybill, 1963, pages 254-6]. Although, in mathematics, an "interval" is not necessarily restricted to one dimension, we shall use the phrase "confidence region" when dealing with two or more dimensions. If the region so constructed is elliptical, it is often called a confidence ellipse. This ellipse has a preassigned probability $(100\gamma\%)$ of enclosing the true values of μ and σ jointly.

The tolerance interval for the individual values of x in the population is of the form

$$\bar{x} \pm ks, \qquad (3.6.1\text{-}3)$$

With k properly chosen, we are $100\gamma\%$ confident that the above interval will contain at least $100\alpha\%$ of the individual values in the population. With σ unknown, we can have $\gamma = 1$ only if k is infinite. It is incorrect to say that 99.73% of the individual values will lie within $\bar{x} \pm 3s$, because $\bar{x} \neq \mu$ and $s \neq \sigma$. The method for obtaining values of k is complicated, since $\bar{x}$ and s are themselves random variables, so that k depends not only on γ and α but also on the sample size n from which $\bar{x}$ and s have been obtained. Values of k for selected values of n, α, and γ are shown in Table 3.6.1-4, which have been extracted from [Bowker and Lieberman 1961, page 227].

Table 3.6.1-4 Values of k such that $(\bar{x} \pm ks)$ has $100\gamma\%$ probability of including at least $100\alpha\%$ of the individual values in the population.

	γ:	.95			.99		
n	α:	.90	.95	.99	.90	.95	.99
10		2.839	3.379	4.433	3.582	4.265	5.594
20		2.310	2.752	3.615	2.659	3.168	4.161
30		2.140	2.549	3.350	2.385	2.841	3.733
40		2.052	2.445	3.213	2.247	2.677	3.518
50		1.969	2.379	3.126	2.162	2.576	3.385

The table shows, for example, that if $\bar{x}$ and s have been calculated from a sample of n = 20 observations, the probability is 99% (γ = .99) that at least 95% (α = .95) of the individual values in the population will be between $\bar{x} \pm 3.168s$. This should be compared with $\mu \pm 1.96\sigma$, in the case where μ and σ are known. The unjustified use of the familiar factors from the normal distribution, when μ and σ are estimated from a sample, can therefore be quite misleading, even if n is as large as 50. The above tolerance interval of $\bar{x} \pm 3.168s$ should also be compared with the narrower confidence interval $\bar{x} \pm 0.468s$ for μ. This is of course to be expected.

We shall now construct a prediction interval for the next independent observation, after having taken n observations giving $\bar{x}$ and s. If the next observation is denoted by X, say, the quantity $(X - \bar{x})$ is normally distributed with zero mean and variance $(1 + \frac{1}{n})\sigma^2$. It follows from statistical theory that

$$t = \frac{(X - \bar{x})}{s\left(\frac{n+1}{n}\right)^{1/2}} \qquad (3.6.1\text{-}4)$$

has the t - distribution with $\nu = (n - 1)$ degrees of freedom. From the above, we readily get the following prediction interval for X:

$$\bar{x} \pm t\, s\left(\frac{n+1}{n}\right)^{1/2} \qquad (3.6.1\text{-}5)$$

The values of t have previously been given in Table 3.6.1-3 and depend on ν and γ. For example, if $\bar{x}$ and s have been obtained from n = 20 observations, the 95% prediction interval for the next observation is $\bar{x} \pm (2.093)\sqrt{21/20}\, s$ or $\bar{x} \pm 2.145s$, compared to $\bar{x} \pm 0.468s$ (confidence interval for μ) and $\bar{x} \pm 3.168s$ (tolerance interval for at least 95% of the population values, with probability of 0.99 of being correct).

If σ is known but μ is unknown, we replace s in equation (3.6.1-5) by σ and take $\nu = \infty$ in obtaining the value of t. If μ is known and σ is unknown, the prediction interval for the next observation is

$$\mu \pm ts. \qquad (3.6.1\text{-}6)$$

For example, from a sample of n = 20 observations, the probability is 95% that the next observation will lie between $\mu \pm 2.093s$, compared to $\bar{x} \pm 2.145s$ previously obtained.

We stress the distinction among confidence, tolerance, and prediction intervals. The first is an interval for the parameters of the population; the second is an interval for including a given proportion of all the individuals in the population; and the last is for predicting the next (single) observation. If the parameters of the population are known, tolerance and prediction intervals coincide.

3.6.2 TWO - DIMENSIONAL CASE

Let x_1 and x_2 have the bivariate normal distribution with means μ_1, μ_2, variances σ_1^2, σ_2^2, and correlation coefficient ρ. As an example, x_1 may be the distance from some origin in an east-west direction and x_2 may be the distance in a north-south direction. If the origin is the bull's eye in a target board, we may be interested in the distribution of the individual shots around the target center. If $\rho = 0$ and $\sigma_1 = \sigma_2 = \sigma$, say, the variables x_1 and x_2 are said to have the bivariate circular normal distribution, because the contours of the probability density function of x_1 and x_2 are circles. In the general case, the contours are ellipses.

Assume that x_1 and x_2 have the circular normal distribution with σ, μ_1, and μ_2 known. We will construct tolerance circles with (μ_1, μ_2) as center and radius $c\sigma$. These are referred to as contour circles in [Hald 1952] and as probability circles in [Burington and May 1958]. The probability is one that this circle contains $100\alpha\%$ of the individuals in the population, each of which has an x_1- and a x_2- value. This tolerance circle will also be a prediction circle. If another observation is taken, the probability is $100\alpha\%$ that it will fall inside the circle. The values of c for various values of α are shown in Table 3.6.2-1. (The values of c^2 are given by the so-called Chi-Square distribution with 2 degrees of freedom.) More extensive tables are to be found in [DiDonato and Jarnagin 1962] and, less extensively, in [Harter, 1960] and [Burington and May, 1958].

Table 3.6.2-1 Radius of Tolerance Circles

Proportion (α) Contained within Circle	Radius of Circle ($c\sigma$)
.3935	1.0000σ
.5000	1.1774σ = CPE
.5440	1.2533σ = MRE
.8647	2.0000σ
.9000	2.1460σ = CMAS
.9500	2.4477σ
.9889	3.0000σ
.9978	3.5000σ = CNCE

From Table 3.6.2-1, we see that if we take an observation from a circular normal distribution, the probability is 39.35% that it will fall inside a circle, centered at (μ_1, μ_2), with a radius of one σ. Here, σ is sometimes called the circular standard error. The values of 1.1774σ, 1.2533σ, 2.1460σ, and 3.5σ are respectively known as the circular probable error (CPE or sometimes written CEP), mean radial error (MRE), circular map accuracy standard (CMAS), and circular near certainty error (CNCE). The CEP is the <u>median</u> of the distribution of <u>radial</u> errors or 'miss' distances. An observation is just as likely to fall inside as outside the circle with the CEP as the radius. The MRE is the average distance of all observations from the origin. It is not zero as all distances from the origin, regardless of directions, are positive. The relationships among σ, CPE, and MRE are summarized below.

$$\begin{aligned} 1\sigma &= 0.8493\ \text{CPE} = 0.7979\ \text{MRE} \\ 1\text{CPE} &= 1.1774\sigma = 0.9394\ \text{MRE} \\ 1\text{MRE} &= 1.2533\sigma = 1.0645\ \text{CPE} \end{aligned} \qquad (3.6.2\text{-}1)$$

By subtraction, we can obtain the probability of an observation falling within the circular ring between two circles. Thus, the probability is .8647 - .3935 = .4712 that the observation will fall in the annulus between two circles with radii σ and 2σ.

The probability of a point falling within an off-set circle of a specified radius, whose center is at a given distance d from the origin (μ_1, μ_2) is also tabulated in [Di Donato and Jarnagin, 1962] and [Burington and May, 1958, page 102]. This distance d is the bias in the observations. Because of the symmetry of the distribution, the probability does not depend on the location of the circle but only on its distance from the origin. The previous case considered corresponds to d = 0.

In [Burington and May 1958, page 98] tolerance ellipses are given for the general case where $\rho \neq 0$ and $\sigma_x \neq \sigma_y$, where these are all known. With (μ_1, μ_2) as origin, the equation of the tolerance ellipse is

$$\frac{1}{1-\rho^2}\left[(x_1/\sigma_1)^2 - 2\rho\,(x_1/\sigma_1)(x_2/\sigma_2) + (x_2/\sigma_2)^2\right] = c^2 \qquad (3.6.2\text{-}2)$$

where c is given in Table 3.6.2-1. Thus, if $\sigma_1 = 5$, $\sigma_2 = 10$, and $\rho = 0.5$, the 95% tolerance ellipse is given by

$$\frac{4}{3}\left[x_1^2/25 - (x_1\,x_2)/\,50 + x_2^2/\,100\right] = (2.4477)^2. \qquad (3.6.2\text{-}3)$$

The ellipse (3.6.2-3) contains 95% of the population values; equivalently, if one observation is taken from the bivariate population, the probability is 95% that it will fall inside the above ellipse.

If tolerance circles are required in the general case, see [Chew and Boyce 1962]. This reference also gives the mean, median, mode, and standard deviation of the distribution of radial error.

Suppose now, more realistically, that μ_1, μ_2, σ_1, σ_2, and ρ are all unknown and have to be estimated from a sample (x_{11}, x_{12}), (x_{21}, x_{22}), ..., (x_{n1}, x_{n2}) of n observations, each observation being a vector of two elements. The mean μ_1 and the variance σ_1^2 of the random variable x_1 will be estimated from $x_{11}, x_{21}, \ldots, x_{n1}$ in the usual way (equation 3.6.1-1). The estimates will be denoted by $\bar{x}_1$ and s_1^2. We similarly define and obtain $\bar{x}_2$ and s_2^2 from $x_{12}, x_{22}, \ldots, x_{n2}$. The covariance σ_{12} between x_1 and x_2 is defined by $\sigma_{12} = \rho\sigma_1\sigma_2$ and is estimated by

$$s_{12} = \sum_{i=1}^{n} (x_{1i} - \bar{x}_1)(x_{2i} - \bar{x}_2)/(n-1) \qquad (3.6.2\text{-}4)$$

Let

$$S = \begin{bmatrix} s_1^2 & s_{12} \\ s_{12} & s_2^2 \end{bmatrix} \qquad (3.6.2\text{-}5)$$

be the estimate of the true variance - covariance matrix Σ

of x_1 and x_2. Define $\underline{\mu} = (\mu_1, \mu_2)'$ and $\underline{\bar{x}} = (\bar{x}_1, \bar{x}_2)'$, where the prime stands for "transpose". In [Anderson 1958, page 108,] the following confidence ellipse for $\underline{\mu}$ is given:

$$n\,(\underline{\bar{x}} - \underline{m})'\, S^{-1}(\underline{\bar{x}} - \underline{m}) \leq \frac{(n-1)p}{n-p} F_{p,n-p} \qquad (3.6.2\text{-}6)$$

In the above equation, p is the number of dimensions (two, here) and $F_{p,n-p}$ is Fisher's F-distribution with parameters p and (n-p). Its values, depending on p, (n-p), and confidence coefficient γ, have been tabulated. Every quantity in the equation is numerically known, except $\underline{m}$. The above represents the interior and boundary of an ellipse containing all values of $\underline{m}$ satisfying the equation. It is centered at $\underline{\bar{x}} = (\bar{x}_1, \bar{x}_2)$, and its shape and size depend on S and γ. The probability is $100\gamma\%$ that the true $\underline{\mu}$ lies on or within the ellipse.

Confidence Ellipse for $\underline{\mu} = (\mu_1, \mu_2)$.

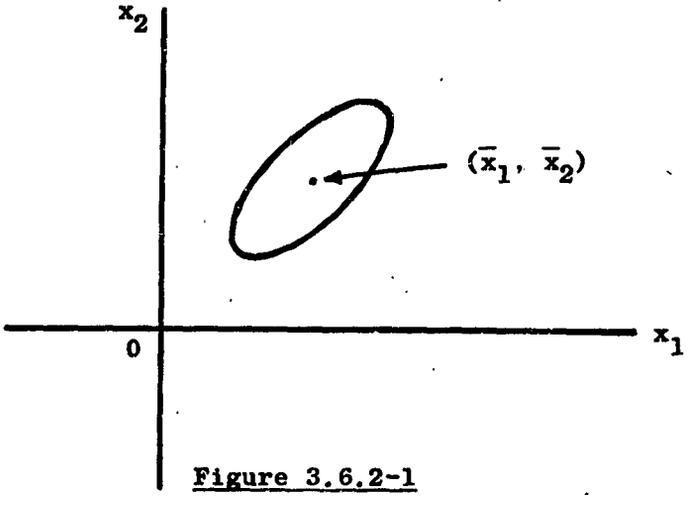


Figure 3.6.2-1

In [Duncan and Ackerson, 1960] the prediction ellipse is given for the next observation $\underline{X}$ in the general case where Σ and $\underline{\mu}$ are unknown. With S and $\underline{\bar{x}}$ defined as before, the prediction ellipse is given by

$$\frac{n}{n+1}(\underline{X} - \underline{\bar{x}})' S^{-1} (\underline{X} - \underline{\bar{x}}) \leq \frac{(n-1)p}{n-p} F_{p,n-p} \quad . \quad (3.6.2\text{-}7)$$

This ellipse is improperly called a tolerance ellipse in the above reference. It does not have $100\lambda\%$ probability of containing at lest $100_\alpha\%$ of the values in the population. For a discussion of tolerance ellipses in the case where μ and Σ are unknown, see [Chew, 1964c].

3.6.3 Three - Dimensional Case

The 3 variables x_1, x_2, and x_3 will be assumed to have the trivariate normal distribution with means μ_1, μ_2, and μ_3; variances σ_1^2, σ_2^2, and σ_3^2; and covariances σ_{12}, σ_{13}, and σ_{23}. Also assume, for the time being, that $\sigma_1 = \sigma_2 = \sigma_3 = \sigma$ and $\sigma_{12} = \sigma_{13} = \sigma_{23} = 0$, in which case we say that x_1, x_2, and x_3 have the spherical normal distribution.

The tolerance region is a sphere, centered at (μ_1, μ_2, μ_3), with radius $C\sigma$, where C^2 is the 100_α percentile of the Chi-Square distribution with 3 degrees of freedom. Recall that in the circular normal distribution, the radius of the tolerance circle is $c\sigma$, where c is the 100_α percentile of the Chi-Square distribution with 2 degrees of freedom.

Values of C are tabulated in statistical text books. The proportions of the population values contained in the tolerance spheres for certain values of the radius $C\sigma$ are given in Table 3.6.3-1. With all parameters known, this tolerance sphere is also the prediction sphere for the next observation; also, $\lambda = 1$ for these tolerance spheres. The values of 1.538σ, and 4.0σ are called the spherical probable error, spherical accuracy standard, and spherical near certainty error respectively.

Table 3.6.3-1 Radii of Tolerance Spheres

Proportion (α) Contained within Sphere	Radius of Sphere ($C\sigma$)
.1990	1.000σ
.5000	1.538σ
.7500	2.027σ
.9000	2.500σ
.9500	2.795σ
.9900	3.368σ
.9989	4.000σ

In the general case where x_1, x_2, and x_3 have known variance-covariance matrix Σ and a known mean vector $\underline{\mu}$, the tolerance ellipsoid given below is certain of containing $100\alpha\%$ of the population values.

$$(\underline{x} - \underline{\mu})' \Sigma^{-1} (\underline{x} - \underline{\mu}) \leq \chi^2_{3d.f.} \qquad (3.6.3\text{-}1)$$

In equation (3.6.3-1), $\chi^2_{3\text{d.f.}}$ is obtained from tables of the Chi-Square distribution with 3 degrees of freedom. The ellipsoid is centered at $\underline{\mu} = (\mu_1, \mu_2, \mu_3)'$. If $\underline{\mu}$ is taken as the origin, this term will drop out from the equation. Equation (3.6.2-2) is a particular case of (3.6.3-1) for two dimensions. This tolerance ellipsoid will also be a prediction ellipsoid.

Finally, if the mean $\underline{\mu}$ and covariance matrix Σ are unknown, they can be estimated from a sample of n vectors of observations $(x_{11}, x_{12}, x_{13}), \ldots, (x_{n1}, x_{n2}, x_{n3})$ as in the two-dimensional case. The confidence ellipsoid for $\underline{\mu}$ will also be given by equation (3.6.2-6), except that p is now equal to three. The prediction ellipsoid will be given similarly by equation (3.6.2-7) with $p = 3$ also. The tolerance ellipsoid in the case of unknown $\underline{\mu}$ and Σ is discussed in [Chew, 1964c].

CHAPTER 4

TECHNIQUES FOR DETERMINING VELOCITY AND ACCELERATION ACCURACIES

At present there is neither direct velocity nor direct acceleration measuring equipment in operation by RCA-MTP on the Eastern Test Range. The basic method for obtaining external velocity and acceleration data is by numerical differentiation of position data (either the original U, V, W data (system coordinates) or the derivative X, Y, Z data). This may be accomplished by the application of digital smoothing (polynomial fitting) or digital frequency filtering techniques. The methods in operation in Data Reduction at ETR are of both types. For many purposes the frequency constrained filters are replacing or have replaced the least squares polynomial filters in many applications. A comparative evaluation between least squares moving arc smoothing techniques and digital filtering based on frequency conditions has been reported by Pavely(1). The frequency constrained filter developed at the ETR is discussed by Gennery(2). The following is a brief outline of polynomial fitting. Further details and applicable charts are given in Appendix I.

Given the position data and corresponding time data

$$U_1, U_2, \ldots, U_n$$

$$t_1, t_2, \ldots, t_n$$

a polynomial of k^{th} degree is fitted by some acceptable criterion to the first m points

$$U_1, U_2, \ldots, U_m$$

$$t_1, t_2, \ldots, t_m$$

---

(1) Pavely, R. F., A Unified Approach to Data Smoothing, Technical Documentary Report MTC-TDR-62-10, June 1962.

(2) Gennery, D. B., An Improved Digital Filter, RCA/MTP Mathematical Services Technical Memo. No. TM-63-8, December 1963.

The first and second derivatives of the polynomial are evaluated at an appropriate time. Then the moving arc technique of fitting the polynomial of k^{th} degree to the data

$$U_2, \ldots, U_{m+1}$$
$$t_2, \ldots, t_{m+1}$$

and evaluating the first and second derivatives is used. This is continued until all desired velocity and acceleration components are computed. In the so called simple differencing method, the degree of the polynomial is unity, and m, the number of points used, is 2. If the data are equispaced in time, that is

$$t_j = t_0 + j(\Delta t)$$

moving average formulas of the form

$$\frac{dU_i}{dt} = \frac{1}{\Delta t} \sum_{j=1}^{m} b_j \; U_{i-j+d}$$

where d is related to the delay (i.e., if m is any odd integer, that is if m = 2n+1 and evaluation is at the mid point d = n+1, if m = 2n+1 and evaluation is at the end point d = m) and

$$\frac{d^2U_i}{dt^2} = \frac{1}{(\Delta t)^2} \sum_{j=1}^{m} c_j \; U_{i-j+d}$$

are available. The b_j and c_j depend on the degree k of the polynomial, the span of points, m, used in the moving average and the number d. The b_j and c_j are fixed constants and they are precomputed.

4.1 CORRELATED DATA

4.1.1 FREE FALL DATA ANALYSIS

Assuming that the observed U, V, W data are serially correlated and processed through smoothing filters in order to obtain velocity data ($\dot{U}$, $\dot{V}$, $\dot{W}$) and acceleration data ($\ddot{U}$, $\ddot{V}$, $\ddot{W}$) then estimates of the error in the derivative data may be obtained as a function of the variance estimate of the random error (correlated plus uncorrelated components) in position. The position error variance which propagates into velocity and acceleration is a composite of the high and low frequency "noise" in the data. This error is perhaps most appropriately described as the total error minus the constant bias error. Constant bias errors in the position data introduce negligible effects in the derivative velocity and acceleration data since by their very nature they tend to disappear in the process of differentiation.* It is the correlated low frequency noise which has the most deleterious effect on the quality of the derivative data since smoothing over spans appreciably shorter than the typical low frequency noise period does little to reduce its influence. The rigorous propagation of correlated errors through any specified smoothing filter requires a knowledge of the autocorrelation function of the

*This does not mean to imply that bias errors in position data do not influence velocity and acceleration information which is obtained in a coordinate system different from that of the derivative data. For example, a constant bias in the observed AZUSA measurement ℓ would not affect the derivative $\dot{\ell}$ or $\ddot{\ell}$ data obtained by numerically differentiating ℓ but would influence Cartesian coordinate velocity and and acceleration information $\dot{X}$ and $\ddot{X}$ if derived from the ℓ, $\dot{\ell}$ and $\ddot{\ell}$ information according to the relationships

$$\dot{X} = r\dot{\ell} + \ell\dot{r}$$

$$\ddot{X} = r\ddot{\ell} + \dot{\ell}\dot{r} + \ell\ddot{r} + \dot{r}\dot{\ell}$$

errors. If the autocorrelation coefficients of lags 0, 1, 2, 3 are 1, P_1, P_2, P_3 . . . , the variance of the value of $\dot{U}$ obtained from the smoothing filter

$$\dot{U}_i = \sum_{j=-m}^{m} b_j \; U_{i+j} \; * \qquad (4.1.1\text{-}1)$$

is given by

$$\sigma^2_{\dot{U}_i} = \sigma^2_U \; b \; R \; b^T \qquad (4.1.1\text{-}2)$$

in which b is the row vector of data multipliers

$$b = (b_{-m} \; b_{-m+1} \; \cdots \; b_{-1} \; b_0 \; b_1 \; \cdots \; b_{m-1} \; b_m)$$

R is the autocorrelation matrix given in (4.1.1-3)

$$\begin{array}{ccccccc} 1 & P_1 & P_2 & P_3 & \cdots & P_{2m} \\ P_1 & 1 & P_1 & P_2 & \cdots & P_{2m-1} \\ P_2 & P_1 & 1 & P_1 & \cdots & P_{2m-2} \\ P_3 & P_2 & P_1 & 1 & \cdots & P_{2m-3} \\ \cdot & \cdot & \cdot & \cdot & & \cdot \\ \cdot & \cdot & \cdot & \cdot & & \cdot \\ \cdot & \cdot & \cdot & \cdot & & \cdot \\ P_{2m} & P_{2m-1} & P_{2m-2} & P_{2m-3} & & 1 \end{array}$$

---

*By setting t = 0 at the i^{th} measurement the expressions given previously for $\frac{dU_i}{dt}$ and $\frac{d^2U_i}{dt^2}$ may be written as (4.1.1-1) and (4.1.1-4).

and σ_U^2 is the variance of U_i.

Similarly, the variance of $\ddot{U}$ obtained from the smoothing filter

$$\ddot{U}_i = \sum_{j=-m}^{m} c_j \; U_{i+j} \qquad (4.1.1\text{-}4)$$

is given by

$$\sigma_{\ddot{U}}^2 = \sigma_U^2 \; c \; R \; c^T \qquad (4.1.1\text{-}5)$$

in which c is the row vector of data multipliers

$$c = (c_{-m} \; c_{-m+1} \cdots c_{-1} \; c_0 \; c_1 \cdots c_{m-1} \; c_m),$$

R is the autocorrelation matrix given in (4.1.1-3)

An estimate of the autocorrelation function is best obtained from the residuals about a free fall ellipse (Keplerian ellipse) fitted to a long span (preferably 100 to 200 seconds) of post burnout data. The autocorrelation function may be obtained from the power spectrum analysis computer program.

Velocity error estimates are also obtained directly from free fall data by the following method. Position parameters are fit to a Taylor series expansion of the equations of motion truncated at the fourth power. Associated with the fit are Keplerian rates. The differences between Keplerian rates and the tracking system derived rates are used to estimate the rate variances.

4.1.2 POWERED FLIGHT DATA ANALYSIS

Velocity error estimates for powered flight data are obtained directly by comparing the velocity data derived from the tracking system's position data with inertial guidance velocity data. As pointed out in Section 3.1.2, inertial guidance data are subject to long term drift errors and very low frequency errors (errors below .05 cycles per second) whereas the data from external tracking systems are subject to errors in the high frequency and low frequency regions (errors above .05 cycles per second) but exhibit good characteristics in the very low frequency or near zero frequency region. It is by virtue of the fact that these differences exist in the frequency characteristics of the two systems (Inertial Guidance and External Tracking) that the Inertial Guidance data may be used as a standard for noise estimation in the external data and the external data in turn as a standard for estimation of long term drifts or biases in the Inertial Guidance data [Pitman, 1962, Chapter 13].

4.2 UNCORRELATED DATA

If it may be assumed that errors in successive values of U_j are uncorrelated and that a polynomial of k^{th} degree approximates the data to a sufficient degree of accuracy over a span of m points, then the variance of the value of $\dot{U}$ obtained from the smoothing filter

$$\dot{U} = \frac{1}{\Delta t} \sum_{j=1}^{m} b_j \, U_{i-j+d} \qquad (4.2\text{-}1)$$

is given by

$$\sigma_{\dot{U}} = \frac{\sigma_U}{\Delta t} \left(\sum_{j=1}^{m} b_j^2 \right)^{1/2} \qquad (4.2\text{-}2)$$

and the standard deviation of the value of $\ddot{U}$ obtained from the smoothing filter

$$\ddot{U} = \frac{1}{(\Delta t)^2} \sum_{j=1}^{m} c_j \, U_{i-j+d} \qquad (4.2\text{-}3)$$

may be expressed as

$$\sigma_{\ddot{U}} = \frac{\sigma_U}{(\Delta t)^2} \left(\sum_{j=1}^{m} c_j^2 \right)^{1/2} \qquad (4.2\text{-}4)$$

The relation between the random errors in velocity and acceleration data and the random errors in position data can be obtained for various values of m, the spread of points used in the curve fitting, and the value k, the degree of the polynomial that fits the data. For example, in the case of midpoint smoothing, equation (4.2-2) becomes for a second degree polynomial fit

$$\sigma_{\dot{U}} = \frac{\sigma_U}{\Delta t} \sqrt{\frac{12}{m(m^2-1)}} \approx \frac{\sigma_U \sqrt{12}}{(\Delta tm)\sqrt{m}} \quad (4.2\text{-}5)$$

and equation (3.7.2-4) becomes for a second and third degree fit

$$\sigma_{\ddot{U}} = \frac{\sigma_U}{(\Delta t)^2} \sqrt{\frac{720}{m(m^2-1)(m^2-4)}} \approx \frac{\sigma_U \sqrt{720}}{(\Delta tm)^2 \sqrt{m}} \quad (4.2\text{-}6)$$

It is evident from the approximations that if the sampling rate is stepped up and the smoothing time span (Δtm) held constant, the velocity and acceleration errors are reduced approximately by a factor of $m^{-1/2}$. Truncation errors limit the extent to which this can be applied.

Figure A1-1, Appendix I gives the relation between σ_U and $\sigma_{\dot{U}}$ for k = 2 and smoothing in velocity determinations obtained by using a span of 2n+1 points and evaluating at points other than the mid point, for the case where U can be expressed as a quadratic function of time and the errors in U are uncorrelated. (Mathematically, it is a plot of the radical in equation 4.2-5). For example, if a span of 21 points is used and evaluation of the derivative is at the mid point, it is seen from the graph that

$$\frac{\sigma_{\dot{U}} \Delta t}{\sigma_U} = .036$$

so if σ_U = 5 ft and $\Delta t = \frac{1}{10}$ sec.,

$$\sigma_{\dot{U}} = 1.8 \text{ ft./sec.}$$

Likewise, if a span of 37 points is used and evaluation of the derivative is made at the 26th point or 7 points from the mid point

$$\frac{\sigma_{\dot{U}} \ \Delta t}{\sigma_U} = .028$$

and if again $\sigma_U = 5$ ft. and $\Delta t = \frac{1}{10}$ sec.,

$$\sigma_{\dot{U}} = 1.4 \text{ ft/sec.}$$

Curves for higher degree polynomial fits for both velocity and acceleration errors are given in Figures A1-2 to A1-6 Appendix I.

CHAPTER 5
ERROR PROPAGATION

If a tracking instrument, or a set of tracking instruments, measures a set of quantities $y_1, y_2, \ldots, y_n$ (which we shall call the measured parameters), then it is common practice to attempt to assess the magnitude of the errors associated with the measured parameters, as well as correlations between these errors. This error evaluation may take the form of a comparison with another tracking system which is used as a standard, or a statistical study of the data obtained from the system. It is customary to display the error estimates thus obtained in the form of a square array of numbers, which is termed the covariance matrix of the set of measured parameters $y_1, y_2, \ldots, y_n$. (A formal definition of this concept will be presented later.)

The covariance matrix of the measurements, then, is a set of numbers which describes the size and interdependence of the associated errors. Many questions which might be raised about the accuracy of the system under consideration can, indeed, be answered by examination of the elements of this array. However, other important questions concerning accuracy cannot be answered by an examination of the covariance matrix. For example the quantities of interest are frequently the coordinates of the target in some specified rectangular coordinate system, or perhaps the velocities or accelerations of these coordinates. Information about the errors in these coordinates is not available from inspection of the covariance matrix of the measured parameters. We are, of course, assuming that mathematical relations exist such that the desired coordinates may be calculated from the set of measured parameters $y_1, y_2, \ldots, y_n$. Error propagation is the term applied to the theory and technique of the utilization of these

mathematical relations, together with the covariance matrix of the measured parameters, with the object of obtaining an estimate of the covariance matrix of the desired quantities, in this case the coordinates. This, then, is the basic problem of error analysis: Given a set of measurements $y_1, y_2, \ldots, y_n$, and an associated covariance matrix, we wish to obtain an estimate of the covariance matrix of some set of desired quantities $x_1, x_2, \ldots, x_k$. We assume that mathematical relations exist such that the x's may be found or approximated knowing the y's. It is in the use of these mathematical relations that the geometry of the situation (geometrical relations between the target and tracker or trackers) becomes involved and influences the final result, namely, the covariance matrix of the x's. Thus, the result is solely determined by two factors. The first is the nature of the errors in the measured parameters, which is given quantitative form in the covariance matrix. The second is what might well be termed the "total geometry" of the situation, which involves the geometric character of the measurements, location of tracking site or sites, location of target, etc. This second factor, as we shall see, is given quantitative form in terms of certain partial derivatives, which in turn depend upon the mathematical relations between the y's and the x's.

The term "geometric dilution of precision," commonly referred to as GDOP, is related to the effect of this second factor upon the covariance matrix of the desired quantities. If we hold the covariance matrix of the y's fixed, we often note drastic changes in the covariance matrix of the x's due to changes in geometry.

As a very simple example of this phenomenon we might consider a point in space determined by a single radar measuring R, A, and E, and another point (along the same ray) with associated measurement 3R, A, and E. For given errors of measurement ΔR, ΔA, and ΔE, the position error of the second point will clearly be much greater than that of the first point, and this larger error will be reflected in the covariance matrix results were we to propagate from R, A, and E to some x, y, z coordinate system.

5.1 ERROR PROPAGATION IN THE JUST-DETERMINED CASE

By the just-determined case we denote that situation wherein the number of parameters measured by the instrumentation is just sufficient to determine the desired quantities, say the target's position and/or velocity. This is distinct from the redundant, or over-determined, case, in which more measurements are available than are mathematically necessary for the determination of the desired parameters.

The basic tool in the just-determined case is the so-called "Law of Covariance Propagation." We shall see how this relation utilizes the two factors mentioned in the introduction, namely, the "total geometry" of the tracking situation, and the covariance matrix of the measured parameters. We shall sketch a proof of this relation.

We approach the proof by using the "expectation" concept discussed in any text on mathematical statistics.

Let x be a continuous random variable with probability density function p(x). The "expectation" of x is defined as

$$E(x) = \int_{-\infty}^{+\infty} x\, p(x)\, d\, x$$

This is often described as the true, or population, mean and shall be denoted by μ. We note that if a is a constant,

$$E(a) = \int_{-\infty}^{+\infty} a\, p(x)\, d\, x = a$$

We further define, if y = f(x),

$$E(y) = E\left[f(x)\right] = \int_{-\infty}^{+\infty} f(x)\ p(x)\ d\,x.$$

From these definitions, we note the following properties

$$E\left[f(x) + g(x)\right] = E\left[f(x)\right] + E\left[g(x)\right] \qquad 5.1\text{-}1$$

$$E\left[a\ f(x)\right] = a\ E\left[f(x)\right]. \qquad 5.1\text{-}2$$

Letting $f(x) = (x-\mu)^k$, we have

$$E(x-\mu)^k = \int_{-\infty}^{+\infty} (x-\mu)^k\ p(x)\ d\,x.$$

This particular function is called the k^{th} moment of x about its mean. The second moment about the mean is called the variance, i.e.

$$\text{var}\ \ x = \sigma_x^2 = E(x-\mu)^2 = \int_{-\infty}^{+\infty} (x-\mu)^2\ p(x)\ d\,x$$

This is clearly a measure of the dispersion of x about its mean. Applying 5.1-1 and 5.1-2, we have

$$\begin{aligned}\sigma_x^2 &= E(x-\mu)^2 \\ &= E\left[x^2 - 2\mu\ x + \mu^2\right] \\ &= E(x^2) - 2\ \mu\ E(x) + \mu^2 \qquad 5.1\text{-}3 \\ &= E(x^2) - 2\mu^2 + \mu^2 \\ &= E(x^2) - \mu^2\end{aligned}$$

Considering now two random variables x_1 and x_2, we define

$$\text{cov}\ \ (x_1, x_2) = \sigma_{x_1\ x_2} = E\left[(x_1-\mu_1)\ (x_2-\mu_2)\right]$$

$$E\,(x_i-\mu_1)(x_2-\mu_2) = \int_{-\infty}^{+\infty}\int_{-\infty}^{+\infty} (x_1-\mu_1)(x_2-\mu_2)p(x_1,x_2)d_{x_1}d_{x_2}$$

where $p(x_1,x_2)$ is the joint probability density function of x_1 and x_2. We note that

$$\begin{aligned}\sigma_{x_1x_2} &= E\left[x_1x_2 - x_1\mu_2 - \mu_1x_2 + \mu_1\mu_2\right] \\ &= E(x_1x_2) - \mu_1\mu_2 - \mu_1\mu_2 + u_1u_2 \qquad 5.1\text{-}4 \\ &= E(x_1x_2) - \mu_1\mu_2\end{aligned}$$

We now consider the variances of certain simple functions.

(A) $y = a_o + a_1x.$

(We note that $E(y) = E(a_o + a_1x) = a_o + a_1\mu.$)

Using 5.1-3,

$$\begin{aligned}\sigma_y^2 &= E(y^2) - \left[E(y)\right]^2 \\ &= E\left[a_o^2 + 2a_oa_1x + a_1^2x^2\right] - (a_o^2 + 2a_oa_1\mu + a_1^2\mu^2) \\ &= a_o^2 + 2a_oa_1\mu + a_1^2\,E(x^2) - a_o^2 - 2a_oa_1\mu - a_1^2\mu^2 \\ &= a_1^2\left[E(x^2) - \mu^2\right] \\ &= a_1^2\,\sigma_x^2\end{aligned}$$

(B) $y = f(x).$

By analogy with (A), if $y = f(x)$ is approximated in the neighborhood of $x = x_o$ by the first two terms of a Taylor

series,

$$y \approx f(x_o) + \frac{df}{dx_o}(x-x_o). \quad \text{Then}$$

$$\sigma_y^2 \approx \left(\frac{df}{dx_o}\right)^2 \sigma_x^2.$$

(C) $$y = a_o + a_1x_1 + a_2x_2$$

We first note that

$$E(y) = E(a_o) + a_1E(x_1) + a_2E(x_2)$$

$$= a_o + a_1\mu_1 + a_2\mu_2$$

Using 5.1-3,

$$\sigma_y^2 = E(y^2) - \mu_y^2$$

$$= E\left[(a_o + a_1x_1 + a_2x_2)^2\right]$$

$$- (a_o + a_1\mu_1 + a_2\mu_2)^2$$

$$= E\left[a_o^2 + 2a_oa_1x_1 + a_1^2x_1^2 + 2a_oa_2x_2 + 2a_1a_2x_1x_2 + a_2^2x_2^2\right]$$

$$-\left[a_o^2 + 2a_oa_1\mu_1 + a_1^2\mu_1^2 + 2a_oa_2\mu_2 + 2a_1a_2\mu_1\mu_2 + a_2^2\mu_2^2\right]$$

$$= E\left[a_1^2x_1^2 + 2a_1a_2x_1x_2 + a_2^2x_2^2\right]$$

$$-\left[a_1^2\mu_1^2 + 2a_1a_2\mu_1\mu_2 + a_2^2\mu_2^2\right]$$

$$= a_1^2\left[E(x_1^2) - \mu_1^2\right] + a_2^2\left[E(x_2^2) - \mu_2^2\right]$$

$$+ 2a_1a_2\left[E(x_1x_2) - \mu_1\mu_2\right]$$

Using 5.1-3 and 5.1-4, this reduces to

$$\sigma_y^2 = a_1^2\sigma_{x_1}^2 + a_2^2\sigma_{x_2}^2 + 2a_1a_2\,\sigma_{x_1x_2} .$$

(D) $\qquad y = f(x_1, x_2)$

By analogy with the step from (A) to (B), if the relation $y = f(x_1, x_2)$ is approximated by

$$y \approx f(x_1^o, x_2^o) + \frac{\partial f}{\partial x_1}\bigg|_o (x_1 - x_1^o) + \frac{\partial f}{\partial x_2}\bigg|_o (x_2 - x_2^o),$$

then this is of the form (C) and $\therefore$

the result is

$$\sigma_y^2 \approx \left(\frac{\partial f}{\partial x_1}\right)^2 \sigma_{x_1}^2 + \left(\frac{\partial f}{\partial x_2}\right)^2 \sigma_{x_2}^2 + 2\,\frac{\partial f}{\partial x_1}\,\frac{\partial f}{\partial x_2}\,\sigma_{x_1x_2} \qquad 5.1\text{-}5$$

Relation 5.1-5 may be expressed in matrix form as follows:

$$\sigma_y^2 = B\,S_x\,B^T, \qquad \text{where}$$

$$B = \left[\frac{\partial y}{\partial x_1} \quad \frac{\partial y}{\partial x_2}\right],$$

$$S_x = \begin{bmatrix} \sigma^2_{x_1} & \sigma_{x_1x_2} \\ \sigma_{x_1x_2} & \sigma^2_{x_2} \end{bmatrix},$$

and B^T is the transpose of B.

We now define the covariance matrix of the set of variables $x_1, x_2, \ldots, x_n$.

$$S_x = \begin{bmatrix} \sigma^2_{x_1} & \sigma_{x_1x_2} & \cdots & \sigma_{x_1x_n} \\ \sigma_{x_2x_1} & \sigma^2_{x_2} & \cdots & \sigma_{x_2x_n} \\ \vdots & & & \\ \sigma_{x_nx_1} & \sigma_{x_nx_2} & \cdots & \sigma^2_{x_n} \end{bmatrix} \qquad 5.1\text{-}6$$

We note that this is a symmetric matrix, since from the definitions it follows that $\sigma_{x_ix_j} = \sigma_{x_jx_i}$

Suppose now that we have a set $y_1, y_2, \ldots, y_m$, where each y_i is a function of the n variables $x_1, x_2, \ldots x_n$, i.e., $y_i = y_i(x_1, x_2, \ldots, x_n)$, $i = 1, 2, \ldots, m$.

5.1 ERROR PROPAGATION IN THE JUST-DETERMINED CASE (CONT'D)

We are now in a position to state the law of covariance propagation. Using considerations entirely similar (but more complicated) to those leading to equation (5.1-5), it may be established that

$$S_y = B\, S_x\, B^T. \qquad 5.1\text{-}7$$

Here S_x and S_y are as described in 5.1-6. B is a matrix of partial derivatives defined as follows.

$$B = \begin{bmatrix} \frac{\partial y_1}{\partial x_1} & \frac{\partial y_1}{\partial x_2} & \cdots & \frac{\partial y_1}{\partial x_n} \\ \frac{\partial y_2}{\partial x_1} & \frac{\partial y_2}{\partial x_2} & \cdots & \frac{\partial y_2}{\partial x_n} \\ \vdots & & & \\ \frac{\partial y_m}{\partial x_1} & \frac{\partial y_m}{\partial x_2} & \cdots & \frac{\partial y_m}{\partial x_n} \end{bmatrix}$$

An important special case of equation (5.1-7) arises when S_x is a diagonal matrix, i.e., when terms of the form $\sigma_{x_i x_j}$ are zero for all $i \neq j$. Another way of stating this is to say that the errors in the x's are uncorrelated. In this case we have

$$\sigma_{y_i y_j} = \frac{\partial y_i}{\partial x_1}\frac{\partial y_j}{\partial x_1}\,\sigma^2_{x_1} + \frac{\partial y_i}{\partial x_2}\frac{\partial y_j}{\partial x_2}\,\sigma^2_{x_2} + \ldots + \frac{\partial y_i}{\partial x_n}\frac{\partial y_j}{\partial x_n}\,\sigma^2_{x_n}, \qquad 5.1\text{-}8$$

and if $y_i = y_j$ we have

$$\sigma_{y_i y_i} = \sigma^2_{y_i} = \left(\frac{\partial y_i}{\partial x_1}\right)^2 \sigma^2_{x_1} + \left(\frac{\partial y_i}{\partial x_2}\right)^2 \sigma^2_{x_2} + \ldots + \left(\frac{\partial y_i}{\partial x_n}\right)^2 \sigma^2_{x_n} \qquad 5.1\text{-}9$$

Relation (5.1-9) is often described as the Gaussian Law of Error Propagation.

We note that m is not, in general, equal to n, and that B is not a square matrix. S_y and S_x will always be both square and symmetric.

As we have seen, relation (5.1-7) is based directly upon approximating the change in the dependent variable by the differential, i.e., the first degree term in the Taylor expansion. Hence, a certain degree of inexactness is inherent in the relation except, of course, for linear functions. However, Tukey [Tukey, 1957] examines this classic relation and reports: "The most important conclusion is that the classical propagation formula is much better than seems to be usually realized. Examples indicate that it is quite likely to suffice for most work."

5.1.1 PROPAGATION OF ERRORS IN POSITION

The basic problem is to determine the effect of the errors of measurement in the instrumental observations - angle, direction cosines, film coordinates, range sums, range differences, etc. on the rectangular coordinate data. The error in the observed U, V, W coordinate data which propagates into the X, Y, Z position coordinate data is the total error which may have been determined by methods outlined in Chapter 3.

As pointed out previously, Chapter 3, the variances of the bias errors arise from analysis of many tests at the same point in space on similar trajectories and, hence, may be treated in a random fashion. Thus, total error comprised of random and systematic (bias) components may be propagated as a single error.

As an example, the following equations present the relationship between space position data and the basic measurements for a radar system.

1. The measured quantities are:
   Slant Range (R)
   Azimuth Angle (A)
   Elevation Angle (E)

2. Space position data X, Y, Z are obtained by:
   $X = R \cos A \cos E$
   $Y = R \sin A \cos E$
   $Z = R \sin E$

3. Errors may exist singly in one of the coordinates R, A, or E or simultaneously in R, A and E. With the

relationships listed in 2, the effects of these errors upon the space position data may be expanded. For example, if errors exist simultaneously in R, A, E:

$$\Delta X = \Delta R \cos E \cos A - R\,\Delta A \cos E \sin A - R\,\Delta E \sin E \cos A$$
$$\Delta Y = \Delta R \cos E \sin A + R\,\Delta A \cos E \cos A - R\,\Delta E \sin E \sin A$$
$$\Delta Z = \Delta R \sin E + R\,\Delta E \cos E$$

Assuming the errors in R, A and E are independent (zero cross-correlation) the GDOP's for a radar according to the Gaussian Law of Error Propagation equation (5.1-9) Section 5.1 may be expressed as:

$$\sigma_X^2 = \left(\frac{\partial X}{\partial R}\right)^2 \sigma_R^2 + \left(\frac{\partial X}{\partial A}\right)^2 \sigma_A^2 + \left(\frac{\partial X}{\partial E}\right)^2 \sigma_E^2$$

$$= (\sigma_R^2 \cos^2 A \cos^2 E + \sigma_E^2 R^2 \cos^2 A \sin^2 E + \sigma_A^2 R^2 \sin^2 A \cos^2 E)$$

$$\sigma_Y^2 = \left(\frac{\partial Y}{\partial R}\right)^2 \sigma_R^2 + \left(\frac{\partial Y}{\partial A}\right)^2 \sigma_A^2 + \left(\frac{\partial Y}{\partial E}\right)^2 \sigma_E^2$$

$$= (\sigma_R^2 \sin^2 A \cos^2 E + \sigma_A^2 R^2 \cos^2 A \cos^2 E + \sigma_E^2 R^2 \sin^2 A \sin^2 E)$$

$$\sigma_Z^2 = \left(\frac{\partial Z}{\partial R}\right)^2 \sigma_R^2 + \left(\frac{\partial Z}{\partial A}\right)^2 \sigma_A^2 + \left(\frac{\partial Z}{\partial E}\right)^2 \sigma_E^2$$

$$= (\sigma_R^2 \sin^2 E + \sigma_E^2 R^2 \cos^2 E)$$

$$\sigma_{XY} = \left(\frac{\partial X}{\partial R}\right)\left(\frac{\partial Y}{\partial R}\right) \sigma_R^2 + \left(\frac{\partial X}{\partial A}\right)\left(\frac{\partial Y}{\partial A}\right) \sigma_A^2 + \left(\frac{\partial X}{\partial E}\right)\left(\frac{\partial Y}{\partial E}\right) \sigma_E^2$$

5.1.1 PROPAGATION OF ERRORS IN POSITION (CONT'D)

$$\sigma_{XY} = (\cos A \sin A \cos^2 E)\,\sigma_R^2 - (R^2 \cos E^2 \sin A \cos A)\sigma_A^2 + (R^2 \cos A \sin^2 E \sin A)\sigma_E^2$$

$$\sigma_{XZ} = \left(\frac{\partial X}{\partial R}\right)\left(\frac{\partial Z}{\partial R}\right)\sigma_R^2 + \left(\frac{\partial X}{\partial A}\right)\left(\frac{\partial Z}{\partial A}\right)\sigma_A^2 + \left(\frac{\partial X}{\partial E}\right)\left(\frac{\partial Z}{\partial E}\right)\sigma_E^2$$

$$\sigma_{XZ} = (\cos A \cos E \sin E)\,\sigma_R^2 - (R^2 \cos A \sin E \cos E)\,\sigma_E^2$$

$$\sigma_{YZ} = \left(\frac{\partial Y}{\partial R}\right)\left(\frac{\partial Z}{\partial R}\right)\sigma_R^2 + \left(\frac{\partial Y}{\partial A}\right)\left(\frac{\partial Z}{\partial A}\right)\sigma_A^2 + \left(\frac{\partial Y}{\partial E}\right)\left(\frac{\partial Z}{\partial E}\right)\sigma_E^2$$

$$\sigma_{YZ} = (\sin A \cos E \sin E)\,\sigma_R^2 - (R^2 \sin A \sin E \cos E)\sigma_E^2$$

σ_X^2, σ_Y^2, σ_Z^2 - Variance Terms

σ_{XY}, σ_{XZ}, σ_{YZ} - Covariance Terms

Hence, given the points (R, A, E) and estimates of the total error σ_R, σ_A, σ_E, estimates of σ_X, σ_Y, σ_Z, the total errors in X, Y, Z can be obtained.

If for some reason it is desired to estimate the effect of one component of the total error then the previous equations hold with the σ_A, σ_R, σ_E estimates of error representing that component of the total error.

A similar set of equations hold for the AZUSA position error GDOP. The standard AZUSA equations are:

$$x = r\ell$$
$$y = rm \qquad \text{where } n = \sqrt{1 - \ell^2 - m^2}$$
$$z = rn$$

The GDOP's for AZUSA thus become:

$$\sigma_x^2 = \left(\frac{\partial x}{\partial r}\right)^2 \sigma_r^2 + \left(\frac{\partial x}{\partial \ell}\right)^2 \sigma_\ell^2 + \left(\frac{\partial x}{\partial m}\right)^2 \sigma_m^2$$
$$= \ell^2 \sigma_r^2 + r^2 \sigma_\ell^2$$

$$\sigma_y^2 = \left(\frac{\partial y}{\partial r}\right)^2 \sigma_r^2 + \left(\frac{\partial y}{\partial \ell}\right)^2 \partial\ell^2 + \left(\frac{\partial y}{\partial m}\right)^2 \sigma_m^2$$
$$= m^2 \sigma_r^2 + r^2 \sigma_m^2$$

$$\sigma_z^2 = \left(\frac{\partial z}{\partial r}\right)^2 \sigma_r^2 + \left(\frac{\partial z}{\partial \ell}\right)^2 \sigma_\ell^2 + \left(\frac{\partial z}{\partial m}\right)^2 \sigma_m^2$$
$$= n^2 \sigma_r^2 + \left(\frac{r\ell}{n}\right)^2 \sigma_\ell^2 + \left(\frac{rm}{n}\right)^2 \sigma_m^2$$

$$\sigma_{xy} = \left(\frac{\partial x}{\partial r}\right)\left(\frac{\partial y}{\partial r}\right) \sigma_r^2 + \left(\frac{\partial x}{\partial \ell}\right)\left(\frac{\partial y}{\partial \ell}\right) \sigma_\ell^2 + \left(\frac{\partial x}{\partial m}\right)\left(\frac{\partial y}{\partial m}\right) \sigma_m^2$$
$$= \ell m \sigma_r^2$$

$$\sigma_{xz} = \left(\frac{\partial x}{\partial r}\right)\left(\frac{\partial z}{\partial r}\right) \sigma_r^2 + \left(\frac{\partial x}{\partial \ell}\right)\left(\frac{\partial z}{\partial \ell}\right) \sigma_\ell^2 + \left(\frac{\partial x}{\partial m}\right)\left(\frac{\partial z}{\partial m}\right) \sigma_m^2$$
$$= \ell n \sigma_r^2 - \left(r \frac{\ell r}{n}\right) \sigma_\ell^2$$

$$\sigma_{yz} = \left(\frac{\partial y}{\partial r}\right)\left(\frac{\partial z}{\partial r}\right) \sigma_r^2 + \left(\frac{\partial y}{\partial \ell}\right)\left(\frac{\partial z}{\partial \ell}\right) \sigma_\ell^2 + \left(\frac{\partial y}{\partial m}\right)\left(\frac{\partial z}{\partial m}\right) \sigma_m^2$$
$$= mn \sigma_r^2 - \left(r \frac{mr}{n}\right) \sigma_m^2$$

5.1.1 PROPAGATION OF ERRORS IN POSITION (CONT'D)

The standard deviation arising from the total errors may then be used to judge the expected accuracy of the reduced position data. However, care must be employed in the interpretation of these standard deviations. If the distribution of the errors of the derived position coordinates were normal, then probability statements (such as "68% of the time the error in y will be less than σ_y in absolute value) may be made concerning the errors. Since the distributions (see [Chew 1964a]) are in general not normal, no such statements may be made with certainty.

It is sometimes desired to estimate the errors in the original observations (σ_U, σ_V, σ_W) when error estimates for the reduced data are specified.

Both the variance and covariance estimates of error for the X, Y, Z data must be known in order to accomplish the task.

$$U = f(X, Y, Z)$$

Since X, Y, Z are dependent the general expression for the GDOP is:

$$\sigma_U^2 = \left(\frac{\partial U}{\partial X}\right)^2 \sigma_X^2 + \left(\frac{\partial U}{\partial Y}\right)^2 \sigma_Y^2 + \left(\frac{\partial U}{\partial Z}\right)^2 \sigma_Z^2$$

$$+ 2\left(\frac{\partial U}{\partial X}\right)\left(\frac{\partial U}{\partial Y}\right)\sigma_{XY} + 2\left(\frac{\partial U}{\partial X}\right)\left(\frac{\partial U}{\partial Z}\right)\sigma_{XZ} + 2\left(\frac{\partial U}{\partial Y}\right)\left(\frac{\partial U}{\partial Z}\right)\sigma_{YZ}$$

5.1.2 PROPAGATION OF ERRORS IN VELOCITY AND ACCELERATION DATA

When cartesian coordinate velocity and acceleration information is obtained by determining the first and second time derivatives of position information in the coordinate system of the observation and then transforming this information into cartesian coordinates, estimates of the total error in position and acceleration information in cartesian coordinates are found by utilizing error propagation techniques. If, on the other hand, the U, V, W position data are transformed to X, Y, Z cartesian position data and then smoothed to obtain velocity and acceleration information, direct methods of estimating the error in the velocity and acceleration data are utilized and error propagation techniques are not required. Both methods of determining cartesian coordinate velocity and acceleration information are employed at ETR.

5.1.2.1 PROPAGATION OF ERRORS IN VELOCITY DATA

The total errors in velocity in cartesian coordinates may be found by differentiating the X, Y, Z equations with respect to time and utilizing the approximation equations (5.1-8) and (5.1-9), Section 5.1.

$$\dot{X},\ \dot{Y},\ \dot{Z} = f\ (U,\ V,\ W,\ \dot{U},\ \dot{V},\ \dot{W}) \qquad (5.1.2.1\text{-}1)$$

The variance terms $\sigma^2_{\dot{X}}$, $\sigma^2_{\dot{Y}}$, $\sigma^2_{\dot{Z}}$ may be written as:

$$\sigma^2_{\dot{X}} = \left(\frac{\partial \dot{X}}{\partial U}\right)^2 \sigma^2_U + \left(\frac{\partial \dot{X}}{\partial V}\right)^2 \sigma^2_V + \left(\frac{\partial \dot{X}}{\partial W}\right)^2 \sigma^2_W + \left(\frac{\partial \dot{X}}{\partial \dot{U}}\right)^2 \sigma^2_{\dot{U}} + \left(\frac{\partial \dot{X}}{\partial \dot{V}}\right)^2 \sigma^2_{\dot{V}} + \left(\frac{\partial \dot{X}}{\partial \dot{W}}\right)^2 \sigma^2_{\dot{W}} \qquad (5.1.2.1\text{-}2)$$

$$\sigma_{\dot{Y}}^2 = \left(\frac{\partial \dot{Y}}{\partial U}\right)^2 \sigma_U^2 + \left(\frac{\partial \dot{Y}}{\partial V}\right)^2 \sigma_V^2 + \left(\frac{\partial \dot{Y}}{\partial W}\right)^2 \sigma_W^2 + \left(\frac{\partial \dot{Y}}{\partial \dot{U}}\right)^2 \sigma_{\dot{U}}^2 + \left(\frac{\partial \dot{Y}}{\partial \dot{V}}\right)^2 \sigma_{\dot{V}}^2 + \left(\frac{\partial \dot{Y}}{\partial \dot{W}}\right)^2 \sigma_{\dot{W}}^2 \qquad (5.1.2.1\text{-}3)$$

$$\sigma_{\dot{Z}}^2 = \left(\frac{\partial \dot{Z}}{\partial U}\right)^2 \sigma_U^2 + \left(\frac{\partial \dot{Z}}{\partial V}\right)^2 \sigma_V^2 + \left(\frac{\partial \dot{Z}}{\partial W}\right)^2 \sigma_W^2 + \left(\frac{\partial \dot{Z}}{\partial \dot{U}}\right)^2 \sigma_{\dot{U}}^2 + \left(\frac{\partial \dot{Z}}{\partial \dot{V}}\right)^2 \sigma_{\dot{V}}^2 + \left(\frac{\partial \dot{Z}}{\partial \dot{W}}\right)^2 \sigma_{\dot{W}}^2 \qquad (5.1.2.1\text{-}4)$$

The expressions for the covariance terms $\sigma_{\dot{X}\dot{Y}}$, $\sigma_{\dot{X}\dot{Z}}$, $\sigma_{\dot{Y}\dot{Z}}$, $\sigma_{\dot{X}\dot{X}}$, $\sigma_{\dot{Y}\dot{X}}$, $\sigma_{\dot{Z}\dot{X}}$, $\sigma_{\dot{X}\dot{Y}}$, $\sigma_{\dot{Y}\dot{Y}}$, $\sigma_{\dot{Z}\dot{Y}}$, $\sigma_{\dot{X}\dot{Z}}$, $\sigma_{\dot{Y}\dot{Z}}$, $\sigma_{\dot{Z}\dot{Z}}$ may be written according to the following expression for $\sigma_{\dot{X}\dot{Y}}$

$$\sigma_{\dot{X}\dot{Y}} = \left(\frac{\partial \dot{X}}{\partial U}\right)\left(\frac{\partial \dot{Y}}{\partial U}\right) \sigma_U^2 + \left(\frac{\partial \dot{X}}{\partial V}\right)\left(\frac{\partial \dot{Y}}{\partial V}\right) \sigma_V^2 + \left(\frac{\partial \dot{X}}{\partial W}\right)\left(\frac{\partial \dot{Y}}{\partial W}\right) \sigma_W^2 + \left(\frac{\partial \dot{X}}{\partial \dot{U}}\right)\left(\frac{\partial \dot{Y}}{\partial \dot{U}}\right) \sigma_{\dot{U}}^2 + \left(\frac{\partial \dot{X}}{\partial \dot{V}}\right)\left(\frac{\partial \dot{Y}}{\partial \dot{V}}\right) \sigma_{\dot{V}}^2 + \left(\frac{\partial \dot{X}}{\partial \dot{W}}\right)\left(\frac{\partial \dot{Y}}{\partial \dot{W}}\right) \sigma_{\dot{W}}^2 \qquad (5.1.2.1\text{-}5)$$

As an example the velocity variance $\sigma_{\dot{X}}^2$ for a radar according to equation (5.1.2.1-2) may be expressed as:

$$\begin{aligned}\sigma_{\dot{X}}^2 = {} & (\dot{E} \sin E \cos A + \dot{A} \cos E \sin A)^2 \sigma_R^2 \\ & + (-\dot{R} \sin E \cos A - \dot{E} R \cos E \cos A + \dot{A} R \sin E \sin A)^2 \sigma_E^2 \\ & + (-\dot{R} \cos E \sin A + \dot{E} R \sin E \sin A - \dot{A} R \cos E \cos A)^2 \sigma_A^2 \\ & + (\cos A \cos E)^2 \sigma_{\dot{R}}^2 + (-R \cos A \sin E)^2 \sigma_{\dot{E}}^2 \\ & + (-R \sin A \cos E)^2 \sigma_{\dot{A}}^2\end{aligned}$$

5.1.2.1 PROPAGATION OF ERRORS IN VELOCITY DATA (CONT'D)

In the same manner the velocity variance $\sigma^2_{\dot{X}}$ for AZUSA may be written as:

$$\sigma^2_{\dot{X}} = \dot{\ell}^2 \sigma^2_{\dot{r}} + \dot{r}^2 \sigma^2_{\dot{\ell}} + \ell^2 \sigma^2_{\dot{r}} + r^2 \sigma^2_{\dot{\ell}}$$

5.1.2.2 PROPAGATION OF ERRORS IN ACCELERATION DATA

The total errors in cartesian acceleration coordinates may be found by differentiating the $\dot{X}$, $\dot{Y}$, $\dot{Z}$ equations with respect to time and utilizing the approximations equations (5.1-8) and (5.1-9) Section 5.1.

$$\ddot{X}, \ddot{Y}, \ddot{Z} = f_{\ddot{X}, \ddot{Y}, \ddot{Z}} (U, V, W, \dot{U}, \dot{V}, \dot{W}, \ddot{U}, \ddot{V}, \ddot{W}) \quad (5.1.2.2\text{-}1)$$

$$\sigma^2_{\ddot{X}} = \left(\frac{\partial \ddot{X}}{\partial U}\right)^2 \sigma^2_U + \left(\frac{\partial \ddot{X}}{\partial V}\right)^2 \sigma^2_V + \left(\frac{\partial \ddot{X}}{\partial W}\right)^2 \sigma^2_W + \left(\frac{\partial \ddot{X}}{\partial \dot{U}}\right)^2 \sigma^2_{\dot{U}} + \left(\frac{\partial \ddot{X}}{\partial \dot{V}}\right)^2 \sigma^2_{\dot{V}} + \left(\frac{\partial \ddot{X}}{\partial \dot{W}}\right)^2 \sigma^2_{\dot{W}} + \left(\frac{\partial \ddot{X}}{\partial \ddot{U}}\right)^2 \sigma^2_{\ddot{U}} + \left(\frac{\partial \ddot{X}}{\partial \ddot{V}}\right)^2 \sigma^2_{\ddot{V}} + \left(\frac{\partial \ddot{X}}{\partial \ddot{W}}\right)^2 \sigma^2_{\ddot{W}} \quad (5.1.2.2\text{-}2)$$

The expressions for $\sigma^2_{\dot{Y}}$ and $\sigma^2_{\ddot{Z}}$ may be written in the same manner. The covariance terms will be of the form:

$$\sigma_{\ddot{X}\ddot{Y}} = \left(\frac{\partial \ddot{X}}{\partial U}\right)\left(\frac{\partial \ddot{Y}}{\partial U}\right) \sigma^2_U + \left(\frac{\partial \ddot{X}}{\partial V}\right)\left(\frac{\partial \ddot{Y}}{\partial V}\right) \sigma^2_V + \left(\frac{\partial \ddot{X}}{\partial W}\right)\left(\frac{\partial \ddot{Y}}{\partial W}\right) \sigma^2_W + \left(\frac{\partial \ddot{X}}{\partial \dot{U}}\right)\left(\frac{\partial \ddot{Y}}{\partial \dot{U}}\right) \sigma^2_{\dot{U}} + \left(\frac{\partial \ddot{X}}{\partial \dot{V}}\right)\left(\frac{\partial \ddot{Y}}{\partial \dot{V}}\right) \sigma^2_{\dot{V}} + \left(\frac{\partial \ddot{X}}{\partial \dot{W}}\right)\left(\frac{\partial \ddot{Y}}{\partial \dot{W}}\right) \sigma^2_{\dot{W}} + \left(\frac{\partial \ddot{X}}{\partial \ddot{U}}\right)\left(\frac{\partial \ddot{Y}}{\partial \ddot{U}}\right) \sigma^2_{\ddot{U}} + \left(\frac{\partial \ddot{X}}{\partial \ddot{V}}\right)\left(\frac{\partial \ddot{Y}}{\partial \ddot{V}}\right) \sigma^2_{\ddot{V}} + \left(\frac{\partial \ddot{X}}{\partial \ddot{W}}\right)\left(\frac{\partial \ddot{Y}}{\partial \ddot{W}}\right) \sigma^2_{\ddot{W}} \quad (5.1.2.2\text{-}3)$$

5.1.2.1 PROPAGATION OF ERRORS IN VELOCITY DATA (CONT'D)

σ_U, σ_V, σ_W are values of the total error in the position coordinates U, V, W. $\sigma_{\dot{U}}$, $\sigma_{\dot{V}}$, $\sigma_{\dot{W}}$, $\sigma_{\ddot{U}}$, $\sigma_{\ddot{V}}$, $\sigma_{\ddot{W}}$ are values of the error in the rate coordinates ($\dot{U}$, $\dot{V}$, $\dot{W}$) and time derivative of rate coordinates ($\ddot{U}$, $\ddot{V}$, $\ddot{W}$) consisting of the random (correlated plus uncorrelated) error components which propagate into the derivative data.

5.1.3 COORDINATE TRANSFORMATION OF ERROR EXPRESSIONS

The errors σ_X, σ_Y, σ_Z, $\sigma_{\dot{X}}$, $\sigma_{\dot{Y}}$, $\sigma_{\dot{Z}}$, $\sigma_{\ddot{X}}$, $\sigma_{\ddot{Y}}$, $\sigma_{\ddot{Z}}$ are associated with the coordinate system X, Y, Z defined by the equations relating the rectangular coordinate data and the original observations. These errors can be expressed in terms of another coordinate system X' Y' Z' as follows:

Assume that the new coordinate system X' Y' Z' is related to the coordinate system X Y Z by

$$X' = a_1 X + b_1 Y + c_1 Z + d_1$$

$$Y' = a_2 X + b_2 Y + c_2 Z + d_2$$

$$Z' = a_3 X + b_3 Y + c_3 Z + d_3 \qquad (5.1.3\text{-}1)$$

Then the following matrix equation holds between the errors in the two systems:

$$\sigma' = \hat{R}\ \sigma\ \hat{R}^T \qquad (5.1.3\text{-}2)$$

where $\hat{R}$ is the matrix of the coefficients of X Y Z in (5.1.3-1) (the transformation matrix) and

5.1.3 COORDINATE TRANSFORMATION OF ERROR EXPRESSIONS (CONT'D)

$\hat{R}^T$ is the transpose of $\hat{R}$

σ is the variance - covariance error matrix in the original system

Also, if Σ', Σ represent the 9 x 9 covariance matrices of position, velocity, and acceleration in the two systems, then

$$\Sigma' = R \Sigma R^T \qquad (5.1.3\text{-}3)$$

where

$$R = \begin{bmatrix} \hat{R} & 0 & 0 \\ 0 & \hat{R} & 0 \\ 0 & 0 & \hat{R} \end{bmatrix}$$

If we partition the matrices in the right member of 5.1.3-3 into 3 x 3 blocks and perform the indicated multiplications of the blocks, we note that each 3 x 3 block of Σ' is of the form 5.1.3-2 i.e., if Σ'_{ij} is the (3 x 3) i,j-th block of Σ', Σ_{ij} the i,j-th block of Σ, then $\Sigma'_{ij} = \hat{R} \Sigma_{ij} \hat{R}^T$.

5.2 ERROR PROPAGATION IN THE OVER - DETERMINED CASE

In the case of an over - determined system a least squares technique is used to estimate the set of parameters that can most closely represent the observations. The GDOP calculation for the over - determined solution is based on the same methods outlined in section 5.1 except that more variables are involved and more complex mathematical manipulations must be carried out.

5.2.1 GENERAL PRINCIPLES

In the framework of the least - squares analysis, that estimate of the coordinates of the target is considered the best, which minimizes the quadratic form:

$$\sum_{i,j} w_{ij}\, r_i\, r_j \qquad (5.2.1\text{-}1)$$

where w_{ij} are the elements of the weight matrix w, which is the inverse of the variance - covariance matrix σ_U of the observations or measurements $u_1, u_2, \ldots u_m \ldots u_M$. The residual r_i is the difference between the observed value of a parameter and the value calculated from the estimate $(X_o, Y_o, Z_o, \dot{X}_o, \dot{Y}_o, \dot{Z}_o)$. It is assumed that the theoretical values of the observations can be unambiguously expressed as functions of the coordinates of the target:

$u_m = u_m\,(X, Y, Z, \dot{X}, \dot{Y}, \dot{Z})$.

From this least - squares principle follows the variance - covariance matrix in the cartesian coordinates of the target as:

5.2.1 GENERAL PRINCIPLES (CONT'D)

$$\sigma(X_n)=\sigma(X,Y,Z,\dot{X},\dot{Y},\dot{Z})=\left\{\left(\frac{\partial u_m}{\partial X_n}\right)^T \sigma_U^{-1} \left(\frac{\partial u_m}{\partial X_n}\right)\right\}^{-1} \quad (5.2.1\text{-}2)$$

where: $\frac{\partial u_m}{\partial X_n} = \frac{\partial(u_1, \cdots u_M)}{\partial(X,Y,Z,\dot{X},\dot{Y},\dot{Z})}$, the matrix of partial derivatives (related to the Jacobian in form) of the observations versus the coordinates.

The observations u_m have up till now been treated as separate entities. In practice, groups of them are considered to belong to one specific tracking system, e.g. range, azimuth and elevation for a radar. In the GDOP calculation it is assumed that the cross - correlations in the errors of the measurements belonging to the same system and the cross-correlation in the errors of the measurements belonging to different systems are small enough that they can be neglected. In the latter case this seems to be warranted in those circumstances where the measurements of one system are clearly set apart from others, physically or geographically, e.g. one radar versus another which is at a large distance. In other cases the system concept is less applicable, and more formal than factual, e.g. a UDOP system with long baselines. The covariance matrix of measurement errors is therefore a diagonal matrix, i.e., covariances are assumed to be zero.

The σ_U matrix may be written as

$$\sigma_U = \begin{bmatrix} \sigma_U^{(1)} & & & \\ & \sigma_U^{(2)} & & \\ & & \sigma_U^{(p)} & \\ & & & \sigma_U^{(P)} \end{bmatrix} \qquad (5.2.1\text{-}3)$$

where $\sigma_U^{(1)}$ ... $\sigma_u^{(p)}$ are themselves diagonal matrices representing the errors of measurement of the different systems. The inverse is simply:

$$\sigma_U^{-1} = \begin{bmatrix} \sigma_U^{(1)^{-1}} & & & \\ & \sigma_U^{(2)^{-1}} & & \\ & & \sigma_U^{(p)^{-1}} & \\ & & & \sigma_U^{(P)^{-1}} \end{bmatrix} \qquad (5.2.1\text{-}4)$$

Now formula (5.2.1-2) is expressible as:

$$\sigma(X_n)=\sigma(X,Y,Z,\dot{X},\dot{Y},\dot{Z})= \sum_1^p \left\{ \left(\frac{\partial u_k^{(p)}}{\partial X_n} \right)^T \sigma_U^{(p)^{-1}} \left(\frac{\partial u_k^{(p)}}{\partial X_n} \right) \right\}^{-1} \qquad (5.2.1\text{-}5)$$

where:

$$\frac{\partial u_k^{(p)}}{\partial X_n} = \frac{\partial(u_1^{(p)}, u_2^{(p)} \text{----- } u_{kp}^{(p)})}{\partial(X_1, \text{---------- } X_n)} \quad , \sum_p k_p = M.$$

The capital X, Y, Z, used to this point were meant to refer to a central or common coordinate system, in which the reduction is performed. Generally it is the pad coordinate system; it is also denoted by "trajectory system."

It simplifies matters if one expresses the measurements in terms of local cartesian coordinates, $x_i^{(p)}$, or $x^{(p)}$, $y^{(p)}$, $z^{(p)}$, $\dot{x}^{(p)}$, $\dot{y}^{(p)}$, $\dot{z}^{(p)}$.

Then $$\frac{\partial u_k^{(p)}}{\partial X_n} = \left(\frac{\partial u_k^{(p)}}{\partial x_i^{(p)}}\right)\left(\frac{\partial x_i^{(p)}}{\partial X_n}\right)$$

The matrix of partial derivatives $\left(\frac{\partial x_i^{(p)}}{\partial X_n}\right)$ is a common orthogonal transformation matrix.

We write the transformation from the central to the local coordinate system in the form:

$$\begin{bmatrix} x^{(p)} \\ y^{(p)} \\ z^{(p)} \end{bmatrix} = R^{(p)} \begin{bmatrix} X \\ Y \\ Z \end{bmatrix} + \begin{bmatrix} x_o^{(p)} \\ y_o^{(p)} \\ z_o^{(p)} \end{bmatrix} \qquad (5.2.1\text{-}6)$$

where the last column consists of the local coordinates of the central system's origin.

In terms of the orthogonal matrix $R^{(p)}$, thus defined, we have:

$$\frac{\partial x_i^{(p)}}{\partial X_n} = \begin{bmatrix} R^{(p)} & 0 \\ 0 & R^{(p)} \end{bmatrix} .$$

Formula (5.2.1-5) can be written as:

$$\sigma(X,Y,Z,\dot{X},\dot{Y},\dot{Z}) = \sum_{p=1}^{P} R^{(p)T} \left(\frac{\partial u_m^{(p)}}{\partial x_i}\right)^T \sigma_u^{(p)-1} \left(\frac{\partial u_m^{(p)}}{\partial x_i}\right) R^{(p)-1} \qquad (5.2.1\text{-}7)$$

The sequence of events in the GDOP analysis may be described as follows:

$\sigma_u^{(p)}$

$w_u^{(p)} = \sigma_u^{(p)-1}$

$w_{local}^{(p)} = \left(\frac{\partial u_m^{(p)}}{\partial x_i}\right)^T w_u^{(p)} \left(\frac{\partial u_m^{(p)}}{\partial x_i}\right)$

Central, in both the literary and configuration sense, are the variance- covariance matrices $\sigma_u^{(p)}$, one for each system. These are inverted to give weight matrices $w_u^{(p)}$, one for each system, in its measurement coordinates. These weight matrices, $w_u^{(p)}$, are transformed into weight matrices in terms of local, cartesian coordinates by matrices of partial derivatives. (It may be remarked here that in the language of differential geometry the weight matrices are transformed in a covariant fashion; the variance - covariance matrices, having the character of coordinate differences, are transformed in a contravariant fashion. Under orthogonal transformations the distinction between

contravariant and covariant can be abolished, and both types of matrices transform in the same way.)

$$w^{(p)}_{central} = R^{(p)^T} w^{(p)}_{local} R^{(p)}$$

$$w_{total} = \Sigma w^{(p)}_{central}$$

$$\sigma(x_n) = w^{-1}_{total}$$

The local weight matrices are transformed into weight matrices expressed in terms of the central coordinate system, $w^{(p)}_{central}$. Adding these weight matrices, and inverting the result yields the desired variance-covariance matrix in central cartesian coordinates. If desired, this matrix may be rotated into any given (earth tangent or earth-centered) coordinate system, or transformed into an earth-centered inertial system.

5.2.2 THE VARIANCE - COVARIANCE MATRICES OF MEASUREMENT ERRORS

In principle, the variance - covariance matrix of measurement errors consists of a sum of matrices, each corresponding to a different source of error: electronic noise, time jitter, refraction correction errors, survey errors, timing, etc.

Sometimes the errors caused by a given source are not correlated between the different tracking systems, e.g. electronic noise. In other cases there exists a more or less strong interdependence; a typical example is the error in the refraction correction, which could be common to systems, depending on their distance. Other errors, e.g.

the error in the velocity of light, being a bias error, is perfectly common to most measurements.

Cross-correlations in errors between different tracking systems are not considered at the present time. This is less serious than it might appear, because e.g. the refraction correction is more important in the interferometer systems, such as AZUSA and MISTRAM, internally, than the combination of these with others at large distances. Still one should keep this point in mind; situations may occur where these cross-correlations change the picture considerably.

Degradation of quality of the measurements at low elevation angles is accounted for in the GDOP calculation in the following manner. Input constants are provided which represent a) the (random) variance at or above 5^{o}, and b) the variance at 2^{o}. (Below 2^{o} the station is not used in the solution.) To obtain a value of the variance between 2^{o} and 5^{o}, the value of an exponential function, fitted between the two input values, is employed.

Some remarks on the uncertainty in the value for the velocity of light are in order here. This is clearly an error that penetrates almost all of the observations. As long as the error due to this source is not larger than other errors in the system there is not much harm in neglecting the cross-correlations due to this effect. To give an idea of the order of magnitude: if e.g. 2 ft. is about the order of magnitude of the other errors involved, then, reckoning the velocity of light to be accurate to 0.2 km/sec., one would not have to worry up to distances of about 600 miles. For very large distances (say, to the moon) the estimated errors, neglecting the cross-correlations, can be excessively large [Rutledge, 1961].

Survey errors are treated in the following manner. The location of a tracking station on the earth's surface is determined by three quantities. Generally these are latitude, longitude, and height above a certain standard ellipsoid. These can be transformed into cartesian coordinates. The basic electric measurements in the tracking instruments are scalars: phase, time delay, etc. Thus in these measurements there is no orientation involved, only the location of the given station. As remarked before, groups of observations are considered to belong to one tracking system. Often the relative locations of the stations constituting a system are better known than the system as a whole relative to some reference point. A typical example is the Eleuthera MISTRAM. In such cases it is useful to distinguish between internal and external survey. The internal survey gives the location of the stations referred to the location of the central station; now also an orientation of this local coordinate system has to be defined. If the relative location of the stations is not better known than the absolute, there is no need to make the distinction between internal and external survey, e.g., the UDOP system, or the Valkaria MISTRAM. Only the external survey inaccuracy is accounted for at the present time.

Let the external survey uncertainty concerning translation be given in the local cartesian coordinates as:

$$\sigma_{\xi\dot{\xi}} = \begin{bmatrix} \sigma_{\xi} & \text{cov. terms} \\ \text{cov. terms} & \sigma_{\dot{\xi}} \end{bmatrix} \qquad (5.2.2\text{-}1)$$

where:

$$\sigma_{\xi} = \begin{bmatrix} \sigma_{\xi}^2 & \sigma_{\xi\eta} & \sigma_{\xi\zeta} \\ \sigma_{\eta\xi} & \sigma_{\eta}^2 & \sigma_{\eta\zeta} \\ \sigma_{\zeta\xi} & \sigma_{\zeta\eta} & \sigma_{\zeta}^2 \end{bmatrix}$$

and $\sigma_{\dot{\xi}}$ is a similar matrix. For land-based stations $\sigma_{\dot{\xi}} = 0$ Then the contribution to the input matrix due to translational inaccuracy is given by:

$$\left[\frac{\partial u_m^{(p)}}{\partial(\xi,\eta,\zeta,\dot{\xi},\dot{\eta},\dot{\zeta})}\right]\left[\sigma_{\xi\dot{\xi}}\right]\left[\frac{\partial u_m^{(p)}}{\partial(\xi,\eta,\zeta,\dot{\xi},\dot{\eta},\dot{\zeta})}\right]^T \qquad (5.2.2\text{-}2)$$

Because the observations are all expressed in terms of coordinate differences, $\xi - x$, $\eta - y$, $\zeta - z$, we notice that:

$$\frac{\partial u}{\partial \xi} = -\frac{\partial u}{\partial x} \text{ etc.} \qquad (5.2.2\text{-}3)$$

and thus (5.2.2-2) can be alternatively written as:

$$\left[\frac{\partial u_m^{(p)}}{\partial(x,y,z,\dot{x},\dot{y},\dot{z})}\right]\left[\sigma_{\xi\dot{\xi}}\right]\left[\frac{\partial u_m^{(p)}}{\partial(x,y,z,\dot{x},\dot{y},\dot{z})}\right]^T \qquad (5.2.2\text{-}4)$$

The orientation of a local coordinate system is physically determined by the plumbline at the central site and true (astronomical) north. In the data reduction the observations are first transformed to a system with the same origin, but oriented relative to the ellipsoid. The error in the deflection of the vertical (defined as the difference between the astronomic and geodetic position) thus is directly connected with the error in the geodetic position. When rotating the system to match the central coordinate system, these two errors cancel, and the only errors left are those due to the astronomic observations.

Let the three angles α_1, α_2, α_3 be infinitesimal rotation angles about the x, y and z axes respectively. The uncertainties in the astronomic observations concerning rotations and rotation rates are expressed in the matrices:

$$\sigma_\alpha = \begin{bmatrix} \sigma_{\alpha_1}^2 & \sigma_{\alpha_1\alpha_2} & \sigma_{\alpha_1\alpha_3} \\ \sigma_{\alpha_2\alpha_1} & \sigma_{\alpha_2}^2 & \sigma_{\alpha_2\alpha_3} \\ \sigma_{\alpha_3\alpha_1} & \sigma_{\alpha_3\alpha_2} & \sigma_{\alpha_3}^2 \end{bmatrix} \qquad (5.2.2\text{-}5)$$

and $\sigma_{\dot\alpha}$, similarly formed.

The contribution to the input matrix of the p^{th} system from rotation inaccuracy is given by:

$$\begin{bmatrix} X_\alpha & 0 \\ \dot X_\alpha & X_\alpha \end{bmatrix} \begin{bmatrix} \sigma_\alpha^{(p)} & \\ & \sigma_{\dot\alpha}^{(p)} \end{bmatrix} \begin{bmatrix} X_\alpha^T & \dot X_\alpha^T \\ 0 & X_\alpha^T \end{bmatrix} \qquad (5.2.2\text{-}6)$$

where:

$$X_\alpha = \begin{bmatrix} 0 & -z & y \\ z & 0 & -x \\ -y & x & 0 \end{bmatrix}$$

and:

$$\dot X_\alpha = \begin{bmatrix} 0 & -\dot z & \dot y \\ \dot z & 0 & -\dot x \\ -\dot y & \dot x & 0 \end{bmatrix}$$

These rotation effects are considered in the GDOP calculation. The influence on land-based stations is negligible. For ships the effect may be appreciable.

PART II

SYSTEM DESCRIPTIONS, ERROR SOURCES AND ACCURACIES

1.0 INTRODUCTION

Part II of this report is devoted to discussions and data pertaining to the individual tracking systems: the specific methods whereby the accuracies are determined, descriptions of the systems to the extent needed properly to utilize the data, discussions of error sources and error models, and the accuracy data themselves. Even though in some cases accuracy data are sparse, as with the new signature, navigation or shipborne radar systems, or classified, as with MILS, the methodology, system description and error source discussions are not abbreviated. Hence, as supplementary accuracy data do become available, the framework for their interpretation will already exist. Also, these discussions should be of value to those engineers using, evaluating, or contemplating the use of these systems.

The tables in Section 2.0 summarizes the accuracy data discussed in the balance of the report. In general these estimates refer to optimum conditions. Succeeding pages amplify, explain and extend the instrumentation accuracies to other conditions since it is recognized that a single number is not representative of an instrumentation system operating under extreme conditions of environment and geometry.

As a result of the inauguration in October 1964 of the Systems Analysis Monthly Accuracy Bulletin, the data in the Summary Tables will in some instances not be the same as those shown in the detailed discussions, since the data in Section 2.0 represent the latest data available at the time of going to press and may include the results of tests more recent than those available at the time of preparation of the main text. Tables similar to those shown in Section 2.0 are now published on a

monthly basis by RCA Systems Analysis for the purpose of keeping current this portion of The Accuracy of ETR Instrumentation.

2.0 SUMMARY OF ETR TRACKING INSTRUMENTATION ACCURACIES

The following is a list of the summary tables included in this Section:

Table	System	Missile Type	Page
2.0-1	Metric Optics	All	2-2
2.0-2	Pulsed Radar	All	2-3
2.0-3	MISTRAM I & II	MINUTEMAN	2-4
2.0-4	MISTRAM I & II	TITAN II, GEMINI, SATURN	2-6
2.0-5	GLOTRAC	ATLAS, SATURN, TITAN III	2-8
2.0-6	AZUSA	ATLAS, SATURN, TITAN III	2-9
2.0-7	UDOP	MINUTEMAN	2-10
2.0-8	ODOP	SATURN	2-11
2.0-9	Ships	- -	2-12

TABLE 2.0-1

ACCURACY ESTIMATES

SYSTEM: METRIC OPTICS (See Section 3.0)
MISSILE TYPE: All
ASSUMED MEAN BIAS: Zero

Instrumentation	Total Error	
	s_x	s_y
CZR oriented with shoot boards*	76	73
CZR oriented with offset boards*	93	70
CZR oriented with dials*	183	139
Ballistic Cameras**		
115 mm F.L.	3.7	2.3
210 mm F.L.	5.3	2.5
300 mm F.L.	4.7	3.9
600 mm F.L.	3.5	5.6
1000 mm F.L.	3.4	5.3
300 mm F.L. (Re-entry Data - Full Synchronous Timing)	4.3	6.0
	s_a	s_e
Cine-Theodolites (Askania)***	19	23

*Uncertainty of the x and y coordinates at the film plane in microns. In use, CZR cameras are usually rolled approximately 90°. Based on 10" focal length.

**Uncertainty of the x and y coordinates at the film plane in microns.

***Uncertainty in seconds of arc at the camera.

TABLE 2.0-2

ACCURACY ESTIMATES

SYSTEM: PULSED RADAR (See Section 4.0)
MISSILE TYPE: All
ASSUMED MEAN BIAS: Zero

Radar FPS-16	Coord.	s_{Bias}	s_{Random}	Radar FPQ-6 TPQ-18	Coord.	s_{Bias}	s_{Random}
1.16	A	0.10	0.10	0.18	A	0.10	0.07
	E	0.15	0.15		E	0.15	0.10
	R	50.0	7.5		R	50.0	7.5
3.16	A	0.10	0.10	19.18	A	0.10	0.07
	E	0.15	0.15		E	0.15	0.10
	R	90.0	15.0		R	100.00	7.5
5.16	A	0.10	0.10	3.18	A	0.10	0.10
	E	0.15	0.15		E	0.15	.15
	R	90.0	15.0		R	100.0	15.0
12.16	A	0.10	0.2	7.18	A	0.10	0.07
	E	0.15	0.2		E	0.15	0.10
	R	90.0	20.0		R	75.0	7.5
13.16	A	0.10	0.2	91.18	A	0.10	0.15
	E	0.15	0.2		E	0.15	0.20
	R	90.0	20.0		R	100.0	15.0
				12.18	A	0.20	0.20
					E	0.20	0.25
					R	160.0	15.0
40.43	A	2.7	3.5				
Trinidad	E	2.7	3.5				
	R(AT)*	15K ft	25 K ft				
	R(FRT)**	2K ft	100 ft				

Note: Angle values in mils, Range in Feet.
A = Azimuth E = Elevation R = Range

*Acquisition Tracking Mode
**Fine Range Tracking Mode

TABLE 2.0-3
ACCURACY ESTIMATES

SYSTEM: MISTRAM I & II (See Section 6.2)
MISSILE TYPE: MINUTEMAN
ASSUMED MEAN BIAS: Zero

Measurement	Position (Ft)			Rate** (Ft/Sec)	Acceleration** (Ft/Sec^2)
	S_{Bias}		S_{Random}	S_{Random}	S_{Random}
	a priori	a posteriori*			
1st Stage					
Valkaria					
R	2.6	1.0	0.2	0.03	0.3
P_1	0.06	0.01	0.04	0.033	0.15
Q_1	0.07	0.02	0.04	0.032	0.15
P_2	1.2	0.08	0.15	0.042	0.20
Q_2	1.0	0.18	0.15	0.046	0.20
2nd Stage					
Valkaria					
R	2.6	1.0	0.2	0.02	0.2
P_1	0.06	0.01	0.02	0.006	0.05
Q_1	0.07	0.02	0.02	0.007	0.05
P_2	1.2	0.08	0.10	0.007	0.07
Q_2	1.0	0.18	0.10	0.007	0.07
Eleuthera (Passive)					
R_S	10^6	1.9	0.8	0.12	0.5
$\dot{R}_S$***	0.1	0.01	- - -	- - -	- - -
P	3.0	0.08	0.15	0.05	0.25
Q	1.5	0.02	0.15	0.05	0.25

*Bias uncertainty after adjustment by GLAD using MISTRAM I in 1st Stage and MISTRAM I & II in 2nd and 3rd Stage.

**Rate and acceleration derived by use of a 23 point, 3rd degree polynomial.

***Rate Bias (Ft/Sec).

TABLE 2.0-3 (Cont'd)
ACCURACY ESTIMATES

SYSTEM: MISTRAM I & II (See Section 6.2)
MISSILE TYPE: MINUTEMAN
ASSUMED MEAN BIAS: Zero

Measurement	Position (Ft)			Rate** (Ft/Sec)	Acceleration** (Ft/Sec^2)
	s_{Bias}		s_{Random}	s_{Random}	s_{Random}
	a priori	a posteriori*			
3rd Stage					
Eleuthera (Active)					
R	5.4	1.5	0.8	0.03	0.3
P	1.6	0.08	0.2	0.006	0.08
Q	1.5	0.02	0.1	0.006	0.05
Valkaria (Passive)					
R_S	10^6	2.6	0.4	0.06	0.30
P_1	0.06	0.01	0.02	0.005	0.01
Q_1	0.07	0.01	0.02	0.005	0.01
P_2	1.2	0.05	0.10	0.010	0.05
Q_2	1.0	0.06	0.10	0.010	0.05

*Bias uncertainty after adjustment by GLAD using MISTRAM I in 1st Stage and MISTRAM I & II in 2nd and 3rd Stage.

**Rate and acceleration derived by use of a 23 point, 3rd degree polynomial.

TABLE 2.0-4
ACCURACY ESTIMATES

SYSTEM: MISTRAM I & II (See Section 6.2)
MISSILE TYPE: TITAN II, GEMINI, SATURN
ASSUMED MEAN BIAS: Zero

Measurement	Position (Ft)			Rate** (Ft/Sec)	Acceleration** (Ft/Sec^2)
	s_{Bias}		s_{Random}	s_{Random}	s_{Random}
	a priori	a posteriori*			
Booster					
Valkaria (Active)					
R	2.7	1.8	0.2	0.05	0.5
P_1	0.16	0.07	0.03	0.017	0.14
Q_1	0.16	0.15	0.03	0.017	0.14
P_2	1.5	1.0	0.15	0.020	0.16
Q_2	1.5	1.1	0.15	0.020	0.16
Sustainer					
Valkaria (Active)					
R	2.7	1.8	0.1	0.03	0.30
P_1	0.16	0.01	0.02	0.002	0.02
Q_1	0.16	0.02	0.02	0.002	0.02
P_2	1.5	0.14	0.10	0.005	0.03
Q_2	1.5	0.22	0.10	0.005	0.03
Valkaria (Passive)					
R_3	10^6	5.0	0.4	0.06	0.3
R_S***	0.1	0.01	- - -	- - -	- - -
P_1	3.0	0.02	0.02	0.002	0.02
Q_1	3.0	0.03	0.02	0.002	0.02
P_2	3.0	0.2	0.10	0.005	0.03
Q_2	3.0	0.3	0.10	0.005	0.03
Eleuthera (Active)					
R	2.3	1.5	0.8	0.03	0.3
P	2.0	0.4	0.2	0.005	0.03
Q	2.0	0.4	0.1	0.005	0.03

*Bias uncertainty after adjustment by GLAD using MISTRAM I in Booster stage and MISTRAM I & II in Sustainer Stage.

**Values derived by use of a 13 point, 2nd degree polynomial.

***Rate Bias (Ft/Sec)

TABLE 2.0-4 (Cont'd)
ACCURACY ESTIMATES

SYSTEM: MISTRAM I & II
MISSILE TYPE: TITAN II, GEMINI, SATURN
ASSUMED MEAN BIAS: Zero

Measurement	Position (Ft)			Rate** (Ft/Sec)	Acceleration** (Ft/Sec^2)
	^{S}Bias		^{S}Random	^{S}Random	^{S}Random
	a priori	a posteriori*			
Sustainer					
Eleuthera (Passive)					
R_S	10^6	4.0	0.8	0.06	0.5
P	2.2	0.7	0.2	0.005	0.03
Q	2.3	0.1	0.1	0.005	0.03

*Bias uncertainty after adjustment by GLAD using MISTRAM I in Booster stage and MISTRAM I & II in Sustainer Stage.

**Values derived by use of a 31 point, 2nd degree polynomial.

TABLE 2.0-5
ACCURACY ESTIMATES

SYSTEM: GLOTRAC (See Section 6.3)
MISSILE TYPE: ATLAS, SATURN, TITAN III
ASSUMED MEAN BIAS: Zero

Station	Position (Ft)			Rate** (Ft/Sec)		
	s_{Bias}		s_{Random}	s_{Bias}		s_{Random}
	a priori	a posteriori*		a priori	a posteriori*	
Range Difference						
Atlantic	10^7	20	0.15	0.20	0.10	0.04
Bermuda	10^7	58	0.15	0.20	0.18	0.08
Grand Turk	10^7	19	0.36	0.20	0.05	0.09
San Salvador	10^7	13	0.33	0.20	0.05	0.06
Antigua	10^7	84	0.50	0.20	0.17	0.08
Eleuthera	10^7	4	0.21	0.20	0.03	0.08
Cape Van	10^7	0.4	0.53	0.20	0.01	0.09
Range Sum						
Atlantic	10^7	87	0.35	0.50	0.11	0.06
Bermuda	10^7	70	0.40	0.50	0.08	0.08
Grand Turk	10^7	41	0.56	0.50	0.05	0.12
San Salvador	10^7	47	0.46	0.50	0.09	0.17
Antigua	10^7	49	0.36	0.50	0.07	0.12
Cape Van	10^7	43	0.42	0.50	0.11	0.06

*These estimates assume that error model coefficients are adjusted by the GLAD Program with AZUSA, GLOTRAC and Radar as inputs.

**Rate derived by use of a 21 point, 2nd degree polynomial.

TABLE 2.0-6
ACCURACY ESTIMATES

SYSTEM: AZUSA MARK II (See Section 6.4)
MISSILE TYPE: TITAN III, ATLAS, SATURN
ASSUMED MEAN BIAS: Zero

Measurements	Position			Rate**
	s_{Bias}		s_{Random}	s_{Random}
	a priori	a posteriori*		
Booster				
ℓ_c	50 ppm	No Data	25 ppm	4.0 ppm/sec
m_c	50 ppm	No Data	25 ppm	3.0 ppm/sec
R_c	15 ft	No Data	0.6 ft	0.2 ft/sec
Sustainer				
ℓ_c	30 ppm	6.3 ppm	6 ppm	1.5 ppm/sec
m_c	30 ppm	9.8 ppm	6 ppm	1.5 ppm/sec
R_c	15 ft	4.5 ft	0.2 ft	0.05 ft/sec

*These estimates assume that the biases are adjusted by the GLAD Program with AZUSA, GLOTRAC, and Radar as input.

**Rate for ℓ_c and m_c derived by use of a 61 point, 2nd degree polynomial.

Rate for R_c derived by use of a 31 point, 2nd degree polynomial.

TABLE 2.0-7

ACCURACY ESTIMATES

SYSTEM: UDOP (See Section 6.5)
MISSILE TYPE: MINUTEMAN
ASSUMED MEAN BIAS: Zero

Sites	Range Sum		Range Sum Rate*
	s_{Bias} (Ft)	s_{Random} (Ft)	s_{Random} (Ft/Sec)
Uprange			
Playalinda Beach	6.5	0.63	0.12
Titusville-Cocoa	2.6	0.49	0.11
Merritt Island	2.9	0.56	0.13
Pluto	2.7	0.58	0.14
Pooled Value	4.1	0.57	0.13
Downrange			
Allans Cay	3.8	0.63	0.15
Walker Cay	4.5	0.60	0.14
Bassett Cove	3.5	0.53	0.11
West End	3.4	0.51	0.14
Pooled Value	3.8	0.57	0.14

*Rate derived by use of a 25 point 3rd degree polynomial filter.

TABLE 2.0-8

ACCURACY ESTIMATES

SYSTEM: ODOP (See Section 6.5)
MISSILE TYPE: SATURN
ASSUMED MEAN BIAS: Zero

Sites	Range Sum		Range Sum Rate*
	S_{Bias} (Ft)	S_{Random} (Ft)	S_{Random} (Ft/Sec)
Merritt Island	13.2	0.31	0.10
Pluto	5.1	0.46	0.09
Site C	10.3	0.37	0.10
Blockhouse 34	11.5	0.34	0.09
Cactus	10.7	0.28	0.11
RMS	10.5	0.36	0.10
	Range Difference		Range Difference Rate*
Allans minus Bassett	5.1	0.27	0.06
Walker minus Bassett	5.1		0.08
Bassett minus West End		0.21	
Allans minus West End	11.1	0.21	0.07
RMS	7.6	0.23	0.07

*Rate derived by use of a 61 point, 3rd degree polynomial.

TABLE 2.0-9

ACCURACY ESTIMATES

SYSTEM: SHIPS

I METRIC ACCURACIES (See Section 5.0)

Instrumentation: General H. H. Arnold, C-Band Radar (909C)
(Tabulated values are based on one evaluation test)

ERROR ESTIMATE	MEASUREMENT		
	A** (MILLI-RADIANS)	E** (MILLI-RADIANS)	R** (FEET)
Mean Bias	0.69	-0.35	284
Standard Deviation (about mean bias)	1.75	0.88	38
Total (Root Sum Square)	1.88	0.95	287
Bias Uncertainty	*	*	*

*Insufficient Data Available

**Based on differences with AZUSA as a standard

II SIGNATURE (CROSS SECTION) ACCURACIES (See Section 9.0)

INSTRUMENTATION	MEASUREMENT	σ_{TOTAL}***
C-Band Radar		
H. H. Arnold	Target cross-section	2.5 db
H. S. Vandenberg	Target cross-section	2.5 db
L-Band Radar		
H. H. Arnold	Target cross-section	2.6 db
H. S. Vandenberg	Target cross-section	3.4 db
X-Band Radar		
H. H. Arnold	Target cross-section	3.7 db

***This value represents the root sum square of 2 components.
(a) Pooled standard deviations from 3 second spans of data.
(b) Standard deviation of span means about the grand mean.

Target radar cross section biases are removed through calibration and data processing.

3.0 OPTICAL INSTRUMENTATION

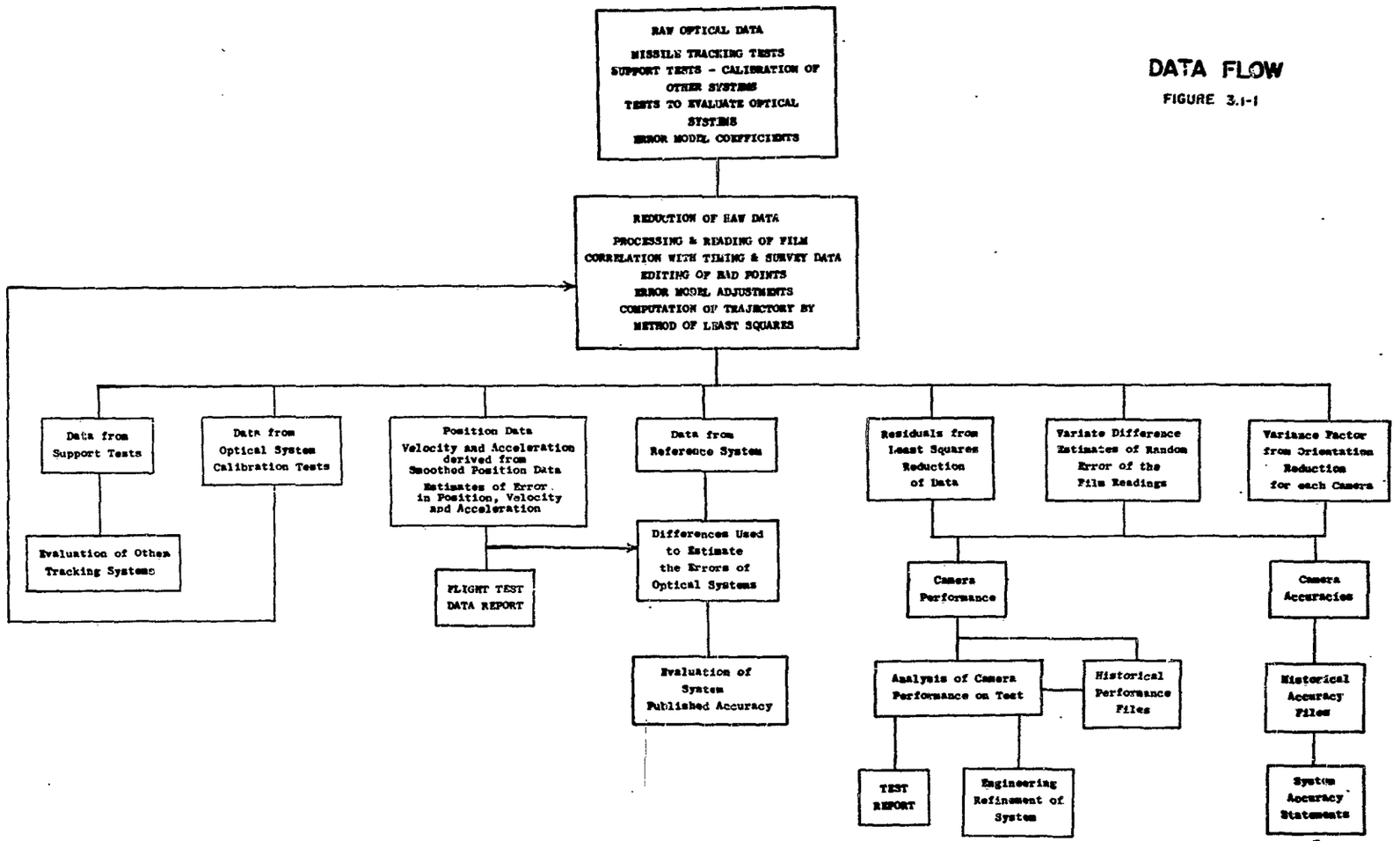
3.1 Procedure for Estimating System Accuracies and Performance

3.1.1 Data Flow

The general flow of optical data is illustrated on Figure 3.1-1. Raw optical data are generated by missile tests, calibration tests in support of other systems, and special tests designed to evaluate and calibrate error models of the optical tracking systems.

The information comes to Data Reduction as exposed film, timing records, and survey information locating cameras and, in some cases, orientation targets. The film records are processed and read and this information, correlated in time, is combined with the survey data and processed to generate position-time information on the path of the object being tracked. Internal consistency checks are performed during this processing and improper data points are edited. Error models covering hardware anomalies of the tracking systems are available and where equipment errors have not been isolated and removed, error model calibration values may be inserted in the calculations to remove their effect. Since the optical systems usually acquire redundant data, the method of least squares is used in the reduction.

Two types of information emerge from this process. They are missile position data and test error information. The additional missile parameters of velocity and acceleration are derived from the position data. Error estimates of the missile parameters are based on nominal system errors combined with error information obtained during the reduction of the data. The missile parameters and the associated estimates of error are published in the Flight Test Data Report. The test error data are used to evaluate camera accuracy and performance.



DATA FLOW

FIGURE 3.1-1

3.1.2 Methodology for Estimating System Accuracies

All metric optical tracking systems have three requirements in common. They are:

(1) The geodetic location of each instrument must be known at the time of the test.

(2) It must be possible to determine the direction that the optical axis bears relative to the location of the instrument at the moment that it acquires tracking information. All measurements and calculations are referred to this axis. This process is known as determining the "orientation" of the instrument.

(3) Since a single optical instrument cannot determine range, information from a second unit must always be available. In addition, the uncertainties of cloud interference make it expedient to cover each launch with more than the minimum number of units.

This redundant information is exploited during the reduction of data by the method of least squares. This approach maximizes the use of all available information on a test.

The test error information that is used to estimate system accuracy includes the following:

(1) The weighted residuals of each camera as determined by a least squares adjustment of the data.

(2) A variate difference estimate of the random error in the digitized film readings for each camera.

(3) An estimate of the variance factor derived during the orientation of each camera.

This information is used to compute the individual camera variances as follows:

$$\begin{bmatrix} s_{xi}^2 & 0 \\ 0 & s_{yi}^2 \end{bmatrix} - \begin{bmatrix} V_i & 0 \\ 0 & U_i \end{bmatrix} \hat{\sigma}_o^2$$

where

s_{xi}^2, s_{yi}^2 = estimates of the error variance in the x and y basic measurement** of the i^{th} camera.

V_i, U_i = estimates of the x and y elements of the relative covariance matrix.

$\hat{\sigma}_o^2$ = an estimate of the variance factor (also known as unit variance).

The estimate of the variance factor ($\hat{\sigma}_o^2$) for each system is computed as:

$$\hat{\sigma}_o^2 = \left\{ \sum_{j=1}^{n} \left[\frac{\sum_{i=1}^{m_j} (v_{ij}^2 + u_{ij}^2)}{(2m_j - 3)} \right] \right\}$$

**This estimate is in the film plane of the camera.

where

v_{ij}, u_{ij} = x and y weighted residuals of the i^{th} camera at the j^{th} time point.

m_j = number of cameras in the solution at the j^{th} time point.

n = number of time points.

$\hat{\sigma}_o^2$ = the estimate of the variance factor.

The relative covariance matrices are the inverse of the weight matrices used in the least squares solution. The covariance matrices of the three metric optical systems are:

Relative Covariance Matrix for Fixed Cameras

$$\begin{bmatrix} v_i & 0 \\ 0 & u_i \end{bmatrix} = \begin{bmatrix} \frac{2C_L^2}{S^2C^2}\left(\frac{S_o^2\ \sigma_{\bar{x}}^2}{S_o^2+\sigma_{\bar{x}}^2}\right) & 0 \\ 0 & \frac{2C_L^2}{S^2C^2}\left(\frac{S_o^2\ \sigma_{\bar{y}}^2}{S_o^2+\sigma_{\bar{y}}^2}\right) \end{bmatrix}$$

where

$\sigma_{\bar{x}}^2$, $\sigma_{\bar{y}}^2$ = estimate of the variance of the x and y film observations as determined by the variate difference technique.

S_o = the mean error from the orientation adjustment.

C = the focal length of the camera.

C_L = a constant (.2548 meters).

S = a constant (10 microns).

Relative Covariance Matrix for Cine-Theodolites

$$\begin{bmatrix} V_i & 0 \\ 0 & U_i \end{bmatrix} = \begin{bmatrix} \frac{\hat{\sigma}_A^2}{\sigma_o^2} & 0 \\ 0 & \frac{\hat{\sigma}_E^2}{\sigma_o^2} \end{bmatrix}$$

where

$\hat{\sigma}_A^2$, $\hat{\sigma}_E^2$ = estimate of the variance of the azimuth and elevation film observations as determined by the variate difference technique.

σ_o^2 = a constant (4.938×10^{-6} degrees^2)

Relative Covariance Matrix for Ballistic Cameras

$$\begin{bmatrix} V_i & 0 \\ 0 & U_i \end{bmatrix} = \begin{bmatrix} \dfrac{2C_L^2\sigma_x^2 S_{ooi}^2}{S_o^2(\sigma_x^2 C_i + S_{ooi}^2 C_L^2)} & 0 \\ 0 & \dfrac{2C_L^2\sigma_y^2 S_{ooi}^2}{S_o^2(\sigma_y^2 C_i + S_{ooi}^2 C_L^2)} \end{bmatrix}$$

where

σ_x^2, σ_y^2 = the random error associated with the x and y plate readings

C_i = the focal length of the ith camera in mm.

C_L = a constant (1000 mm).

S_o = a constant (3 microns)

S_{ooi} = the standard error of the orientation of the i^{th} camera.

The following assumptions are germane to this methodology:

(1) It is assumed that errors from one camera plate are independent of those from any other plate and so are errors from the same camera at different times. We can express this assumption mathematically as

$$\text{cov}\ (\epsilon_{ij}, \epsilon_{i'j'}) = 0, \text{ if either } i \neq i' \text{ or } j \neq j' \text{ or both.}$$

$$\text{and cov}\ (\eta_{ij}, \eta_{i'j'}) = 0, \text{ if either } i \neq i' \text{ or } j \neq j' \text{ or both.}$$

where $(\epsilon_{ij}, \eta_{ij})$ denote true errors in the unadjusted plate coordinates (systematic error removed). Subscripts i and j refer to camera and time instant respectively.

This assumption is believed to be reasonable for the camera systems.

(2) It is assumed that the covariance matrix of $(\epsilon_{ij}, \eta_{ij})$ is

$$\underline{\Sigma}_{ij} = \underline{\Sigma}_i = \underline{V}_i \sigma^2 = \begin{bmatrix} V_i & c_i \\ c_i & U_i \end{bmatrix} \sigma^2 = \underline{W}_i^{-1} \sigma^2$$

where

$\underline{\Sigma}_{ij} = \underline{\Sigma}_i$ = the covariance matrix of $(\epsilon_{ij}, \eta_{ij})$

$c_i = 0$ because it is assumed that there is no correlation between x and y.

$\underline{V}_i = \underline{W}_i^{-1}$ = the relative covariance matrix

σ^2 = the unit variance (variance factor)

V_i = covariance matrix element of x or ϵ

U_i = covariance matrix element of y or η

The above assumption implies the following:

(a) the relative covariance matrix of $(\epsilon_{ij}, \eta_{ij})$ is known for all exposures;

(b) the absolute covariance matrices are identical for data from all exposures of the same camera;

(c) the relative (and hence also the absolute) covariance matrices of data from different cameras are different;

(d) the variances of the errors in the x- and in the y- coordinates from camera i are $\sigma^2 V_i$ and $\sigma^2 U_i$ respectively.

The estimation of the unit variance is based on the assumption that the errors follow a multivariate normal distribution with zero means (i.e. all systematic error has been removed).

The derivation of this methodology is given in [Chew, 1964b].

3.1.3 Methodology of Analysis of System Performance

Closely allied with the accuracy of optical tracking systems is the problem of maintaining this accuracy at a high level. Most tracking systems operate from fixed locations. Over a period of time it becomes possible to detect and measure some of their systematic

errors. The constant errors can either be physically removed from the equipment or mathematically removed from the data.

In contrast, most optical tracking systems are designed to be highly mobile. This increases their flexibility of application and permits optimization of geometry. However, the lack of a stable site-camera configuration makes it necessary to monitor the performance of each sub-system frequently to prevent the inclusion of systematic errors in the data. The situation is further complicated by the fact that a single camera does not determine a spatial point and often the error characteristics of one camera are influenced by the quality of other cameras in the solution.

However, one advantage of optical trackers should be emphasized. Each camera in the network is self initializing and, if track should be lost temporarily for any reason, the subsequent data are just as valid as the initial portion. Then too, the commitment of several cameras on each launch insures the continuity of track in any environment that is suitable for optical tracking. Cameras may leave and re-enter the solution with minimal disturbance of the resultant data.

The best approach to determining performance of an optical system is the direct comparison of each camera's projected ray to the equivalent ray as defined by a reference system. In the optical coverage time span the two independent reference systems sometimes available are inertial guidance and "best estimate of trajectory" solutions. These reference systems are not available on the majority of missile tests, however, so another reference system must be used.

One reference system used is the optical solution itself. This is convenient since the needed error information is generated during

the reduction of data. It is not, of course, an "independent" system, and hence its ability to determine bias errors particuarly is limited. The information consists of residuals (i.e. the difference of the individual camera measurements with those generated by the solution) and an estimate of "noise" in the digitized camera data (i.e. azimuth and elevation, x and y plate coordinates). The following performance criteria are used:

The criterion "camera total error of residuals" is defined as the standard deviation of the residuals of a single camera about a mean of zero. If the total error of residuals of a camera significantly exceeds that of other c ameras on the same test or of long term expected values, an investigation of the cause of the camera's high total error is instituted.

"Camera mean bias error of residuals" is defined as the arithmetic mean of the residuals of a camera. If the bias error significantly exceeds that of other cameras on the same test or falls outside of control limits based on similar camera conditions it is interpreted as an indication of internal or external systematic error.

The "random error of the film readings" is defined as the root mean square of the noise estimates in a camera's digitized data. This value is compared to that of other cameras on the test and to the long term expected value. In this case a high value indicates problems in the film imagery or in digitizing of the camera's data.

Table 3.1-1 summarizes the results of an analysis of the residuals from the reduction of a hypothetical set of data. It also summarizes the estimates of random error in the film readings of each camera as indicated by the variate difference of these readings. In each case, the estimate of error has been compared with the long term values of these performance estimates for cameras used under the same circumstances. If the test error was greater than expected, the word "high" has been entered in the table. If the estimate was in the normal range, the word "normal" has been entered. The last two columns of the table indicate the performance areas that should be searched for the causes of the higher than expected errors.

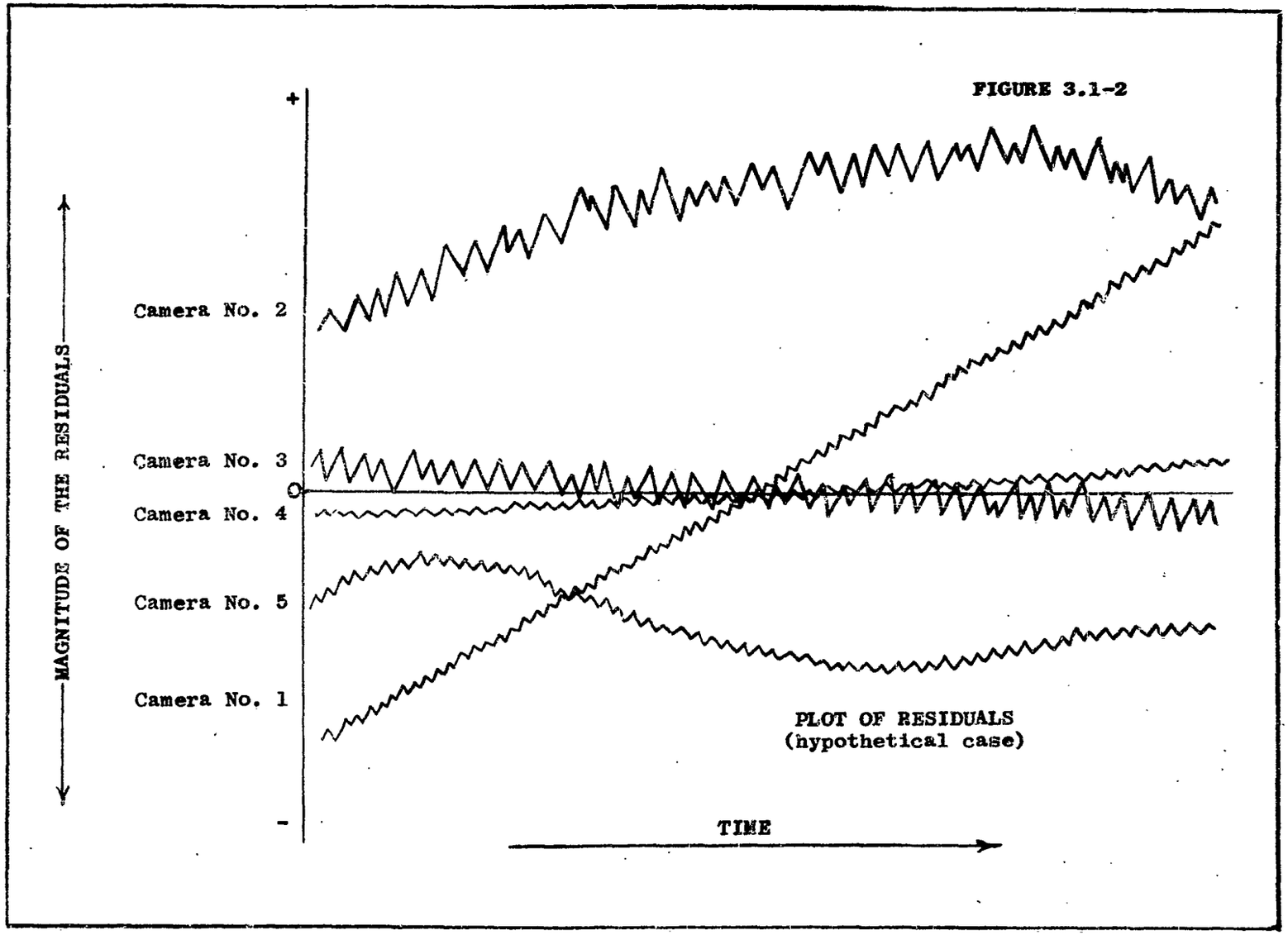
Table 3.1-1
Performance Characteristics Derived from Hypothetical Data

Camera No.	Estimates of			Search for Causes of	
	Total Error	Mean Bias Error	Random Error	Systematic Error	Random Error
1	High	Normal	Normal	Yes	No
2	High	High	High	Yes	Yes
3	Normal	Normal	High	No	Yes
4	Normal	Normal	Normal	No	No
5	High	High	Normal	Yes	No

Table 3.1-1 indicates that of the five hypothetical cameras, only one (No. 4) did not have some sort of problem on the test. Cameras No. 2 and 3 showed high random error in the film readings. Cameras No. 1, 2 and 5 showed high estimates of the total error of camera residuals with a high mean bias error of residuals indicated by the latter two. At this point in the analysis, plots of the residuals of each of the problem cameras would be made.

Figure 3.1-2 shows plots of the residuals that could correspond to each of the cameras in the hypothetical test. The zero line of the plot represents the least squares solution for all cameras in the test. The residuals of one of the parameters for each of the cameras on the test have been plotted about this system solution. The plots of Cameras No. 2 and 3 do show greater than normal "noise" in the residuals. This had been indicated from the engineering estimates based on the variate difference of the film readings and confirms the need for study of the film digitizing areas of these two cameras. The plots of Cameras No. 1, 2 and 5 indicate some form of systematic error in the data gathered by these cameras. These error patterns would be compared with the patterns of known errors. A hypothesis of the cause of error would be set up. This hypothesis would be checked by review of film evaluations, camera logs and other information defining the test results. Appropriate field investigations such as checks of camera calibration, resurveys of sites, and rereading of films would be made. In some cases, computer simulation of test conditions could be used as an analysis method. Camera No. 4 showed close adherence to the system solution and no investigation would be conducted. The number of problem cameras on this test has been exaggerated for the

FIGURE 3.1-2


+
MAGNITUDE OF THE RESIDUALS
Camera No. 2
Camera No. 3
Camera No. 4
Camera No. 5
Camera No. 1
-
TIME
PLOT OF RESIDUALS
(hypothetical case)

purpose of illustration. In the usual analysis, great caution must be observed if more than 30 or 40 percent of the cameras indicate problems. As noted earlier, the apparent behavior of one camera can be influenced by the quality of other cameras in the solution and caution must be employed when several problem cameras are turned up by the analysis.

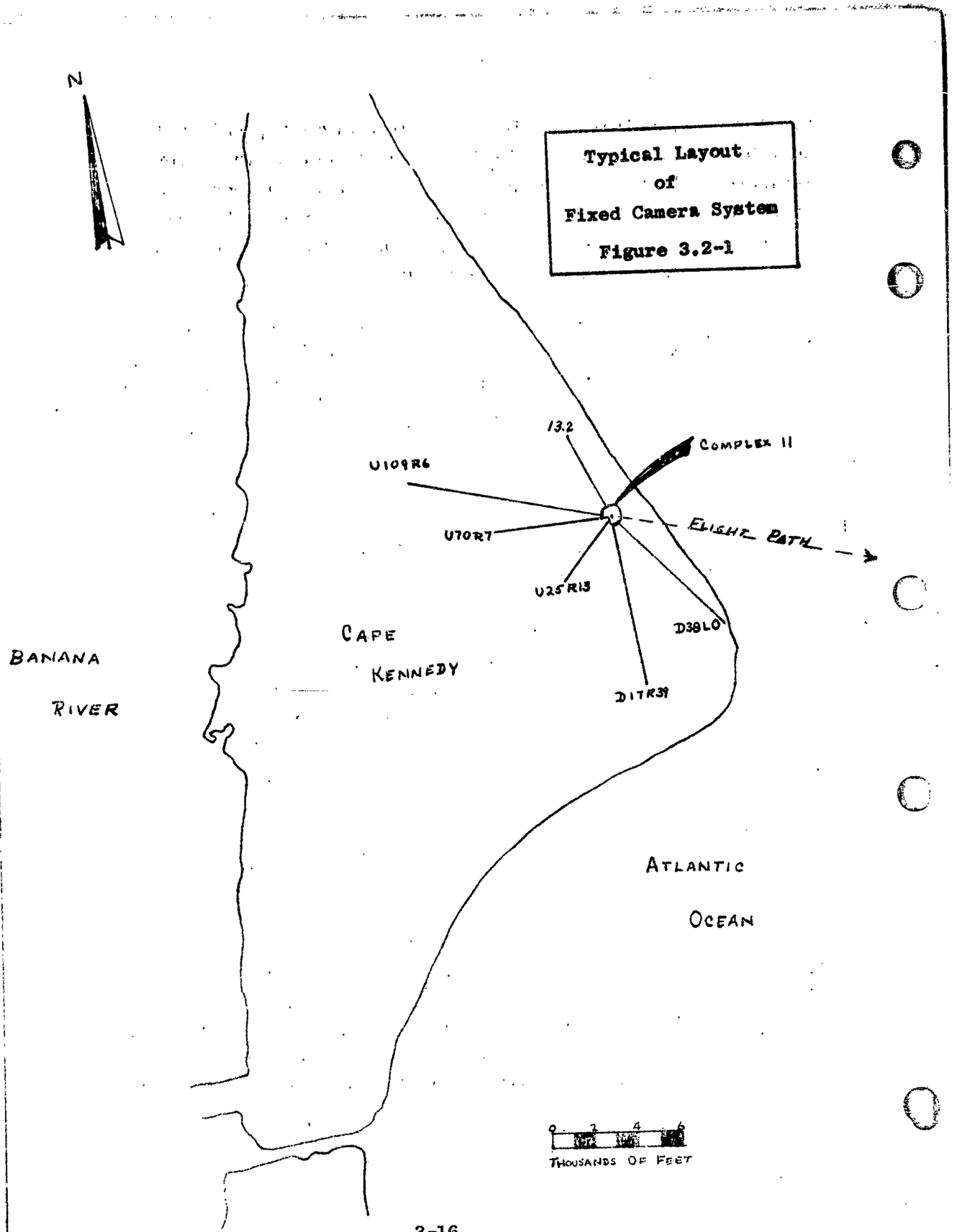
The results of the analysis and conclusions about the committed system's performance on the test are published in a test report. Corrective action is initiated on any system problems which are defined by the analysis.

3.2 FIXED CAMERA

3.2.1 System Description

The Fixed Camera System is used to obtain missile data from lift-off to approximately 2000 feet. This coverage can be extended to 10,000 feet by "stacking" several sets of cameras and reducing their data as a single trajectory. Velocity and acceleration information is derived from the position data. There are approximately 50 Fixed Camera sites spread over the Cape Kennedy area. There are 25 cameras available to equip these sites. When a shot is planned, certain of these sites are selected for the test so as to provide redundant coverage of the expected trajectory of the missile during the committed interval. Most of the Fixed Cameras are mounted on trailers and are towed to the selected camera sites on the day before the test. A typical layout for the launch of an Atlas Missile from Complex 11 is shown on Figure 3.2-1.

Each of the cameras is fastened to a precision three-axis mount and enclosed in a protective dome whose controlled atmosphere pre-conditions the camera to the thermal environment that is forecast for the time of launch. This is to prevent thermal shock to the equipment when the dome is opened to acquire data.


N
Typical Layout
of
Fixed Camera System
Figure 3.2-1
13.2
COMPLEX II
U109R6
U70R7
FLIGHT PATH
U25R13
D38LO
D17R31
CAPE
KENNEDY
BANANA
RIVER
ATLANTIC
OCEAN
0 2 4 6
THOUSANDS OF FEET

Each camera site is provided with range timing so that the cameras may be synchronized with it and with each other. Located near each camera site are one or more tall poles carrying illuminated orientation targets. The locations of the pad, the camera sites, and the orientation targets are all accurately determined shortly before the date of launch.

The Fixed Cameras (CZR) record a motion picture type of record on film that is 5-1/2 inches wide. Each frame is approximately 1 inch by 5-1/2 inches. Range timing is recorded along one edge of the film and a set of fiducial marks is recorded down the center of each frame.

Prior to the test, orientation data are recorded on the first portion of each roll of film. These data consist of the images of orientation targets and, in the case of offset orientations, certain other angular measurements, which will be explained later, are noted. The orientation of a Fixed Camera establishes the relationship between the film coordinate system and a local camera coordinate system centered at the survey point for the camera station. This relationship is expressed in terms of three angles: the azimuth angle, α, of the vertical plane containing the z axis of the film coordinate system, measured positive clockwise from true north in the tangent plane; the elevation angle, ω, of the principal axis of the camera measured positive upward from the tangent plane; and the roll angle, κ, which is the inclination of the x film coordinate axis with the tangent plane. These angles are computed from the directions of orientation targets whose images are exposed on the camera film.

After orientation, each camera is directed toward a specific portion of the trajectory and "fixed" or locked in that position. During the flight, data are recorded as a series of photographs with the missile occupying a sequence of positions as it advances along its trajectory. After processing, the film is read (measured) on a precision film reader and successive positions of the missile image are determined with respect to the fiducials which appear at the same location on each frame.

The missile trajectory is computed on a point by point basis. The film coordinates of each image are combined with the orientation data to construct a projected ray from each camera to the region of a single missile point in space. Since these rays do not meet in a unique point, because of measuring errors, the method of least squares is used to estimate the unknown point. The amount by which each ray is shifted in space is reflected back to the film of each camera. The shift on each film from the measured location of the image to the shifted point as determined by the method of least squares solution is called the residual for that camera at that time point. It is measured in microns in the x and y coordinates of the frame of that camera.

Three procedures of varying precision are used to determine the orientation of each camera. In one configuration, the orientation targets appear on the same frames as the missile data. This is referred to as a "shoot" orientation. When multiple targets are available, the method of least squares is used to estimate the three angles of orientation (azimuth, elevation and roll of each camera) as well as some factors of the internal geometry of the camera. Assuming equal care in all procedures, a "shoot" orientation will yield the most

precise orientation.

If the orientation targets and the missile trajectory do not occupy the camera field of view simultaneously, the former are photographed first and the dials on the axes of the mount are read and recorded. The camera is then turned to the trajectory and locked after which the dials are recorded again. This procedure is known as an "offset" orientation. It contains all of the errors associated with the "shoot" procedure plus the errors involved in determining two dial readings for each axis through which the camera may be turned.

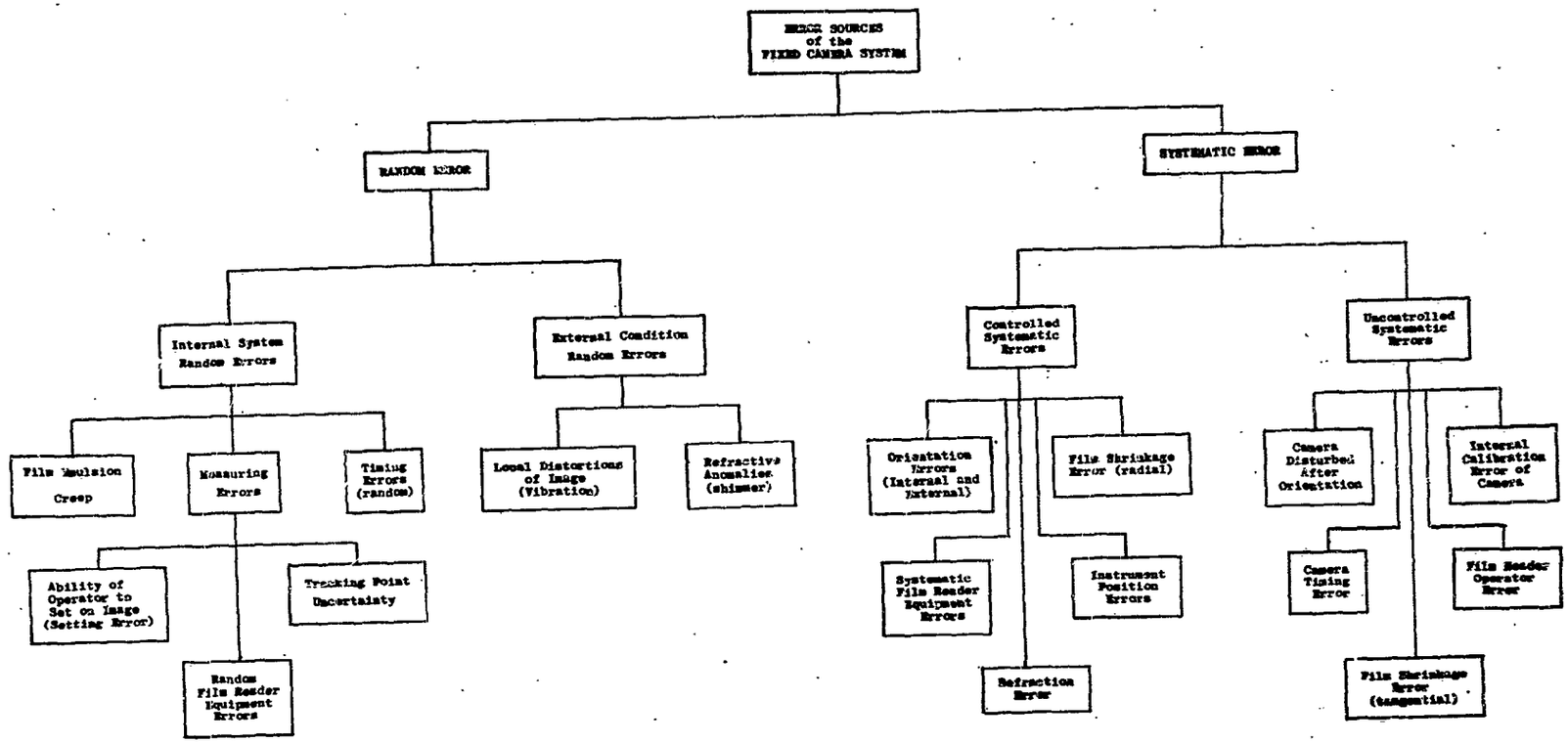
A third procedure is used when the film contains no orientation targets. Before taking any orientation exposures, a tall structure on the range is always photographed by each camera in the net. This "reference" shot is used as insurance against the failure of any portion of the other types of orientation. A "dial" orientation uses this single reference point as a zero set for the azimuth dial of the camera. The azimuth, elevation and roll angles of the camera are determined from the readings of the camera dials referenced to the dial zero set and the level of the camera. There are many sources of error in this procedure. They include reading and recording twelve dial values, periodic and secular errors in the dials themselves, non-perpendicularity of the three mount axes and mislevel of the camera. A "dial" orientation is the least precise of the three and is used to retrieve data where the usual procedures have failed.

3.2.2 Error Sources

The error sources of the Fixed Camera System are shown in Figure 3.2-2. In this figure the error sources have been

SOURCES OF ERROR
FIXED CAMERA SYSTEM

FIGURE 3.2-2



classified as random and systematic. Random errors are sub-classified by origin and systematic errors by the degree of control. The following paragraphs briefly define and explain these classifications.

Systematic errors are defined as those errors which affect the results of the system in a mathematically describable manner. The effect of random error and its reduction is discussed under the random error sub-classifications.

The sub-classification "Controlled Systematic Error" contains those error sources to which some method of control is applied. Instrument position and reader equipment errors are controlled by monitoring the survey process and instrument condition respectively. Orientation errors and radial film shrinkage are mathematically corrected during the orientation reduction. Refraction errors are reduced mathematically during both the orientation reduction and the triangulation reduction. The completeness of these corrections is dependent on the availability of sufficient calibration and test condition information.

The effects of "Uncontrolled Systematic Errors" are considered to be negligible in most operations of the system. The possible exception is film reader operator bias error which is currently under study. "Internal System Random Errors" are defined as those errors which directly affect the digitized film data. These errors are inherent in the system, but their magnitudes can be reduced by hardware or procedural changes that improve the system's resolution. The effect of random error can be minimized by proper mathematical data processing techniques.

"External Condition Random Errors" are defined as those errors which are generated by test conditions. The magnitude of these errors can be deduced from the physical conditions of the test if sufficient information is available. The effect of these errors can be minimized by proper mathematical data processing procedures.

3.2.3 System Accuracies

Fixed Camera accuracy estimates and data characteristics contained in this report are based on analysis of data from the missile tests shown in Table 3.2-1.

Table 3.2-1
Missile Types and Test Numbers

THOR	ATLAS	SATURN	POLARIS	MINUTEMAN	CENTAUR	TITAN III
3680	5145	0169	6090	3775	5175	4751
6900	3686	2769	5844			
5332	0250	4444	3599			
0475						
0136						
0131						

3.2.3.1 Accuracy Estimates

Using the methodology of Section 3.1.2, the estimates of Total Error are shown in Tables 3.2-2, 3.2-3 and 3.2-4. These values

are based on 10" focal length cameras. Too few data are available to generate values for other focal lengths.

Table 3.2-2
CZR Estimates of Total Error by Orientation

METHOD OF ORIENTATION	Estimates of Total Error	
	x-coordinate	y-coordinate
Shoot	76	73
Offset	93	70
Mixed	92	74

Units = Microns at the Film Plane*

Table 3.2-3
CZR Estimates of Total Error by Tracking Point

TRACKING POINT	Estimates of Total Error	
	x-coordinate	y-coordinate
Nose of the Missile	83	63
Nose of the Escape Tower	76	73
Base of the Nozzle	107	94

Units = Microns at the Film Plane*

*See Page 3-49 for table of unit conversion factors.

Table 3.2-4
Estimates of Total Error by Missile Type

TYPE OF MISSILE	CZR System Estimates of Total Error	
	x-coordinate	y-coordinate
THOR	114	85
SATURN	76	73
TITAN-III	51	41

Units = Microns at the Film Plane*

Based on the error values listed above for a Saturn missile, Figure 3.2-3 shows the Geometrical Dilution of Precision that might be expected for a Saturn launch from Complex 37 which was supported by five CZR cameras located at camera sites 34-1, U190L62, U236L87, U257L119 and U268L172.

3.2.3.2 Performance Data

Fixed camera performance on a test is judged by comparisons with the values shown in Tables 3.2-5, 3.2-6 and 3.2-7. The definition and use of these values is given in Section 3.1.3. Only those values that are germane to the detection of camera performance problems are presented. These performance values should not be used to estimate system accuracy or other characteristics. All values are based on 10" focal length because of insufficient data at other focal lengths.

*See page 3-20 for table of unit conversion factors.

Geometric Dilution of Precision
Fixed Camera System
Saturn Launch
Figure 3.2-3
Five Camera Configuration
Sites: U2680172
U2570119
U2361487
U1980162
34-2
Feet
3.0
2.0
1.0
0.0
0
5
10
15
Time in Seconds
$\sqrt{\sigma_x^2 + \sigma_y^2 + \sigma_z^2}$

Table 3.2-5
Orientation Performance Standards

METHOD OF ORIENTATION	Total Error		Bias Uncertainty*	
	S_x	S_y	S_x	S_y
Shoot	95.0	54.0	54.9	21.9
Offset	127.4	103.8	103.7	83.4
Dial	182.8	138.6	167.2	124.1

Units = Microns at the Film Plane**

Table 3.2-6
Tracking Point Performance Standards

Tracking Point	High Frequency Random Error	
	x-Coordinate	y-Coordinate
Flame	14	11
Nose of Missile	23	13
Nose of Escape Tower	24	20
Base of Missile	25	17

Units = Microns at the Film Plane**

*The mean Bias of the Fixed Camera system is assumed to be zero.

**See Page 3-29 for table of unit conversion factors.

Table 3.2-7
OZR Camera Performance Standards by Missile Type

MISSILE TYPE	OZR Camera Total Error**	
	S_x	S_y
SATURN	106	40
POLARIS	138	57
ATLAS*	146	108
MINUTEMAN	108	177
CENTAUR	68	60
TITAN III	40	23
THOR	126	92

Units = Microns at the Film Plane***

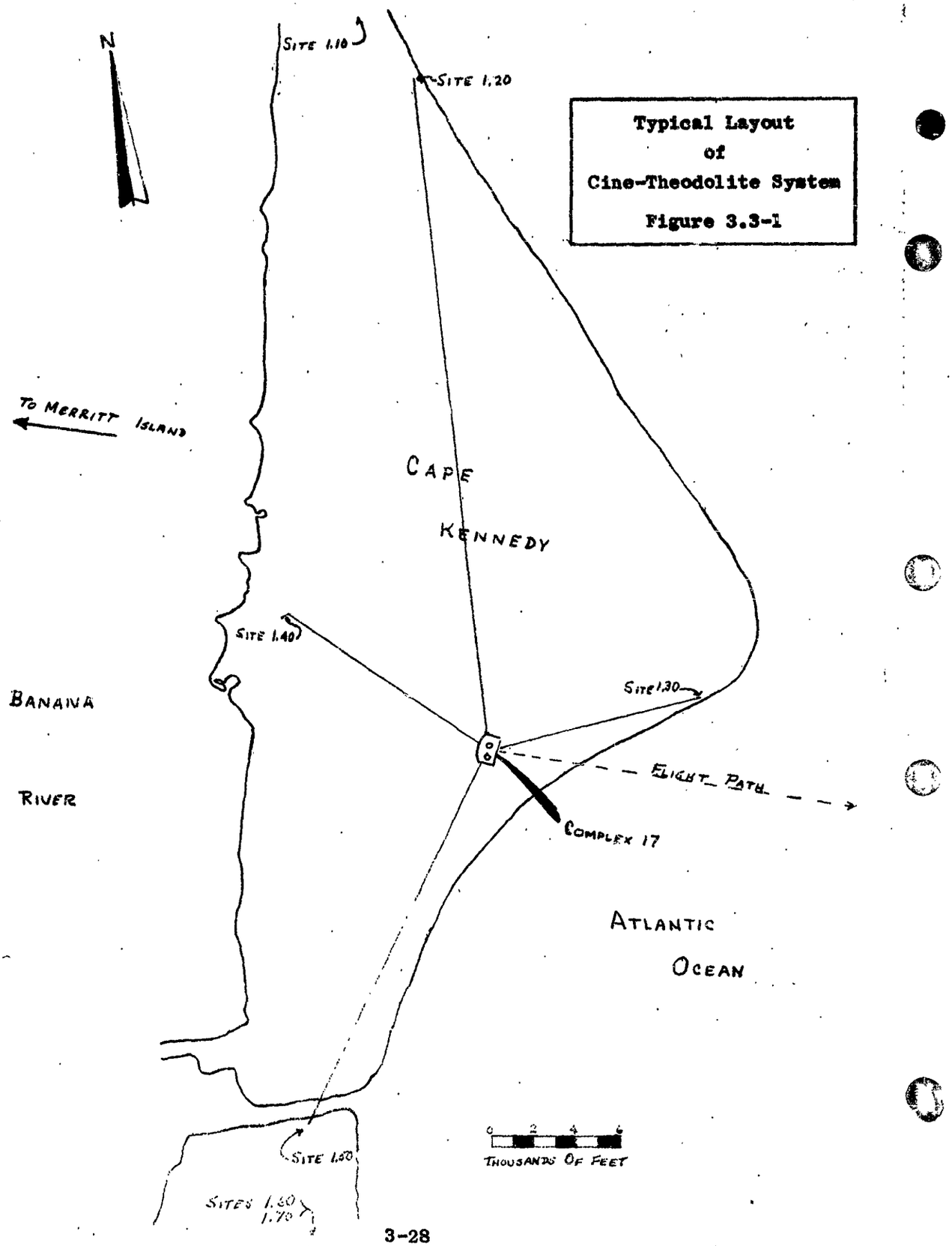
3.3 CINE-THEODOLITE (ASKANIA)

3.3.1 System Description

The Cine-Theodolite System is used to obtain optical data from 1500 feet to approximately 100,000 feet. The point at which it takes over from the Fixed Camera System depends on the lower atmospheric conditions.

There are four Cine-Theodolite sites placed within the general Cape Kennedy area. They are supplemented by three more (one north of and two south of the area) that are used to extend the coastal base of the system to about 22 miles. See Figure 3.3-1 for a typical Cine-Theodolite System layout.

*ATLAS values contain a number of dial oriented cameras.
**The mean Bias of the Fixed Camera system is assumed to be zero.
***See Page 3-49 for table of unit conversion factors.



Typical Layout
of
Cine-Theodolite System
Figure 3.3-1

The Theodolites are cine-type cameras fastened to two axis mounts. They are mounted in permanent towers and protected by controlled atmosphere domes. In use, a single operator uses a built-in telescope to track the missile in azimuth and elevation to be sure that the missile image is recorded on the center of the film frame. Since only the camera's location on the range is fixed, it must acquire continuous camera orientation data during tracking so that missile data may be reduced. This is done by photographing the mount axis dials on the same 35 millimeter film that records missile position data.

Before a missile is to be tracked, each instrument is pointed in turn at a series of illuminated targets that surround its location and short bursts of film are exposed. Survey information on these orientation targets and on the camera location is used to determine the dials' "zero set", and to obtain collimation and mislevel information. After this a missile may be tracked and photographed in flight. Then the film is processed and read. The zero set, collimation and level data are combined with the dial readings of each frame and a correction is added to adjust for any mistracking of the missile.

As with the Fixed Camera System, the missile trajectory is computed on a point by point basis. The azimuth and elevation readings, corrected for refraction, are combined with the orientation data to construct a projected ray from each Cine-Theodolite site to the region of a single missile point in space. Since the rays do not meet in a unique point, because of measuring errors, the method of least squares is used to estimate the unknown point. Velocity and acceleration

information are derived from the position data. The angular amount by which the projected ray is shifted to meet the solution is called the camera residual. It is measured in seconds of arc in the azimuth and elevation of each camera.

The geometric strength of the Cine-Theodolite System has been limited by the weakness of the net between Sites 1.30 and 1.40. In 1965 the strength of the net will be augmented by the addition of seven mobile instruments and the availability of Universal Camera Sites in the Merritt Island Launch Area.

3.3.2 Error Sources

The error sources of the Cine-Theodolite System are shown in Figure 3.3-2. In this figure the error sources have been classified as random and systematic. Random errors are subclassified by origin and systematic errors by degree of control. Although the Fixed Camera and the Cine-Theodolite error charts have several blocks in common, the specific errors represented by these blocks vary with the system. The following paragraphs briefly define and explain the classifications of the errors of the Cine-Theodolite System.

Systematic errors are defined as those errors which affect the results of the system in a mathematically describable manner. The effect of systematic errors can, in theory, be reduced or removed by calibration, procedural changes, or mathematical treatment of the data.

Random error sources are defined as those error sources which affect the results of the system in an arbitrary manner and can only be described mathematically in terms of probability distributions. The effect of random error and its reduction

is discussed under random error sub-classifications.

The sub-classification "Controlled Systematic Error" contains those error sources to which some method of control is applied. The instrument position errors, long term calibration errors and film reading equipment errors are controlled by monitoring the equipment or the procedure involved. Orientation errors and refraction error are corrected mathematically before triangulation. The effects of "Uncontrolled Systematic Errors" are considered to be negligible in most operations of the system. The possible exception is reader operator bias which is currently under study.

"Internal System Random Errors" are defined as those errors which directly affect the digitized film data. These errors are inherent in the system, however their magnitudes can be reduced by hardware or procedural changes which improve the system's resolution. The effect of random error can be minimized by proper mathematical data processing techniques.

"External Condition Random Errors" are defined as those errors which are generated by test conditions. The magnitude of these errors can be deduced from the physical conditions of the test if sufficient information is available. The effect of these errors can be minimized by proper mathematical data processing procedures.

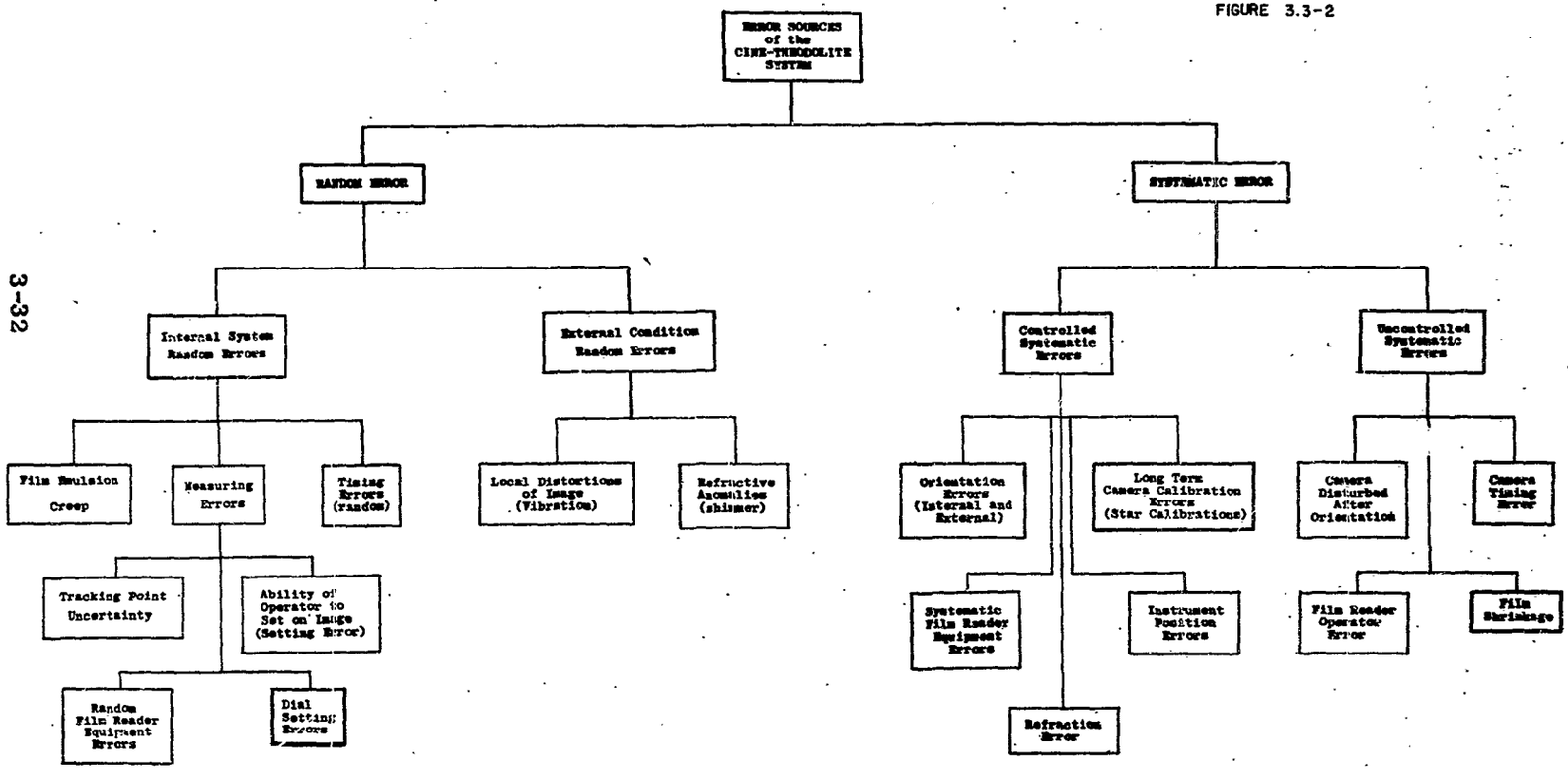
3.3.3 System Accuracies

Cine-Theodolite accuracy estimates and data characteristics contained in this report are based on an analysis of the data

SOURCES OF ERROR

CINE - THEODOLITE SYSTEM

FIGURE 3.3-2



from the missile tests shown in Table 3.3-1.

Table 3.3-1
Missile Types and Test Numbers

THOR	ATLAS	SATURN	POLARIS	MINUTEMAN	CENTAUR	TITAN-III	TITAN-II
3600	5145	0169	5120	5003	5175	4751	0275
6900	3686	2769	6090	3775			
5332		4444	5844	0430			
0475			3599				
0136							
0131							

3.3.3.1 Accuracy Estimates

Using the methodology of Section 3.1.2, the estimates of the Total Error for a number of individual Cine-Theodolite cameras have been generated. These estimates have been combined as weighted* RMS values to derive an estimate for all stations (Table 3.3.2) and by missile types (Table 3.3-3).

Table 3.3-2
Estimates of Total Error for the Cine-Theodolite System

	Estimates of Total Error	
	Azimuth	Elevation
All Stations	18.5	22.8

Units = seconds of arc at the camera**

*Weighted by the degrees of freedom associated with each camera.
**See Page 3-49 for table of unit conversion factors.

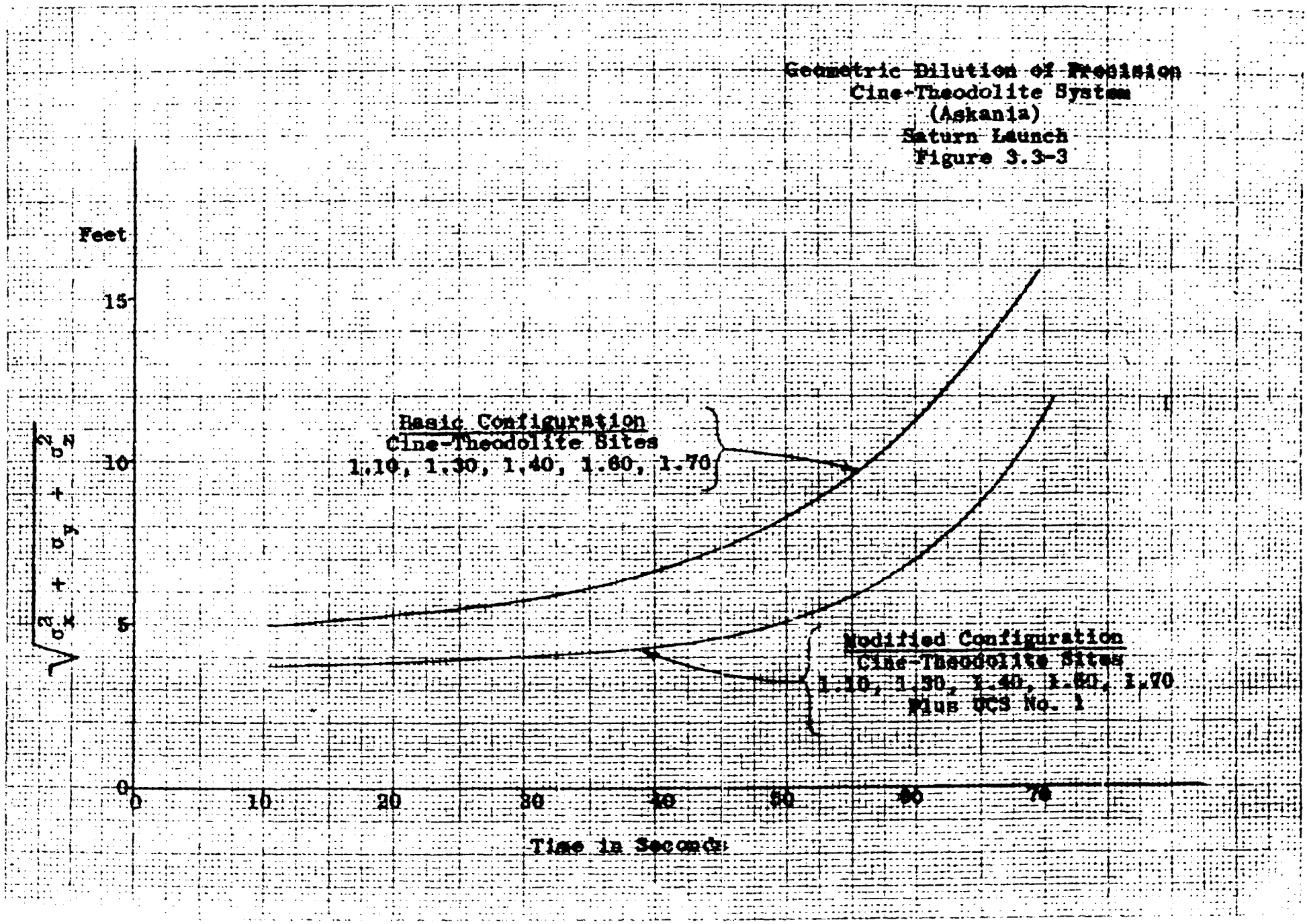
Table 3.3-3
Estimates of Cine-Theodolite Total Error by Missile Type

Missile Type	Estimates of Total Error	
	Azimuth	Elevation
THOR	18	23
SATURN	16	16
MINUTEMAN	14	14
TITAN-III	22	32

Based on the error values listed above for Saturn and Minuteman missiles, Figures 3.3-3 and 3.3-4 show the Geometric Dilution of Precision that might be expected for launches that were supported by five Cine-Theodolite cameras located at Sites 1.10, 1.30, 1.40, 1.60 and 1.70. In each instance the reduction in G.D.O.P.'s that would result from the inclusion of a single Merritt Island site in the net is also shown. The increased depth in geometry is particularly helpful after 30 to 40 seconds from lift off.

3.3.3.2 Performance Data

Cine-Theodolite performance on a test is judged by comparisons with the following values. The definition and use of these values are given in Section 3.1.3. These performance values (Table 3.3-4) should not be used to estimate system accuracy.


Geometric Dilution of Precision
Cine-Theodolite System
(Askania)
Saturn Launch
Figure 3.3-3
Feet
15
10
5
0
$\sqrt{\sigma_x^2 + \sigma_y^2 + \sigma_z^2}$
Basic Configuration
Cine-Theodolite Sites
1.10, 1.30, 1.40, 1.60, 1.70
Modified Configuration
Cine-Theodolite Sites
1.10, 1.30, 1.40, 1.60, 1.70
Plus OCS No. 1
0
10
20
30
40
50
60
70
Time in Seconds

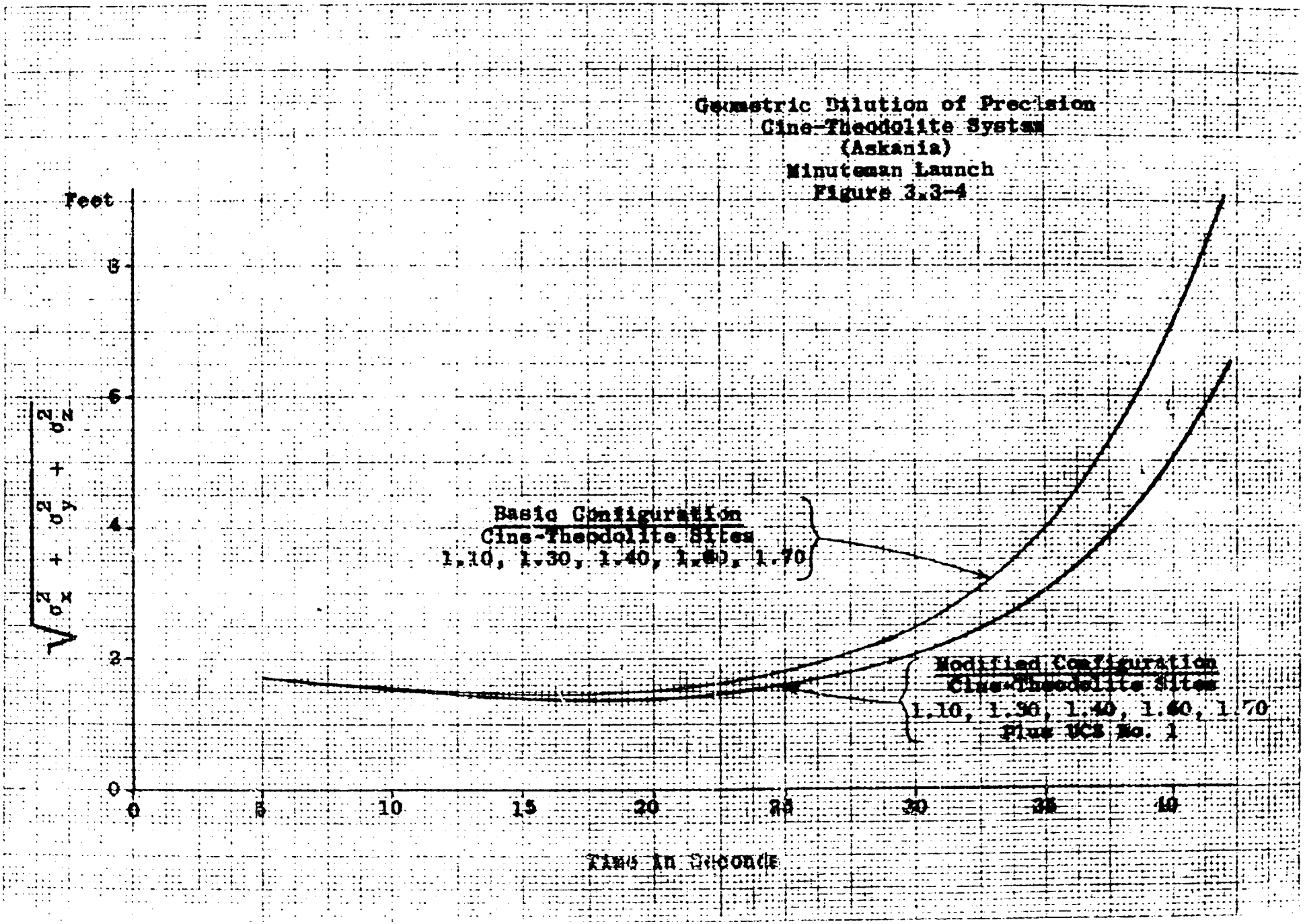

Geometric Dilution of Precision
Cine-Theodolite System
(Askania)
Minuteman Launch
Figure 3.3-4
Feet
8
6
4
2
0
$\sqrt{\sigma_{x_o}^2 + \sigma_{y_o}^2 + \sigma_{z_o}^2}$
Basic Configuration
Cine-Theodolite Sites
1.10, 1.30, 1.40, 1.60, 1.70
Modified Configuration
Cine-Theodolite Sites
1.10, 1.30, 1.40, 1.60, 1.70
Plus UCS No. 1
0
5
10
15
20
25
30
35
40
Time in Seconds

Table 3.3-4
Cine-Theodolite Performance Standards by Missile Type

Missile Type	Total Error		Bias* Uncertainty		High Frequency Random Error	
	s_A	s_E	s_A	s_E	s_A	s_E
THOR	16	21	9	20	8	10
SATURN	23	30	12	16	11	12
POLARIS	17	16	11	14	10	9
ATLAS	19	16	13	13	10	9
MINUTEMAN	14	15	3	14	10	9
CENTAUR	14	16	10	9	9	10
TITAN-III	14	16	12	14	8	9
TITAN-II	16	24	10	26	8	12
BLUE SCOUT	20	18	4	12	11	10
ALL MISSILES	18	19	11	16	10	10

Units = Seconds of Arc at the Camera**

3.4 BALLISTIC CAMERA

3.4.1 System Description

The Ballistic Camera systems are used for the optical tracking of both intermediate range and distant objects. They are used successfully for the following purposes:

(1) To determine the trajectories of distant missiles.

(2) To determine the paths of highly lofted missiles or of

*The mean Bias of the Cine-Theodolite system is assumed to be zero.

**See Page 3-49 for table of unit conversion factors.

orbiting satellites. In this instance they provide an important link in the improvement of world-wide geodetic nets.

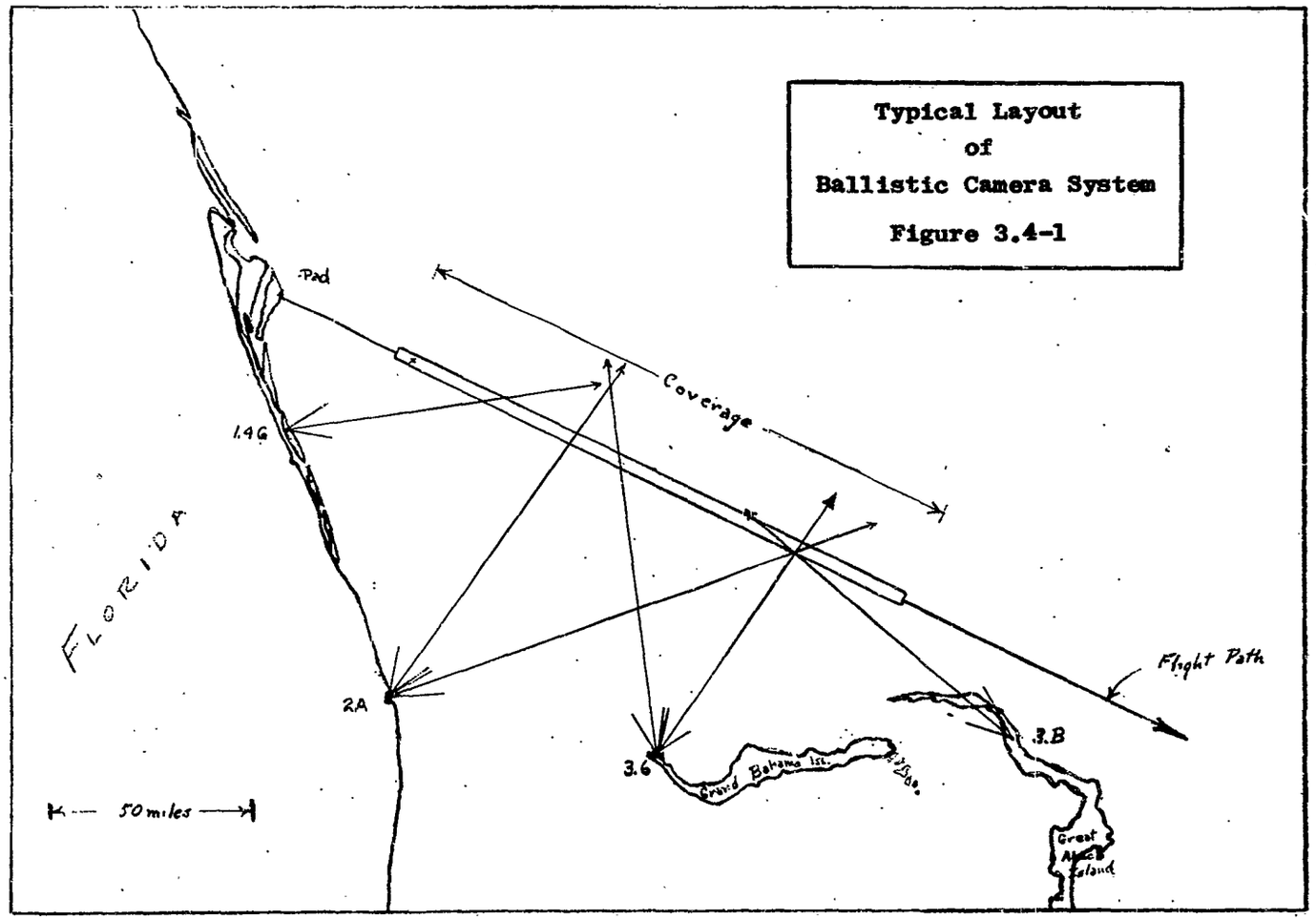
(3) To determine the paths of self luminous bodies such as missiles re-entering the atmosphere.

(4) To determine the flight paths of aircraft that are being used to evaluate other tracking systems.

3.4.1.1 Conventional Ballistic Camera System

The basic camera consists of a rigid, box-type instrument in which a lens system and a shutter are mounted. Provision is made to introduce a photographic glass plate into the box and lock it in place. Optical projectors within the camera expose fiducial marks onto this plate at the time that the data are recorded so that the coordinates of the images on the plate may be referenced to the optical axis of the lens system. The camera weighs less than 100 pounds and, after packing in a special container, may be transported from site to site without disturbing its internal geometry. On site, it is mounted on a semi-permanent, stable pedestal and protected against the sun and weather until it is time for the mission.

The camera mount is provided with leveling screws. Other adjustments are provided so that its optical axis may be directed toward any portion of the range. Prior to the test, the camera is directed toward the assigned portion of the expected trajectory and approximate values of the azimuth and elevation angles of the optical axis are noted. A typical test lay-out is shown on Figure 3.4-1.


Typical Layout
of
Ballistic Camera System
Figure 3.4-1
Pad
Coverage
1.4G
FLORIDA
2A
3.6
3.B
Flight Path
50 miles
Grand Bahama Isl.
Great Abaco Island

The general procedure for acquiring ballistic camera data is as follows: A few minutes before the flight is to be made, a photographic plate is loaded into the camera and all final adjustments are made. The camera will not be touched again until after the operation. A pre-orientation exposure is made as closely as possible to event-time. Shutter operation for all star orientation exposures is controlled by signals generated by Central Timing and transmitted to each site. Timing signals operate the shutters in the following sequence: open two seconds; closed 30 seconds; open one second; closed 30 seconds; open one-half second; closed 30 seconds; open one-quarter second; then closed until the time for the event to be recorded. The result will be a series of four exposures of each star in the field of view producing images of decreasing length. If there is sufficient time, the shutter may be opened for one minute and closed for 30 seconds before the beginning of the above sequence to aid in identification.

The orientation of a ballistic camera establishes the relationship between the plate coordinate system and a cartesian local camera coordinate system centered at the survey point for the camera station. This relationship is expressed in terms of three angles: The azimuth angle, α, of the vertical plane containing the z axis of the plate coordinate system, measured positive clockwise from true north in the tangent plane; the elevation angle, ω, of the principal axis measured positive upward from the tangent plane; and the roll angle, κ, which is the inclination of the x plate coordinate axis with the tangent plane measured positive counterclockwise from the tangent plane. These angles are computed from the directions of control points whose images are exposed on the camera plate.

The control points may be any objects in space which will expose identifiable points on the camera plate and whose direction or positions are known or can be determined. The control points normally used for ballistic cameras are stars whose directions from the camera can be accurately determined if the time of exposure is accurately known.

Just before the main event is to be recorded, the shutters of the cameras will be opened and will remain open until the desired portion of the trajectory has been recorded. The light flashes from the missile's strobe light will produce a series of point exposures across the plate while the stars will produce unbroken lines. The shutters will then be closed and will remain closed until the post-orientation series of star exposures which should be made as soon as possible after the main event. Post-orientation is carried out in the same manner as pre-orientation except that the order of shutter-cycling is reversed. This results in star exposures of one-quarter second, one-half second, one second, and two seconds. Reversal of the order provides a means of identifying the star traces as pre- and post-orientation. After the test the plates are processed and the coordinates of each image point are measured on a plate reading microscope known as a comparator. The digitized data are now ready for reduction.

The missile trajectory is computed on a point by point basis. The plate coordinates of each image point are combined with the orientation data to construct a projected ray from each camera to the region of a single missile point in space. Since these rays do not meet in a unique point because of measuring errors, the method of least squares is used to estimate the unknown point. The amount by which each ray is

shifted in space is reflected back to the plate of each camera. On each plane, the displacement of the ray from the measured location of the image to the new point that has been determined by the method of least squares, is called the residual for that camera at that time point. It is measured in microns at the plate in the x and y coordinates of that camera. The adjustment of each point in space produces a pair of coordinate residuals for each camera in the net.

3.4.1.2 Modified Ballistic Camera System

A modified ballistic camera system is being used to determine the position of bodies re-entering the atmosphere from space. Re-entry bodies have continuous luminosity from their friction with the atmosphere and would be recorded by a conventional ballistic camera as a continuous image without time correlation. The modified ballistic camera is designed to break this continuous image into short segments corresponding in function to the image points of the conventional ballistic camera (see Section 3.4.1.1).

The modification consists primarily of replacing the single camera capping shutter by a twin shutter. The first of these shutters has the same capping function as that of the conventional ballistic camera. The second or chopping shutter opens and closes 5 or 10 times per second. This shutter provides the chopping action required to record the trajectory of the luminous body as a series of position images.

By operating two or more cameras with synchronized chopping shutters at different sites, film records similar to those of the conventional ballistic camera are obtained. These records

have different time coding and are of poorer image quality than those produced by conventional ballistic cameras, but the data can be reduced in the same manner. The time synchronization accuracy of the modified system is critical. If the shutters of the several cameras are not opened and closed simultaneously, the recorded images will not represent common spacial points of the re-entry body.

During the period September 1964 to the present time most downrange re-entry tests employed a semisynchronous method of timing. Independent time generators were located at each camera site. These generators were individually referenced to WWV and to LORAN prior to the test. Time coordination among cameras was, of course, a problem under these circumstances.

Recently, a new method of synchronization has been installed at one downrange location. Full-synchronous timing employs a single time generator that is referenced to WWV and to LORAN. The shutter pulses are delivered to the individual camera sites by hard wire from this generator. Just prior to the test the time delay from the generator to each site is measured. This delay is introduced into the common generator pulse that is sent to each site to pulse the chopping shutters. Improved shutter synchronization has greatly reduced system errors.

3.4.2 Error Sources

The errors of the ballistic camera system are shown in Figure 3.4-2. In this figure the error sources have been classified as random and systematic. Random errors are sub-classified by origin and systematic errors by degree of control. The following paragraphs briefly define and explain these classifications.

Systematic errors are defined as those errors which affect the output of the system in a mathematically describable manner. The systematic errors of the conventional ballistic cameras are either under control or of negligible magnitude in most uses of the system.

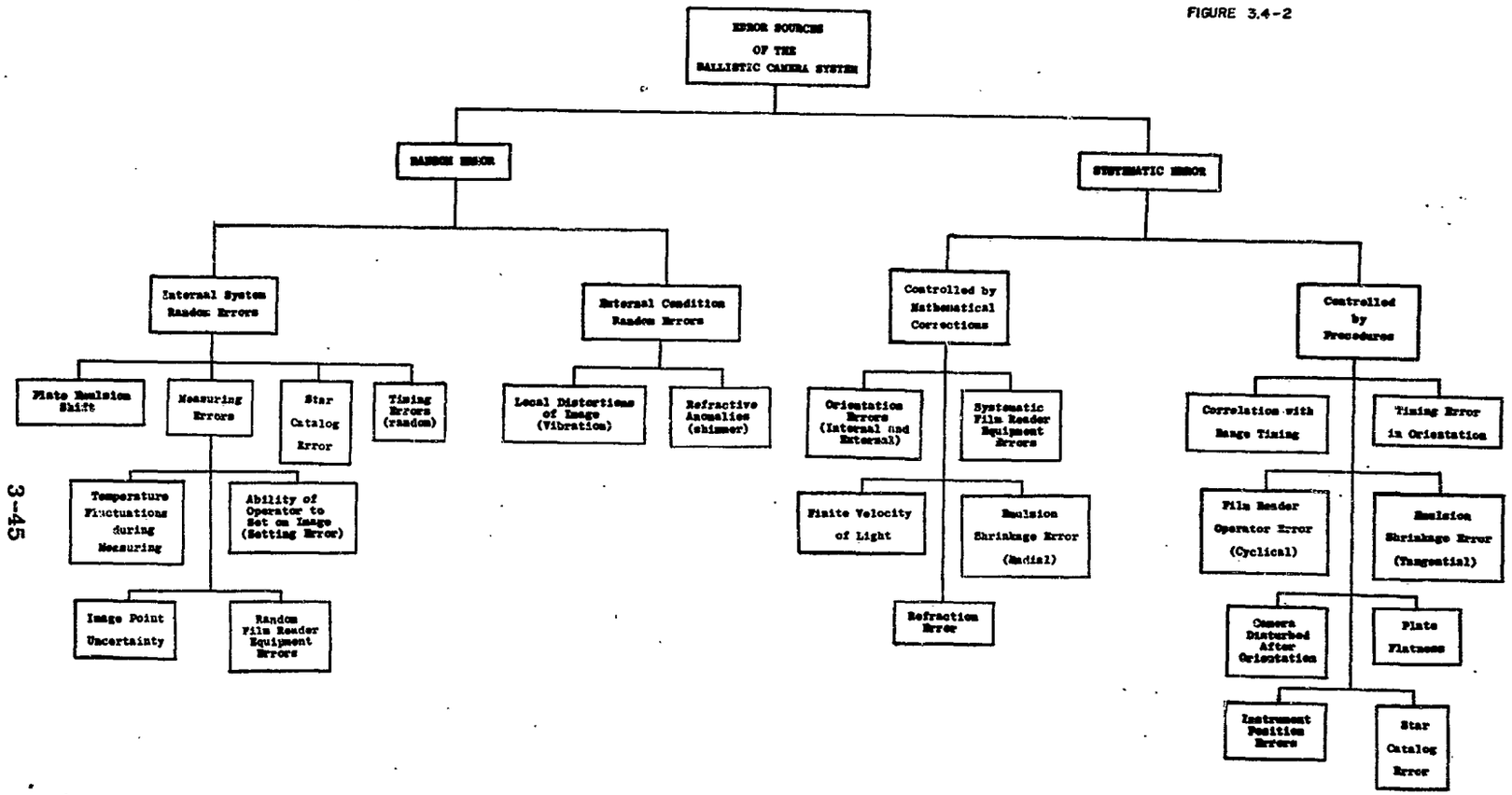
Random errors are defined as those errors which affect the output of the system in an arbitrary manner and can only be described mathematically in terms of probability distributions. Extensive studies have been made to determine the magnitudes of the various random errors and to provide methods for reducing their effects.

The sub-classification "Controlled by Mathematical Corrections" contains those systematic errors which are directly controlled by calibration of the instrumentation or by mathematical correction of the data during the reduction. The sub-classification "Controlled by Procedures" contains those systematic errors which are controlled by implementing proper procedures to limit them to a negligible level. An exception in this category is star catalog error. The influence of this error is dependent on the number of usable stars on the several plates of the test and on the accuracy of the catalog information available on the stars that are used. Generally, the level of the error from this source is much lower in the northern hemisphere than it is in the southern hemisphere. An improved star catalog is under preparation.

"Internal System Random Errors" are defined as those errors which are inherent in the design of the system. The measuring errors and emulsion shift are errors which occur in the digitized plate data. The magnitude of the random error in

SOURCES OF ERROR
BALLISTIC CAMERA SYSTEM

FIGURE 3.4-2



emulsion shift has been determined as 0.7 microns when proper photographic processes are employed in plate development [Starbird, 1964]. The measuring errors are dependent on image quality and film reading conditions. The star catalog errors are discussed above. The random component of star catalog error will affect the final results of the system only indirectly (through the covariance matrix of the triangulation).

"External Condition Random Errors" are defined as those errors which are generated by test conditions. Ballistic camera tests are usually designed to minimize the effect of these error sources.

The modified ballistic camera system is subject to all of the errors mentioned above. Because of poorer image quality, measuring errors are significantly larger. A major additional error found in this system is that of camera to camera time synchronization in the chopping of the image. This source is generally systematic in nature.

3.4.3 System Accuracies

Ballistic camera data characteristics contained in this report are based on an analysis of the data from support tests shown in Tables 3.4-1, 2, 3.

Table 3.4-1
Test Numbers

Conventional Ballistic Cameras (in Support of Mistram and AZUSA Evaluations)		
1911	6665	6556
1954	6254	6743
1839	6276	6433
6494	6434	6434
	6646	

Table 3.4-2
Test Numbers

Conventional Ballistic Cameras (Used to Improve Geodetic Locations)	
3806	6609
4112	4114

Table 3.4-3
Test Numbers

Synchronous Ballistic Camera System (Used to Track Re-Entry Bodies)	
Semi-Synchronous	Full-Synchronous
0104	0158
0040	0225
0037	
0201	
0227	
0430	

3.4.3.1 Accuracy Estimates

Accuracy estimates for the ballistic camera system are given in Tables 3.4-4 and 3.4-5.

Table 3.4-4
Estimates of Accuracy for the
Conventional Ballistic Camera

CAMERA FOCAL LENGTH (in mm)	ERROR ESTIMATES					
	Total Error		Bias Uncertainty		Random Error	
	Coordinate		Coordinate		Coordinate	
	X	Y	X	Y	X	Y
115	3.7	2.3	2.5	1.6	2.7	1.7
210	5.3	2.5	4.2	2.0	3.2	1.5
300	4.7	3.9	2.4	2.0	4.1	3.3
600	3.5	5.6	2.1	4.3	2.8	3.6
1000	3.4	5.3	2.1	4.4	2.7	3.0

Units = Microns at the plate*

Table 3.4-5
Estimates of Accuracy for the
Modified Ballistic Camera

CAMERA FOCAL LENGTH (mm)	NO. OF OPER.	TIMING OF THE CHOPPING SHUTTER	ERROR ESTIMATES					
			Total Error		Bias Uncertainty		Random Error	
			Coordinate		Coordinate		Coordinate	
			X	Y	X	Y	X	Y
300	7	S	13.4	19.6	5.6	13.1	12.2	14.6
210	11	S	2.0	16.1	1.3	11.0	1.5	11.8
300	7	F	4.3	6.0	2.9	4.1	3.2	4.4

S = Semi-Synchronous Timing, F = Full-Synchronous Timing.

Units = Microns at the plate*

*See Page 3-49 for table of unit conversion factors.

TABLE OF UNIT CONVERSION FACTORS

$$\text{Seconds of Arc} = \frac{8.118}{\text{F L in Inches}} \times \text{Microns at the Film Plane}$$

$$\text{Milliradians} = 2.062 \times 10^{2} \times \text{Seconds of Arc}$$

$$\text{Milliradians} = \frac{3.937 \times 10^{-2}}{\text{F L in Inches}} \times \text{Microns at the Film Plane}$$

F L = Focal Length

4.0 PULSED RADARS - LAND BASED

4.1 Procedure for Estimating System Accuracies

4.1.1 Introduction

The investigation of radar errors is oriented toward furnishing the data user with accurate position data and reliable estimates of random and bias errors. In addition to supplying the user with periodic updating information, the following objectives indicate the scope of the endeavor:

(a) To supply Data Processing with estimates of systematic and low-frequency random errors which, combined with high-frequency random error estimates (extracted from the data over 21 - point spans by the variate difference method), are transformed into the XYZ system and published in the Flight Test Data Report as total error estimates.

(b) To determine estimates of random and bias errors from experimental results, particularly for newly installed systems, in order to develop initial and updating information.

(c) To furnish estimates of radar errors in a form suitable for propagation into position and velocity components of Geometrical Dilution of Precision (GDOP), i.e., error magnitudes along the trajectory in the XYZ reference frame, for planning purposes.

(d) To determine the form of the radar error model and to evaluate the coefficients with which raw radar data may be corrected at the radar site or during the data processing stage.

4.1.2 Method of Error Determination

Comparisons are made by means of differences in time-coincident

azimuth, elevation and range (AER) data with respect to data from another independent tracking system of equal data rate and superior precision or accuracy. With the advent of improved BET/GLAD programs in which observations from several tracking instruments are adjusted by least squares, this type of reference is given preference over other comparisons. It is expected that more reliable and more useful results will be obtained from a combined instrument trajectory, particularly when this trajectory has contributions from downrange radars.

4.1.2.1 Flow Diagrams

Figure 4.1-1 illustrates the general approach to radar accuracy evaluations in the form of a flow diagram which characterizes the sequential actions and supporting functions. Figure 4.1-2 shows the details of the Data Processing (Computer) support, applicable processing routines and the data output required for subsequent accuracy analyses. Both figures apply to evaluations as outlined and may be augmented as required.

4.1.2.2 Test Conditions in Support of Accuracy Evaluation

Radar accuracy evaluations pursue the determination of the radar system's performance from several aspects which are characterized below:

a) Instrument performance under ideal (non-fluctuating point source) target signal conditions and controlled dynamic target behavior. This type of evaluation reflects the results from experiments designed to determine basic radar capabilities and limitations.

Figure 4.1-1

ETR PULSE RADAR SYSTEMS ANALYSIS
PLANNING AND PROCESSING

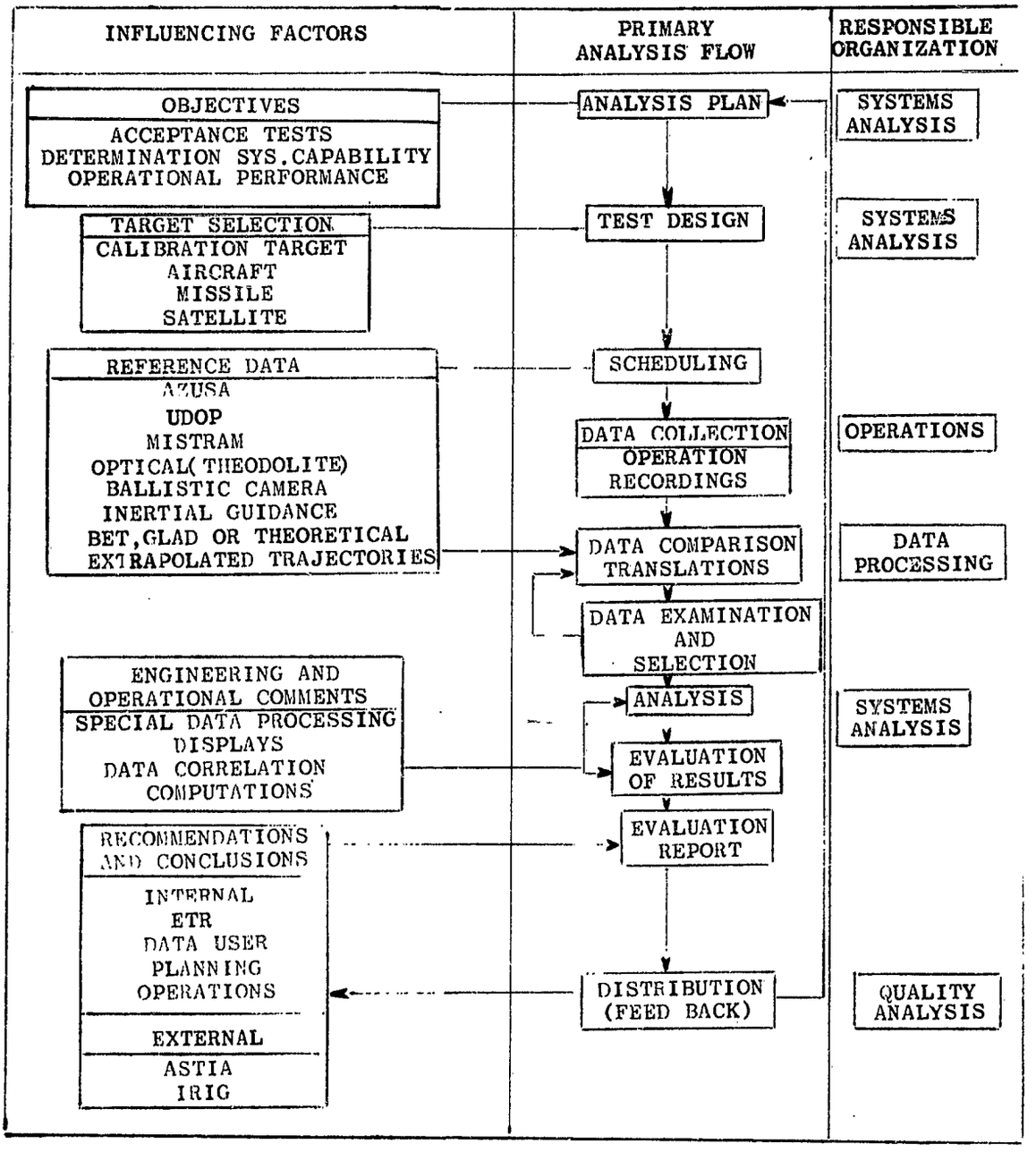
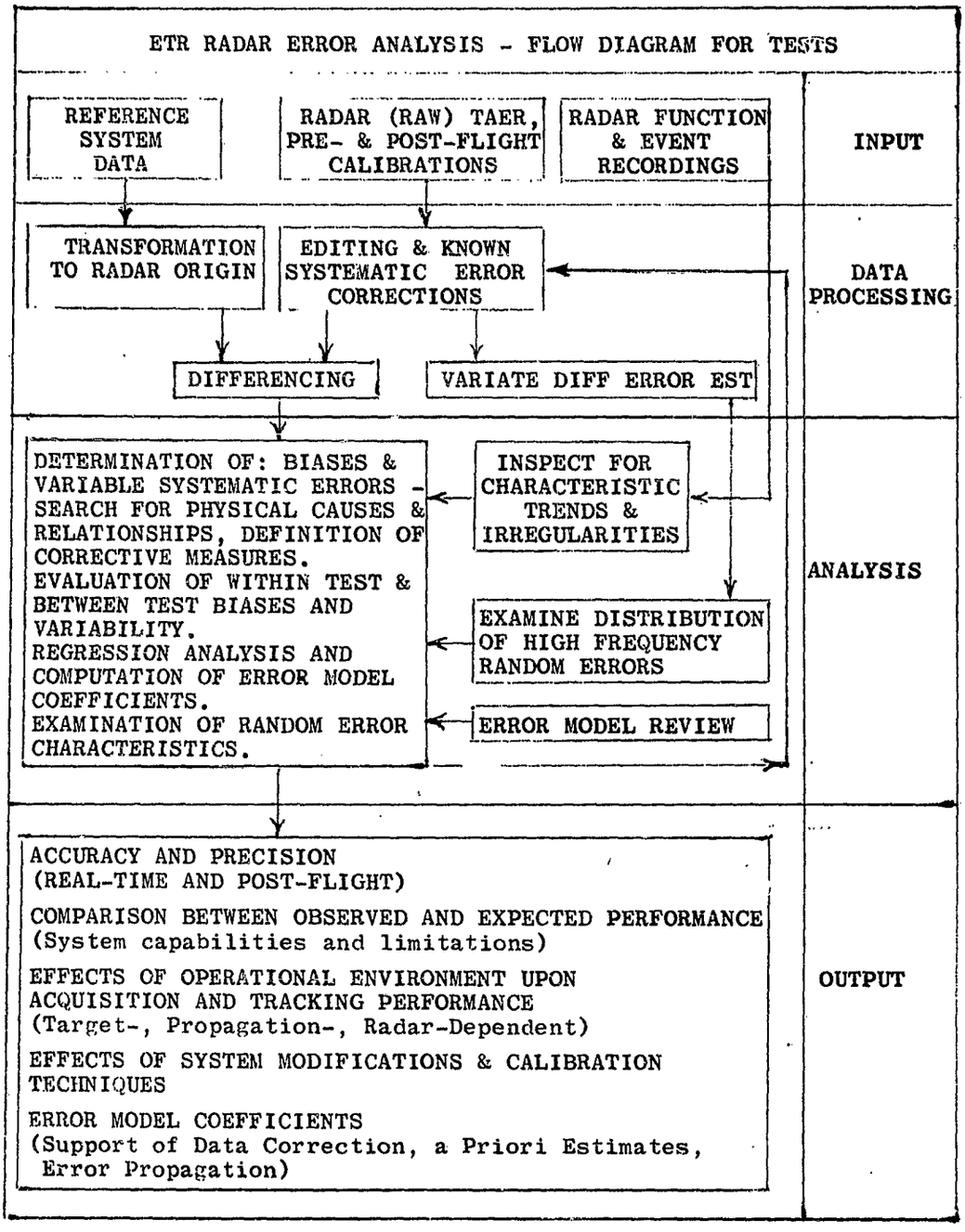


Fig. 4.1-2


ETR RADAR ERROR ANALYSIS - FLOW DIAGRAM FOR TESTS
REFERENCE SYSTEM DATA
RADAR (RAW) TAER, PRE- & POST-FLIGHT CALIBRATIONS
RADAR FUNCTION & EVENT RECORDINGS
INPUT
TRANSFORMATION TO RADAR ORIGIN
EDITING & KNOWN SYSTEMATIC ERROR CORRECTIONS
DIFFERENCING
VARIATE DIFF ERROR EST
DATA PROCESSING
DETERMINATION OF: BIASES & VARIABLE SYSTEMATIC ERRORS - SEARCH FOR PHYSICAL CAUSES & RELATIONSHIPS, DEFINITION OF CORRECTIVE MEASURES.
EVALUATION OF WITHIN TEST & BETWEEN TEST BIASES AND VARIABILITY.
REGRESSION ANALYSIS AND COMPUTATION OF ERROR MODEL COEFFICIENTS.
EXAMINATION OF RANDOM ERROR CHARACTERISTICS.
INSPECT FOR CHARACTERISTIC TRENDS & IRREGULARITIES
EXAMINE DISTRIBUTION OF HIGH FREQUENCY RANDOM ERRORS
ERROR MODEL REVIEW
ANALYSIS
ACCURACY AND PRECISION (REAL-TIME AND POST-FLIGHT)
COMPARISON BETWEEN OBSERVED AND EXPECTED PERFORMANCE (System capabilities and limitations)
EFFECTS OF OPERATIONAL ENVIRONMENT UPON ACQUISITION AND TRACKING PERFORMANCE (Target-, Propagation-, Radar-Dependent)
EFFECTS OF SYSTEM MODIFICATIONS & CALIBRATION TECHNIQUES
ERROR MODEL COEFFICIENTS (Support of Data Correction, a Priori Estimates, Error Propagation)
OUTPUT

b) Instrument performance under operational missile-tracking conditions. This type of evaluation, concentrating on one radar or on one missile-type at a time, determines the effects of target-dependent signal conditions and dynamic loads peculiar to the station trajectory geometry. Comparisons of the results from these studies with those of a) indicate the degree of data degradation due to non-ideal target characteristics.

c) Test-by-test evaluation of operational tracking performance. This type of evaluation verifies the tracking precision and accuracy of all radars participating in missile data acquisition in the quality control sense. The results of these evaluations serve to establish standards of performance by radar and missile type, monitor trends and consistency, detect departures requiring special investigations, and assist planning functions.

4.1.2.3 Mathematical Model for Treatment of Error Data

We shall consider a residual to mean the <u>difference</u> (ΔA, ΔE, ΔR), between radar observation at a given instant, t, and the estimate of the true trajectory from a reference system (e.g., BET or GLAD).

Let x_{ijk} denote the kth residual in the jth span of the ith test ($i = 1, 2, \ldots n$, $j = 1, 2, \ldots n_i$ $k = 1, 2, \ldots n_{ij}$)

The x_{ijk} is part of a model:

$$x_{ijk} = \mu_i + \gamma_{ij} + e_{ijk} \qquad (1)$$

In which the following are assumed:

a) $\mu = 0$ (or constant, bias)
b) $\mu_i \cong$ Normally distributed (μ, σ_b^2)
c) $\gamma_{ij} \cong$ Normally distributed $(0, \sigma_w^2)$
d) $e_{ijk} \cong$ Normally distributed $(0, \sigma_o^2)$

Unless a means is available for removing the error of the reference, the radar error estimates will of course, contain this component.

In the data processing phase, residuals are combined over 20-second spans and the means and standard deviations are extracted for detailed analysis. In summarizing for periodic reports, the span means, by test, are subjected to analysis of variance in order to obtain the within-test and between-test estimates of variability. The standard deviations about span means are pooled to provide estimates of random error. The pooled random error is obtained by weighting the standard deviation of residuals about each span mean by the degrees of freedom, f, per Equation (2).

$$s_o^2 = \sum_j f_j \sigma_j^2 / \sum_j f_j \qquad (2)$$

Between-test and within-test components combine as shown in Equation (3) to form an estimate of the bias error variance, s_B^2:

$$s_B^2 = s_b^2 + s_w^2 \qquad (3)$$

where the subscripts b and w denote between-test and within-test components over the several test results considered.

An estimate of the variability expected during a particular test may be obtained from a combination of the within-test error, s_w and the random error, s_o similar to that shown by Equation (3).

For an estimate of total error that may be expected for any test at any time, combination of bias and random components as shown in Equation (4) may be used.

$$s_T^2 = s_B^2 + s_o^2 \qquad (4)$$

These errors may be propagated into position and velocity GDOPs by combining them as shown below:

CONDITION	VARIANCE
Any test, any time:	$(s_b^2 + s_w^2 + s_o^2)$
Specific test:	$(s_w^2 + s_o^2)$

Input for the second category shown will yield smaller dispersion and may be applied when the uncertainty of between-test bias may be ignored.

4.2 Error Sources

The errors of a tracking radar in measuring Azimuth, Elevation and Range to a target are composed of contributions by the radar itself, the propagation medium, and the target.

4.2.1 Pulsed Radar Error Model

For analysis of the effects of individual errors upon the radar data accuracy, for realistic error budgeting, and for propagation of errors into spatial coordinates, the known error components are suitably arranged in the form of an error model. For the land-based radars, an error model has been formulated which refers to terms of systematic and random nature and accounts with separated equations for the errors peculiar to each tracking coordinate (Azimuth, Elevation, Range). The error model, deliberately, encompasses only those terms which can be related to physically measurable quantities of mechanical and electrical nature with magnitudes near or larger than the data resolution, and which can be theoretically predicted on the basis of physically established relationships. The error model equations are listed in Figure 4.2-1 with a breakdown of the systematic errors and their sources, and Figure 4.2-2 gives a separate account of the components of variance representing the data noise sources.

The category of systematic errors (Figure 4.2-1) comprises misalignments in the nature of bias and those low-frequency error components which are not amenable to mathematical smoothing but rather to position data corrections which can be described in functional form. The e_A, e_E and e_R terms represent residual random and unmodeled error.

The category of noise type errors refers to the sources of tracking jitter of random or oscillatory character about constant mean values, and considers those components which do not permit point-to-point correction but can be improved by mathematical smoothing.

The AN/FPS-16 radars permit on-site error model corrections only for fixed (static)misalignments, e.g. orientation, and beacon delay. In contrast, the RCA-4101 real-time processor of the AN/FPQ-6 and AN/TPQ-18 radars applies real-time error model corrections to the radar angle data which are derived from stored calibrations and measurements of residual servo errors. The error model terms covered by the 4101 processor are indicated by asterisks in Figure 4.2-1 and stress the intention of generating real-time radar data with minimized systematic error components.

Except by implication in the terms e_A, e_E and e_R, the error model of Figures 4.2-1 and 4.2-2 does not list potential error sources such as angle balance point shifts due to RF phase-front distortion or flame interference effects, since events of this type are either external to the radar or non-standard in occurrence and thus are not readily subject to mathematical predictions.

TRACKING RADAR ERROR MODEL

$$\Delta A(t) = \overbrace{a_o^* + a + g_a}^{\text{Static}} + \overbrace{a_1 \dot{A}(t) + a_2 \ddot{A}(t) + a_3 \dddot{A}(t)}^{\text{Dynamic*}} + \overbrace{a_4 \sin A(t) \tan E(t) + a_5 \cos A(t) \tan E(t)}^{\text{Mislevel*}}$$
$$+ \overbrace{a_6 \sec E(t)}^{\text{Misalignment*}} + \overbrace{a_7 \tan E(t)}^{\text{Non-orthog.*}} + \overbrace{a_8 R(t) \dot{A}(t)}^{\text{Time Dilation}} + \overbrace{a_9 f_A(\lambda)}^{\text{Boresight Shift*}} + \overbrace{a_{10} \sin A(t) + a_{11} \cos A(t)}^{\text{Encoder Non-linearity*}} + e_A$$

$$\Delta E(t) = \overbrace{b_o^* + b + g_b}^{\text{Static}} + \overbrace{b_1 \dot{E}(t) + b_2 \ddot{E}(t) + b_3 \dddot{E}(t)}^{\text{Dynamic*}} + \overbrace{b_4 \cos A(t) + b_5 \sin A(t)}^{\text{Mislevel*}} + \overbrace{b_6 h_e}^{\text{Misalignment*}}$$
$$+ \overbrace{b_7 p}^{\text{Residual Refraction}} + \overbrace{b_8 R(t) \dot{E}(t)}^{\text{Time Dilation}} + \overbrace{b_9 f_h(\lambda)}^{\text{Boresight Shift*}} + \overbrace{b_{10} \sin E(t) + b_{11} \cos E(t)}^{\text{Encoder Non-linearity*}} + \overbrace{b_{12} \cos E(t)}^{\text{Droop*}} + e_E$$

$$\Delta R(t) = \overbrace{c_o^* + c + g_c}^{\text{Static}} + \overbrace{c_1 \dot{R}(t)^{**} + c_2 \ddot{R}(t) + c_3 \dddot{R}(t)}^{\text{Dynamic}} + \overbrace{c_4 f(S/N)}^{\text{Beacon Delay}} + \overbrace{c_5 p}^{\text{Residual Refraction}} + \overbrace{c_6 R(t) \dot{R}(t)}^{\text{Time Dilation}}$$
$$+ \overbrace{c_7 R(t)}^{\text{Reference Oscillator}} + \overbrace{c_8 \sin(\omega R(t)) + c_9 \cos(\omega R(t))}^{\text{Resolver Non-linearity*}} + e_R$$

* Denote provisions for real-time corrections by RCA-4101 processor in AN/FPQ-6 and AN/TPQ-18 radars.

** Applies to AN/FPS-16 radars only.

Figure 4.2-1

TRACKING RADAR COMPONENTS OF NOISE VARIANCE

$$\sigma_A^2 = \sigma_{th}^2 + \sigma_g^2 + \sigma_p^2 + \sigma_m^2 + \sigma_\alpha^2$$

(Thermal + Glint + Propagation + Mechanical + Residual Variance)

$$\sigma_E^2 = \sigma_{th}^2 + \sigma_g^2 + \sigma_{f_E(E)}^2 + \sigma_p^2 + \sigma_m^2 + \sigma_\beta^2$$

(Thermal + Glint + Multipath Propagation + Mech. + Residual Variance)

$$\sigma_R^2 = \sigma_{th}^2 + \sigma_g^2 + \sigma_{f_R(E)}^2 + \sigma_p^2 + \sigma_b^2 + \sigma_m^2 + \sigma_\gamma^2$$

(Thermal + Glint + Multipath Propagation + Beacon Jitter + Mech. + Residual Variance)

Figure 4.2-2

The coefficients of the various error model terms are determined by means of measurements performed in connection with the system design and manufacture, by experiments and calibrations conducted in the field, by theoretical predictions, or upon analysis of tracking error data.

4.2.2 Error Breakdown by Frequencies

It may be desirable to separate the errors into classes which are analogous to frequency bands and which relate to the physical system's characteristics:

a) <u>High Frequency Errors</u> (0.5 cps $\leq f_c \leq f_N$ * cps)

These errors are primarily due to receiver thermal noise, random mechanical disturbances, data granularity and target signal fluctuations.

b) <u>Low Frequency Errors</u> ($\frac{1}{2.26T}$**cps $\leq f_c <$ .5 cps)

These deviations reflect dynamic lags due to target motion, long-term beacon delay variations, target-induced balance point shifts, refraction correction errors, etc.

c) <u>Virtual Zero Frequency Errors</u> (0 cps $\leq f_c \leq \frac{1}{2.26T}$**cps)

The errors in this category are biases which are considered constant during a test and originate from zero-setting, system alignment, delay corrections, and changes due to the boresight conditions of the pre-flight check and operational flight conditions.

*f_N - Nyquist frequency = to 1/2 the data sampling rate

**T - length of data span in seconds

4.3 C-BAND RADARS

4.3.1 Systems Description

4.3.1.1 General

The Eastern Test Range C-Band tracking radars are represented by systems of the AN/FPS-16 and AN/FPQ-6 types. The AN/FPS-16 radars include the AN/MPS-25 as a trailerized version, whereas the AN/FPQ-6 radars include the AN/TPQ-18 as a transportable model. These radars have been designed specifically as high-precision instrumentation radars for missle echo and beacon tracking applications. Interference-free multiple radar coverage on beacon targets is accomplished by controlled beacon time-sharing. The present locations of these radars provide ETR with a chain of radars which are compatible and complementary. Their designations and locations (exclusive of shipborne systems) are listed in Table 4.3-1.

TABLE 4.3-1

Designation, Type and Location of ETR C-Band Radars

DESIGNATION	TYPE	LOCATION
1.16	AN/FPS-16	Cape Kennedy
19.18	AN/TPQ-18	Merritt Island
0.18	AN/FPQ-6	Patrick AFB
3.18	AN/TPQ-18	Grand Bahama Island
3.16	AN/FPS-16	Grand Bahama Island
5.16	AN/FPS-16	San Salvador Island
7.18	AN/TPQ-18	Grand Turk Island
91.18	AN/FPQ-6	Antigua Island
12.16	AN/FPS-16	Ascension Island
12.18	AN/TPQ-18	Ascension Island
13.16	AN/MPS-25	Pretoria, S. Africa

The tracking performance achieved during a particular test depends largely on target parameters (e.g., tracking geometry, radar cross-sectional area, beacon system characteristics) and, consequently, predictions of coverage and performance are derived individually under consideration of these factors. In general, the limits of full-performance coverage are determined on the basis that the signal-to-noise ratio (S/N) shall be sufficient to hold random errors below a specified level, taking into account the tracking servo bandwidth and P.R.F. required during the test. Regardless of the S/N criteria, track is maintained until loss of signal except when terminated by operation directive (such as to observe beacon sharing limitations). At present, there are three commitment criteria:

a) For Range Safety purposes, commitments are limited to S/N $\geq$ 6 db and:

ELEVATION ANGLE	AN/FPS-16	AN/FPQ-6
At Acquisition	$\geq 2^{o}$	$\geq 2^{o}$
At Loss of Track	$\geq 2^{o}$	$\geq 0.5^{o}$

b) For Metric Data Commitment, the criteria are designed to avoid engaging the radars under tracking conditions handicapped by inherent random errors greater than 0.2 mils in angle data. Elevation criteria are as in (a), above. Additional criteria for AN/FPS-16 radars: S/N $\geq$ 20 db if PRF = 160 and if angle servo bandwidth is 1.2 to 2.4 cps. Additional criteria for AN/FPQ-6 radars: S/N $\geq$ 15 db if PRF = 160 and the radar operates with medium angle servo bandwidths.

c) For Data Publication, the criteria are designed to make available a maximum amount of reliable data. The criteria are that elevation $\geq 1.5^{o}$, S/N $\geq$ 12 db, and that data quality appear uniform, unless altered by data user. The criterion of elevation $\geq 1.5^{o}$ may not be followed strictly at short slant ranges.

These criteria were followed in the selection of data used in the accuracy evaluations contained in this report.

Analog/F-M converted AGC measurements of AN/FPS-16 radars can be processed on a production basis to provide digital data of signal power (S/N) or of radar cross-sectional area (A_e) at sampling rates of 100/sec.(unfiltered) or 10/sec. (filtered). With the presently employed calibration and processing methods, the quality of radar cross-sectional area data is characterized by errors of less than 3 db at the 95% confidence level for measurements taken within the signal limits 10 db $\leq$ S/N $\leq$ 50 db.

4.3.1.2 AN/FPS-16 and AN/MPS-25 Radars

The AN/FPS-16 radar was designed specifically to provide accurate and precise position measurements for missile and satellite tracking. The radars operate on the monopulse principle, and each radar provides a set of original position measurements in spherical coordinates independent of external tracking instrumentation. The up-range and mid-course radars are linked so that they can be "slaved" and thereby assist one another in acquiring a target. Echo and beacon-track operation are both commonly used, but beacon tracking applications are predominant at ETR. The AN/MPS-25 radar is essentially identical to the AN/FPS-16 except that it is housed in a trailer and has a larger antenna. A unique feature of these radars is their capability of being plunged, i.e., their elevation angle covers 180 degrees, so that they may be boresighted in two positions (normal and plunged). Some measurement characteristics are shown in Table 4.3-2.

TABLE 4.3-2

AN/FPS-16 and AN/MPS-25 RADAR MEASUREMENT CHARACTERISTICS

CHARACTERISTIC	ANGLE	RANGE
Word Capacity	17 Bits	20 Bits
Resolution, Least Significant Digit	.0488 mil	3 Feet
R_n* (Echo Track, 1 m^2 Target, S/N = 0 db, Ant. Dia. = 12 ft.)		270 Kyds
Data Rate (except 12.16 & 13.16)	10 pps	10 pps
R_n* MPS-25, (Ant.Dia. = 16 ft.)		360 Kyds
Data Rate (13.16 & 12.16)	20 pps	20 pps

* R_n: Range capability normalized for listed conditions

4.3.1.3 AN/FPQ-6 and AN/TPQ-18 radars

These radars are second-generation systems to the AN/FPS-16 metric tracking instruments with the following improvements:

a) Tracking capability to greater distances achieved by: 1) increased transmitter power, 2) higher antenna gain and 3) greater receiver sensitivity.

b) Higher angle tracking precision, resulting from use of hydraulic instead of electric angle drive systems and hydrostatic azimuth bearing.

c) Extension of unambiguous range during continuous track at high PRF to maximum range, through the use of digital servo techniques.

d) Incorporation of features facilitating rapid target detection and lock-on.

e) Capability of real-time data corrections, achieved by use of an RCA-4101 computer. The AN/TPQ-18 is identical to the FPQ-6 except that it is housed in transportable modular shelters. Some measurement characteristics are listed in Table 4.3-3

TABLE 4.3-3

AN/FPQ-6 and AN/TPQ-18 MEASUREMENT CHARACTERISTICS

CHARACTERISTIC	ANGLE	RANGE
Word Capacity	19 Bits	25 Bits
Resolution, Least Significant Digit	.122 mil	5.86 ft.
R_n* (Echo Track, 1 m^2 Target, S/N = 0 db, Ant. Dia = 20 ft.)		925 Kyds
Data Rate	20 pps	20 pps

*R_n: Range Capability normalized for listed conditions.

4.3.2 System Accuracies

C-Band Radar accuracy estimates and data characteristics contained in this report are based on analysis of data from the missile tests shown in Table 4.3-4.

Tables 4.3-5 and 4.3-6 give current estimates of C-Band radar accuracies. The experimental results for radars 19.18 and 91.18 (Table 4.3-6) are based on only six tests each, hence are still tenuous. This applies particularly to the between-test component of bias error.

F-ratio tests were made at the 5% level of significance with the following results.

For range errors only, F-ratio tests of within-test and random error variances, ($F = s_w^2/s_o^2$), indicated significance for all radars except 7.18. This is interpreted as indication that external effects, such as beacon anomalies, variation in refraction and refraction corrections themselves, as well as uncertainties in the reference instrument, contribute to the range variability within a test for both C-Band radar types.

In the analysis of variance, F-ratio tests of the between-test and within-test mean squares are significant and indicate that the magnitude of between-test variability is significant for all C-Band radars, in all three coordinates. Thus one surmises that improvements in the zero-set and alignment areas may result in greater calibration consistency between tests.

The mean biases of all C-Band radars appear reasonably close to zero in the angle coordinates but not in range. Notable exceptions appear to be radars 0.18 and 7.18 in which elevation biases were greater than expected. These are being investigated to determine the course of appropriate corrective actions or calibration techniques.

TABLE 4.3-4

TESTS, MISSILES, AND TIME SPANS OF DATA IN RADAR ANALYSES

TEST	MISSILE	TIME SPAN Seconds
Radar 0.18		
45	Polaris	193 - 313
136	Delta Sysncom	33 - 433
169	Saturn	45 - 115
448	Ranger	65 - 300
2769	Saturn	13 - 246
2925	Atlas	60 - 260
4307	OGO	132 - 233
4444	Saturn	37 - 137
4751	Titan	123 - 342
5145	Atlas	182 - 348
5800	Mariner C	120 - 300
6505	Titan III	23 - 403
		360 - 520

TABLE 4.3-4 (Cont.)

TIME, MISSILES, AND TIME SPANS OF DATA IN RADAR ANALYSES

TEST	MISSILE	TIME SPAN Seconds
Radar 19.18		
136	Delta Syncom	35 - 495
2769	Saturn	25 - 145
4751	Titan	123 - 343
6505	Titan III	63 - 403
		360 - 500
Radar 7.18		
136	Delta Syncom	172 - 512
448	Ranger	228 - 288
2769	Saturn	312 - 492
4444	Saturn	217 - 297
4751	Titan	220 - 340
5800	Mariner C	320 - 490
6505	Titan III	229 - 389
Radar 91.18		
169	Saturn	630 - 809
448	Ranger	420 - 520
5800	Mariner C	480 - 540
6900	Delta Imp	397 - 477
6505	Titan III	427 - 862
Radar 1.16		
136	Delta Syncom	71 - 491
169 I & II	Saturn	12 - 372
448	Ranger	75 - 300
3303	Titan	211 - 271
4307	OGO	93 - 319
4444	Saturn	14 - 377
4951	Minuteman	7 - 49
6001	Minuteman	8 - 171

TABLE 4.3-4 (Cont.)

TESTS, MISSILES AND TIME SPANS OF DATA IN RADAR ANALYSES

TEST	MISSILE	TIME SPAN Seconds
Radar 3.16		
136	Delta Syncom	53 - 313
169	Saturn	100 - 423
448	Ranger	90 - 360
3303	Titan	82 - 325
4307	OGO	85 - 325
4444	Saturn	114 - 237
4951	Minuteman	46 - 145
6001	Minuteman	37 - 159
8505	Titan III	110 - 390
		360 - 440
Radar 5.16		
136	Delta Syncom	113 - 633
169	Saturn	172 - 554
201	Minuteman	80 - 141
3303	Titan	151 - 311
4444	Saturn	153 - 297
4951	Minuteman	102 - 142
		635 - 675
6001	Minuteman	77 - 159

TABLE 4.3-5

ACCURACY ESTIMATES, C-BAND RADARS

SYSTEM: AN/FPS-16 and AN/MPS-25 s_o = Random Err: Std Dev,Ind Obsvns about Span Mean

MISSILE TYPES: ALL s_w = W/in Test: Std Dev,Span Means about Test Mean

TRACKING MODE: BEACON s_b = Between T: Std Dev,Test Means about Grand Mean

RADAR NO. TESTS	COORDINATE	s_o	s_w	s_b	TEST PERIOD
1.16 (11)	Az (mil)	0.099	0.066	.051	Sept.63 - Dec. 64
	El (mil)	.119	.077	.116	
	R (Ft)	6.1	13.4	33.7	
3.16 (11)	Az (mil)	.086	.080	.074	Oct.63 - Dec. 64
	El (mil)	.167	.184	.112	
	R (Ft)	8.4	24.8	43.6	
5.16 (8)	Az (mil)	.114	.070	.067	Oct.63 - Dec. 64
	El (mil)	.157	.120	.077	
	R (Ft)	12.2	24.8	57.8	

NOTE: Estimates for radars 12.16 and 13.16 omitted for lack of sufficient comparison data.

TABLE 4.3-6

ACCURACY ESTIMATES, C-BAND RADARS

SYSTEM: AN/FPQ-6 and AN/TPQ-18
MISSILE TYPES: SEE TABLE 4.2.2.3
TRACKING MODE: BEACON

s_o = Random Err: Std.Dev.,Ind Obsvns about Span Mean
s_w = W/in Test: Std.Dev, Span Means about Test Mean
s_b = Between T: Std.Dev, Test Means about Grand Mean

RADAR	NO. TESTS	COORDINATE	s_o	s_w	s_b	TEST PERIOD
19.18	(6)	Az (mil)	0.055	0.056	0.083	May 64 - Dec. 64
		El (mil	.067	.104	.053	
		R (ft)	5.5	22.5	110.5	
0.18	(15)	AZ (mil)	.069	.040	.082	Oct.63 - Dec. 64
		EL (mil)	.117	.082	.195	
		R (ft)	7.8	16.0	62.5	
7.18	(7)	AZ (mil)	.071	.034	.110	July 64 - Dec. 64
		El (mil)	.132	.072	.119	
		R (ft)	7.4	13.9	73.7	
91.18	(6)	Az (mil)	.116	.041	.053	Oct.63 - Dec. 64
		El (mil)	.177	.111	.046	
		R (ft)	9.9	37.1	114.1	

NOTE: Estimates for radar 12.18 omitted for lack of sufficient comparison data.

4.4 S-BAND RADARS (MOD II)

4.4.1 System Description

The ETR MOD II radar is an outgrowth of the SCR-584 radar for missile tracking applications. It has improved angle and range tracking performance, operates on echo or beacon targets and records high-resolution data on paper tape. The distribution and location of ETR MOD II radars are given in Table 4.4-1, and some of the radar's measurement characteristics in Table 4.4-2.

TABLE 4.4-1

LOCATIONS OF ETR MOD II RADARS

STATION	NUMBER	LOCATION
1	3	Cape Kennedy
3	2	Grand Bahama Island
5	1	San Salvador Island
7	1	Grand Turk Island
12	1	Ascension Island

TABLE 4.4-1

MOD II RADAR MEASUREMENT CHARACTERISTICS

CHARACTERISTIC	ANGLE	RANGE
Word Capacity	N/A	N/A
Resolution Least Significant Digit	.1 mil	3 ft.
R_n *(Echo Track, 1 m^2 Target, S/N = 0 db, Ant. Dia. = 10 ft.)		80 Kyd
Data Rate	2 pps	2 pps

* R_n: Range capability normalized for listed conditions.

4.4.2 System Accuracies

Comments which apply to the estimates of total dispersion and bias given in Table 4.4-3 are as follows:

The operationally observed data precision applies to beacon track at a receiver S/N ratio exceeding 12 db. In echo track, the angular dispersions usually increase as the result of glint and/or signal scintillations, showing a typical data quality degradation between 20% and 30%.

The angle tracking precision refers to track at elevation angles above 2.5^{o}.

The use of instrumentally smoothed angle track is limited to those conditions where the dynamic lags due to angular accelerations can be tolerated. Lag errors of 1 mil are experienced at $\ddot{A}, \ddot{E} \simeq 0.017^{o}/sec^{2}$ when operating with the shortest filter constant of the smoothing units, and the acceleration capabilities decrease in the other smoothing steps according to their time constant.

Metric Data Commitments and Range Safety Commitments are based on tracking conditions such that Elevation $\geq 2.5^{o}$ and S/N $\geq$ 12 db.

TABLE 4.4-3

ACCURACY ESTIMATES, S-BAND (MOD II) RADARS

	Az (mil)	El (mil)	R (ft.)
s_{random}	1.5	1.5	45
s_{bias}	1	1	100

4.5 X-BAND RADARS (MOD IV)

4.5.1 System Description

Two X-Band radars of the NIKE AJAX type, modified as MOD IV "High Resolution Trackers" are located at Cape Kennedy and operated for the specific purpose of providing present-position plotting board information during the early flight phase of missile launches.

Forthcoming equipment with digital encoders will permit use of these radars as data sources for the real-time Impact Prediction computer. Some of the measurement characteristics are listed in Table 4.5-1 and accuracies in Table 4.5-2.

To achieve fine angle tracking accuracy as early as possible after launch, both radars are equipped with infrared detectors (IR), which are used to control the radar's angle tracking servo systems during the time when multipath and target glint would degrade the angle data quality in the radar mode. The range measurements must be obtained by radar echo track.

TABLE 4.5-1

X-BAND RADAR (MOD IV) MEASUREMENT CHARACTERISTICS

CHARACTERISTIC	ANGLE	RANGE
Word Capacity (Planned)	18 Bits	17 Bits
Resolution, Least Significant Digit	0.0244 mil	3 ft.
R_n*(Echo Track, 1 m^2 Target, S/N = 0 db, Ant. Dia. = 6 ft.		57 Kyd
Data Rate	10 or 20 pps	

* R_n: Range capability normalized for listed conditions

4.5.2 System Accuracies

TABLE 4.5-2

ACCURACY ESTIMATES X-BAND (MOD IV) RADARS

	Spherical			Plotting Board (Ft)		
	Az(mil)	El(mil)	R(ft)	X	Y	Z
s_{random}	0.2	0.2	30	7	7	7
s_{bias}	.3	.3	50	20	20	60

4.6 UHF DOWNRANGE RADAR (TRINIDAD)

4.6.1 System Description

The Trinidad UHF Radar system, consisting of an AN/FPS-43 tracker and an AN/FPS-44 scanner, is operated by ETR in support of missile tests, space vehicle observations and radar signature studies of single and multiple targets. To perform these functions, the radar is designed for echo track of small targets at very long distances, for measurements of target reflectivity in different signal return polarizations and for measurements of target velocity by means of the pulse-doppler principle. Some measurement characteristics are given in Table 4.6-1.

In addition to the basic RF characteristics of the AN/FPS-43, which are similar to those of the M.I.T. Millstone Hill Radar, the system includes pulse compression for improved target signal-to-noise ratio and for increased resolution in the range coordinate. The data recording facilities are designed to acquire all data essential to meet the system's application objectives (see Table 4.6-2).

TABLE 4.6-1

UHF RADAR (AN/FPS-43) MEASUREMENT CHARACTERISTICS (METRIC DA

CHARACTERISTIC	ANGLE	RANGE	SIGNAL AMPLITUDE
Resolution at LSD,* Magtape (30 pps)	E = 0.01098° A = .00549°	30 ft.	0.2 db (S/N Dependent)
Resolution at LSD,* Teletype (100 wds/min)	.01°	0.01 N.M.	

* LSD: Least Significant Digit

TABLE 4.6-2

AN/FPS-43 RADAR DATA ACQUISITION CHARACTERISTICS (SIGNAL AMPLITUDE DATA)

a. Film Recording 1) Log Amplitude vs. Time (pulse-to-pulse), both polarizations, tracked target only. 2) Log Amplitude vs. Range (pulse -to-pulse), 2 FRT segments, tracked polarization. 3) Log Amplitude vs. Range (pulse-to-pulse, 15 FRT segments, tracked polarization. 4) Log Amplitude intensified vs. Range vs. Time, 2 FRT segments, tracked polarization. 5) Log Amplitude intensified vs. Range vs. Time, 15 FRT segments, tracked polarization.
b. Strip Chart Recording 1) Visicorder Log Amplitude vs. Time (pulse-to-pulse), both polarizations, tracked target only. 2) CRT Recorder Range/Amp. Intensified vs. Time, 15 FRT segments, tracked polarization.
c. IF Tape Recording (Mag. Tape) Time, rel. Range, Amplitude (pulse-to-pulse), both polarizations, all target.

NOTE: Playback of the tape recordings c. through the radar receiver produces digital amplitude and relative range data (at 30/sec) of the targets selected for playback track, and film recordings corresponding to a.1) through a.5). The playback operation provides the above data in both polarizations.

4.6.2 System Accuracies

The tracking accuracy of the AN/FPS-43 radar was studied by using translated data from overlapping C-Band radar coverages as reference values or by analyzing orbital residuals. As the result of tracking geometry and error propagation, the listed values reflect the combined errors of radar and reference data and, consequently, will be conservative estimates of the Trinidad Tracker's accuracy. Since echo track is the standard operating mode, the tracking errors will vary with the echo level and its scintillation content. The listed values refer to spans of data where the signal-to-noise ratio is fairly consistent and above 12 db.

The angle tracking performance of the Trinidad Tracker is characterized by large low-frequency error components (between 0.1 and 0.2 cps), whereas the digital range tracker does not indicate pronounced cyclic components in the error frequency spectrum.

Table 4.6-3 gives the current estimates of the Trinidad Radar's accuracies.

TABLE 4.6-3 ACCURACY ESTIMATES, UHF AN/FPS-43 RADAR (TRINIDAD

Parameter (1)		Az (Deg)	El (Deg)	Range	Signal Amplitude
Magtape (MTU) Data (2)					
AT Mode	s_{Random}	0.2	0.2	25 Kft	1 db
	s_{Bias}	.15	.15	15 Kft	
FRT Mode	s_{Random}	.2	.2	-100 Ft	
	s_{Bias}	.15	.15	2 Kft	
Punched Tape (TTY) Data (3)					
AT Mode	s_{Random}	.35	.2	8.5 n.m.	
	s_{Bias}	.07	.22	7 n.m.	
FRT Mode	s_{Random}	.2	.2	2 n.m.	
	s_{Bias}	.08	.22	0.9 n.m.	

(1) Accuracy of measured parameters depends on the received signal-to-noise ratio.

(2) Obtained from comparisons with ETR Radars.

(3) Obtained from analysis of orbital residuals.

5.0 PULSED RADARS - SHIPBORNE

5.1 Advanced Range Instrumentation Ships (ARIS)

5.1.1 System Description

The Advanced Range Instrumentation Ships (ARIS) systems are contained in two ships, the General H. H. Arnold (ARIS I), and the General H. S. Vandenberg (ARIS II) which are essentially identical with respect to design tracking capabilities. Figure 5.1-1 shows the physical arrangement of the equipment and a block diagram of signal flow paths between subsystems. The subsystems essential to collection of metric data are:

(1) The Integrated Instrumentation Radar, IIR;

(2) The Navigation and Stabilization subsystem;

(3) The Optical Equipment subsystem;

(4) The Data Handling subsystem; and

(5) The Meteorological subsystem.

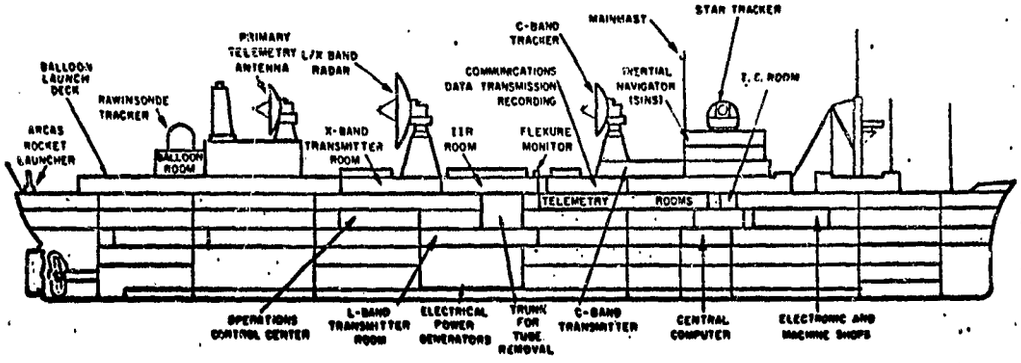
Additional capabilities include collection of telemetry data and signature data as described elsewhere in this document.

The IIR consists, in part, of a C-band tracking radar capable of providing accurate coordinates of range, elevation and train with respect to the reference orientation of its mount. The Stabilization and Navigation subsystem provides correctors for the radar coordinates to permit translation to coordinate systems common to other range instrumentation (see Section 8.3). Additional coordinate correctors are provided by the Flexure Monitor Optical Equipment to correct for flexure of the ship between the radar mount and the stable platform. The meteorological subsystem provides data on the physical properties of the local atmosphere so that refraction effects may be corrected.

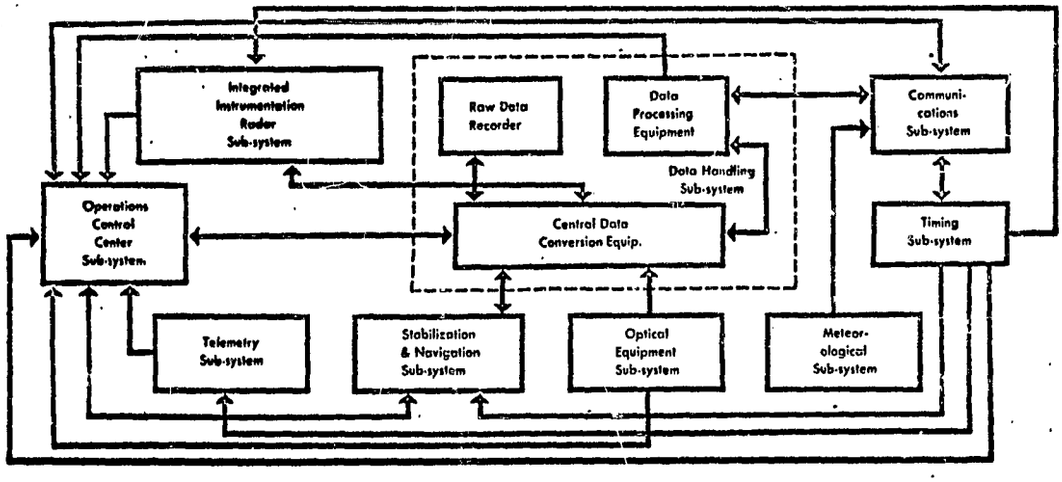
Figure 5.1-1

ARIS SHIP EQUIPMENT CONFIGURATION

PHYSICAL ARRANGEMENT



SIGNAL FLOW BLOCK DIAGRAM



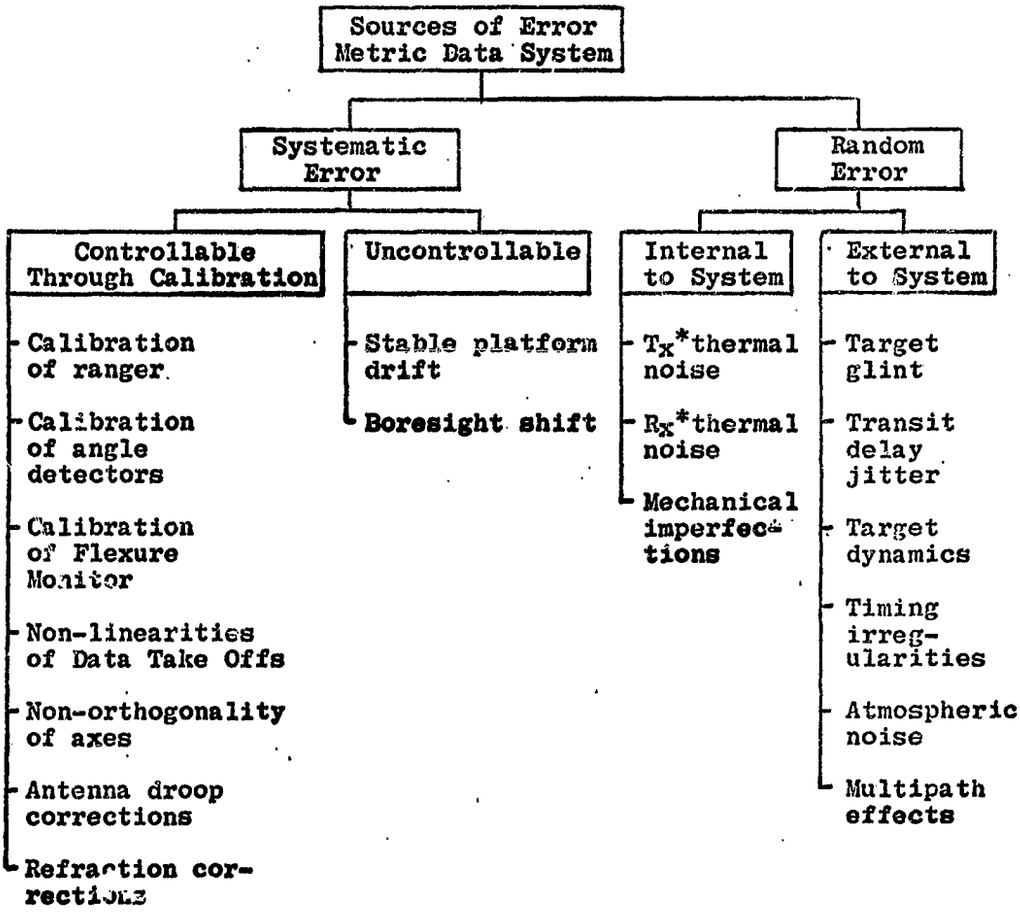
5.1.2 Error Sources

The problems encountered in providing accurate trajectory data from a shipborne radar include all of the error sources of land based radars plus the uncertainties of translating the ship's position and attitude to a given reference position, attitude, and time and the continuous variation in tilt due to ship's motion. A block diagram of these error sources is shown in Figure 5.1-2 where the total "error" of the system is composed of the residual systematic errors or biases upon which is superimposed a range of random variation. Neither of these entities is defineable without due regard for the target, the geometry of the measurements, the mission requirements, and the accuracy of the supporting subsystems. The normally measured quantities of range, train and elevation with respect to the C-band radar mount (polar coordinates) are very well determined with respect to the ship's local coordinate system, but ship's roll (R), pitch (P), and yaw (Y), intra-ship flexure, (θ_R, θ_P and θ_Y), and uncertainty as to ship's reference location, heading and attitude degrade the ability of the system accurately and precisely to define the space coordinates of a target with reference to a central (land based) coordinate system.

The Navigation and Stabilization subsystem and the Flexure Monitor subsystem, therefore, are vital elements of the Integrated Instrumentation Radar system in correcting the deck referenced train and elevation angles to accurate angles of true azimuth and true elevation with respect to the local earth's tangent plane and azimuth reference direction. The latitude and longitude of the ship must also be provided by the SINS in order to allow the IIR to yield data capable of translation to coordinate systems common to oth r range instrumentation.

Figure 5.1-2

SOURCES OF ERROR
SHIPBORNE RADAR



*T_x = transmitter R_x = receiver

Calibration procedures have been established to determine the accuracy of the SINS and the Flexure Monitor.

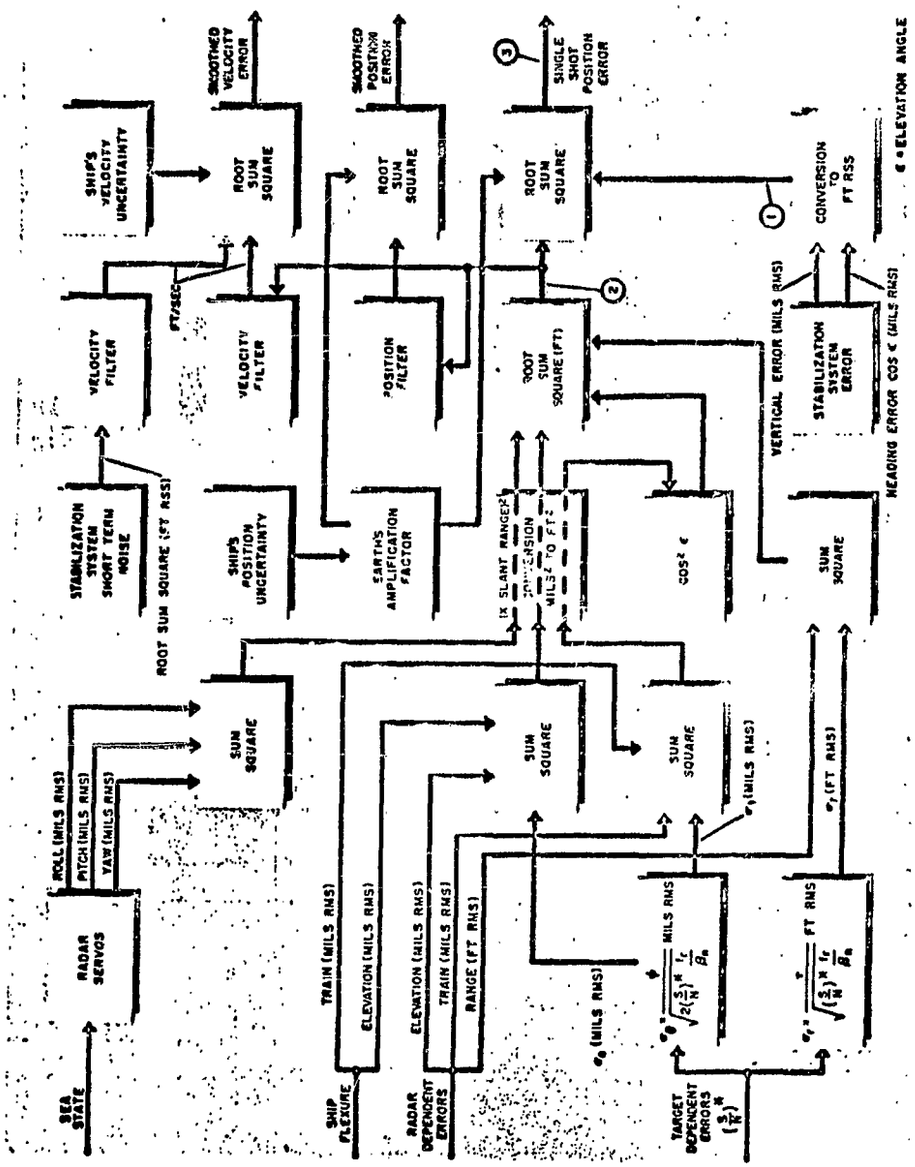
Since this calibration utilizes optical targets (stars, aircraft, balloons, etc), the angle errors between the radar electrical and optical axes require another set of corrections for the radar deck angles which are further diluted in accuracy by uncertainties in the radar refraction determinations. Non-orthogonality between the train and elevation axes of the radar, antenna droop, and the accuracy and precision with which a target of given characteristics (S/N) can be determined in angle and range with respect to the antenna reference must be determined to permit computer corrections for static radar errors. Finally, the servo lags must be read out and weighed with the computer delays and data recording delays to permit corrections for target dynamics and time dilation. Errors due to uncertainty in wave length, λ, can generally be ignored since the transmitting frequency is controlled to very high accuracy.

5.1.3 Error Model

The error sources listed in Section 5.1.2 may be statistically resolved into an appropriate set of coefficients representing estimators of errors due to each cause. These coefficients may then be used in a mathematical expression or error model from which the expected errors in the system may be predicted. The significant parameters of the shipborne radar tracking system are deck referenced train, T (t), elevation, E (t), and Range, R (t), as functions of time during a tracking mission. The errors (inaccuracies) of these parameters at any given time are composed of unpredictable residuals of the systematic errors and unseparable random errors due to noise in the measurements.

Figure 5.1-3

ERROR ANALYSIS PROCESS BLOCK DIAGRAM



The Ship's Inertial Navigation System stable platform and the Flexure Monitor subsystem are the major contributors to the error model term for "tilt". The familiar land based radar error model with tilt appearing as a small fixed component of mis-level in two fixed coordinate directions is replaced in the ship-borne radar error model with a tilt error which now adds variation in tilt due to ship's flexure with respect to the ship's reference (SINS stable platform), tilt in the reference vertical with respect to the space coordinate system and variation in the direction of the tilt vector with ship's heading, H, which is also an additional source for azimuth error. Figure 5.1-3 shows, in block diagram form, how the error sources are processed through data reduction.

When the vertical and azimuthal corrections from the SINS stable platform are utilized to provide "true" azimuth, A', "true" elevation, E', and include the tilt corrections from the Flexure Monitor subsystem along the roll, pitch and yaw axes of the ship, the error model equations become:

Azimuth Error Model

$$\Delta A'(t) = a_o \qquad \text{static}$$

$$+ \; a_1 \dot{T}(t) + a_2 \ddot{T}(t) + a_3 \dddot{T}(t) \qquad \text{dynamic}$$

$$+ \; \tan E(t) \left[a_4 \cos T(t) + a_5 \sin T(t) \right] \qquad \text{FM tilt}$$

$$+ \; \tan E(t) \left[a_6 \cos (T+H)(t) + a_7 \sin (T+H)(t) \right] \qquad \text{SINS tilt}$$

$$+ \; a_8 \sec E(t) \qquad \text{misalignment}$$

$$+ \; a_9 \tan E(t) \qquad \text{non-orthogonality}$$

$$+ \; a_{10} R(t) \dot{T}(t) \qquad \text{time dilation}$$

$$+ \; a_{11} f_A(\lambda) \qquad \text{boresight shift}$$

$$+ \; a_{12} \sin T(t) + a_{13} \cos T(t) \qquad \text{DTO non-linearity}$$

$$+ \; e_A \qquad \text{residual.}$$

Elevation Error Model

$\Delta E'(t) = b_o$	static
$+ b_1\dot{E}(t) + b_2\ddot{E}(t) + b_3\dddot{E}(t)$	dynamic
$+ b_4 \cos T(t) + b_5 \sin T(t)$	FM tilt
$+ b_6 \cos (T+H)(t) + b_7 \sin (T+H)(t)$	SINS tilt
$+ b_8 h_e$	misalignment
$+ b_9 p$	residual refraction
$+ b_{10} R(t)\dot{E}(t)$	time dilation
$+ b_{11} f_h(\lambda)$	boresight shift
$+ b_{12} \sin E(t) + b_{13} \cos E(t)$	DTO non-linearity
$+ b_{14} \cos E(t)$	droop
$+ e_E$	residual

Range Error Model

$\Delta R'(t) = c_o$	static
$+ c_1\dot{R}(t) + c_2\ddot{R}(t) + c_3\dddot{R}(t)$	dynamic
$+ c_4 f(S/N)$	echo delay
$+ c_5 p$	residual refraction
$+ c_6 R(t)\dot{R}(t)$	time dilation
$+ c_7 R(t)$	reference oscillator
$+ e_R$	residual

5.1.4 Methodology for Estimating System Accuracies

Determination of the error model coefficients requires statistical analysis of a large amount of data from calibrations, experiments and tracking runs adequately referenced to independent sources of tracking data. The first stage is the calibration of the ship's stable platform to provide a shipborne reference for heading and local vertical. This program is described in Section 8.3.9, Navigations Systems.

The second stage is the calibration of the ship's Flexure Monitor subsystem using the Star Tracker. With the Star Tracker tracking a star, this procedure collects output angle data from the Star Tracker, the output angle data from the Flexure Monitor and the output angle data from the slaved C-band radar mount. The C-band radar pointing angles are corrected to the C-band Optical axis using boresight camera film records time correlated to angle Data Take Off outputs.

The third stage is to allow the ship to steam along prescribed courses in an area which can also be covered by a "standard" tracking system such as Azusa, MISTRAM, Ballistic Cameras, Land Based Radars, etc. and simultaneously collect tracking data on aircraft for statistical determination of a reference trajectory for regression analysis of the shipborne radar tracking errors from which the error model coefficients are determined.

The identifiable systematic errors are removed from the ARIS metric data and the total error is estimated as the RSS value of residual bias and "noise" variances of all useable 10-second spans of data.

5.1.5 System Accuracies

One successful test has been run in which the Arnold collected useable data for comparison with AZUSA data. Editing yielded 207, 186 and 231 useful spans of data for azimuth, elevation and range data processing out of a total of 253 10-second spans. Two successful Vandenberg tests yielded 566, 566 and 542 useful spans of azimuth, elevation and range data out of a total of 576 10-second spans. Table 5.1-1 shows the estimates of error after correction for correctible systematic errors.

Table 5.1-1
ARIS Metric Data Accuracy Estimates
(Correctible Errors Removed)

ARIS I (ARNOLD) ERRORS

	$\Delta A'$ Milli-rad.	$\Delta E'$ Milli-rad.	$\Delta R'$ Feet
Sample Mean (Bias Estimate)	0.69	-0.35	284
Standard Deviation	1.75	0.88	38
Total (Root Sum Square)	1.88	0.95	287
Bias Uncertainty	*	*	*

ARIS II (VANDENBERG) ERRORS

	$\Delta A'$ Milli-rad.	$\Delta E'$ Milli-rad.	$\Delta R'$ Feet
Sample Mean (Bias Estimate)	0.516	0.703	45
Standard Deviation	0.186	0.170	11
Total (Root Sum Square)	0.564	0.729	46
Bias Uncertainty	0.203	0.268	18

*Insufficient data available for significant estimate.

5.2 Twin Falls Victory

5.2.1 System Description

The Twin Falls Victory ship metric data system consists, basically, of an AN/FPS-16 C-band radar, and an N7C SINS. Lorac and Loran systems are provided for fixing position but are inadequate for broad ocean area (BOA) coverage. See Figures 5.2-1 and 5.2-2 for present system configuration and system block diagram.

Modification plans are being prepared to replace the N7C SINS with a MK-IV SINS and to add to an Acoustic Ship Positioning System (ASPS). Additionally, the radar will be modified to incorporate parametric amplifiers and a side-lobe detection system to eliminate the possibility of tracking on a side lobe. A radar calibration system will be added to provide the capability of measuring any misalignment between the radar antenna optical and RF axes at sea.

5.2.2 System Accuracy Determination

After completion of modifications, the TFV ship will have improved metric data capabilities. The same sources of error and methodology for calibration and reduction of systematic errors will be used for determining overall accuracy as for the ARIS systems except for the ship's flexure which can not be monitored in the TFV ship system.

Due to the imminent modifications, the accuracy data previously quoted are not included in this report. As soon as new data are available, they will be included in the Monthly Accuracy Bulletin.

Figure 5.2-1

SYSTEM CONFIGURATION
TWIN FALLS VICTORY

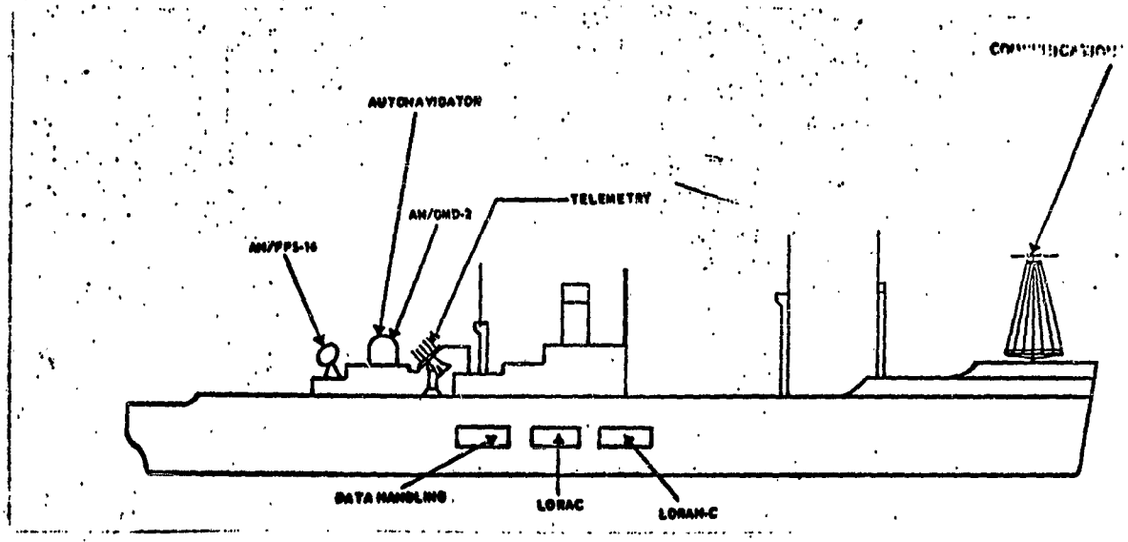


Figure 5.2-2
SYSTEM BLOCK DIAGRAM

6.0 CW RADARS

6.1 Procedure for Estimating System Accuracies

The procedure for estimating CW Radar Measurement Accuracies is illustrated in Figure 6.1-1.

Each CW Radar measurement is compared to a BET or GLAD determination, Inertial Guidance and/or to other CW Radars. Differences in CW Radar coordinates are subjected to additional analysis as follows:

(1) Estimation of error model coefficients.
(2) Analysis of variance (within test and between test variation).
(3) Spectral Analysis of least squares residuals.
    (a) Power spectrum.
    (b) Autocorrelation and cross correlation coefficients.
(4) Error estimates by frequency band.
    The total error variance may be considered to have component error variances as follows:

$$\sigma_T^2 = \sigma_B^2 + \sigma_L^2 + \sigma_H^2$$

where

σ_T^2 = Total error variances

σ_B^2 = Error variance due to bias or other systematic error with near zero frequency

σ_L^2 = Error variance due to low frequency components

σ_H^2 = Error variance due to high frequency components

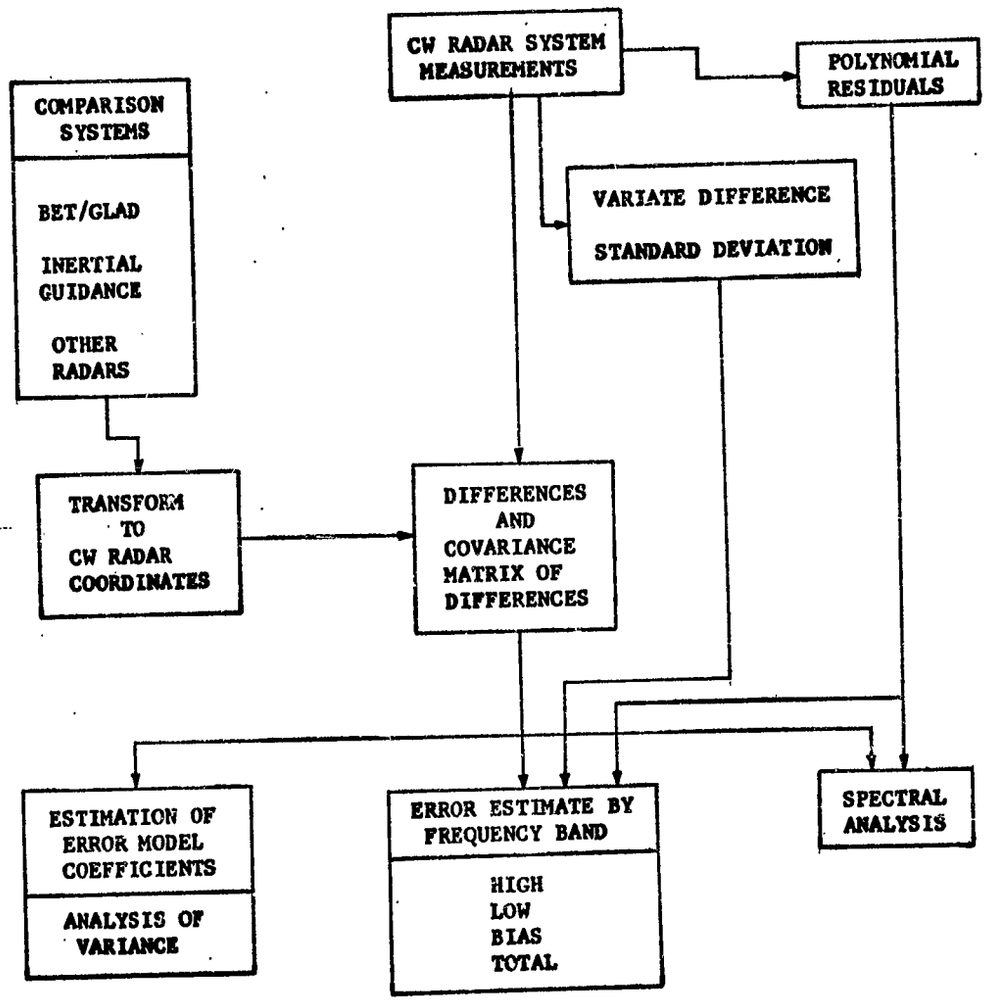
The approximate frequency bands for these components are:

(Text continued on page 6-3)

FIGURE 6.1-1

CW RADAR

ACCURACY ESTIMATION



Error Component	Frequency Band (cycles per second)
Bias	0 to $\frac{1}{2.26T^{*}}$
Low	$\frac{1}{2.26T}$ to filter cutoff
High	Filter cutoff to $\frac{1}{2\Delta t^{**}}$
Total	0 to $\frac{1}{2\Delta t}$

High frequency errors, σ_H, are estimated by the variate difference method adjusted to the high frequency band or by computing the standard error of polynomial residuals.

Low frequency errors, σ_L, are estimated by computing the square root of the variance of differences or BET/GLAD residuals minus the high frequency error variance, i.e.

$$\sigma_L = \left[\sigma^2_{\text{Residuals}} - \sigma_H^2\right]^{1/2}$$

The bias error, σ_B, is estimated from the bias and bias uncertainties computed by the BET/GLAD. The total error is the root sum square of the high, low, and bias frequency errors.

*T is the data time span (seconds) used in the estimate.

**Δt is the interval between successive data points.

6.2 MISTRAM

6.2.1 System Description

6.2.1.1 MISTRAM I

This system is composed of five sites arranged in the shape of a capital L (See Figure 6.2-1). The Central Transmitting and Receiving Site is located at the vertex and is designated as Site Zero. Each leg has two receiving sites located at distances of about 10,000 and 100,000 feet from the central site. Range sum is measured between the central transmitter and the central receiver; range differences are measured between each outlying site and the central site. One of the 100,000 foot baseline stations is at an azimuth of approximately 167° from the central station relative to true north. The other 100,000 foot station is at an azimuth of approximately 249° relative to true north. The range sum is usually divided by two and in the active track mode this is approximately equal to the target range from the central station. The terminology is summarized in the following tabulation:

R = (Range sum from central transmitter to the vehicle to central receiver) ÷ 2.

P_1 = Range difference to the vehicle between the west 10,000 foot site and the central site.

Q_1 = Range difference to the vehicle between the south 10,000 foot site and the central site.

P_2 = Range difference to the vehicle between the west 100,000 foot site and the central site.

Q_2 = Range difference to the vehicle between the south 100,000 foot site and the central site.

(Text continued on page 6-6)

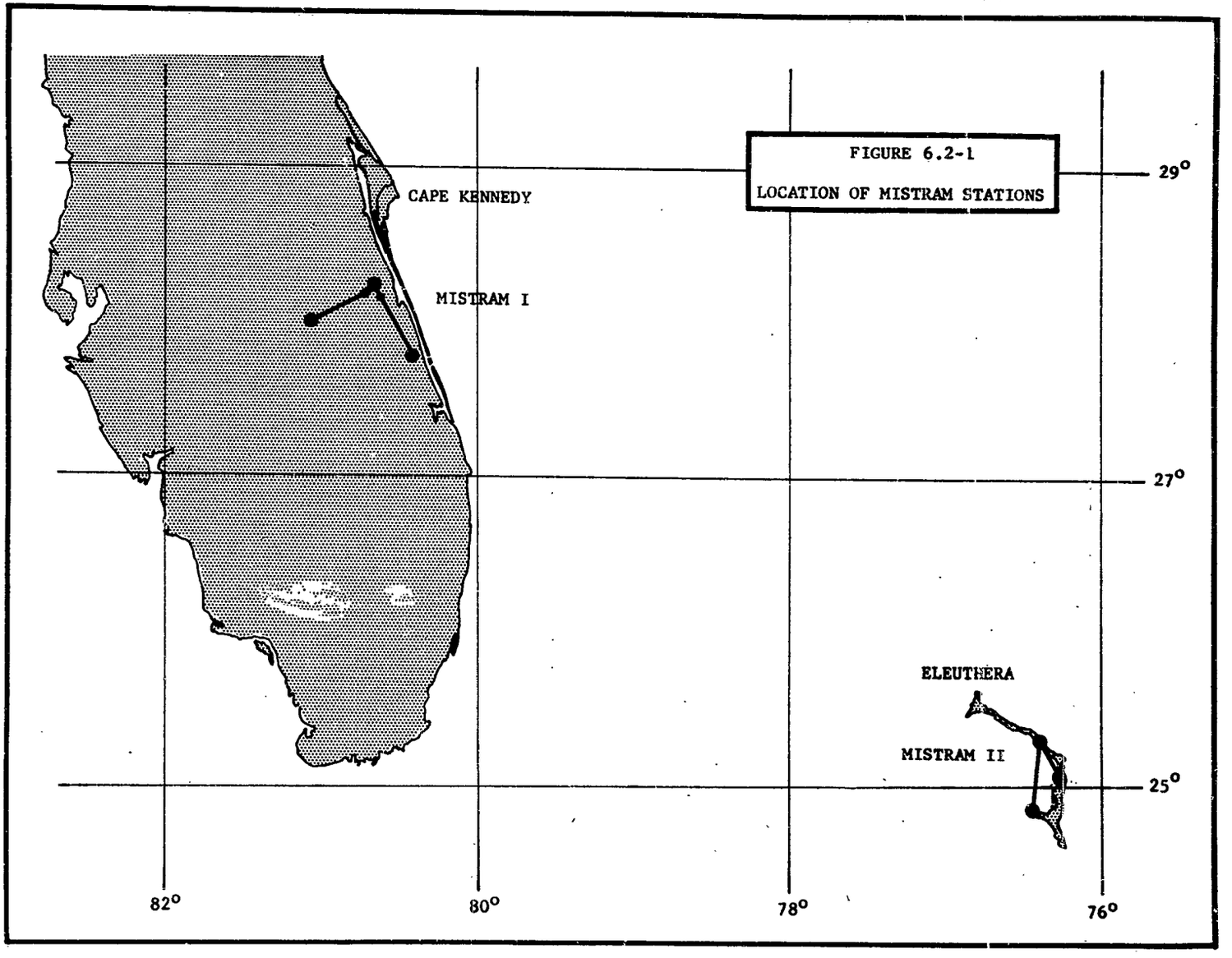


FIGURE 6.2-1

LOCATION OF MISTRAM STATIONS

6.2.1.2 MISTRAM II

This system is composed of three sites arranged such that the lines joining the outlying sites and the central site form an acute angle of approximately 45°. The short leg (Q) forms an angle of 138.9° with true north and the long leg (P), an angle of 183.4° with true north. The P and Q legs are 156,000 and 87,000 feet in length, respectively.

6.2.1.3 Measurement Techniques

The measurements made by both systems are based on phase comparison techniques. Two X-band signals (approximately 8000 mc) are generated and transmitted via the ATSS* antenna to the transponder in the missile. The transponder receives the signals, shifts them in frequency, amplifies them and transmits them to the receiving sites.

One of the signals, called the continuous signal, is a pure X-band sine wave. At the central station, a difference frequency between the received and transmitted signals is generated. A continuing cycle count of this Doppler frequency yields an integrated range sum rate. To this must be added an integration constant to obtain a meaningful measurement of range to the missile.

The other transmitted signal, called the calibrate signal, is used to provide the integration constant and to periodically check it. The calibrate signal frequency is periodically swept through an 8

*Acquisition and Tracking Subsystem.

megacycle variation. While equipment considerations require the frequency change to be smooth and relatively slow, the comparison between transmitted and received signals can be shown to be mathematically equivalent to the same comparison with a step change in frequency. Figure 6.2-2 shows graphically the actual frequency change and the step frequency change. In both cases the area between the transmitted and received frequency curves (excluding Doppler frequencies) can be shown to be equal to $\Delta F \cdot \Delta t$, where ΔF is 8 megacycles and $\Delta t = \frac{2R}{c}$ (c = velocity of propagation). The MISTRAM System measures this area, from which the range R is determined.

The procedure for the range difference measurements is the same as the above discussion for the range measurement except that the comparisons are made between two received signals instead of between transmitted and received signals.

In the passive mode, the range measurement is replaced by an uninitialized measurement of range sum from active transmitter to passive central receiver. The initializing constant, or constant of integration, is estimated from redundant data by the GLAD Program.

6.2.1.4 Characteristics and Specifications

Volume of Coverage

Azimuth:	360 degrees
Elevation:	5 to 85 degrees, full accuracy; zero to 90 degrees, decreased accuracy (The full accuracy coverage is limited by the elevation angle from any one antenna).
Range:	20 to 600 nautical miles, full accuracy; 600 to 1000+ nautical miles, decreased accuracy

(Text continued on page 6-9)

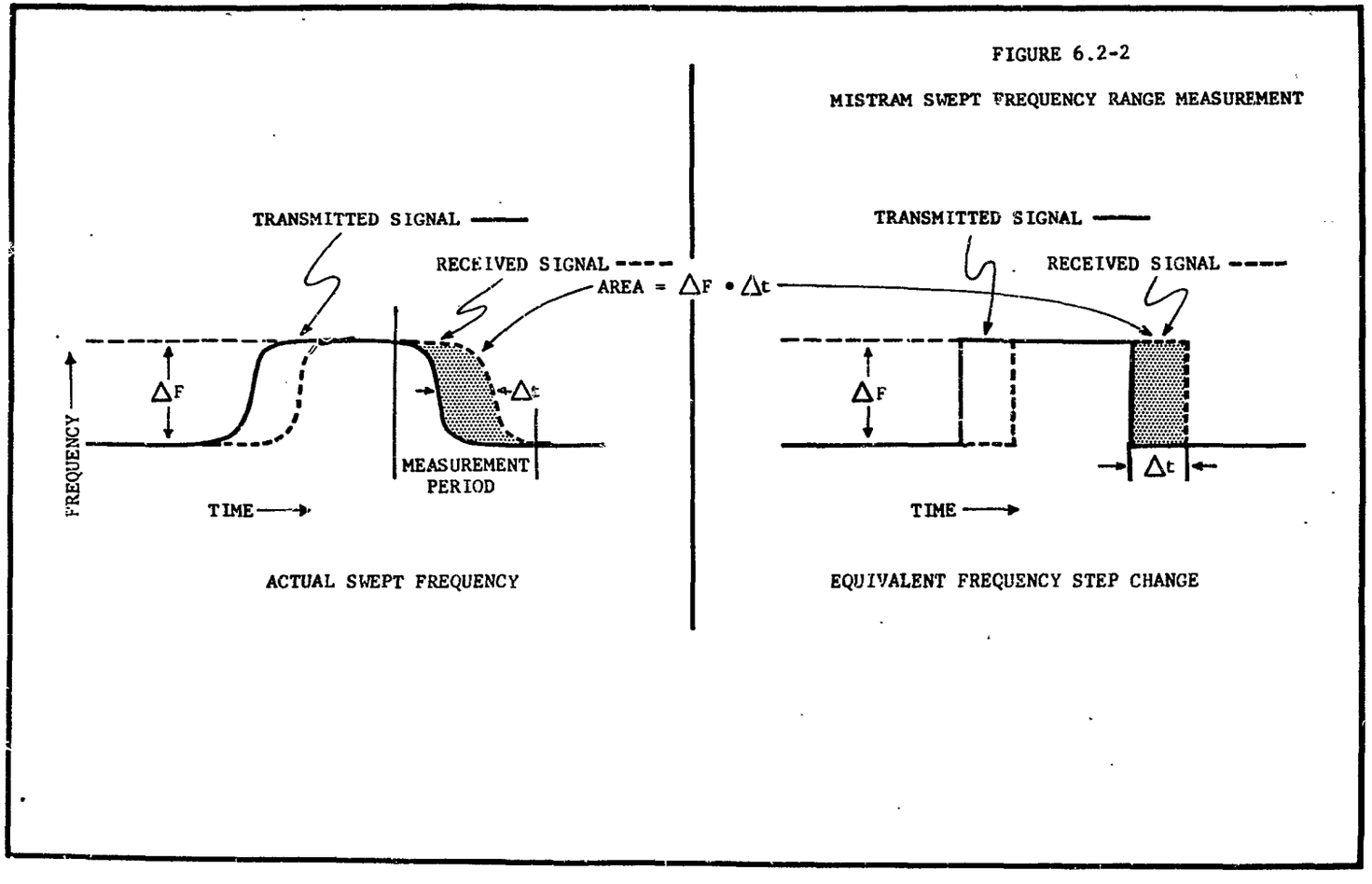


FIGURE 6.2-2

MISTRAM SWEPT FREQUENCY RANGE MEASUREMENT

(Range is signal level limited, and full range depends upon the application).

Rate and Acceleration Limits

Range Rate:	zero to 50,000 Ft/Sec
Range Acceleration:	zero to 750 Ft/Sec^2
Rate of change of range acceleration:	zero to 50 Ft/Sec^3
Range difference rate:	zero to 3,000 Ft/Sec
Azimuth and elevation tracking rate:	zero to 45 Degrees/Sec
Azimuth and elevation acceleration:	zero to 250 $Degrees/Sec^2$

Sampling Rate

MISTRAM I	20 points per second
MISTRAM II	200 points per second sampled but 20 points per second digitized output, each based on an 11-point linear fit to 200 pps data.

System Accuracy Specifications

Table 6.2-1 gives equipment accuracy specifications for the MISTRAM range and range difference measurements.

TABLE 6.2-1
MISTRAM EQUIPMENT ACCURACY SPECIFICATIONS

	MISTRAM I					MISTRAM II		
	R	P_1	Q_1	P_2	Q_2	R	P	Q
Position, Ft.	0.4	0.03	0.03	0.3	0.3	0.4	0.3	0.3
Rate, Ft/Sec	0.02	0.002	0.002	0.002	0.002	0.02	0.002	0.002

6.2.2 Error Sources

6.2.2.1 MISTRAM Error Models

The MISTRAM error models for Range and Range Difference measurements are shown below:

$$\Delta R = a_0 + a_1 R + a_2 \dot{R} + a_3 \csc E_0 + a_4 t + e_r$$

$$\Delta P = b_0 + b_1 P + b_2 \dot{P} + b_3 (\csc E_0 - \csc E_P) + b_4 t + e_P$$

$$\Delta Q = c_0 + c_1 Q + c_2 \dot{Q} + c_3 (\csc E_0 - \csc E_Q) + c_4 t + e_Q$$

Where:

ΔR, ΔP, ΔQ are observed differences between MISTRAM Range and Range Difference measurements and the corresponding data from a comparison standard.

E_0 = Elevation angle with respect to the central site

$E_{P,Q}$ = Elevation angle with respect to the outlying site

t = time (in seconds) of observation

e_R, e_P, e_Q are residual errors

The terms of the error model may be interpreted as follows:

(a) The terms in the error model subscripted with a zero are included to account for the presence of a constant bias or offset in the data due to errors in the pre-test and post-test determination of delays through the ground equipment (and in the case of Range, through the airborne transponder). This bias also includes two foot ambiguities in the data due to incorrect determination of the integration constant or starting point for the count of Doppler frequency cycles. All of these errors are generally termed zero-set errors.

(b) The terms subscripted with a one are scale factor errors arising from lack of exact knowledge of the vacuum velocity of electromagnetic propagation, and from frequency errors. The raw output of the system may be considered to be in units of cycles to which a scale factor with dimension ft/cycle must be applied to convert to feet. This scale factor is determined from $\lambda = c/f$ and will be in error if either c or f is not correctly known. For a velocity of light error, the component is equal to $\frac{\Delta c}{c}$ and for a frequency error, the component is approximately equal to $\frac{\Delta f}{f}$.

(c) The terms subscripted with a two are included to account for a timing bias with respect to the standard Range Timing. The coefficient will have units of seconds, since for a timing bias Δt, the range error ΔR is approximately $\Delta R = R\Delta t$.

(d) The terms subscripted with a three are included to account for uncorrected (i.e., residual) refraction errors. If a flat earth is assumed, the Range refraction correction can be shown to be equal to

$-\csc E \int_0^h N(h)dh \times 10^{-6}$, and thus the coefficient can be regarded as an error in the estimation of the definite integral. The refractivity is usually assumed to decay exponentially from a measured value N_0 at the surface of the earth to $\frac{N_0}{2.718}$ at a fixed scale height H. This error model term attempts to account for the deviation of the actual refractivity along the ray paths from that of the model atmosphere used. For the range difference measurements, the refraction correction equals

$\left\{-\csc E_0 \int_0^h N(h)dh - -\csc E_1 \int_0^h N(h)dh\right\} \times 10^{-6}$ or

$10^{-6} \left\{\csc E_1 - \csc E_0\right\} \int_0^h N(h)dh$, and again the coefficient is representative of an error in the estimation of the definite integral.

(e) The terms with subscript four are included to account for an error which varies linearly with time. Such an error could be caused by "warm-up" phenomena at many points in the system. In the passive mode, this term represents range sum rate bias errors arising from difference in frequency of the reference oscillators at the passive and active stations.

(f) The "e" terms in the error model are included to account for so-called "random" errors. The actual make-up of the "e" terms cannot be fully known, but its components are the following:

(1) Atmospheric phenomena which are not accounted for by the $(\csc E_0 - \csc E_{P,Q})$ refraction term of the error model
(2) Errors in the comparison standard resulting from errors in other tracking systems, uncorrected survey errors, and point-of-track errors.
(3) Thermal noise in the electronic equipment. The magnitude of the noise power depends on the absolute temperature of the equipment and on the bandwidth of the equipment. This is suppressed by the receiver AGC except at signal levels near threshold.
(4) Other "unmodeled" error sources.

6.2.2.2 Survey Error Estimates

The latest Coast and Geodetic Survey estimates of the standard error of the Valkaria and Eleuthera survey measurements relative to Cape Kennedy are tabulated below:

	Valkaria (Central)	Eleuthera (Central)
σ_X, Ft.	0.2	3.04
σ_Y, Ft.	0.2	3.04
σ_Z, Ft.	0.14	3.4

The error in location of remote stations relative to their central site is much smaller, and is considered negligible as an error source in published trajectory data. The errors in location of the systems relative to Cape Kennedy are not large enough to cause serious errors in terms of current accuracy requirements.

6.2.3 System Accuracies

MISTRAM accuracy estimates and data characteristics contained in the report are based on analysis of data from the missile tests shown in Table 6.2-2.

Table 6.2-2

MISSILE TYPES AND TEST NUMBERS

MINUTEMAN		TITAN II		SATURN	
Range Test Number	Missile Number	Range Test Number	Missile Number	Range Test Number	Missile Number
3301	431	0354	N-24	0169	SA-5
3302	432	3303	N-25	2769	SA-6
3815	433	3787	N-29	4444	SA-7
4951	435	0525	N-31		
6001	446	0227	N-32		
6080	447	0104	N-33		
0305	438	0275	GLV-1		
0376	448	0158	N-3A		
0526	436				
0201	437				
0430	439				
0351	440				
0050	442				
0037	441				
0040	443				
1060	444				
3552	449				

6.2.3.1 Accuracy Estimates

Tables 6.2-3, 6.2-4 and 6.2-5 give current estimates of MISTRAM accuracy for MINUTEMAN, TITAN, and SATURN, respectively. The a priori column represents bias uncertainty before adjustment to a

(Text continued on page 6-19)

TABLE 6.2-3

ACCURACY ESTIMATES

SYSTEM: MISTRAM I & II
MISSILE TYPE: MINUTEMAN

Measurement	Position (Ft)					Rate[2] (Ft/Sec)			Acceleration[2] (Ft/Sec^2)		
	s_{Bias}		s_{Random}			s_{Random}			s_{Random}		
	a priori	a pos-teriori[1]	1st Stage	2nd Stage	3rd Stage	1st Stage	2nd Stage	3rd Stage	1st Stage	2nd Stage	3rd Stage
Valkaria											
R	2.6	1.0	0.3	0.3		0.06	0.05		0.3	0.3	
P_1	0.06	0.01	0.03	0.02		0.033	0.006		0.15	0.05	
Q_1	0.07	0.02	0.03	0.02		0.032	0.007		0.15	0.05	
P_2	1.2	0.08	0.15	0.10		0.042	0.011		0.20	0.10	
Q_2	1.0	0.18	0.15	0.10		0.046	0.012		0.20	0.10	
Eleuthera (Active)											
R	5.4	1.5			0.3			0.04			0.3
P	1.6	0.08			0.1			0.010			0.08
Q	1.1	0.02			0.1			0.006			0.05
Eleuthera (Passive)											
R	10^6[4]	1.9		0.6			0.07			0.5	
$\dot{R}_S$[3]	0.5	0.02									
P	3.0	0.08		0.1			0.010			0.08	
Q	1.5	0.02		0.1			0.006			0.05	

(1) Uncertainty after adjustment by GLAD using MISTRAM I & II data only.
(2) Derived by use of a 23 point, 3rd degree polynomial.
(3) Rate bias (Ft/Sec).
(4) R is ambiguous and must be initialized. Hence an arbitrary large number such as 10^6 is entered as the a priori uncertainty.

TABLE 6.2-4

ACCURACY ESTIMATES

SYSTEM: MISTRAM I & II
MISSILE TYPE: TITAN

Measurement	Position (Ft)			Rate[2] (Ft/Sec)	Acceleration[2] (Ft/Sec^2)
	s_{Bias}		s_{Random}	s_{Random}	s_{Random}
	a priori	a posteriori[1]			
Booster					
Valkaria					
R	1.8	1.8	0.2	0.06	0.60
P_1	0.07	0.07	0.03	0.014	0.14
Q_1	0.22	0.15	0.03	0.014	0.14
P_2	1.0	1.0	0.15	0.023	0.20
Q_2	2.0	1.5	0.15	0.027	0.20
Sustainer					
Valkaria					
R	1.8	1.6	0.1	0.05	0.30
P_1	0.07	0.02	0.03	0.002	0.02
Q_1	0.22	0.02	0.03	0.002	0.02
P_2	1.0	0.2	0.1	0.004	0.03
Q_2	2.0	0.2	0.1	0.005	0.03
Eleuthera (Passive)					
R_S	10^6[4]	4.0	0.4	0.07	1.0
P	2.1	0.2	0.1	0.005	0.03
Q	1.5	0.1	0.1	0.005	0.03
$\dot{R}_S$[3]	0.5	.02	- - -	- - -	- - -

(1) Bias uncertainty after adjustment by GLAD using MISTRAM I in Booster stage and MISTRAM I & II in Sustainer stage.

(2) Values derived by use of a 13 point, 2nd degree polynomial.

(3) Rate Bias. (Ft/Sec).

(4) See Table 6.2-3

TABLE 6.2-5

ACCURACY ESTIMATES

SYSTEM: MISTRAM I & II
MISSILE TYPE: SATURN

Measurement	Position (Ft)			Rate[2] (Ft/Sec)	Acceleration[2] (Ft/Sec^2)
	S_{Bias}		S_{Random}	S_{Random}	S_{Random}
	a priori	a posteriori[1]			
Booster					
Valkaria (Active)					
R	2.7	1.8	0.2	0.10	0.8
P_1	0.16	0.07	0.03	0.017	0.14
Q_1	0.16	0.15	0.03	0.017	0.14
P_2	1.5	1.0	0.15	0.020	0.16
Q_2	1.5	1.1	0.15	0.020	0.16
Sustainer					
Valkaria (Active)					
R	2.7	1.8	0.1	0.05	0.30
P_1	0.16	0.01	0.02	0.002	0.02
Q_1	0.16	0.02	0.02	0.002	0.02
P_2	1.5	0.14	0.10	0.005	0.03
Q_2	1.5	0.22	0.10	0.005	0.03
Valkaria (Passive)					
R_S	10^6[4]	5.0	0.4	0.07	0.3
$\dot{R}_S$[3]	0.5	0.01	- - -	- - -	- - -
P_1	3.0	0.02	0.02	0.002	0.02
Q_1	3.0	0.03	0.02	0.002	0.02
P_2	3.0	0.2	0.10	0.005	0.03
Q_2	3.0	0.3	0.10	0.005	0.03

(1) Bias uncertainty after adjustment by GLAD using MISTRAM I in Booster stage and MISTRAM I & II in Sustainer stage.
(2) Values derived by use of a 13 point, 2nd degree polynomial.
(3) Rate bias.(Ft/Sec).
(4) See Table 6.2-3.

TABLE 6.2-5 (Continued)

ACCURACY ESTIMATES

SYSTEM: MISTRAM I & II
MISSILE TYPE: SATURN

Measurement	Position (Ft)			Rate[2] (Ft/Sec)	Acceleration[2] (Ft/Sec^2)
	s_{Bias}		s_{Random}	s_{Random}	s_{Random}
	a priori	a posteriori[1]			
Sustainer					
Eleuthera (Active)					
R	2.3	1.5	0.1	0.05	0.7
P	2.0	0.4	0.1	0.005	0.03
Q	2.0	0.4	0.1	0.005	0.03
Eleuthera (Passive)					
R_S	10^6[4]	4.0	0.4	0.07	1.0
$\dot{R}_S$[3]	0.5	0.01	- - -	- - -	- - -
P	2.2	0.7	0.1	0.005	0.03
Q	2.3	0.1	0.1	0.005	0.03

(1) Bias uncertainty after adjustment by GLAD using MISTRAM I in Booster stage and MISTRAM I & II in Sustainer stage.
(2) Values derived by use of a 13 point, 2nd degree polynomial.
(3) Rate bias.(Ft/Sec).
(4) See Table 6.2-3.

constant bias error model (except constant plus $a_4 t$ for the passive range sum) by the GLAD Program, and the a posteriori column gives bias uncertainty after the adjustment.

For TITAN, it is assumed that all five MISTRAM I measurements are available during booster stage and that all five MISTRAM I active measurements plus the three MISTRAM II passive measurements are available during sustainer stage. A three second dropout at staging is assumed.

For MINUTEMAN, it is assumed that the five MISTRAM I active measurements are available through first stage, the five MISTRAM I active plus the three MISTRAM II passive measurements are available during second stage, and the three MISTRAM II active plus the five MISTRAM I passive measurements are available during third stage.

For SATURN, it is assumed that the five MISTRAM I active measurements are available during booster stage and the five MISTRAM I measurements plus the three MISTRAM II measurements are available during sustainer stage. The a posteriori estimates apply whether or not the passive measurements are initialized. A three second dropout at staging is assumed.

Figures 6.2-3, 6.2-4, and 6.2-5 are plots of the propagation of MISTRAM errors in total rectangular coordinate velocity errors for the MINUTEMAN, TITAN, and SATURN trajectories, respectively. The upper curve in each case is for MISTRAM I only, while the lower curve applies to a combined solution using MISTRAM I and MISTRAM II. For the MINUTEMAN case, it is assumed that data are

(Text continued on page 6-23)

FIGURE 6.2-3
MISTRAM ERROR PROPAGATION
MINUTEMAN TRAJECTORY

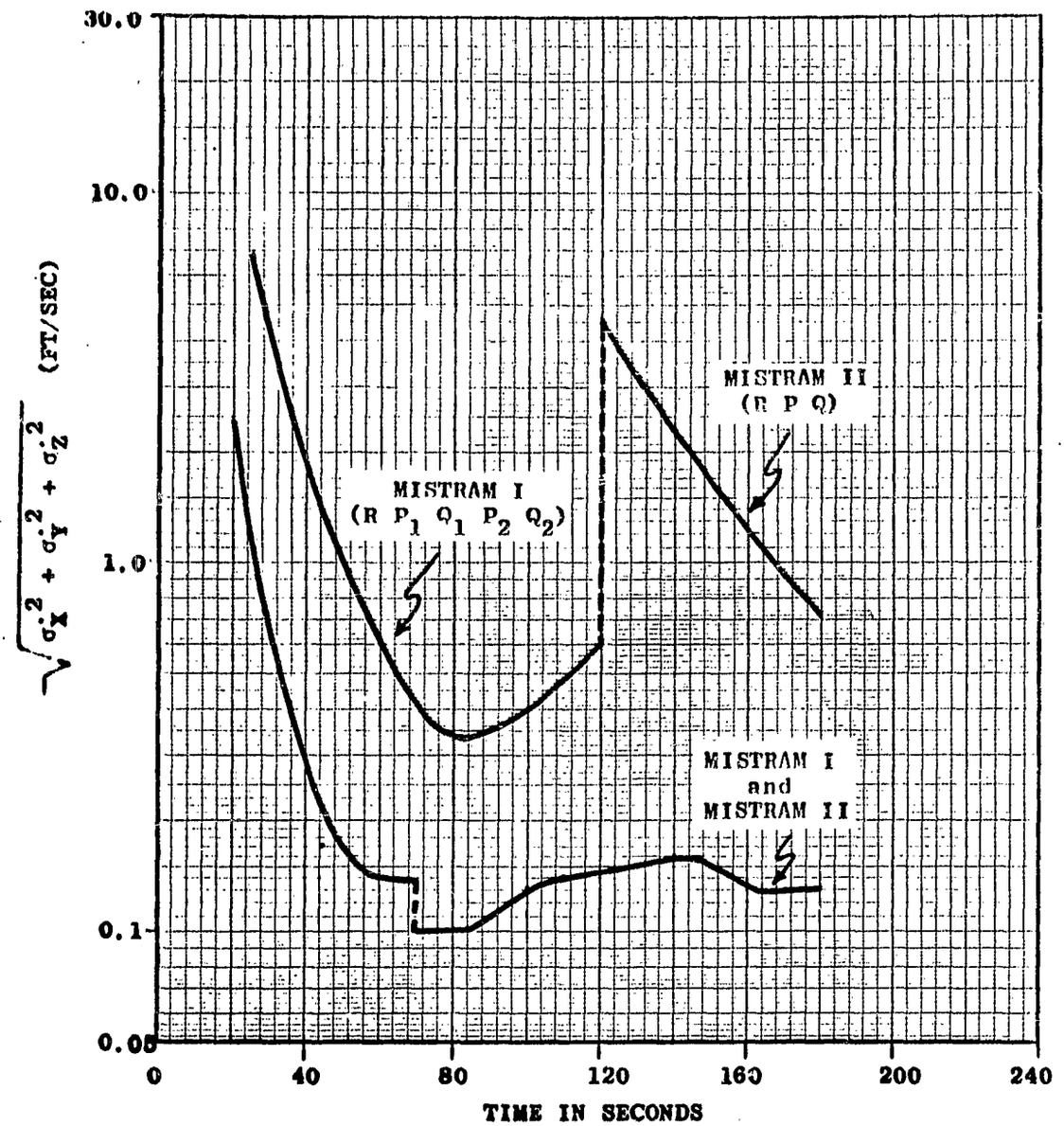


FIGURE 6.2-4

MISTRAM ERROR PROPAGATION

TITAN TRAJECTORY

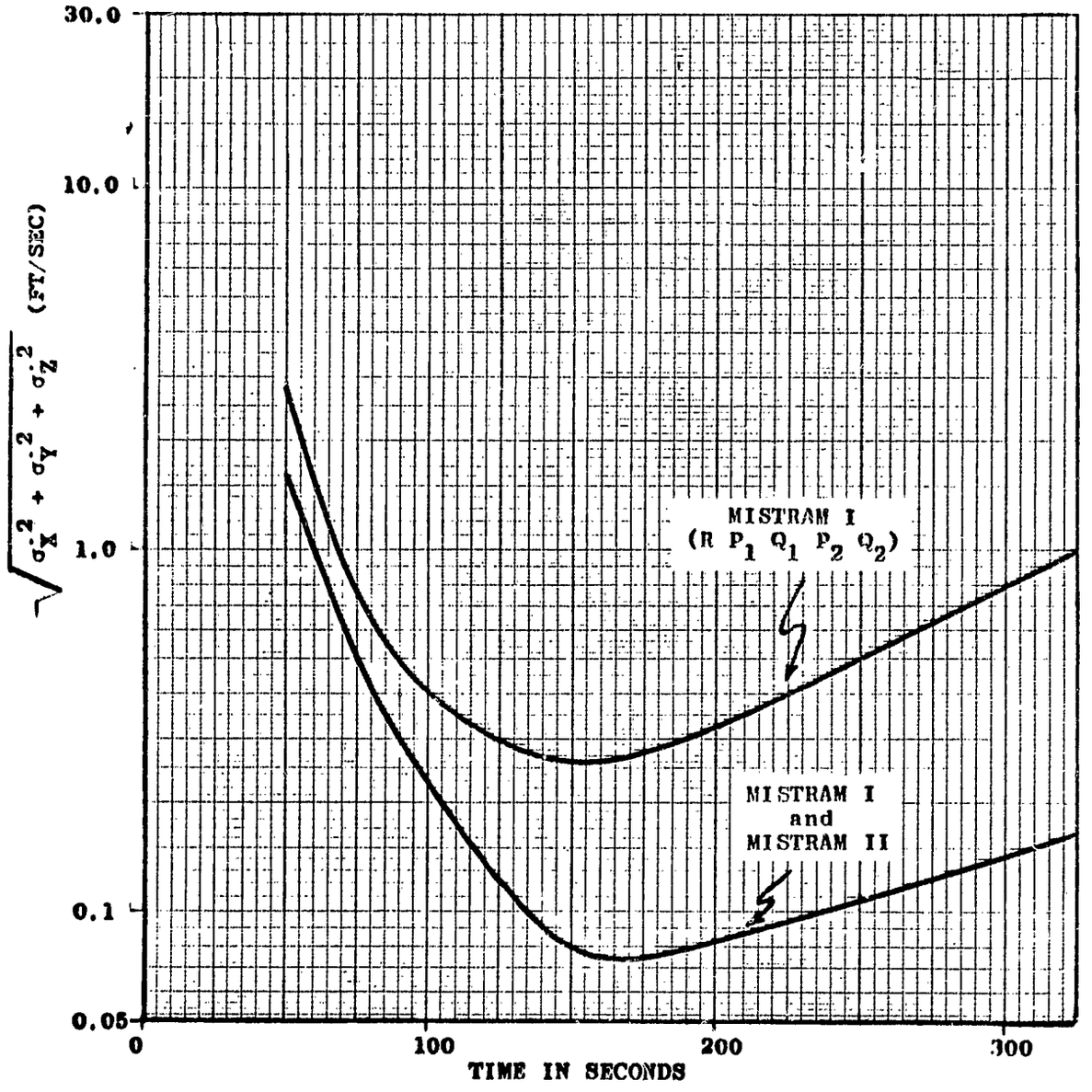
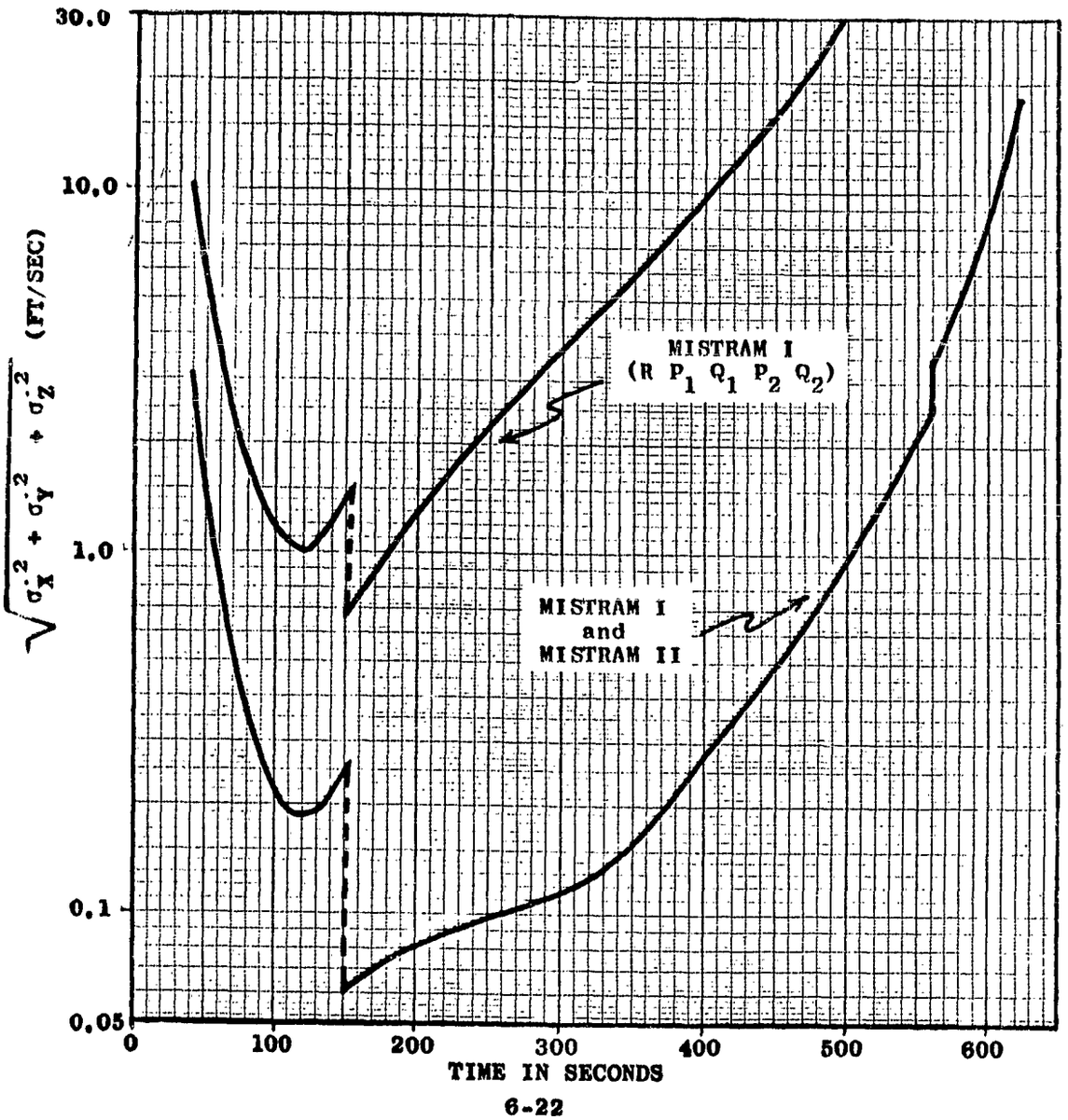


FIGURE 6.2-5
MISTRAM ERROR PROPAGATION
SATURN TRAJECTORY



available as follows:

MISTRAM I active 10 to 120 seconds
MISTRAM II passive 70 to 120 seconds
MISTRAM II active 122 to 182 seconds
MISTRAM I passive 122 to 182 seconds

For the TITAN case it is assumed that data are available as follows:

MISTRAM I active 50 to 320 seconds
MISTRAM II passive 150 to 350 seconds

For the SATURN trajectory it is assumed that data are available as follows:

MISTRAM I active 40 to 330 seconds
MISTRAM II passive 150 to 330 seconds
MISTRAM II active 332 to 620 seconds
MISTRAM I passive 332 to 552 seconds

6.2.3.2 Data Characteristics - MINUTEMAN

Tables 6.2-6 through 6.2-10 are tabulations of MISTRAM I error estimates by frequency band for MINUTEMAN tests. The high frequency numbers are fourth order variate-difference estimates adjusted to the frequency band, $7.4 < f \leq 10$ cps. The low frequency numbers are the standard deviation of BET or GLAD residuals, and are applicable to the frequency band $\frac{1}{2.26T} < f < 7.4$ cps, where T is the length of the time span in seconds. The bias estimates are means of MISTRAM minus BET differences or GLAD bias error model coefficient estimates.

Tables 6.2-11 and 6.2-12 give estimates of MISTRAM II high frequency and bias errors. Estimates of low frequency error

(Text continued on page 6-31)

TABLE 6.2-6

ESTIMATED MISTRAM I ERRORS BY FREQUENCY BAND
MINUTEMAN
R MEASUREMENT

Test	First Stage				Second Stage			
	High Freq. (Ft)	Low Freq. (Ft)	Bias (Ft)	Total (Ft)	High Freq. (Ft)	Low Freq. (Ft)	Bias (Ft)	Total (Ft)
3301	0.0018	0.29	3.8	3.8	0.0021	1.25*	1.3	1.8
3302	0.0020	2.16*	0.7	2.3	0.0017	0.12	2.2	2.2
3815	0.0015	0.02	6.4	6.4	0.0019	0.01	6.4	6.4
4951	0.0016	0.01	9.3	9.3	0.0047	0.02	9.3	9.3
6001	0.0022	0.40	3.4	3.4	0.0018	0.10	3.3	3.3
6080	0.0010	0.40	1.0	1.1	0.0014	0.0	1.0	1.0
0376	0.0009	0.20	5.8	5.8	0.0012	0.20	5.8	5.8
0050	0.0008	0.50	2.2	2.2	0.0013	0.50	2.2	2.2
1060	0.0008	0.40	1.8	1.8	0.0010	1.60*	1.8	2.4
Root Mean Square	0.0015	0.33	4.7	4.8	0.0022	0.21	4.6	4.7
Mean Bias			3.8				3.7	
Standard Error about Mean Bias			2.9				2.9	

*Excluded from Root Mean Square Calculations.

TABLE 6.2-7

ESTIMATED MISTRAM I ERRORS BY FREQUENCY BAND
MINUTEMAN
P_1 MEASUREMENT

Test	First Stage				Second Stage			
	High Freq. (Ft)	Low Freq. (Ft)	Bias (Ft)	Total (Ft)	High Freq. (Ft)	Low Freq. (Ft)	Bias (Ft)	Total (Ft)
3301	0.0010	0.03	-0.19	0.19	0.0006	0.02	-0.21	0.21
3302	0.0014	0.05	0.14	0.15	0.0003	0.01	-0.16	0.16
3815	0.0010	0.04	-0.10	0.11	0.0002	0.01	-0.09	0.09
4951	0.0007	0.04	0.11	0.12	0.0004	0.02	0.10	0.10
6001	0.0015	0.00	0.00	0.00	0.0004	0.01	0.01	0.01
6080	0.0006				0.0002			
0376	0.0002	0.02	-0.02	0.03	0.0002	0.02	-0.02	0.03
0050	0.0005	0.14	-0.08	0.17	0.0003	0.01	-0.08	0.08
1060	0.0007	0.07	-0.09	0.11	0.0002	0.05	-0.09	0.10
Root Mean Square	0.0009	0.06	0.11	0.12	0.0003	0.02	0.11	0.11
Mean Bias			-0.03				-0.08	
Standard Error about Mean Bias			0.11				0.11	

TABLE 6.2-8

ESTIMATED MISTRAM I ERRORS BY FREQUENCY BAND
MINUTEMAN
Q_1 MEASUREMENT

Test	First Stage				Second Stage			
	High Freq. (Ft)	Low Freq. (Ft)	Bias (Ft)	Total (Ft)	High Freq. (Ft)	Low Freq. (Ft)	Bias (Ft)	Total (Ft)
3301	0.0017	0.01	0.07	0.07	0.0004	0.01	0.03	0.03
3302	0.0019	0.06	0.11	0.13	0.0003	0.01	0.15	0.15
3815	0.0012	0.03	0.20	0.20	0.0003	0.06	0.24	0.25
4951	0.0006	0.02	0.17	0.17	0.0004	0.02	0.23	0.23
6001	0.0023	0.05	-0.08	0.09	0.0024	0.01	-0.05	0.05
6080	0.0006				0.0002			
0376	0.0002	0.01	0.02	0.02	0.0002	0.01	0.02	0.02
0050	0.0006	0.13	0.03	0.13	0.0003	0.02	0.03	0.04
1060	0.0007	0.09	-0.01	0.09	0.0002	0.05	-0.01	0.05
Root Mean Square	0.0013	0.06	0.11	0.12	0.0008	0.03	0.13	0.13
Mean Bias			0.06				0.08	
Standard Error about Mean Bias			0.11				0.11	

TABLE 6.2-9

ESTIMATED MISTRAM I ERRORS BY FREQUENCY BAND

MINUTEMAN

P_2 MEASUREMENT

Test	First Stage				Second Stage			
	High Freq. (Ft)	Low Freq. (Ft)	Bias (Ft)	Total (Ft)	High Freq. (Ft)	Low Freq. (Ft)	Bias (Ft)	Total (Ft)
3301	0.0012	0.13	-2.5	2.5	0.0005	0.03	-2.3	2.3
3302	0.0024	0.43	-1.7	1.8	0.0006	0.02	-1.5	1.5
3815	0.0017	0.01	-0.7	0.7	0.0009	0.00	-0.7	0.7
4951	0.0008	0.00	0.9	0.9	0.0005	0.03	0.9	0.9
6001	0.0016	0.07	-0.6	0.6	0.0007	0.09	-0.6	0.6
6080	0.0015	0.03	0.8	0.8	0.0007	0.01	0.8	0.8
0376	0.0015	0.02	0.8	0.8	0.0002	0.02	0.8	0.8
0050	0.0017	0.17	-0.3	0.3	0.0010	0.16	-0.4	0.4
1060	0.0010	0.70	-1.1	1.3	0.0004	0.20	-1.1	1.1
Root Mean Square	0.0015	0.28	1.2	1.2	0.0006	0.09	1.1	1.1
Mean Bias			-0.5				-0.4	
Standard Error about Mean Bias			1.1				1.1	

TABLE 6.2-10

ESTIMATED MISTRAM I ERRORS BY FREQUENCY BAND
MINUTEMAN
Q_2 MEASUREMENT

Test	First Stage				Second Stage			
	High Freq. (Ft)	Low Freq. (Ft)	Bias (Ft)	Total (Ft)	High Freq. (Ft)	Low Freq. (Ft)	Bias (Ft)	Total (Ft)
3301	0.0017	0.07	1.1	1.1	0.0006	0.11	1.0	1.0
3302	0.0020	0.45	0.4	0.6	0.0006	0.04	0.3	0.3
3815	0.0014	0.02	1.1	1.1	0.0008	0.01	1.1	1.1
4951	0.0012	0.01	2.2	2.2	0.0006	0.01	2.2	2.2
6001	0.0011	0.13	-0.1	0.2	0.0006	0.02	0.0	0.02
6080	0.0011	0.17	0.2	0.3	0.0018	0.01	0.3	0.3
0376	0.0004	0.12	0.3	0.3	0.0003	0.12	0.3	0.3
0050	0.0005	0.30	0.1	0.3	0.0005	0.39	0.04	0.4
1060	0.0010	0.20	0.1	0.2	0.0002	0.40	0.1	0.4
Root Mean Square	0.0012	0.21	0.9	0.9	0.0008	0.19	0.9	0.9
Mean Bias			0.6				0.6	
Standard Error about Mean Bias			0.7				0.7	

TABLE 6.2-11

MISTRAM II (Passive) HIGH FREQUENCY ERROR ESTIMATES
MINUTEMAN

Test	Time Span (Seconds)	Position (Ft)		
		R_{Sum}	P	Q
0376	90 - 120	.0009	.0004	.0003
0201	80 - 120	.0010	.0002	.0002
0430	80 - 120	.0010	.0002	.0002
0351	80 - 120	.0012	.0002	.0002
0050	80 - 120	.0010	.0002	.0002
0037	70 - 120	.0014	.0002	.0002
0040	95 - 120	.0013	.0002	.0002
1060	80 - 120	.0015	.0002	- - -

MISTRAM II (Active) HIGH FREQUENCY ERROR ESTIMATES

Test	Time Span (Seconds)	Position (Ft)		
		R	P	Q
0376	150 - 180	.0006	.0002	.0002
0526	145 - 190	.0006	.0002	.0001
0201	120 - 185	.0008	.0002	.0002
0430	140 - 190	.0007	.0002	.0002
0351	140 - 180	.0007	.0002	.0002
0050	130 - 210	.0007	.0002	.0002
0037	135 - 180	.0006	.0002	.0002
0040	150 - 183	.0007	.0002	.0002
1060	120 - 170	.0006	.0002	- - -

TABLE 6.2-12

MISTRAM II BIAS ESTIMATES
MINUTEMAN

Test	Approximate Time Span (Seconds)	Comparison	Position (Ft)		
			R	P	Q
Passive Track					
3301	80 - 121	MISTRAM II-I		-3.9	0.3
3302	106 - 117	MISTRAM II-I		1.9	1.6
3815	83 - 122	MISTRAM II-UDOP		-1.4	2.1
4951	70 - 119	MISTRAM II-I		1.2	-0.7
6001	62 - 122	MISTRAM II-I		-0.2	-3.6
6080	69 - 129	MISTRAM II-I		1.5	0.1
0526	115 - 126	MISTRAM II-GLAD		2.6	2.7
0050	68 - 122	MISTRAM II-GLAD		3.1	-0.5
Root Mean Square				2.3	1.9
Active Track					
3302	123 - 152	MISTRAM II-BET	21.2	1.4	2.3
4951	124 - 150	MISTRAM II-BET	19.3	-6.5	-0.1
6001	127 - 185	MISTRAM II-BET	24.4	-2.9	-1.3
6080	134 - 180	MISTRAM II-BET	17.4	-1.6	-1.5
0526	147 - 188	MISTRAM II-GLAD	1.5	-0.2	2.5
0201	129 - 187	MISTRAM II-MISTRAM I-UDOP Tie-in	-4.2	2.6	2.9
0430	135 - 195	MISTRAM II-MISTRAM I-UDOP Tie-in	5.6	-5.7	-5.9
0351	132 - 180	MISTRAM II-MISTRAM I-UDOP Tie-in	14.8	2.0	1.6
0050	128 - 212	MISTRAM II-MISTRAM I-UDOP Tie-in	4.9	-1.2	-1.6
1060	150 - 185	MISTRAM II-MISTRAM I-UDOP Tie-in	0.3	0.2	0.1

are omitted for MISTRAM II because survey error (especially before the survey was corrected) may cause large low-frequency components which are not representative of the system's present performance.

MISTRAM data on MINUTEMAN flights have been of generally high quality, but published flight test data have not always been as good as could be desired for several reasons:

(1) Losses of signal associated with missile events have resulted in the publication of several short independent spans of data instead of a single longer span on some tests. Performance in this respect has been much improved on recent tests due to procedural changes, changes in missile characteristics, and use of UDOP data to bridge discontinuities.

(2) Signal degradation and attenuation due to a solid fuel flame have seriously affected MISTRAM I performance during third stage. Anticipation of this problem was the original reason for installing MISTRAM II. On many tests, MISTRAM I was unable to acquire passive data during third stage. This resulted in a weak solution, with no redundancy to reduce MISTRAM II bias errors. For this period, it makes little difference whether the MISTRAM I passive data are initialized or not. Again, performance on recent tests appears to be better.

(3) During the earlier tests in the MINUTEMAN Program, the filter (13 point, 2nd degree polynomial) used to derive velocity and acceleration data was not optimum for the dynamic characteristics of the missile. This caused errors in velocity and acceleration near staging times when the third derivative became large. This problem has been corrected by use of a 23 point, 3rd degree polynomial filter.

6.2.3.3 Data Characteristics - TITAN

Tables 6.2-13 through 6.2-17 are tabulations of MISTRAM I error estimates by frequency band for TITAN tests. The methods of estimation are the same as those described in 6.2.3.2 for MINUTEMAN tests.

Tables 6.2-18 and 6.2-19 give estimates of MISTRAM II high frequency and bias errors.

Low frequency error estimates are omitted from MISTRAM II because the actual data errors are confounded with errors due to survey uncertainty.

MISTRAM I performance on TITAN II was generally quite good during the sustainer portion of flight and rather poor during the booster portion. This is largely due to the use of an antenna on the missile which was too highly directional. The antenna main beam was oriented toward MISTRAM I at the end of powered flight, providing signal levels in excess of those required for satisfactory track. During the booster portion, however, rapidly fluctuating signals were obtained, with variable phase relationships among the various transmitted and received frequencies. Since MISTRAM depends on the measurement of phase to determine the trajectory, any phase variations which are not due to target motion appear as errors. In addition, errors due to refraction are most serious at lower elevation angles.

Because the TITAN II antenna system was designed before the decision to proceed with MISTRAM II was made, the orientation of the antenna was not very favorable for MISTRAM II on most flights. MISTRAM II was not required to obtain data and was not, at the time of the TITAN II flights, considered acceptable as a source of

(Text continued on page 6-39)

TABLE 6.2-13

ESTIMATED MISTRAM I ERRORS BY FREQUENCY BAND
TITAN II
R MEASUREMENT

Test	Booster				Sustainer			
	High Freq. (Ft.)	Low Freq. (Ft.)	Bias (Ft)	Total (Ft)	High Freq. (Ft)	Low Freq. (Ft)	Bias (Ft)	Total (Ft)
0354	0.0010	0.20	-0.1	0.2	0.0034	0.20	---	---
3303	0.0009	---	-0.8	---	0.0039	0.10	2.6	2.6
3787	0.0010	0.30	0.2	0.36	0.0038	1.90*	0.2	1.9
0525	0.0009	---	-8.5	8.5	0.0037	---	-8.5	8.5
0227	0.0008	0.07	-7.4	7.4	0.0012	0.02	-7.4	7.4
0104	0.0008	0.06	-0.5	0.5	0.0010	0.03	-4.4	4.4
0275	0.0009	---	0.5	---	0.0010	---	-14.1	14.1
0158	0.0010	0.10	1.8	1.8	0.0010	0.02	3.1	3.1
Root Mean Square	0.0009	0.17	4.1	4.1	0.0029	0.10	7.2	7.2
Mean Bias			-1.8				-4.1	
Standard Error about Mean Bias			3.8				5.7	

*Excluded from Root Mean Square Calculations.

TABLE 6.2-14

ESTIMATED MISTRAM I ERRORS BY FREQUENCY BAND
TITAN II
P_1 MEASUREMENT

Test	Booster				Sustainer			
	High Freq. (Ft)	Low Freq. (Ft)	Bias (Ft)	Total (Ft)	High Freq. (Ft)	Low Freq. (Ft)	Bias (Ft)	Total (Ft)
0354	0.0005	0.06	0.12	0.13	0.0003	0.01	---	---
3303	0.0006	---	-0.4	0.4	0.0002	0.01	0.003	0.01
3787	0.0006	0.02	0.07	0.07	0.0002	0.02	0.07	0.07
0525	0.0007	---	0.06	---	0.0003	---	0.06	---
0227	0.0003	0.02	-0.02	0.03	0.0002	0.02	-0.02	0.03
0104	0.0005	0.01	-0.19	0.19	0.0002	0.01	0.03	0.03
0275	0.0005	---	-0.02	---	0.0002	---	0.04	---
0158	0.0003	0.01	-0.01	0.01	0.0002	0.01	0.04	0.04
Root Mean Square	0.0005	0.03	0.16	0.16	0.0002	0.01	0.04	0.04
Mean Bias			-0.05				0.03	
Standard Error About Mean Bias			0.16				0.04	

TABLE 6.2-15

ESTIMATED MISTRAM I ERRORS BY FREQUENCY BAND
TITAN II
Q_1 MEASUREMENT

TEST	Booster				Sustainer			
	High Freq. (Ft)	Low Freq. (Ft)	Bias (Ft)	Total (Ft)	High Freq. (Ft)	Low Freq. (Ft)	Bias (Ft)	Total (Ft)
0354	0.0005	0.04	-0.02	0.04	0.0002	0.01	---	---
3303	0.0008	---	-0.03	---	0.0008	0.03	0.17	0.17
3787	0.0012	0.01	0.24	0.24	0.0002	0.02	0.24	0.24
0525	0.0006	---	-0.37	---	0.0002	---	-0.37	0.37
0227	0.0003	0.02	0.02	0.02	0.0002	0.01	0.02	0.02
0104	0.0004	0.01	0.31	0.31	0.0002	0.02	0.15	0.15
0275	0.0005	---	-0.09	---	0.0002	---	0.22	---
0158	0.0002	0.01	-0.14	0.14	0.0002	0.03	0.16	0.16
Root Mean Square	0.0006	0.02	0.20	0.20	0.0009	0.02	0.21	0.21
Mean Bias			-0.01				0.08	
Standard Error About Mean Bias			0.20				0.21	

TABLE 6.2-16

ESTIMATED MISTRAM I ERRORS BY FREQUENCY BAND
TITAN II
P_2 MEASUREMENT

Test	Booster				Sustainer			
	High Freq. (Ft)	Low Freq. (Ft)	Bias (Ft)	Total (Ft)	High Freq. (Ft)	Low Freq. (Ft)	Bias (Ft)	Total (Ft)
0354	0.0011	0.07	0.2	0.2	0.0005	0.04	---	---
3303	0.0012	---	-2.3	---	0.0004	0.13	1.1	1.1
3787	0.0012	0.02	1.8	1.8	0.0003	0.13	1.8	1.8
0525	0.0010	---	0.9	---	0.0004	---	0.9	---
0227	0.0004	0.45	-0.6	0.7	0.0002	0.17	-0.6	0.6
0104	0.0005	0.34	-0.9	0.9	0.0002	0.13	1.4	1.4
0275	0.0008	---	-0.6	---	0.0002	---	-0.3	---
0158	0.0009	0.42	-0.7	0.7	0.0004	0.07	0.1	0.1
Root Mean Square	0.0009	0.31	1.2	1.2	0.0004	0.12	1.1	1.1
Mean Bias			-0.3				0.6	
Standard Error about Mean Bias			1.2				0.9	

TABLE 6.2-17

ESTIMATED MISTRAM I ERRORS BY FREQUENCY BAND
TITAN II
Q_2 MEASUREMENT

Test	Booster				Sustainer			
	High Freq. (Ft)	Low Freq. (Ft)	Bias (Ft)	Total (Ft)	High Freq. (Ft)	Low Freq. (Ft)	Bias (Ft)	Total (Ft)
0354	0.0008	0.08	-0.4	0.4	0.0004	0.05	---	---
3303	0.0010	---	-1.1	---	0.0005	0.09	2.4	2.4
3787	0.0016	0.00	2.4	2.4	0.0020	0.18	2.4	2.4
0525	0.009	0.60	-2.6	---	0.0002	---	-2.6	---
0227	0.004	0.60	0.7	0.9	0.0002	0.17	0.7	0.7
0104	0.0005	0.23	1.7	1.7	0.0002	0.14	0.9	0.9
0275	0.0010	---	0.9	---	0.0002	---	0.6	---
0158	0.0005	0.23	-1.9	1.9	0.0002	0.03	0.9	0.9
Root Mean Square	0.0009	0.31	1.7	1.7	0.0007	0.12	1.7	1.7
Mean Bias			-0.04				0.8	
Standard Error about Mean Bias			1.7				1.7	

TABLE 6.2-18

MISTRAM II (PASSIVE) HIGH FREQUENCY ERROR ESTIMATES
TITAN II

Test	Time (Seconds)	Position (Feet)		
		R	P	Q
0525	150 - 230	0.0013	0.0004	0.0004
	230 - 359	0.0013	0.0002	0.0002
0104	144 - 346	0.0010	0.0005	0.0005
0275	156 - 251	0.0021	0.0003	0.0003

TABLE 6.2-19

MISTRAM II (PASSIVE) BIAS ESTIMATES
TITAN

Test	Time (Seconds)	Comparison	Position (Feet)	
			P	Q
3303	178 - 223	MISTRAM II-GLAD	0.7	0.7
	228 - 349	MISTRAM II-GLAD	-0.02	2.4
0227	148 - 346	MISTRAM II-GLAD	1.1	-3.0
0104	144 - 346	MISTRAM II-GLAD	2.2	0.1
0275	156 - 251	MISTRAM II-GLAD	2.4	-0.03
0158	148 - 241	MISTRAM II-GLAD	---	---
	255 - 326	MISTRAM II-GLAD	0.5	-0.1

Range Safety data. Therefore, the system tracked only passively during powered flight.

The GEMINI flights use TITAN II boosters and the same MISTRAM antenna system. Again there is no requirement for MISTRAM II data. Although a handover was made during the first GEMINI flight (Test 0275), it is planned to use MISTRAM II passively during future GEMINI missions.

6.2.3.4 Data Characteristics - SATURN

Tables 6.2-20 through 6.2-24 give MISTRAM I error estimates by frequency band for SATURN missiles SA-5, SA-6, and SA-7. The methods of estimation are the same as those described for MINUTEMAN under 6.2.3.2. Tables 6.2-25 and 6.2-26 give estimates of high frequency and bias errors for MISTRAM II. Low frequency estimates are omitted because the actual data errors are confounded with survey errors.

SATURN flights have yielded long continuous spans of MISTRAM I and II data, usually interrupted only briefly at staging and handover. The missile-borne antenna system has yielded generally good results. SATURN also carries many comparison systems, so that excellent MISTRAM error estimates are available. The BET on SATURN usually contains MISTRAM I, MISTRAM II, UDOP, and GLOTRAC. The bias estimates for MISTRAM I P_1 and P_2 on Test 2769 (SA-6) have been adjusted to remove biases introduced into the data by procedural errors in processing.

6.2.3.5 Estimation of Passive Range Sum Rate Biases

Table 6.2-27 gives estimates of bias and bias uncertainty in Valkaria and Eleuthera passive range sum rates, obtained from the GLAD Program. The passive range sum is an integration

(Text continued on page 6-45)

TABLE 6.2-20

ESTIMATED MISTRAM I ERRORS BY FREQUENCY BAND
SATURN
R MEASUREMENT

Test	Booster				Sustainer (Active)				Sustainer (Passive)			
	High Freq. (Ft)	Low Freq. (Ft)	Bias (Ft)	Total (Ft)	High Freq. (Ft)	Low Freq. (Ft)	Bias (Ft)	Total (Ft)	High Freq. (Ft)	Low Freq. (Ft)	Bias (Ft)	Total (Ft)
0169	0.0008	0.2	6.0	6.0	0.0010	0.1	-19.0	19.1	0.0018			
2769	0.0007	0.3	4.9	4.9	0.0009	0.1	- 5.7	5.7	0.0019	5.8		
4444	0.0007	0.3	5.0	5.02	0.0009	0.24	- 1.1	1.1	0.0017	1.4		

TABLE 6.2-21

ESTIMATED MISTRAM I ERRORS BY FREQUENCY BAND
SATURN
P_1 MEASUREMENT

Test	Booster				Sustainer (Active)				Sustainer (Passive)			
	High Freq. (Ft)	Low Freq. (Ft)	Bias (Ft)	Total (Ft)	High Freq. (Ft)	Low Freq. (Ft)	Bias (Ft)	Total (Ft)	High Freq. (Ft)	Low Freq. (Ft)	Bias (Ft)	Total (Ft)
0169	0.0002	0.02	0.26	0.26	0.0003	0.01	0.20	0.20	0.0011	0.02	0.17	0.17
2769	0.0003	0.03	-0.02	0.03	0.0003	0.03	-0.13*	0.13	0.0008	0.03	0.07	0.07
4444	0.0003	0.04	0.40	0.40	0.0004	0.02	0.09	0.09	0.0013	0.04	0.03	0.04

*Corrected for procedural error.

TABLE 6.2-22

ESTIMATED MISTRAM I ERRORS BY FREQUENCY BAND
SATURN
Q_1 MEASUREMENT

Test	Booster				Sustainer (Active)				Sustainer (Passive)			
	High Freq. (Ft)	Low Freq. (Ft)	Bias (Ft)	Total (Ft)	High Freq. (Ft)	Low Freq. (Ft)	Bias (Ft)	Total (Ft)	High Freq. (Ft)	Low Freq. (Ft)	Bias (Ft)	Total (Ft)
0169	0.0002	0.05	-0.03	0.06	0.0003	0.02	0.14	0.14	0.0012	0.04	-0.04	0.06
2769	0.0003	0.09	0.15	0.18	0.0003	0.01	0.04	0.04	0.0009	0.05	-0.01	0.05
4444	0.0003	0.03	-0.20	0.20	0.0004	0.02	0.09	0.09	0.0015	0.04	0.21	0.21

TABLE 6.2-23

ESTIMATED MISTRAM I ERRORS BY FREQUENCY BAND
SATURN
P_2 MEASUREMENT

Test	Booster				Sustainer (Active)				Sustainer (Passive)			
	High Freq. (Ft)	Low Freq. (Ft)	Bias (Ft)	Total (Ft)	High Freq. (Ft)	Low Freq. (Ft)	Bias (Ft)	Total (Ft)	High Freq. (Ft)	Low Freq. (Ft)	Bias (Ft)	Total (Ft)
0169	0.0010	0.05	2,98	2.98	0.0003	0.06	2.57	2.57	0.0009	0.05	0.58	0.58
2769	0.0004	0.12	-0.96	0.97	0.0003	0.12	-0.32*	0.33	0.0011	0.09	-0.57	0.58
4444	0.0003	0.13	2.21	2.22	0.0005	0.04	0.10	0.10				

*Corrected for procedural error.

TABLE 6.2-24

ESTIMATED MISTRAM I ERRORS BY FREQUENCY BAND
SATURN

Q_2 MEASUREMENT

Test	Booster				Sustainer (Active)				Sustainer (Passive)			
	High Freq. (Ft)	Low Freq. (Ft)	Bias (Ft)	Total (Ft)	High Freq. (Ft)	Low Freq. (Ft)	Bias (Ft)	Total (Ft)	High Freq. (Ft)	Low Freq. (Ft)	Bias (Ft)	Total (Ft)
0169	0.0003	0.21	0.93	0.95	0.0004	0.05	1.30	1.30	0.0014	0.09	-2.83	2.83
2769	0.0005				0.0004							
4444	0.0007	0.17	-1.21	1.22	0.0007	0.11	0.52	0.53	0.0018	0.06	4.09	4.09

TABLE 6.2-25

MISTRAM II HIGH FREQUENCY ERROR ESTIMATES
SATURN

Test	Time Span (Seconds)	Position (Ft)		
		R_{sum}	P	Q
Passive				
0169	252-328	0.009	0.0003	0.0003
2769	220-296	0.0011	0.0003	0.0002
4444	154-349	0.0020	0.0004	0.0004
Active				
0169	332-618	0.0007	0.0001	0.0001
2769	314-576	0.0006	0.0003	0.0001
4444	353-579	0.0012	0.0005	0.0005

TABLE 6.2-26

MISTRAM II BIAS ESTIMATES
SATURN

Test	Time Span (Seconds)	Comparison	Position (Ft)		
			R	P	Q
Passive Track					
0169	252-328	MISTRAM II-GLAD	- -	-1.43	-2.07
2769	220-296	MISTRAM II-GLAD	- -	-10.40	2.92
4444	154-349	MISTRAM II-GLAD	- -	1.26	2.53
Active Track					
0169	252-328	MISTRAM II-GLAD	-4.60	2.10	-0.02
2769	314-576	MISTRAM II-GLAD	1.60	-3.60	-1.43
4444	353-579	MISTRAM II-GLAD	2.19	-0.03	2.26

TABLE 6.2-27

ESTIMATES OF MISTRAM PASSIVE
RANGE SUM RATE BIASES

Test	Rate Biases ΔR_S (Ft/Sec)	Rate Bias Uncertainty $s_{\Delta R_S}$ (Ft/Sec)	Passive Station
3303	0.2	0.2	Eleuthera
0169	1.1	0.01	Eleuthera
	-1.1	0.01	Valkaria
0526	1.3	0.13	Eleuthera
	-1.3	0.06	Valkaria
0227	1.1	0.01	Eleuthera
0050	1.1	0.05	Eleuthera
0104	1.1	0.01	Eleuthera
0037	0.5	0.05	Eleuthera
0275	0.3	0.03	Eleuthera
0158	0.2	0.01	Eleuthera
2769	0.43	0.02	Eleuthera
	-0.45	0.073	Valkaria
4444	0.53	0.03	Eleuthera
	-0.60	0.005	Valkaria
3552	0.44	0.02	Eleuthera
	-0.35	0.035	Valkaria
4943	0.047*	0.009	Eleuthera
	-0.047*	0.009	Valkaria

*Absolute values constrained to be equal.

(cycle count) of the frequency difference between the signal received at the passive station and a locally synthesized signal which is as nearly as possible identical in frequency with the active station's transmitter. This difference frequency corresponds to the rate of change of the sum distance from active transmitter to vehicle to passive receiver, plus a bias due to a discrepancy between the active and passive frequency standards. The MISTRAM I frequency standard is a crystal oscillator which is phase-locked to a Range Timing 100 KC standard frequency sent by microwave from Cape Kennedy. It should thus be immune to differences in frequency with Range Timing over time periods longer than a few seconds. MISTRAM II has a rubidium frequency standard of excellent stability over long time periods. A LORAN C receiver has recently been installed at Eleuthera to standardize the Eleuthera standard. Range Timing is also checked against LORAN C. It is hoped eventually to obtain agreement between the Valkaria and Eleuthera frequency standards to 5 parts in 10^{11}. The values estimated for the range sum rate bias in Table 6.2-27 appear to show a decline with time. The value for Test 4943 corresponds approximately to the 5 parts in 10^{11} goal.

6.3 GLOTRAC

6.3.1 System Description

GLOTRAC is an integrated, high precision tracking system. Operational acceptance of Segment 1 occurred early in 1965. The Segment 1 configuration now in service is shown in Figure 6.3-1. Equipment presently in use is listed in Table 6.3-1. The system employs strong geometry and simple field equipment. The data reduction features an error model, minimum variance trajectory adjustment technique which is similar to the Best Estimate of Trajectory (BET) methods which have been employed by the Range for some time.

Each GLOTRAC station as presently implemented measures only one quantity, a range sum or range difference. This quantity is derived by phase comparing a nominal 5000 mc received signal with a local, highly stable, signal referenced to an Atomichron Frequency Standard. A carrier wavelength of only 6 cm is involved. The data are ambiguous and must be initialized in the data re-reduction process. Frequency standard phase drift is also removed in data reduction.

GLOTRAC may either share the AZUSA transponder or may employ its own specially designed unit. With either arrangement GLOTRAC and AZUSA are compatible. When AZUSA MARK II is in control of the transponder, (See Figure 6.3-2), each slave site measures a range difference quantity referenced to the AZUSA central receiver. When a GLOTRAC transmitter is in control each slave site measures a range sum quantity referenced to the transmitter site.

GLOTRAC, aside from AZUSA, presently does not have real-time capability. GLOTRAC may be modified for this purpose in the future.
(Text continued on page 6-50)

FIGURE 6.3-1

GLOTRAC FIELD COMPLEX

(SEGMENT 1)

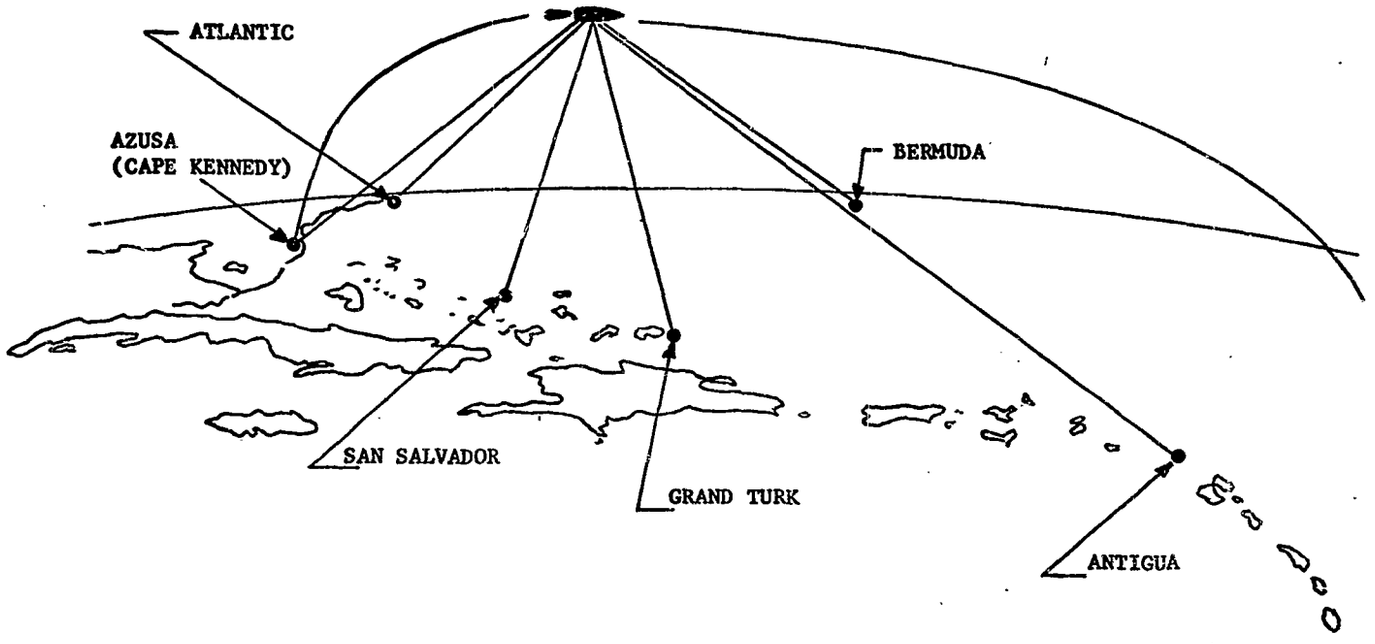


TABLE 6.3-1

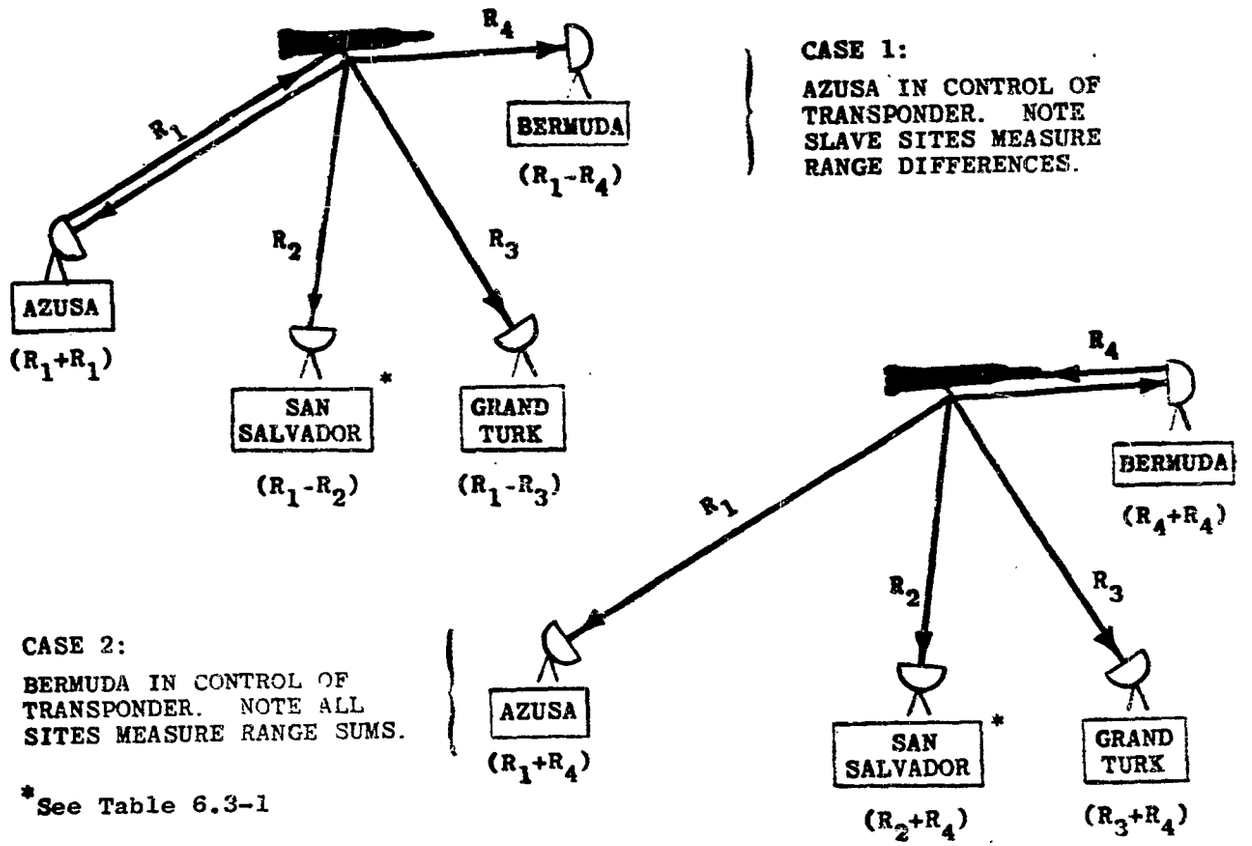
GLOTRAC SEGMENT 1 CONFIGURATION

Station	Special GLOTRAC Equipment	Other Equipment
Antigua	Range Rate Receiver	FPQ-6 (91.19)
Atlantic	Range Rate Receiver	
Bermuda	Range Rate Receiver including a Range Measurement Module, Transmitter	
Cape Kennedy		MARK II AZUSA FPS-16 (1.16)
Grand Bahama		FPS-16 (3.16)
PAFB		FPQ-6 (0.18)
Grand Turk	Range Rate Receiver, Transmitter	FPS-16 (5.16)
Eleuthera	Range Rate Receiver	
San Salvador*		

*The San Salvador GLOTRAC station was recently decommissioned. The FPS-16 Radar (5.16) at San Salvador is in two week call-up status. The San Salvador GLOTRAC transmitter was moved to Grand Turk.

FIGURE 6.3-2

GLOTRAC MEASURED QUANTITIES



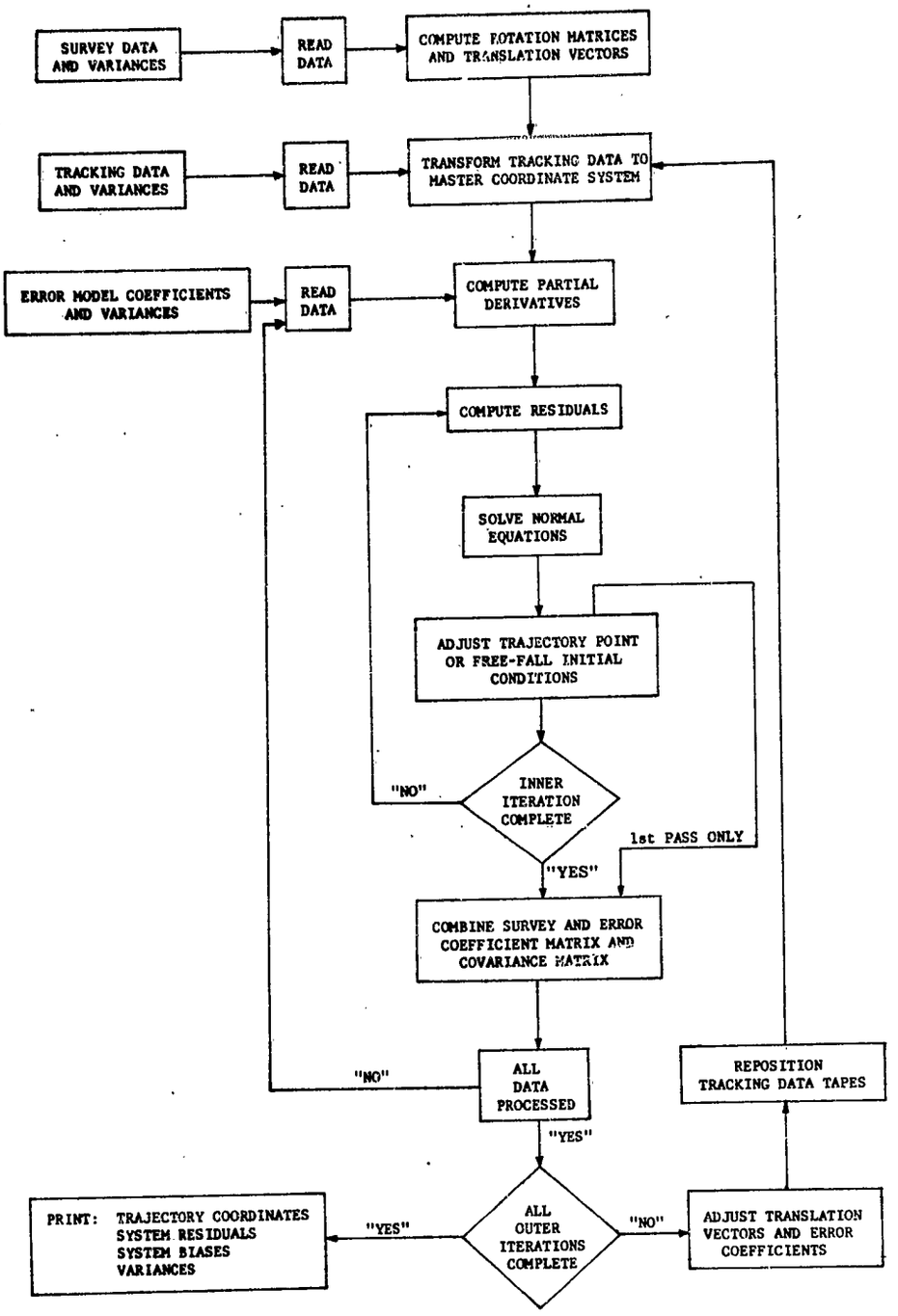
*See Table 6.3-1

The data reduction method employed by GLOTRAC is known as GLAD and gets its name from GLOTRAC Adjustment. Since the data reduction process is an integral part of the GLOTRAC concept and, in a sense, constitutes part of the "system," a brief description follows. Timing, transit time and refraction corrections are made to the data during the pre-GLAD editing process. Figure 6.3-3 is a flow chart illustrating the GLAD reduction. The GLAD processing is started by reading into memory from tape, survey data including uncertainties for all stations. Rotational matrices and translation vectors are computed and used to transform GLOTRAC input data (which are also read in from tape) to the master rectilinear coordinate system. A priori error model coefficients and their variances for all stations are read in from cards and partial derivatives of all measurements are computed with respect to x, y, z (approximate trajectory point), survey and error model parameters. Residuals are computed for all systems in their natural measurement coordinates for each datum point. The normal equations for a least squares adjustment are formulated and solved and error model coefficients including survey are combined (summed) into a common matrix. At the end of the point by point trajectory sequence this matrix contains the accumulated information necessary for the first "outer loop" adjustment. It is important to note that because of relatively poor GLOTRAC initialization at the start of the process individual trajectory points are <u>not adjusted</u> by the "inner loop" on the first pass.

The first outer loop adjustment consists of simultaneously correcting survey values and error model coefficients for all systems across a trajectory span. Tapes are then repositioned and the entire process restarted. The inner loop is allowed to operate (one or more times) on the second and subsequent passes since a good GLOTRAC initialization has now been obtained.
(Text continued on page 6-52)

FIGURE 6.3-3

GLAD DATA PROCESSING FLOW CHART



Measurements are weighted by the reciprocal of their random error variance.

After the adjustment is complete, a newly determined trajectory is read out. A printout is made of the following items:

(a) Measurement residuals (in the natural coordinates of the system).
(b) Survey adjustments with their estimated uncertainties.
(c) Estimated error model coefficients with their estimated uncertainties.
(d) Estimated errors in cartesian coordinates (usually position and velocity) based on uncertainties in the GLAD estimated error model coefficients and the a priori random errors.
(e) The correlation matrix of the estimated error model coefficients.

6.3.2 Error Sources

The GLAD Program will presently accomodate a generalized error model of the form:

$$\Delta R = R - R_m = a_0 + a_1 R + a_2 \dot{R} + a_3 \csc E_0 + a_4 \csc E_i + a_5 t + \epsilon_R$$

where:

R_m = Measured range sum (or range difference)

R = Adjusted range sum (or range difference)

E_0 = Elevation angle at the transmitter site

E_i = Elevation angle at the remote site

a_0 = Initializing constant (Note: Since GLOTRAC data are ambiguous, a_0 is the entire initializing constant)

$a_1 R$ = Error due to frequency bias in active ranging or to

uncertainty in the measured velocity of propagation of electromagnetic waves

$a_2\dot{R}$ = Timing bias error at a particular GLOTRAC station with respect to central timing

$a_3 \csc E_0$ = Residual refraction error (central site)

$a_4 \csc E_i$ = Residual refraction error (remote site)

$a_5 t$ = Error due to frequency bias (remote site with respect to central)

ϵ_R = Residual error (includes thermal noise, multipath variations, transponder delay variations, digital resolution, computer round-off, remaining or unaccountable systematic error, etc.)

The terms of the generalized model are essentially the same as those of the MISTRAM error model. For a term-by-term treatment, the reader is referred to MISTRAM Section 6.2.2.1.

To date, simplified forms of the model have been employed to reduce computational complexity and to conserve available degrees of freedom. Analyses to date have shown that the unused terms are small compared to the terms being estimated. The models currently in use are:

GLOTRAC	$\Delta R = a_0 + a_5 t + \epsilon_R$
AZUSA and Pulse Radar Range	$\Delta R = a_0 + \epsilon_R$
AZUSA l and m	$\Delta l = b_0 + \epsilon_l$
	$\Delta m = c_0 + \epsilon_m$

The GLAD program is also capable of estimating the survey for ten tracking locations up to a maximum of 30 survey adjustments.

When considering GLOTRAC System error sources, it is necessary to consider several additional factors some of which are not error sources in the usual sense, but which contribute heavily to the ability of GLAD to recover error model coefficients accurately.

1. Inadequate Redundancy
   This may be due simply to an insufficient number of deployed sites or to site reliability factors such as inadequate signal coverage (missile antenna pattern), ground station antenna pointing errors, inability to acquire and hold phase lock, poor handover coordination, etc.

2. Inadequate Geometric Strength
   Geometry must be considered in the field deployment of GLOTRAC stations and an attempt must be made to provide optimized geometry at all times of flight.

3. Inadequate Trajectory Span
   GLAD determines error model coefficients by an iterative adjustment which essentially optimizes the fit of data over a trajectory span. In the free fall case GLAD applies the equations of motion to a span of data. Obviously, to maximize accuracy, the fit should be made over as long a trajectory span as permitted by the uncertainty in the earths gravitational model and the fit of the system error models.

4. Inadequate or Incorrect Error Model

5. Inadequate A Priori Knowledge of Input Parameters (particularly as it applies to survey adjustments, weighting and error propagation)

6. Capacity of the GLAD Program
   The GLAD Program is currently limited to estimating 50 error model coefficients including 10 survey adjustments. GLAD capacity is a limiting factor on the accuracy of the reduced GLAD data in some instances.

6.3.3 System Accuracies

GLOTRAC as a system has produced data on relatively few missions to date due to lack of adequate signal coverage of the large GLOTRAC complex.

Estimates of GLOTRAC accuracies are based on data for the following missile tests:

Range Test	Date	Type of Missile
5175	11-27-63	ATLAS/CENTAUR
2769	5-28-64	SATURN SA-6
0448	7-28-64	ATLAS/RANGER-7
4444	9-18-64	SATURN SA-7

6.3.3.1 Accuracy Estimates

Estimates of GLOTRAC accuracy for ATLAS and SATURN missiles are tabulated in Table 6.3-2. The a priori estimates represent bias uncertainty before adjustment of the GLOTRAC error model by the GLAD Program, and the a posteriori estimates illustrate bias uncertainty after the adjustment.

Figures 6.3-4 and 6.3-5 are plots of the propagation of current GLOTRAC total errors (Table 6.3-2) into rectangular coordinate position and velocity errors respectively for the ATLAS and SATURN trajectories for the above listed tests.

6.3.3.2 Data Characteristics

Tables 6.3-3, 6.3-4, 6.3-5 and 6.3-6 are tabulations of GLOTRAC error estimates by frequency band for Tests 5175, 2769, 0448, and 4444 respectively. The high frequency numbers are obtained from mid-point deviations about a three second moving arc, 31 point, 2nd degree polynomail fit to GLOTRAC data. The high

(Text continued on page 6-61)

TABLE 6.3-2

ACCURACY ESTIMATES

GLOTRAC Station	Range Difference				Range Difference Rate (3)			
	s_{Bias} (Ft)			s_{Random} (Ft)	s_{Bias} (Ft/Sec)			s_{Random} (Ft/Sec)
	a priori (4)	a pos-(1) teriori	a pos-(2) teriori		a priori	a pos-(1) teriori	a pos-(2) teriori	
Van 4	10^7	0.4	- - -	0.40	0.50	0.001	- - -	0.10
Van 10	10^7	- - -	5.2	0.40	0.50	- - -	0.02	0.10
Atlantic	10^7	15.8	21.1	0.40	0.50	0.07	0.06	0.10
Bermuda	10^7	67.6	- - -	0.40	0.50	0.18	- - -	0.10
San Salvador	10^7	17.3	6.7	0.40	0.50	0.05	0.01	0.10
Grand Turk	10^7	26.5	6.0	0.40	0.50	0.07	0.02	0.10
Antigua	10^7	100.3	- - -	0.40	0.50	0.21	- - -	0.10

(1) These estimates assume that error model coefficients are adjusted by the GLAD Program with AZUSA, GLOTRAC and Radar as inputs.

(2) These estimates assume that error model coefficients are adjusted by the GLAD Program with AZUSA, GLOTRAC and Radar as inputs including about 75 seconds of free fall data.

(3) Rate derived by use of a 21 point, 2nd degree polynomial.

(4) Must be initialized.. Hence arbitrary large numbers used for initial a priori error estimate.

Best Available Copy

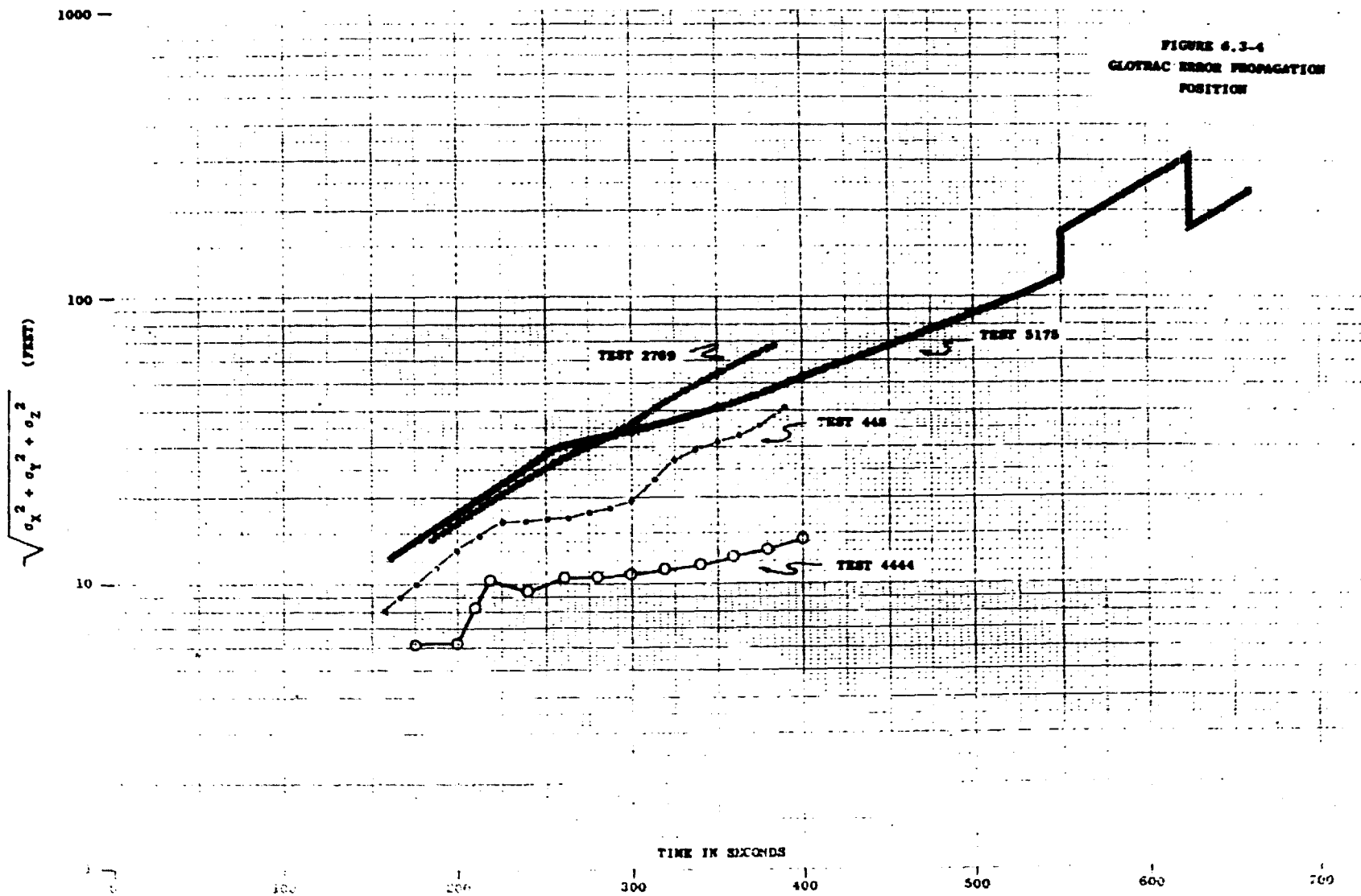


FIGURE 6.3-4
GLOTRAC ERROR PROPAGATION
POSITION

Best Available Copy

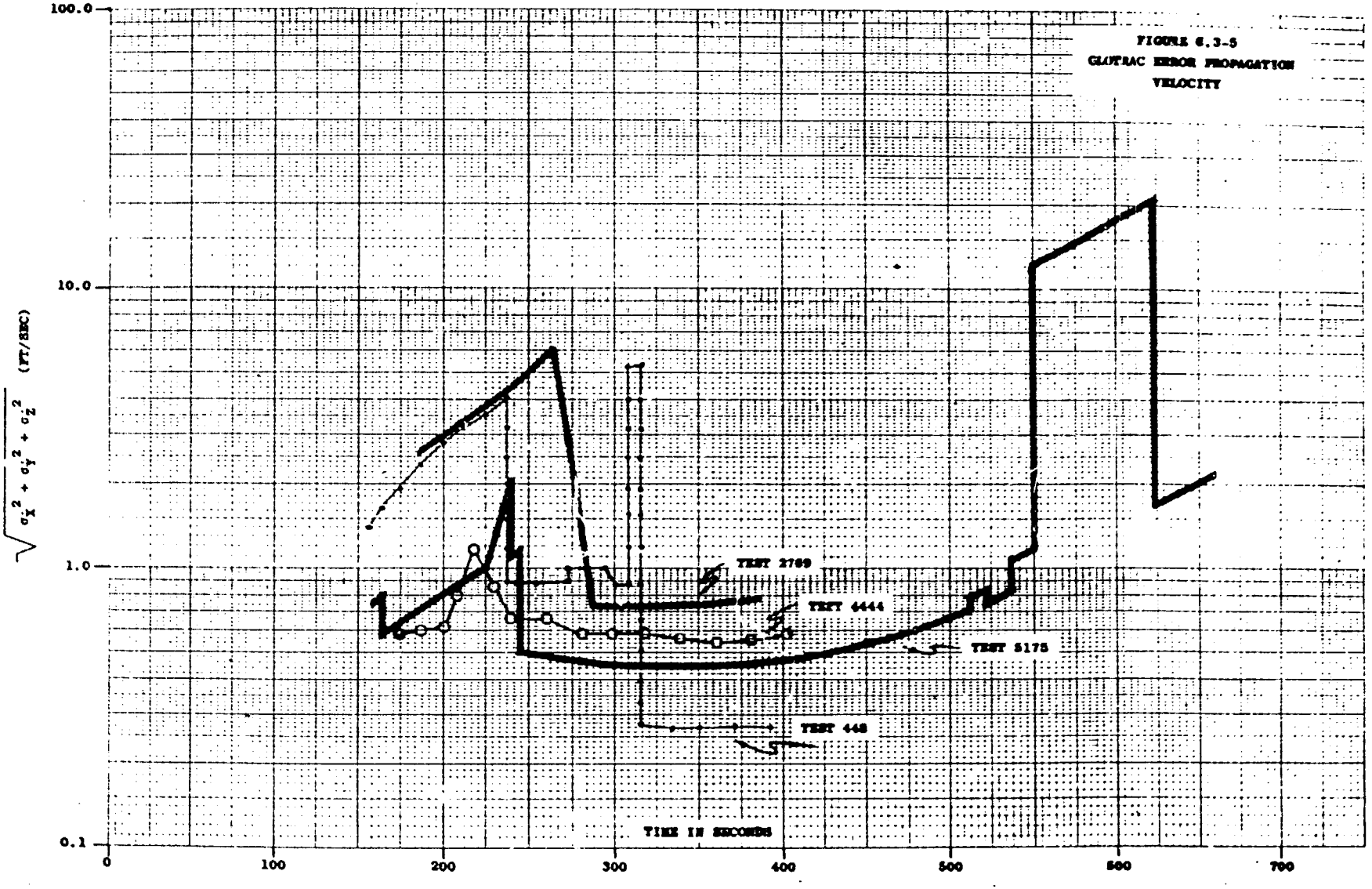


FIGURE 6.3-5
GLOTRAC ERROR PROPAGATION
VELOCITY

TABLE 6.3-3

ESTIMATED GLOTRAC ERRORS BY FREQUENCY BAND
ATLAS CENTAUR TEST 5175

Station	Time Span (Seconds)	Range Difference (Ft)			Range Difference Rate (Ft/Sec)			
		High Freq.	Low Freq.	Bias*	High Freq.	Low Freq.	Bias	Total
Atlantic	298-512	0.16	0.72	19.6	0.06	0.19	0.10	0.22
Bermuda	245-512	0.16	0.45	94.9	0.06	0.13	0.10	0.17
San Salvador	165-512	0.12	0.37	18.0	0.04	0.04	0.05	0.08
Grand Turk	265-430	0.16	0.24	39.4	0.06	0.00	0.10	0.12
Antigua	350-512	0.34	0.54	105.7	0.12	0.00	0.07	0.14

TABLE 6.3-4

ESTIMATED GLOTRAC ERRORS BY FREQUENCY BAND
SATURN TEST 2769

Station	Time Span (Seconds)	Range Difference (Ft)			Range Difference Rate (Ft/Sec)			
		High Freq.	Low Freq.	Bias*	High Freq.	Low Freq.	Bias	Total
Van 4	254-499	0.05	0.90	0.4	0.02	0.15	0.00	0.15
Grand Turk	214-499	0.14	0.52	22.3	0.05	0.09	0.07	0.12
San Salvador	184-499	0.05	0.49	23.0	0.02	0.05	0.07	0.09
Bermuda	279-454	0.05	0.04	61.5	0.02	0.02	0.29	0.29
Antigua	434-499	0.03	0.29	95.8	0.01	0.08	0.28	0.29

*Does not include contribution of $A_5 t$ term

TABLE 6.3-5

ESTIMATED GLOTRAC ERRORS BY FREQUENCY BAND
ATLAS RANGER TEST 0448

Station	Time Span (Seconds)	Range Difference (Ft)			Range Difference Rate (Ft/Sec)			
		High Freq.	Low Freq.	Bias*	High Freq.	Low Freq.	Bias	Total
Powered Flight								
Atlantic	156-316	0.09	0.15	21.10	0.03	0.00	0.06	0.06
Van 10	156-316	0.07	3.82	5.25	0.03	0.40	0.02	0.40
Grand Turk	156-316	0.08	0.39	5.99	0.03	0.12	0.02	0.12
San Salvador	156-316	0.07	0.34	6.66	0.02	0.10	0.01	0.10
Free Fall								
Atlantic	316-392	0.07	0.39	21.10	0.02	0.16	0.06	0.17
Van 10	316-392	0.09	9.39	5.25	0.03	0.39	0.02	0.39
Grand Turk	316-392	0.14	1.41	5.99	0.05	0.22	0.02	0.23
San Salvador	316-392	0.08	0.57	6.66	0.03	0.26	0.01	0.26

TABLE 6.3-6

ESTIMATED GLOTRAC ERRORS BY FREQUENCY BAND
SATURN TEST 4444

Station	Time Span (Seconds)	Range Difference (Ft)			Range Difference Rate (Ft/Sec)			
		High Freq.	Low Freq.	Bias*	High Freq.	Low Freq.	Bias	Total
Atlantic	173-403	0.07	0.12	9.87	0.03	0.03	0.02	0.05
Bermuda	274-403	0.08	0.21	11.27	0.03	0.00	0.04	0.05
San Salvador	174-403	0.09	0.41	6.36	0.03	0.06	0.02	0.07
Grand Turk	219-403	0.20	0.33	4.99	0.07	0.00	0.02	0.07

*Does not include contribution of $A_5 t$ term

frequency rate data estimates were computed as the product of the position data and a scale factor derived for a 21 point, second degree filter. The applicable frequency band for high frequency error is 0.15 cps $< f \leq$ 5 cps.

The low frequency error estimates represent the square root of the variance of the GLAD residuals minus the variance of the high frequency error. The average frequency band for low frequency error is 0.0019 cps $< f \leq$ 0.15 cps.

The bias uncertainties are the standard deviation of the error model coefficients computed by the GLAD program. The average frequency band for bias estimates is 0 cps $< f \leq$ 0.0019 cps.

Total range difference error was not computed on the tests included in this report because the standard deviation of the second term of the error model ($a_5 t$) was not available.

6.4 AZUSA MARK II

6.4.1 System Description

6.4.1.1 General

The AZUSA MARK II System is a microwave interferometer which measures the position in space of an airborne target. It provides information for real time impact prediction and post flight trajectory analysis. The system is the operational counterpart of the experimental AZUSA MARK I System (recently decommissioned). Together these systems have participated in over 500 ballistic missile launches to date.

The AZUSA MARK II System has been modified for use with the GLOTRAC System and works with either an AZUSA or GLOTRAC transponder.

6.4.1.2 Measurement Techniques

The basic AZUSA position measurements are slant range and two direction cosines, the latter being determined for the direction angles formed by the range vector and two mutually perpendicular, bisecting baselines. The AZUSA MARK II baseline arrangement is shown in Figure 6.4-1. The "rate" antennas (X_{Rate} and Y_{Rate}) are used to provide high resolution, ambiguous range difference data. A high resolution, ambiguous range measurement is made in addition to non-ambiguous modulation range.

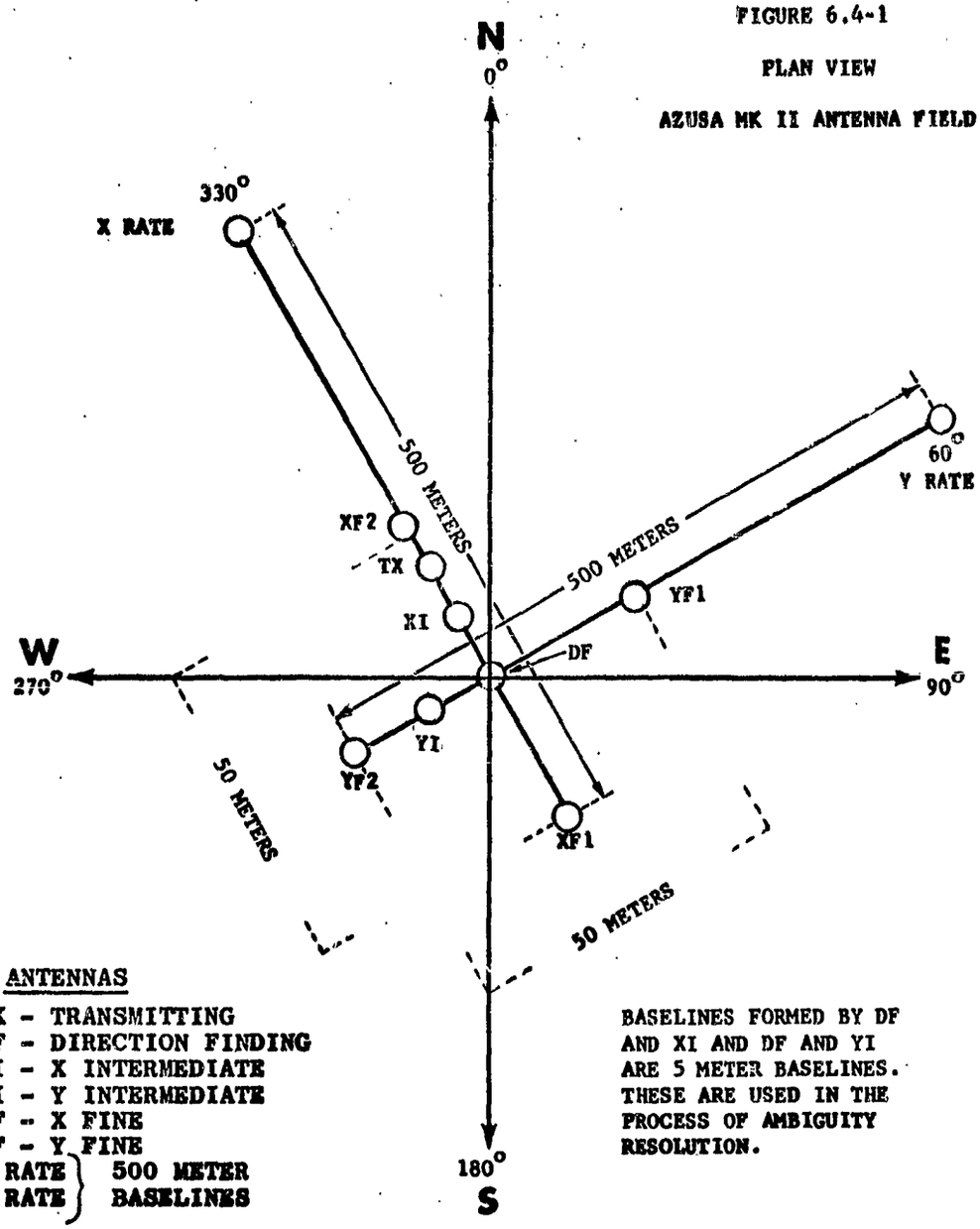
Slant range measurements are accomplished by means of phase comparison (See Figure 6.4-2). The ground to air carrier signal of approximately 5060 mc is frequency modulated with three harmonically related ranging tones. In the transponder, these are extracted and used to modulate the return carrier. At the AZUSA MARK II site the transmitted and received ranging signals are phase compared. The phase delay encountered in propagating to

(Text continued on page 6-65)

FIGURE 6.4-1

PLAN VIEW

AZUSA MK II ANTENNA FIELD



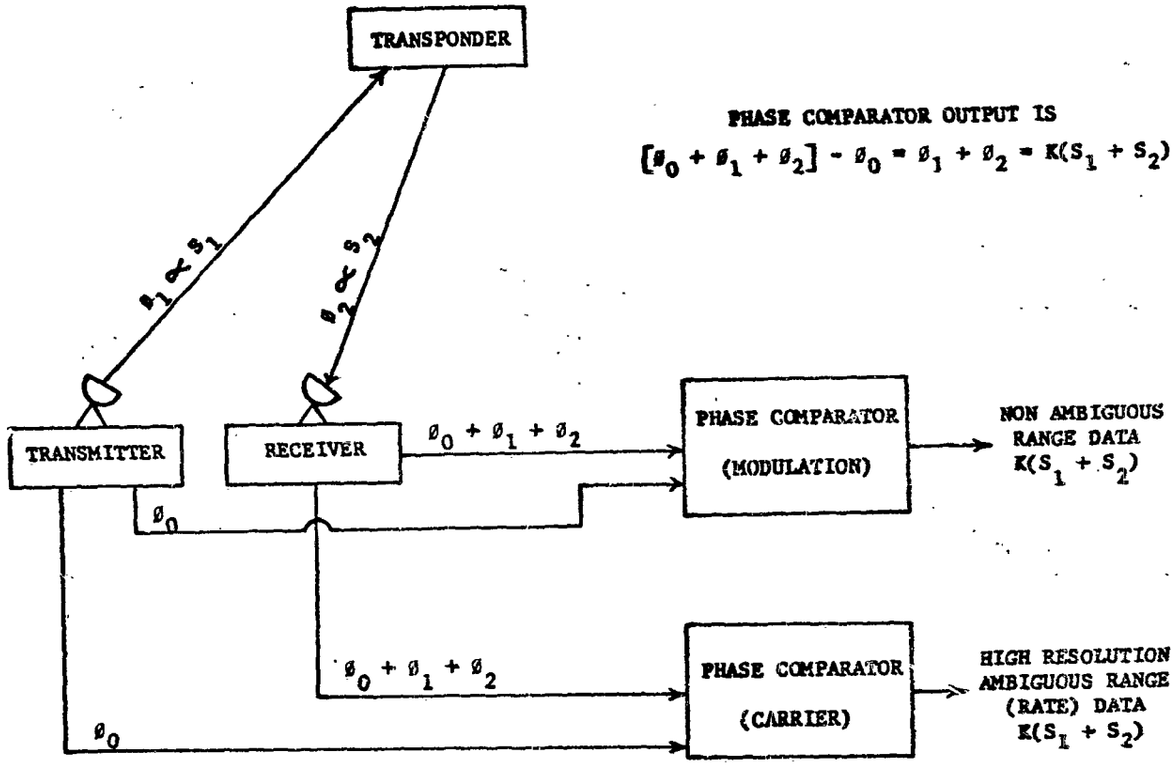
ANTENNAS

TX - TRANSMITTING
DF - DIRECTION FINDING
XI - X INTERMEDIATE
YI - Y INTERMEDIATE
XF - X FINE
YF - Y FINE
X RATE } 500 METER
Y RATE } BASELINES

BASELINES FORMED BY DF AND XI AND DF AND YI ARE 5 METER BASELINES. THESE ARE USED IN THE PROCESS OF AMBIGUITY RESOLUTION.

FIGURE 6.4-2

AZUSA RANGE MEASUREMENT



and from the target is proportional to the slant range. Three modulation frequencies are required to resolve range ambiguities. The range thus derived is referred to as modulation range. Coherent carrier range, R_C, an ambiguous quantity, is derived in a similar manner using the microwave carrier. Coherence between the transmitted and received carriers is maintained through the transponder by means of phase lock circuitry. Coherent carrier range data, having a resolution of approximately 0.1 foot, (3.0 cm) are normally published as AZUSA range data.

Baseline data (ℓ and m) are derived as follows (See Figure 6.4-3). A microwave carrier of 5000 mc (nominal) is emitted from the target. The signal will encounter a phase delay, ϕ_1, in propagating to antenna 1 and a phase delay, ϕ_2, in propagating to antenna 2. The phase comparator accepts ϕ_1 and ϕ_2 as inputs and provides $(\phi_1 - \phi_2) = K\,(S_1 - S_2)$ as an output. The output quantity may be "normalized" to provide a direction cosine as follows:

From the Law of Cosines,

$$S_1^2 = R^2 + (\frac{D}{2})^2 + 2R\,(\frac{D}{2})\cos\beta$$

$$S_2^2 = R^2 + (\frac{D}{2})^2 - 2R\,(\frac{D}{2})\cos\beta$$

$$S_1^2 - S_2^2 = 2RD\cos\beta$$

$$(S_1 - S_2)(S_1 + S_2) = 2RD\cos\beta$$

But

$$S_1 + S_2 \simeq 2R \text{ for } R >> D$$

Therefore

(Text continued on page 6-67)

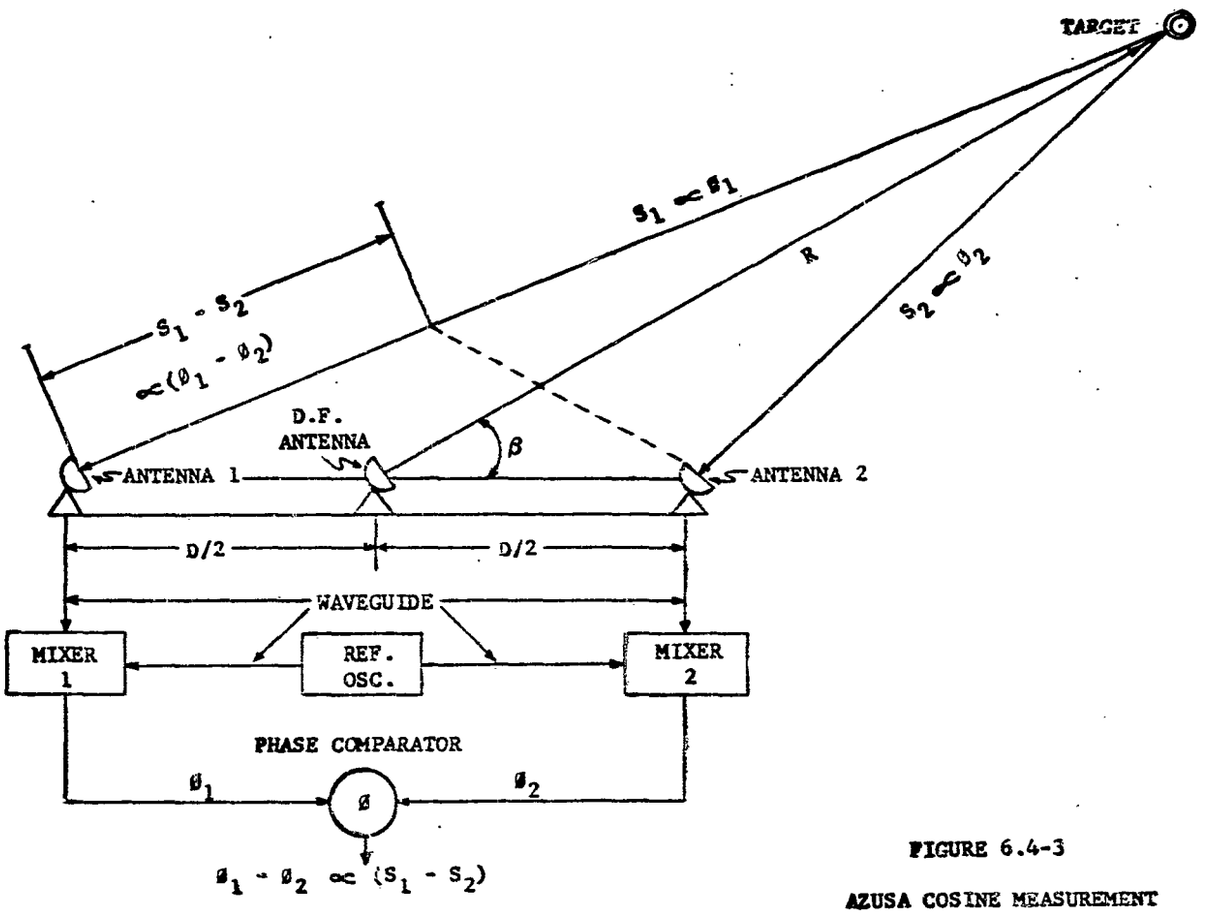


FIGURE 6.4-3

AZUSA COSINE MEASUREMENT

$S_1 - S_2 \simeq D \cos \beta$, or

$$\text{Cos } \beta \simeq \frac{S_1 - S_2}{D}, \text{ for } R >> D$$

In practice this approximation is very good, the error involved being less than 50 ppm cosine error at a tracking distance of one mile.

6.4.1.3 Characteristics and Specifications

Volume of Coverage

- Azimuth: 360 degrees
- Elevation: 5 to 85 degrees (The lower limit is associated with increased errors due to multipath and refraction)
- Range: Up to 1000 nautical miles

Rate Limits

- Range Rate: 0 to 60,000 feet/second
- Angular Rate:
  - Azimuth: 0 to 1.0 radian/second
  - Elevation: 0 to 0.4 radian/second
  - Cosine: 0 to 0.1 per second

Sampling Rate: 20 points per second

Digital Data Least Significant Bit Values

- Range: 0.98 feet
- Coherent Carrier Range: 0.098 feet
- Direction Cosines:
  - 50 Meter Baselines: 1.87×10^{-6}
  - 500 Meter Baselines: 1.87×10^{-7}

Shadowing occurs at the baseline ends since one antenna may block the view of another. This shadow zone has a half angle of about 18°.

The system has a signal threshold of about -155 dbw as measured at the microwave mixers. For metric data commitments the signal must be at least -135 dbw. For range safety the signal must be at least -145 dbw. The five foot AZUSA parabolic antennas have an effective gain ahead of the mixers of approximately +33 db.

6.4.2 Error Sources

The current AZUSA error model is of the generalized form

$$\Delta R = a_0 + a_1 R + a_2 \dot{R} + a_3 \csc E_0 + a_4 t + \epsilon_R$$

$$\Delta \ell = b_0 + b_1 \ell + b_2 \dot{\ell} + b_3 (\csc E_{\ell_1} - \csc E_{\ell_2}) + b_4 t + \epsilon_\ell$$

$$\Delta m = c_0 + c_1 m + c_2 \dot{m} + c_3 (\csc E_{m_1} - \csc E_{m_2}) + c_4 t + \epsilon_m$$

Where:

ΔR, $\Delta \ell$, and Δm are differences between the AZUSA measurements, R, ℓ, and m, and corresponding data from a comparison standard.

E_0 = elevation angle at the central antenna

E_{ℓ_1}, E_{ℓ_2} = elevation angles at the X_{f_1} and X_{f_2} antennas respectively

E_{m_1}, E_{m_2} = elevation angles at the Y_{f_1} and Y_{f_2} antennas respectively

t = time of observation

ϵ_R, ϵ_ℓ, ϵ_m = unmodeled errors in R, ℓ, and m

a_0, b_0, c_0 = initialization errors in R, ℓ, and m. In the case of range this term also accounts for unknown transponder delays.

a_1R, $b_1\ell$, c_1m = scale factor errors in R, ℓ, and m due to frequency standard error and uncertainty in the determination of the velocity of propagation of electromagnetic waves in space.

$a_2\dot{R}$, $b_2\dot{\ell}$, $c_2\dot{m}$ = timing errors in R, ℓ, and m with respect to AFETR timing central

$a_3 \csc E_0$, $b_3 (\csc E_{\ell_1} - \csc E_{\ell_2})$, $c_3 (\csc E_{m_1} - \csc E_{m_2})$ = residual (uncorrected) refraction errors in R, ℓ, and m

a_4t, b_4t, c_4t = warm up type errors in AZUSA. (NOTE: The use of this term for passive operation no longer applies to AZUSA since MARK I has been decommissioned.)

For a more detailed term-by-term discussion of similar error models, the reader is referred to the GLOTRAC and MISTRAM sections.

Some simplifications of the AZUSA error models are possible from physical considerations. The zero subscript terms must be retained. These terms as well as their uncertainties are generally large.

The subscript one terms may usually be dropped from consideration since frequency standard error is known to be better than 1.0×10^{-6} and uncertainties in the velocity of propagation of light are also on this order.

Timing at AZUSA MARK II with respect to AFETR central is known to within one or two microseconds, therefore the subscript two terms may be dropped.

Analysis has shown that the residual refraction (subscript 3) terms are usually small with respect to the bias terms. This is because the standard refraction corrections made in data processing are generally good. Furthermore, in the case of AZUSA ℓ and m cosine, the difference in elevation angle at the baseline ends is quite small in any practical tracking situation.

Drift errors in the system are suppressed significantly by providing adequate warm-up time before a mission. It is therefore permissible, in general, to eliminate the subscript 4 terms.

The remaining models, consisting simply of bias error terms and residual (random) error terms have provided a basis for AZUSA accuracy studies. Analysis has shown that the bias terms and their uncertainties are generally predominant which supports the previous argument on elimination of terms. The argument is also supported by frequency band analysis which has shown bias type errors (near zero frequency errors) to be large with respect to higher frequency errors.

Transit time errors are not considered in the error model since the corrections made in data processing for this error are essentially exact.

The residual (random) error terms, of course, include all unmodeled and non-systematic errors such as thermal noise at low signal levels, variations in propagation (multipath) and in transponder delay, measurement resolution, approximation and round-off error, etc.

6.4.3 System Accuracies

AZUSA MARK II accuracy estimates and data characteristics contained in this report are based on analysis of data from the

following missile tests:

Range Test	Launch Date	Type of Missile
5175	11-27-63	ATLAS/CENTAUR
0169	1-29-64	SATURN SA-5
2769	5-28-64	SATURN SA-6
0448	7-28-64	ATLAS/RANGER-7
4751	9-1-64	TITAN III
4307	9-5-64	ATLAS (OGO)
4444	9-18-64	SATURN SA-7

6.4.3.1 Accuracy Estimates

Table 6.4-1 indicates current estimates of AZUSA MARK II accuracy. The a priori column represents bias uncertainty before adjustment of the AZUSA error model by the GLAD program, and the a posteriori column illustrates bias uncertainty after the adjustment.

Figure 6.4-4 is a plot of the propagation of current AZUSA a priori total errors (Table 6.4-1) into rectangular coordinate position and velocity errors for the SATURN trajectory.

6.4.3.2 Data Characteristics

Tables 6.4-2, 6.4-3, and 6.4-4 are tabulations of AZUSA MARK II error estimates by frequency band. The high frequency estimates are obtained by a 3rd order variate difference method adjusted to the frequency band 7.4 cps $< f \leq$ 10 cps. The low frequency estimates are the square root of the variance of the GLAD residuals minus the variance of the high frequency error and are applicable to the frequency band .0022 cps $< f \leq$ 7.4 cps. The bias estimates are means of BET residuals or GLAD bias error model coefficient estimates. The average frequency band for the bias estimates is $0 < f \leq .0022$ cps.

(Text continued on page 6-76)

TABLE 6.4-1

ACCURACY ESTIMATES - AZUSA MARK II

Measurement	Position			Rate**
	s_{Bias}		s_{Random}	s_{Random}
	a priori	a posteriori*		
Booster				
ℓ_c	50 ppm	No Data	25 ppm	4.0 ppm/sec
m_c	50 ppm	No Data	25 ppm	3.0 ppm/sec
R_c	15 ft	No Data	.6 ft	0.2 ft/sec
Sustainer				
ℓ_c	30 ppm	5.0 ppm	6 ppm	1.0 ppm/sec
m_c	30 ppm	7.0 ppm	6 ppm	1.0 ppm/sec
R_c	15 ft	4.0 ft	.6 ft	0.1 ft/sec

*These estimates assume that the biases are adjusted by the GLAD Program with AZUSA, GLOTRAC, and Radar as input.

**Rate for ℓ_c and m_c derived by use of a 61 point, 2nd degree polynomial.

Rate for R_c derived by use of a 31 point, 2nd degree polynomial.

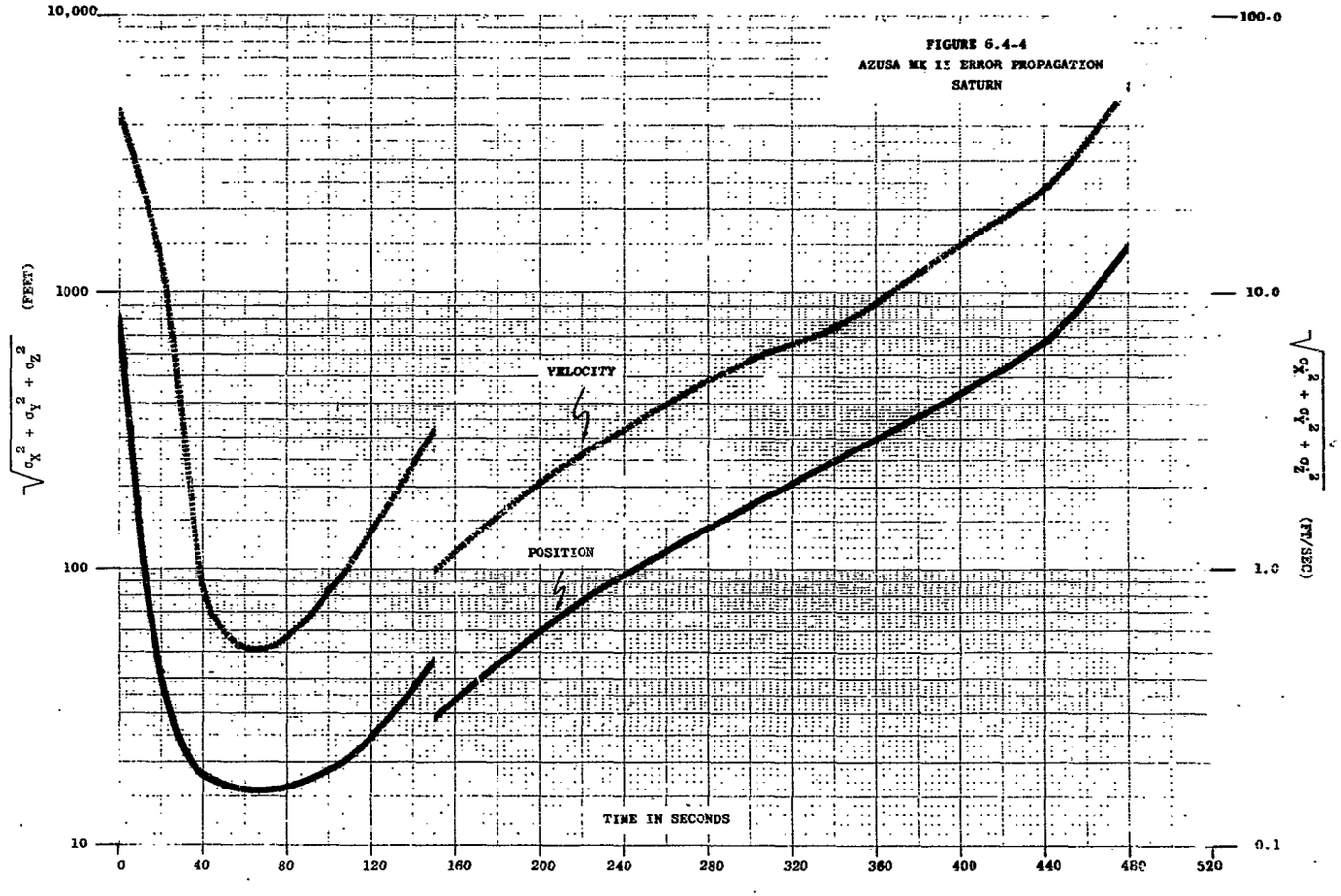

FIGURE 6.4-4
AZUSA MK II ERROR PROPAGATION
SATURN
10,000
1000
100
10
100.0
10.0
1.0
0.1
VELOCITY
POSITION
TIME IN SECONDS
0
40
80
120
160
200
240
280
320
360
400
440
480
520
(FEET)
(FT/SEC)

TABLE 6.4-2

ESTIMATED AZUSA MARK II ERRORS BY FREQUENCY BAND
$\dot{\ell}_c$ MEASUREMENT

Test	Booster				Sustainer			
	High Freq. (ppm)	Low Freq. (ppm)	Bias (ppm)	Total (ppm)	High Freq. (ppm)	Low Freq. (ppm)	Bias (ppm)	Total (ppm)
5175	- - -	- - -	- - -	- - -	0.22	1.63	31.0	31.1
0169	1.68	11.58	108.6	109.2	0.17	8.19	53.9	54.5
2769	0.56	29.77	3.2	39.9	0.28	8.54	61.2	61.8
0448	0.56	31.92	-17.0	36.2	0.56	8.89	49.3	50.1
4444	1.12	13.28	143.0	143.6	0.56	- - -	35.4	- - -
4751	0.56	- - -	- - -	- - -	0.17	3.94	40.7	40.9
4307	0.56	- - -	70.8	- - -	0.57	- - -	17.6	- - -
RMS	0.94	23.54	86.7	89.8	0.40	6.89	43.5	44.0
Mean Bias			61.7				41.3	
Standard Error about Mean			60.9				13.7	

TABLE 6.4-3

ESTIMATED AZUSA MARK II ERRORS BY FREQUENCY BAND
m_c MEASUREMENT

Test	Booster				Sustainer			
	High Freq. (ppm)	Low Freq. (ppm)	Bias (ppm)	Total (ppm)	High Freq. (ppm)	Low Freq. (ppm)	Bias (ppm)	Total (ppm)
5175	- - -	- - -	- - -	- - -	0.28	1.88	-10.3	10.5
0169	1.68	23.34	-37.8	44.5	0.28	4.67	-30.9	31.3
2769	0.56	30.41	11.9	32.7	0.39	6.66	-93.2	93.4
0448	0.56	46.55	-19.4	50.4	0.56	5.43	29.5	30.0
4444	1.12	6.56	5.0	8.3	1.12	- - -	-5.2	- - -
4751	0.56	- - -	- - -	- - -	0.34	2.65	-10.2	10.5
4307	1.12	- - -	67.5	- - -	0.56	- - -	-41.2	- - -
RMS	1.02	30.33	36.1	47.2	0.57	4.61	42.2	42.4
Mean Bias			5.4				-23.1	
Standard Error about Mean			35.7				35.3	

TABLE 6.4-4

ESTIMATED AZUSA MARK II ERRORS BY FREQUENCY BAND
R_c MEASUREMENT

Test	Booster				Sustainer			
	High Freq. (Ft)	Low Freq. (Ft)	Bias (Ft)	Total (Ft)	High Freq. (Ft)	Low Freq. (Ft)	Bias (Ft)	Total (Ft)
5175	- - -	- - -	- - -	- - -	0.022	0.20	9.7	9.7
0169	0.022	0.00	6.4	6.4	0.017	1.39	-16.3	16.4
2769	0.022	0.51	1.7	1.8	0.017	0.76	-0.8	1.1
0448	0.022	1.18	-35.6	35.6	0.017	0.46	20.1	20.1
4444	0.022	0.48	16.4	16.4	0.017	2.78	-14.0	14.3
4751	0.017	- - -	- - -	- - -	0.017	0.82	-3.7	3.8
4307	0.017	- - -	-34.5	- - -	0.017	- - -	-34.5	- - -
RMS	0.020	0.69	23.5	23.5	0.018	1.36	17.6	17.7
Mean Bias			-9.1				-5.6	
Standard Error about Mean			21.7				16.7	

A recent re-survey of the AZUSA baseline resulted in significant adjustments to the location of the AZUSA antennas. It is expected that the improved survey will result in lower total AZUSA errors in future tests.

6.5 UDOP

6.5.1 System Description

UDOP is an Ultra High Frequency CW Doppler missile velocity and position measurement system developed for use on the Air Force Eastern Test Range. It employs phase comparison techniques to determine missile position and velocity; however, the data are ambiguous and must be initialized using a known position. There are two UDOP Systems on the AFETR, one located on the Florida mainland covering the launch area (see Figure 6.5-1) and the second located in the vicinity of Grand Bahama Island covering the post-launch phase (see Figure 6.5-2). The launch area system is operated by NASA and is similar to the downrange system operated by the Range Contractor. The launch area system can also be operated as an ODOP or Offset Ultra High Frequency Doppler system.

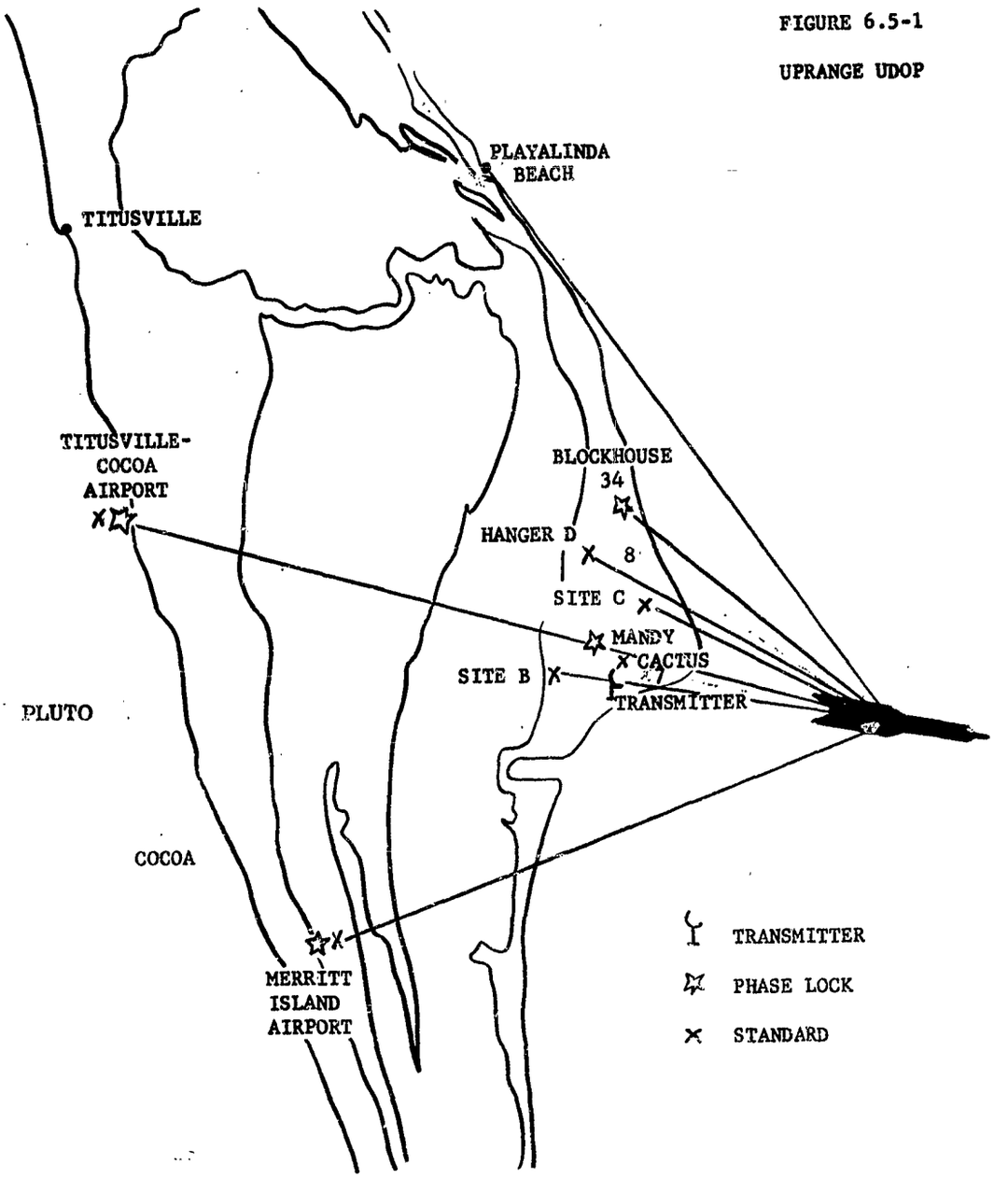
The sites of the downrange UDOP System are located at Walker, Little Carter, Allans Cays, Bassett Cove (GBI), and West End (GBI). Sites at Cape Kennedy, Cocoa (Pluto), Merritt Island, Playalinda Beach, and the Cocoa-Titusville Airport are used by the NASA operated uprange system.

The UDOP System consists of a UHF-VHF transmitting station, a missile transponder, several receiving stations and a central recording station. The UHF transmitter sends a 450 mc signal to the transponder while the VHF transmitter sends a signal of approximately 50 mc to the ground receivers. Both transmitters are excited by the same oscillator so that the signals are phase coherent (see Figure 6.5-3). The transponder receives the 450 mc signal, including a doppler shift which is proportional to the radial velocity of the missile relative to the transmitter and to the transmitter frequency. The transponder doubles the

(Text continued on page 6-81)

FIGURE 6.5-1

UPRANGE UDOP



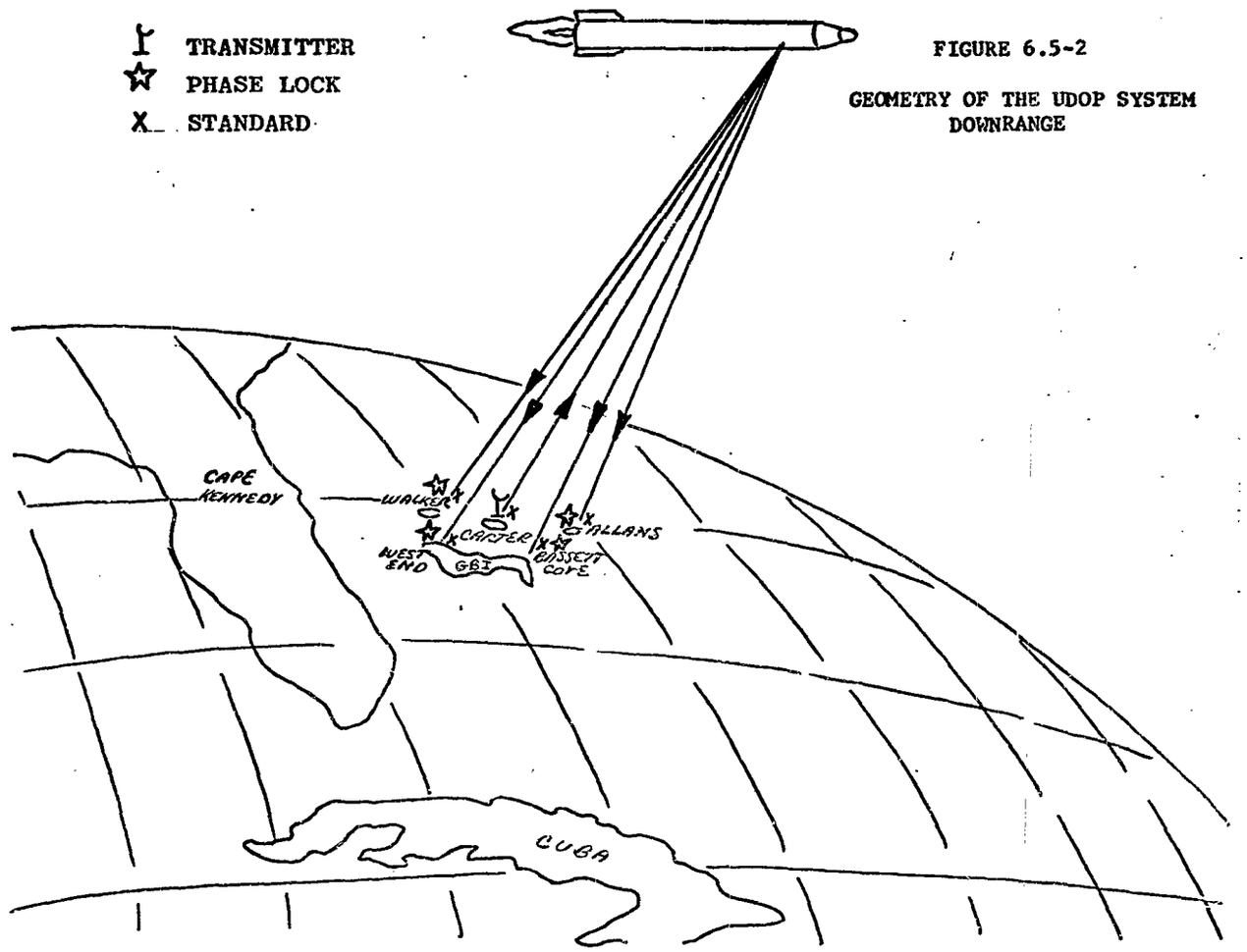
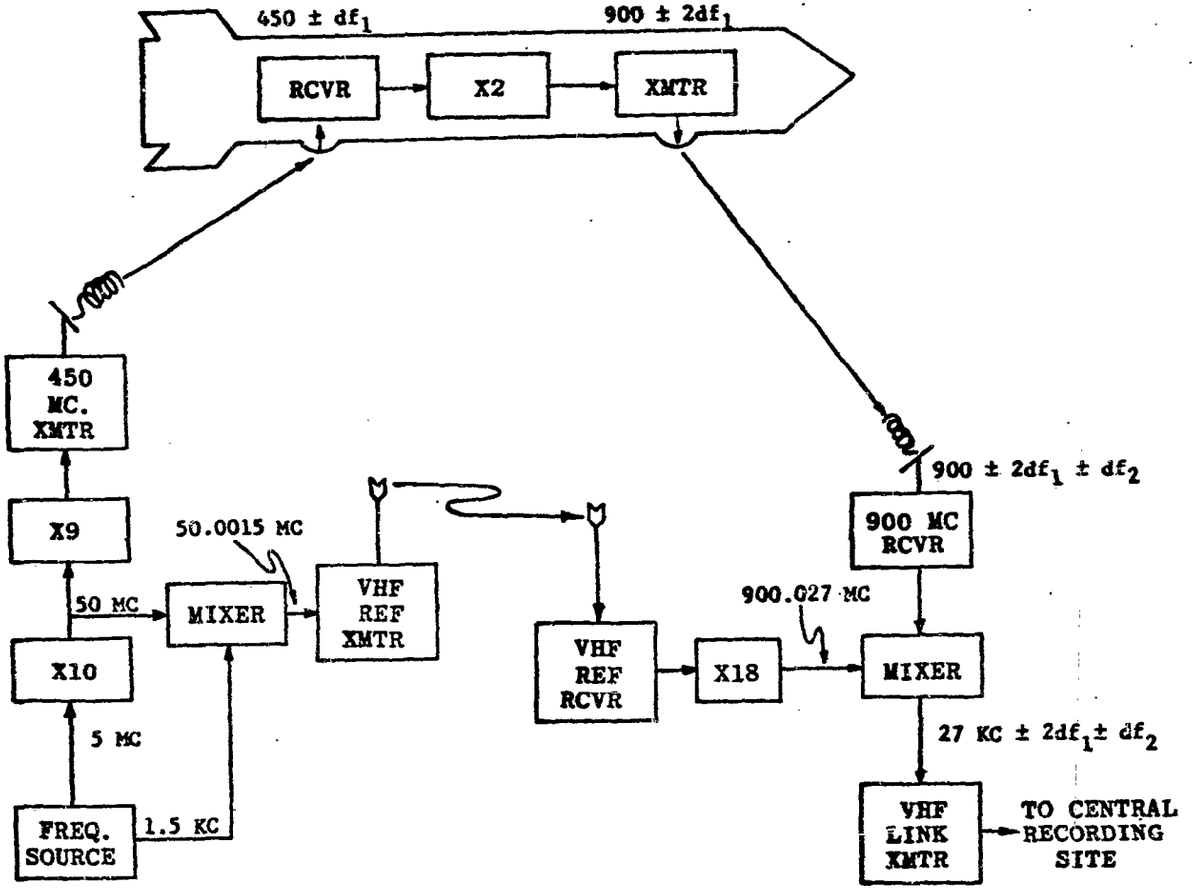


FIGURE 6.5-2

GEOMETRY OF THE UDOP SYSTEM DOWNRANGE

FIGURE 6.5-3
DOWNRANGE UDOP
FUNCTIONAL BLOCK DIAGRAM

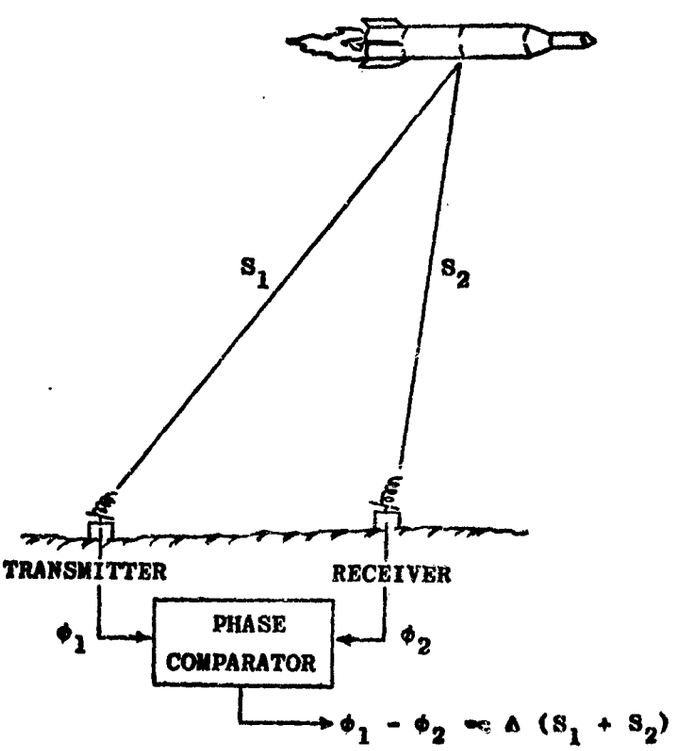


received signal and retransmits it to the ground receivers. The signal undergoes an additional Doppler shift which is proportional to the radial velocity of the missile relative to each receiving site, and to the transponder output frequency. The receivers compare the UHF signal to the eighteenth harmonic of VHF signal to obtain the difference (Doppler shift of the UHF signal) as an output. The signal is also used to frequency modulate the data transmitters operating near 140 mc. These signals are received at the Central Recording Station and fed to a tracking filter to eliminate noise and then into a digitizer which converts them to cycle counts. The cycle counts from the various UDOP receiver stations are translated to a data transmission format for recording on site and at the same time data from the remote downrange sites are transmitted by VHF radio link to Bassett Cove where each of the signals is recorded (ANALOG) and digitized at 10 samples per second. These are multiplexed and fed to an AN/GSC-4 transmitter for relay to Cape Kennedy over the subcable to the real-time computer center at Cape Kennedy. Before use, the incremental cycle counts are totalized to obtain an ambiguous range sum. At the Cape, the signal is received by the data receiver, converted to the required format, recorded and sent to the computer for impact prediction. The recorded data are utilized for off-line reduction.

The basic interpretation of data from UDOP is as follows: The range sum (total distance) from the transmitter to the transponder to each receiver site (see Figure 6.5-4) is determined initially from either the surveyed position of the launch pad or a position determined by other range instrumentation systems after launch. Each range sum describes an ellipsoid with the transmitter at one focus and a receiver at the other focus. For a minimal solution, a transponder is located at the intersection of three such ellipsoids. If more than three receivers are used, a least squares solution is made.

FIGURE 6.5-4

UDOP RANGE SUM MEASUREMENT



6.5.2 Error Sources

The following generalized error model is currently being employed in the analysis of UDOP data:

$$\Delta R = a_0 + a_1 R + a_2 \dot{R} + a_3 \csc E_0 + a_4 \csc E_1 + a_5 t + \epsilon_R$$

Where:

- ΔR = the measured difference of a UDOP range sum parameter and the equivalent quantity determined from a standard of comparison
- E_0 = elevation angle at the transmitting site
- E_1 = elevation angle at the receiving site
- t = the time of measurement
- a_0 = initialization error
- $a_1 R$ = scale factor error
- $a_2 \dot{R}$ = timing error (differences in local and central timing, servo delays, recording delays, digitizer delays, etc.)
- $a_3 \csc E_0$ = residual (uncorrected) refraction error (transmitting site)
- $a_4 \csc E_1$ = residual (uncorrected) refraction error (receiving site)
- $a_5 t$ = drift error due to warm up, etc. or, in the passive mode, drift error due to the use of separate frequency standards at the transmitting and receiving sites
- ϵ_R = residual (random and/or unmodeled) error

The UDOP error model is quite similar to the current AZUSA, GLOTRAC and MISTRAM error models. The reader is referred to the MISTRAM section for a more detailed term-by-term discussion of the model.

UDOP is subject to errors due to transponder and receiver delay variation, digitizer noise, digitizer resolution, computer approximations and round-off, cycle count distortion at low count rates, tropospheric and ionospheric propagation variations, timing variations and other non-systematic errors. These unmodeled errors are included in the ϵ_R term.

It has been found in the case of all CW Radar Systems that the constant bias (a_0) term of the error model is usually predominant. Consequently most data analysis to date has employed simple constant term error models of the form:

$$\Delta R = a_0 + \epsilon_R \quad \text{(active)}$$

and

$$\Delta R = a_0 + a_5 t + \epsilon_R \quad \text{(passive)}$$

Residual analysis to date has not justified the general use of a more complex form. Frequency band analysis further supports the use of a simple model.

6.5.3 System Accuracies

UDOP accuracy estimates and data characteristics contained in the report are based on analysis of data from the 17 missile tests shown in the following table.

TABLE 6.5-1
MISSILE TYPES AND TEST NUMBERS

MINUTEMAN		SATURN	
Range Test Number	Missile Number	Range Test Number	Missile Number
6001	446	0169	SA-5
6080	447	2769	SA-6
0305	438	4444	SA-7
0376	448		
0526	436		
0201	437		
0430	439		
0351	440		
0050	442		
0037	441		
0040	443		
1060	444		
3552	449		
4943	450		

6.5.3.1 Accuracy Estimates

Tables 6.5-2 and 6.5-3 give current accuracy estimates for MINUTEMAN and SATURN tests respectively. Tables 6.5-4, 6.5-5 and 6.5-6 are summaries of high frequency, low frequency and bias error estimates for all the MINUTEMAN tests analysed during the past year. Tables 6.5-7, 6.5-8 and 6.5-9 give similar estimates for SATURN tests.

Error estimates for bias and low frequency error were made using BET as a standard. High frequency noise was estimated by the variate difference method using third differences.

The approximate frequency band for high frequency noise is 3.5 to 5 cycles per second based on the variate difference method of estimation. For the low frequency noise estimation, the frequency band is $\frac{1}{2.26\ t}$ to 3.5 cycles per second where t is the length of the data span in seconds. For the bias estimate, the frequency band is 0 to $\frac{1}{2.26\ t}$ cycles per second.

The current UDOP bias error estimates shown in Table 6.5-2 were obtained using tests 0351, 0050, 0040 and 4943. Tests 6001, 6080, 0305 and 0376 had survey errors due to a misidentification of the antenna location at the Pluto site and tests 1060 and 3552 used the GLAD/BET program which at that time included an error due to a four foot difference in point of track. This does not apply to later tests.

Test 0169 was the last SATURN test to carry a UDOP transponder and therefore was not pooled in the current estimate of accuracy.

Several blanks appear in the tables which follow. This is due to the fact that not all stations listed were employed in every

(Text continues on page 6-95)

TABLE 6.5-2
ESTIMATED ERRORS FOR UDOP
IN RANGE SUM PARAMETERS
MINUTEMAN TESTS

SITES	Range Sum		Range Sum Rate*
	s_{Bias} (Ft)	s_{Random} (Ft)	s_{Random} (Ft/Sec)
Uprange			
Playalinda Beach	6.3	0.55	0.08
Titusville/Cocoa	4.7	0.41	0.09
Merritt Island	3.7	0.47	0.11
Pluto	3.6	0.44	0.13
RMS	4.7	0.52	0.10
Downrange			
Allans Cay	4.6	0.45	0.13
Walker Cay	5.5	0.46	0.09
Bassett Cove	3.4	0.34	0.06
West End	2.8	0.50	0.09
RMS	4.2	0.43	0.09

*Rate derived by use of a 25 point, 3rd degree polynomial.

TABLE 6.5-3

ESTIMATED ERRORS FOR ODOP DATA

SATURN TESTS 2769 and 4444

Sites	Range Sum		Range Sum Rate*
	s_{Bias} (Ft)	s_{Random} (Ft)	s_{Random} (Ft/Sec)
Merritt Island	13.2	0.31	.10
Pluto	5.1	0.46	.09
Site C	10.3	0.37	.10
Blockhouse 34	11.5	0.34	.09
Cactus	10.7	0.28	.11
RMS	10.5	0.36	.10
	Range Difference		Range Difference Rate
Allans minus Bassett	5.1	0.27	.06
Walker minus Bassett	5.1		.08
Bassett minus West End		0.21	
Allans minus West End	11.1	0.21	.07
RMS	7.6	0.23	.07

*Rate derived by use of a 61 point, 3rd degree polynomial.

TABLE 6.5-4
HIGH FREQUENCY ERROR ESTIMATES IN RANGE SUMS FOR UDOP DATA*
MINUTEMAN TESTS

Uprange Sites	6001 (Ft)	6080 (Ft)	0305 (Ft)	0376 (Ft)	0526 (Ft)	0430 (Ft)	0351 (Ft)	0050 (Ft)	0037 (Ft)	0201 (Ft)	1060 (Ft)	RMS
Playalinda Beach	.03	.04	.04	.02	.01	.04	.02		.04	.02	.02	.03
Titusville-Cocoa	.02	.04	.03	.03	.03	.04	.09		.04	.09	.03	.05
Merritt Island	.03	.04	.03	.03	.03	.03	.02		.03	.03	.03	.03
Site C	.03	.03	.02	.03	.02	.04	.03		.02	.02		.03
Pluto	.03	.15	.03	.03	.01	.04	.08	.04		.02		.06
Downrange Sites												
Allans Cay	.04	.03	.03	.02	.03	.03	.03	.05	.03	.04	.03	.03
Walker Cay	.12	.04	.03	.02	.02	.04	.04	.03		.03	.03	.05
Bassett Cove	.02	.04	.02	.02	.02	.03	.04	.03		.03	.02	.03
West End	.03	.04	.03	.02	.02	.04	.04	.03		.08	.02	.04

*High frequency error estimates were not available for Tests 0040, 3552 and 4943.

TABLE 6.5-5

LOW FREQUENCY ERROR ESTIMATES IN RANGE SUMS FOR UDOP DATA*

MINUTEMAN TESTS

Uprange Sites	6001 (Ft)	6080 (Ft)	0305 (Ft)	0376 (Ft)	0351 (Ft)	0050 (Ft)	1060 (Ft)	3552 (Ft)	RMS (Ft)
Playalinda Beach	.54	.51	.14			.31	.85	.64	.55
Titusville - Cocoa	.49	.24	.22	.32	.16	.41	.29	.79	.41
Merritt Island	.21	.24	.28	.54				.80	.47
Site C	.28		.19						.24
Pluto	.28	.17		.65		.51	.49	.39	.44
Downrange Sites									
Allans Cay	.36	.18	.20	.33			.60	.72	.45
Walker Cay	.39	.46	.47	.09		.37	.50	.84	.46
Bassett Cove	.50	.32	.28	.27			.53	.46	.34
West End	.22	.40	.30			.30	.86	.63	.50

*Low frequency error estimates were not available for Tests 0526, 0430, 0037, 0201, 0040 and 4943.

TABLE 6.5-6

BIAS ESTIMATES IN RANGE SUMS FOR UDOP DATA*

MINUTEMAN TESTS

Uprange Sites	6001 (Ft)	6080 (Ft)	0305 (Ft)	0376 (Ft)	0050 (Ft)	0040 (Ft)	0351 (Ft)	1060 (Ft)	3552 (Ft)	4943 (Ft)	RMS (Ft)	Mean (Ft)	S_{Mean} (Ft)
Playalinda Beach	5.8	8.2	7.9	8.8	5.1	5.8		10.5	15.0	8.9	8.9	8.4	2.9
Titusville Cocoa	4.7		7.0	8.8		4.5	-0.2	11.2	14.0		8.8	8.4	2.8
Merritt Island	6.5	11.7	7.4	10.7	3.2	1.6	-0.7				7.2	5.8	4.3
Site C		10.6	5.4	9.7				10.0		6.8	8.7	8.5	2.0
Pluto	6.6	11.1	7.6	10.9	2.0	0.4			6.7	4.9	7.2	6.3	3.6
Downrange Sites													
Allans Cay	9.2	-13.3	-16.0	-14.4	1.2	-3.0	6.3	16.8	6.2	3.9	10.5	0.3	10.5
Walker Cay	11.2	-11.3	-15.3	-11.5	1.0	-2.1	6.5	18.8	8.3	5.9	10.5	2.6	10.2
Bassett Cove	10.8	-11.5	-16.3	-12.8		-2.5	5.3	15.9	-0.3	3.5	10.4	-0.9	10.4
West End	10.2	-10.5	-17.8		0.6	-4.0		14.5	-0.3	3.8	9.8	-4.4	9.8

*These estimates are biases computed in the BET for the tests listed.

TABLE 6.5-7

ESTIMATED RANGE SUM ERRORS BY FREQUENCY BAND FOR UDOP DATA

SATURN TEST 0169

Receiver Sites	High Freq. (Ft)	Low Freq. (Ft)	Bias (Ft)	Total (Ft)
Playalinda Beach	.05	1.5	19.5	19.6
Titusville-Cocoa	.05	1.3	11.9	12.0
Merritt Island	.04	0.5	26.3	26.3
Pluto	.04	- -	9.8	9.8
Site C	.05	0.1	20.8	20.8
RMS	.04	1.1	18.7	18.7
Allans Cay	.06	- -	21.1	21.1
Bassett Cove	.04	1.9	6.5	6.8
West End	.04	1.8	11.4	11.5
Walker Cay	.04	4.0	- -	4.1
RMS	.05	2.8	14.3	14.6

TABLE 6.5-8

ESTIMATED ERRORS BY FREQUENCY BAND
FOR ODOP DATA

SATURN TEST 2769

Receiver Sites	High Freq. (Ft)	Low Freq. (Ft)	Bias (Ft)	Total (Ft)
		Range Sums		
Merritt Island	.03	.35	16.5	16.5
Pluto	.02	.35		
Site C	.01	.10		
Cactus	.02	.09		
Blockhouse No. 34	.01	.10		
		Range Differences		
Allans minus Bassett		.13	5.1	
Walker minus Bassett		.11	8.3	
Allans minus West End		.21	8.1	
Bassett minus West End		.21		

TABLE 6.5-9

ESTIMATED ERRORS BY FREQUENCY BAND
FOR ODOP DATA

SATURN TEST 4444

Receiver Sites	High Freq. (Ft)	Low Freq. (Ft)	Bias (Ft)	Total (Ft)
		Range Sums		
Merritt Island	.04	.24	8.6	8.6
Pluto	.05	.51	5.1	5.1
Site C	.05	.36	10.3	10.3
Cactus	.05	.39	10.7	10.7
Blockhouse No. 34	.15	.39	11.5	11.5
		Range Differences		
Allans minus Bassett		.36	5.0	
Walker minus Bassett		.83*	-6.0	

*Not used in pooled values.

test, data obtained from some stations were not usable, and a BET solution which included UDOP was not available for every test.

Figure 6.5-5 is a plot of propagation of current UDOP errors (Table 6.5-2) into Cartesian coordinates for the MINUTEMAN trajectory based upon the station utilization shown in Figure 6.5-6.

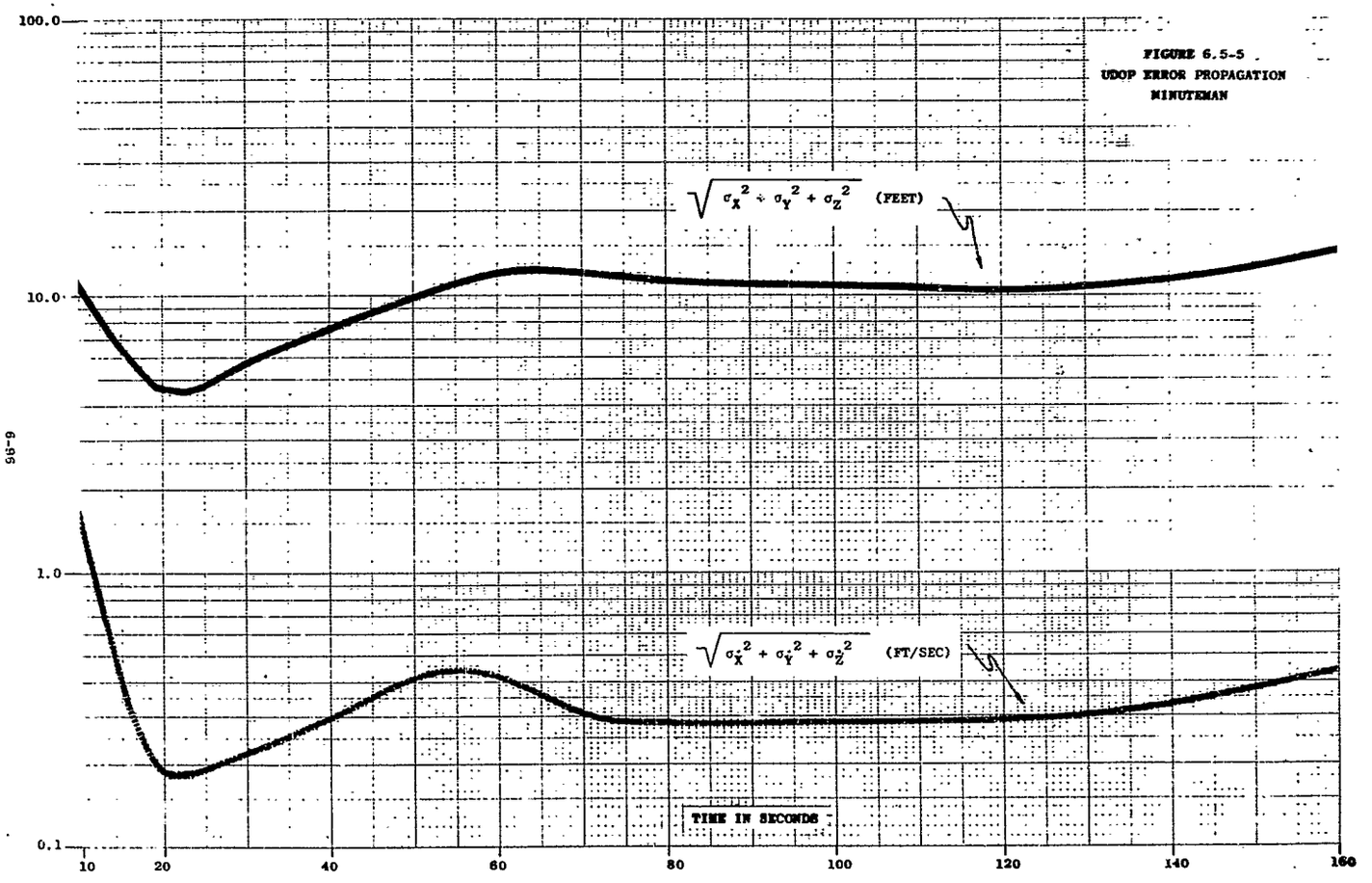
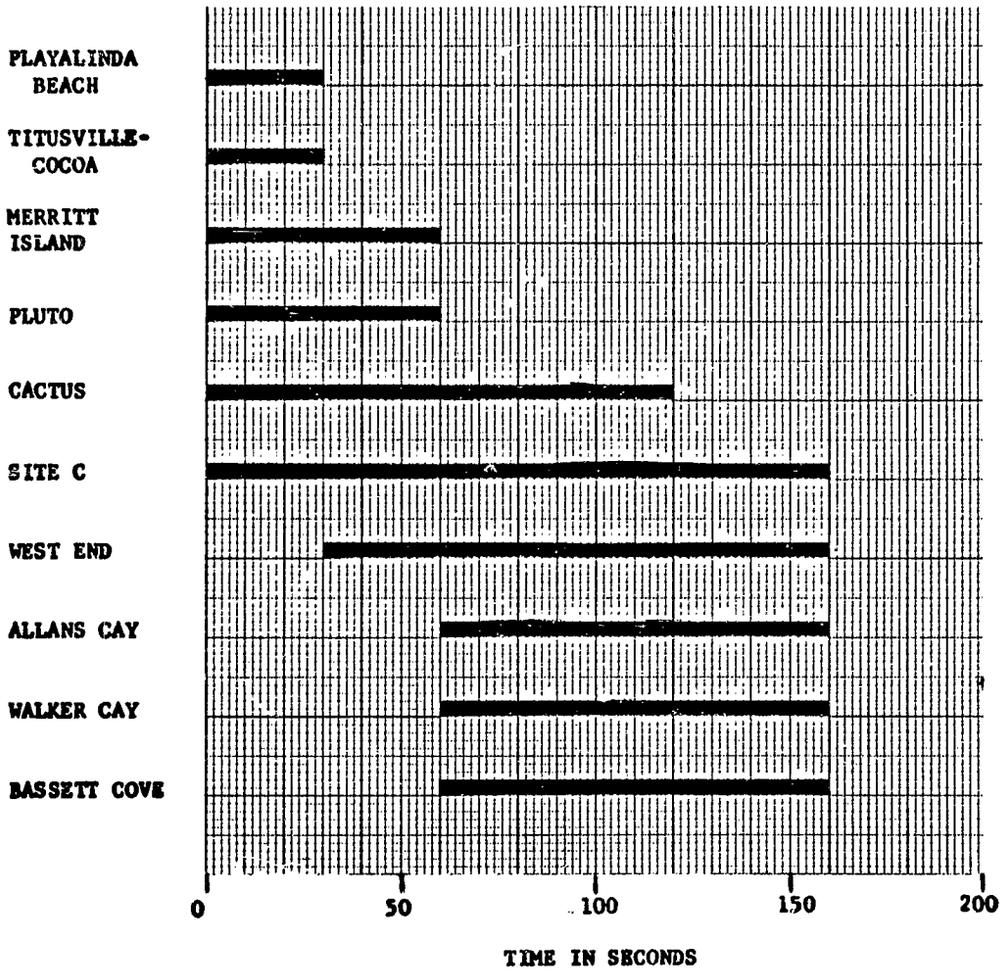


FIGURE 6.5-5
UDOP ERROR PROPAGATION
MINUTEMAN

FIGURE 6.5-6
STATION UTILIZATION
FOR ERROR PROPAGATION



7.0 IMPACT SYSTEMS

There are four distinct types of impact systems at AFETR:

(1) Impact Prediction - Range Safety
(2) Impact Location - Recovery and "quick look" guidance evaluation
(3) Impact Determination - Post Flight using ETR tracking data
(4) Impact Calculation based on MILS-BOA and MILS-Target Array systems

With the exception of the MILS-BOA and MILS-Target Array systems, all the impact systems depend upon tracking data from the various instrumentation sites and the 3600 computer with associated hardware and software.

Generally speaking, the systems are numbered above in the order of increasing accuracy and sophistication of the solution.

7.1 Impact Prediction, Location and Determination

7.1.1 Procedure for Estimating System Accuracies

The accuracy of these systems depends on many factors, for example (a) the trajectory, (b) the accuracy of the tracking or instrumentation system and its sampling rate, (c) the mathematical model used in the computer program, i.e., standard atmosphere, drag curves, velocity of propagation, etc., (d) the computer techniques used - smoothing techniques, number of calculations made per second in real time, etc. Since most of these factors are changing from time to time, it is difficult to state a nominal accuracy for one of these systems in a simple manner. Estimates of accuracy may be obtained by using the specific information pertaining to a particular test.

Estimates of the accuracy of the range safety impact prediction system are obtained as follows. During the powered portion of the trajectory several data points approximately evenly spaced in time are chosen. For purposes of analysis, thrust termination and nose cone separation are assumed to occur at each of these points. Corresponding to a time t there is a real time impact prediction. There is also available in the reduced metric data a position-velocity point corresponding to time t. Introducing this position velocity point into the impact determination computer program (FIAT)* results in a computed vacuum impact point and a computed drag corrected impact point which may be compared with the real time impact point. The real time point is from a vacuum calculation. The average deviation of the real time point from the FIAT vacuum point is of the order of a half mile.

The estimates of the accuracy of Recovery Impact Location and Final Impact Determination (Post Flight) are based on the direct comparison of results from individual impact systems with the MILS data obtained in the Target Array. Results of the comparison are presented in the form of "deviation in nautical miles from MILS Target Array" on a test-by-test basis and in the form of "average deviation in nautical miles from MILS target array" over a period of a year. Results of the comparison are also given in terms of "95% accuracy ellipses" over a period of a year.

* FIAT is the program used for Post Flight Impact Determination.

The accuracy ellipse is defined as the region in space which contains the true impact with probability .95. If there is an indicated bias, then the amount and orientation are given also. The accuracy ellipse is a true measure of overall accuracy and includes all errors such as survey, drag coefficient, wind, thrusts from attitude control, air density, etc. A complete treatment of the 95% accuracy ellipse is given in [O'Connor, 1962].

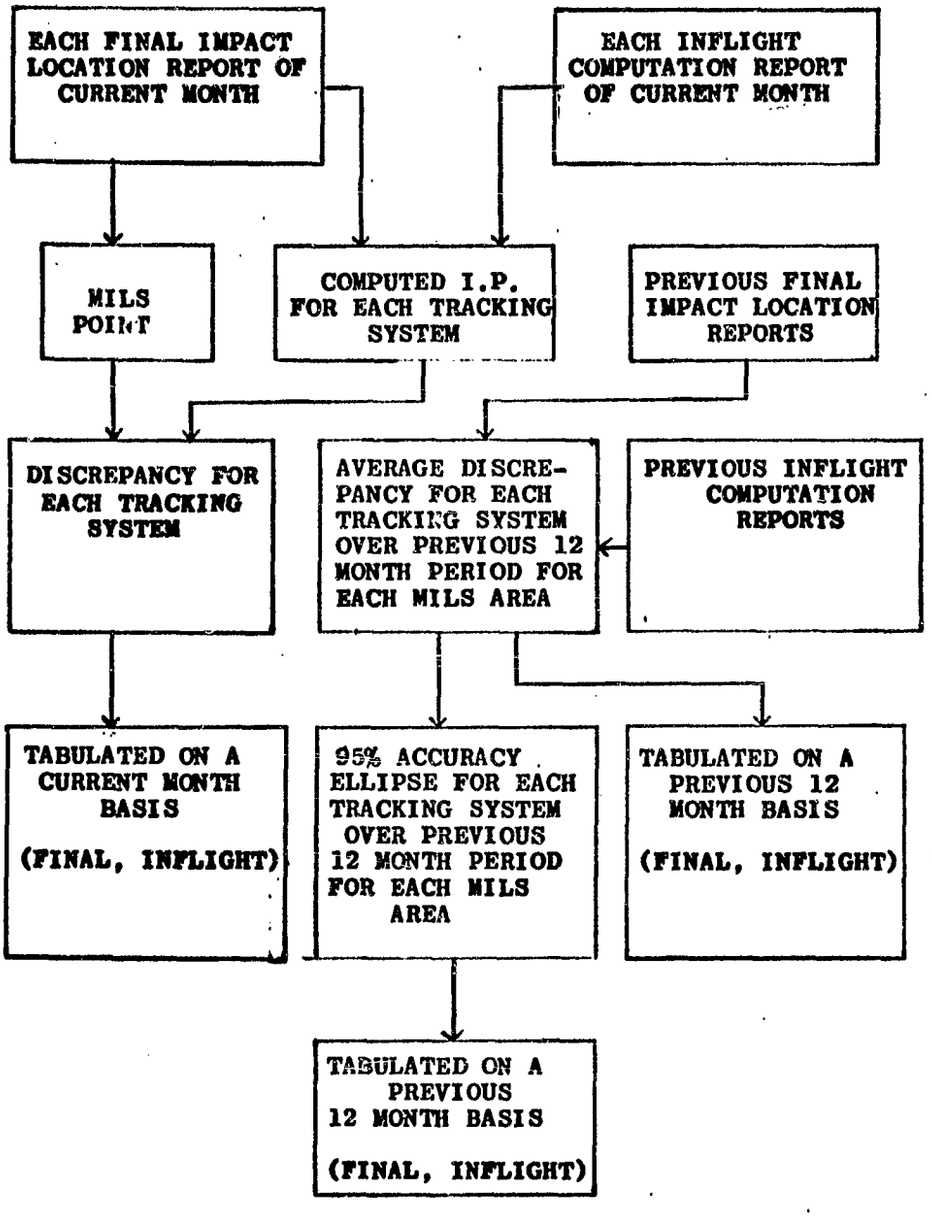
In addition to these estimates of accuracy, an I.P. confidence ellipse is published on a test by test basis in each Final Impact Location Report. This ellipse represents a post flight propagation to impact of the estimated random and systematic errors in the tracking data. Since this propagation does not include all the errors associated with the accuracy ellipse, the confidence ellipse on the average is smaller than the accuracy ellipse.

The general data flow for I.P. error analysis is given in Figure 7.1-1.

7.1.2 System Description

For Range Safety Impact Prediction, the calculations are made in real time. The methods used are essentially the closed form solution for elliptic orbits from celestial mechanics. Emphasis is placed on obtaining results satisfying range safety accuracy requirements but, because of limitations of time allowed for calculations, certain refinements such as correction for drag on re-entry and the gravitational field of the oblate earth are not performed. Data are presented to the Range Safety Officer on a plotting board with minimum (0.5-2.7 sec.) delay.

FIGURE 7.1-1
FLOW CHART FOR ERROR ANALYSIS



Impact Location calculations are made to assist in recovery operations and for quick look evaluation of guidance systems. They are made using rigorous numerical solutions of the trajectory equations with best drag and gravitational potentials available. Two types of results are given: one approximately 10 minutes after burnout and a final one within two hours after burnout.

Post Flight Impact Determinations using ETR data are based on essentially the same methods as the recovery solution.

Since the results are not required sooner than three days to two weeks, various refinements are applied to the data in order to improve the accuracy of the calculation. Examples of such refinements are:

(a) more detailed editing and correction of the tracking data (a limited editing is performed in real time)

(b) utilization of longer spans of tracking data for velocity determination.

(c) utilization of a more sophisticated mathematical technique for determination of the velocity vector.

An impact position is normally given for each separate tracking system used in the test. In addition an impact position is computed from the Best Estimate of Trajectory and published in the Final Impact Location Report. This computation uses a position and velocity vector immediately after burnout and the complete equations of motion. The Most Probable Impact Position (MPIP) is also published in the Final Impact Location Report. The (MPIP) is a weighted average of the impact determinations of the individual tracking systems. The weights

are the inverses of the covariance matrices of each impact position. The confidence ellipse associated with (MPIP) is computed from the inverse of the sum of the inverses of the individual covariance matrices of impact position.

7.1.3 Error Sources

The most influential source of error in most cases is uncertainty in the velocity vector at burnout. The accuracy of this vector is dependent upon the accuracy of the tracking data. Other sources of error whose relative importance varies with the particular missile test and physical conditions are (1) winds at re-entry, (2) ballistic coefficients, (3) missile stability, (4) survey errors, (5) atmospheric density, (6) parameters in equations of motion, (8) computational errors, (9) figure of the earth, (10) residual thrust, (11) thrusts in attitude control. Most of these effects are quite small. Some the Range has no control over. The remainder, including the error in velocity vector, are being actively studied in order to minimize them.

7.1.4 System Accuracies

The accuracy data in this report are based on analysis of the tests listed in Table 7.1-1. As discussed in Section 7.1.1 the accuracy of Recovery Impact Location and Final Impact Determination (Post Flight) information based on the direct comparison of results from individual impact systems with the MILS data are presented in the form of the "deviation in nautical miles from MILS Target Array" over a period of a typical month an example of which is given in Table 7.1-2. Results of the comparisons are also given in terms of the

"deviation" over a period of a year in Table 7.1-3 and in terms of 95% accuracy ellipses in Table 7.1-4.

TABLE 7.1-1

TEST NUMBERS AND MISSILE TYPES

TEST	MISSILE
2901 2875 2949 3610 3622 3651 238 38 45 303 501 41 2033 2084 6100 7678 6090 5844 22 5344	POLARIS
376 351 37 50 526 430 40 1060 6001 6080 305	MINUTEMAN
104 158 227 3303 3787	TITAN II
150 575	ATLAS

TABLE 7.1-2

IMPACT POSITION

DEVIATION IN NAUTICAL MILES FROM MILS POINT

April 1964

TEST	INSTRUMENT	TARGET AREA	IMPACT LOCATION	IMPACT DETERMINATION
40	MISTRAM II	12		.75
	RADAR 12.16	12	.19	.14
158	MISTRAM I	12	1.03	1.14
	RADAR 5.16	12		.51
	RADAR 12.16	12		.08
2033	AZUSA MK II	9	.51	.41
	RADAR 0.18	9		.36
	RADAR 3.16	9		1.04
	RADAR 5.16	9		.19
2084	AZUSA MK II	9	.42	.58
	RADAR 0.18	9		.29
	RADAR 3.16	9		.86
	RADAR 5.16	9		.50
1060	RADAR 12.16	12	.09	.07
575	AZUSA MK II	12		.72
	RADAR 5.16	12		2.13
	RADAR 12.16	12	.19	.04
38	AZUSA MK II	9	.46	.47
	RADAR 0.18	9	.46	2.35
	RADAR 91.18	9		.37

TABLE 7.1-3

IMPACT POSITION

AVERAGE DEVIATION IN NAUTICAL MILES FROM MILS POINT

Sept. 1963 to Aug. 1964

INSTRUMENT	IMPACT LOCATION		IMPACT DETERMINATION	
	AREA 9	AREA 12	AREA 9	AREA 12
AZUSA MK I	1.17 (2)	-----	1.06 (7)	-----
AZUSA MK II	.38 (10)	-----	.42 (16)	.75 (2)
MISTRAM I	-----	.45 (4)	-----	.54 (4)
MISTRAM II	-----	-----	-----	1.39 (10)
UDOP	-----	-----	-----	1.80 (6)
BET	-----	-----	-----	.58 (6)
RADAR 0.16	-----	-----	.61 (5)	-----
RADAR 0.18	.54 (5)	-----	.60 (12)	-----
RADAR 1.16	2.15 (1)	1.34 (4)	.43 (8)	.66 (7)
RADAR 3.16	-----	2.05 (4)	.98 (13)	1.19 (5)
RADAR 5.16	-----	4.23 (3)	.66 (6)	1.08 (11)
RADAR 12.16	-----	.72 (9)	-----	.14 (18)
RADAR 91.18	2.90 (3)	-----	.23 (5)	-----

Numbers in parentheses represent the total number of tests included in the average.

TABLE 7.1-4

IMPACT POSITION

95% ACCURACY ELLIPSES AND BIASES

Sept. 1963 to Aug. 1964

INSTRUMENT	MILS TARGET AREA	TYPE OF IMPACT PCSITION	ACCURACY ELLIPSE			BIAS	
			SEMI-MAJOR AXIS (n.m.)	SEMI-MINOR AXIS (n.m.)	AZIMUTH (Deg.)	AMOUNT (n.m.)	ORIEN-TATION (Deg.)
AZUSA MK II	9	Location	1.02	0.69	83	None	---
RADAR 0.18	9	Location	1.98	0.80	13	None	---
AZUSA MK I	9	Determ.	4.32	1.08	135	.45	42
AZISA MK II	9	Determ.	1.45	0.48	125	None	---
RADAR 0.16	9	Determ.	2.42	1.06	20	.49	138
RADAR 0.18	9	Determ.	2.19	0.85	127	None	---
RADAR 1.16	9	Determ.	1.08	0.94	9	None	---
RADAR 3.16	9	Determ.	2.18	1.97	28	None	---
RADAR 5.16	9	Determ.	2.01	1.03	135	None	---
RADAR 91.18	9	Determ.	0.73	0.48	119	None	---
MISTRAM I	12	Location	2.07	0.64	24	None	---
RADAR 1.16	12	Location	4.72	2.80	115	None	---
RADAR 3.16	12	Location	11.3	1.53	123	None	---
RADAR 12.16	12	Location	2.42	1.37	136	None	---
BET	12	Determ.	2.36	0.38	125	None	---
MISTRAM I	12	Determ.	2.37	0.26	129	None	---
MISTRAM II	12	Determ.	5.80	0.55	124	None	---
UDOP	12	Determ.	9.46	0.49	129	None	---
RADAR 1.16	12	Determ.	1.82	1.49	119	None	---
RADAR 3.16	12	Determ.	4.39	2.02	17	None	---
RADAR 5.16	12	Determ.	2.70	1.93	8	.61	---
RADAR 12.16	12	Determ.	0.60	0.18	107	None	---

7.2 MILS

7.2.1 Procedures for Estimating System Accuracies

This section consists of discussions of some of the procedures utilized in MILS for determining system accuracies, [Whitehead and Beall, 1964].

7.2.1.1 Definition of Terms

The following definitions are provided for some of the basic terms utilized in this section.

Confidence Ellipse - That area, centered at the computed (estimated) impact point, which has $100\gamma\%$ probability of enclosing the true impact point (where γ is the confidence coefficient, e.g., 0.95).

Geodetic Confidence Ellipse - A confidence ellipse computed from a "geodetic accuracy covariance matrix" for a given impact is referred to as a "geodetic confidence ellipse."

Precision - A measure of the dispersion of a set of observations of an event is referred to as precision. In this sense, a tolerance ellipse (see below) has the connotation of precision.

Tolerance Ellipse - That area, centered at the mean of a sample which has $100\gamma\%$ probability of enclosing $100\alpha\%$ of the individuals in the population (where γ is the confidence coefficient and α is an appropriate multiplier.)

Accuracy - The term accuracy refers to the closeness of computations or estimates to the exact or true values. In this sense a geodetic confidence ellipse as defined above is a measure of the accuracy obtained by the system making the

observations. The same is true of the method of estimating accuracy outlined in Paragraph 7.2.1.3.

7.2.1.2 Computation of Confidence Ellipses, MILS/BOA

The following is a general description of the method utilized in computing, from MILS data, a geodetic confidence ellipse about an estimated impact point for a missile test in the Broad Ocean Area (BOA).

From the results of pre- and post-test calibrations of a given BOA surveyed area (the missile aim point), an "a priori" estimate of the standard deviation in timing is determined for each hydrophone. After missile test data have been acquired, these error estimates from calibration are propagated (as a by-product of the least squares adjustment for the test) to provide a solution covariance matrix due to these timing errors. This matrix is referred to as the "timing covariance matrix," and is computed using the maximum likelihood "a posteriori" estimate of the variance factor, (unit variance), viz., the square of the mean error.

If the missile impact occurred in a BOA surveyed area, a "hydrophone motion covariance matrix" (sometimes referred to as the "survey covariance matrix") due to the motion of suspended hydrophones is estimated. A "geodetic survey covariance matrix" is estimated on the basis of the uncertainties in the geodetic survey of this BOA area. These three matrices are summed to yield a "geodetic accuracy covariance matrix" for the missile test.

If the missile did not impact in a BOA surveyed area, then in place of the hydrophone motion and geodetic survey

covariance matrices, a "hydrophone survey and velocity covariance matrix" is estimated due to errors in the estimated acoustic velocities and in the geodetic positions of the hydrophones. This matrix and the timing covariance matrix are then summed to provide a geodetic accuracy covariance matrix for the test.

If the terms of the geodetic accuracy covariance matrix are represented by

$A = S_{\phi}^2$ (estimated variance in latitude (ϕ) of impact point)

$B = S_{\lambda}^2$ (estimated variance in longitude (λ) of impact point) (7.2.1-1)

$C = S_{\phi\lambda}$ (estimated covariance of ϕ and λ),

then a geodetic confidence ellipse (at a one-sigma confidence level) is computed as follows [Duncan, Ackerson, 1960]:

$$M_{\sigma} = \left[.5\left(A+B+ \sqrt{(A-B)^2+4C^2} \right) \right]^{\frac{1}{2}} \qquad (7.2.1\text{-}2)$$

$$m_{\sigma} = \left[.5\left(A+B- \sqrt{(A-B)^2+4C^2} \right) \right]^{\frac{1}{2}} \qquad (7.2.1\text{-}3)$$

$$\alpha = \tan^{-1} \left[\frac{2C}{A-B+\sqrt{(A-B)^2+4C^2}} \right] \qquad (7.2.1\text{-}4)$$

$$\text{Azimuth (of major axis)} = \begin{cases} 180^{\circ}-\alpha, & \alpha > 0 \\ -\alpha, & \alpha < 0 \end{cases} \qquad (7.2.1\text{-}5)$$

where:

M_{σ} = semi-major axis, at a "one sigma" confidence level

m_{σ} = semi-minor axis, at a "one sigma" confidence level

For computing an ellipse at a 95% or an 86.5% (2σ) confidence level, the following conversions are necessary:

$$M_{95\%} = (2.4477)M_{\sigma} \qquad m_{95\%} = (2.4477)m_{\sigma}$$

or $$M_{86.5\%} = 2M_{\sigma} \qquad m_{86.5\%} = 2m_{\sigma}$$

7.2.1.3 Estimation of BOA Accuracy in the Antigua Target Array

For a portion of the missiles impacting in the Antigua Target Array (TA), both TA and BOA data are obtained to provide a TA solution and a BOA solution. Using the TA as the reference system, an estimate of the accuracy achieved by the BOA system for these missile tests can be obtained by determining (1) an estimate of the bias, if any, existing between the BOA impact solutions and the true impact points, (2) a measure of the confidence that can be placed in the estimate of the true bias, and (3) a measure of the precision

of the BOA estimates of the missile impact locations.

Portions of the method used here to obtain the above "measures of accuracy" parallel to some extent the method developed in [O'Connor, 1962]. Consider the following discussion.

Using the Target Array computed impact as reference, the latitude (ϕ_{TA_i}) and longitude (λ_{TA_i}) of the i^{th} impact estimate as computed from TA data, are subtracted from the ϕ_{BOA_i} and λ_{BOA_i} of the impact estimate as computed from BOA data, yielding the differences, $\Delta\phi_i$ and $\Delta\lambda_i$, for the i^{th} test.

These differences can now be thought of as being plotted in a rectangular coordinate system (North latitude and West longitude positive) with the TA solutions superimposed at the origin, (0,0), and the plot of the differences considered a scattering of data points.

The total error in the BOA and TA estimates, respectively, for the i^{th} test, can be separated into a systematic error, or bias, assumed to be constant over all the i's, and a random error, assumed to be normally distributed with mean zero (unbiased). Thus, for the i^{th} test,

$$\phi_{BOA_i} = \phi_{TRUE_i} + \Delta x + \zeta_i$$

$$\lambda_{BOA_i} = \lambda_{TRUE_i} + \Delta y + \epsilon_i$$

and

$$\phi_{TA_i} = \phi_{TRUE_i} + \Delta u + \eta_i$$

$$\lambda_{TA_i} = \lambda_{TRUE_i} + \Delta v + \gamma_i$$

where $(\Delta x, \Delta y)$ = true BOA bias

(ζ_i, ϵ_i) = random error in the i^{th} BOA estimate

$(\Delta u, \Delta v)$ = true TA bias

(η_i, γ_i) = random error in the i^{th} TA estimate

Therefore, the i^{th} differences are

$$\Delta\phi_i = (\Delta x - \Delta u) + (\zeta_i - \eta_i)$$

$$\Delta\lambda_i = (\Delta y - \Delta v) + (\epsilon_i - \gamma_i)$$

From the foregoing assumptions, the mean of the differences is then given by

$$\overline{\Delta\phi} = (\Delta x - \Delta u) + (\overline{\zeta} - \overline{\eta})$$

$$\overline{\Delta\lambda} = (\Delta y - \Delta v) + (\overline{\epsilon} - \overline{\gamma})$$

and the expectations of the means are

$$E\left(\overline{\Delta\phi}\right) = \Delta x - \Delta u$$

$$E\left(\overline{\Delta\lambda}\right) = \Delta y - \Delta v \qquad (7.2.1\text{-}6)$$

Now by choosing k_1 properly, there is a probability, P, that $E\left(\overline{\Delta\phi}\right)$ lies in the confidence interval given by

$$\overline{\Delta\phi} - k_1 s_{\overline{\Delta\phi}} \leq E\left(\overline{\Delta\phi}\right) \leq \overline{\Delta\phi} + k_1 s_{\overline{\Delta\phi}}$$

and likewise for $E\left(\overline{\Delta\lambda}\right)$,

$$\overline{\Delta\lambda} - k_1 s_{\overline{\Delta\lambda}} \leq E\left(\overline{\Delta\phi}\right) \leq \overline{\Delta\lambda} + k_1 s_{\overline{\Delta\lambda}}$$

where $s_{\overline{\Delta\phi}}$, $s_{\overline{\Delta\lambda}}$ are the sample standard deviations of the means, $\overline{\Delta\phi}$ and $\overline{\Delta\lambda}$, respectively, and k_1 is the appropriate multiplying factor. These last two inequalities, using the two previous equations, can be put in the form

$$\overline{\Delta\phi} - k_1 s_{\overline{\Delta\phi}} \leq (\Delta x - \Delta u) \leq \overline{\Delta\phi} + k_1 s_{\overline{\Delta\phi}}$$

$$\overline{\Delta\lambda} - k_1 s_{\overline{\Delta\lambda}} \leq (\Delta y - \Delta v) \leq \overline{\Delta\lambda} + k_1 s_{\overline{\Delta\lambda}}$$

Adding Δu and Δv, respectively, to the above two inequalities yields

$$\overline{\Delta\phi} + \Delta u - k_1 s_{\overline{\Delta\phi}} \leq \Delta x \leq \overline{\Delta\phi} + \Delta u + k_1 s_{\overline{\Delta\lambda}} \qquad (7.2.1\text{-}7)$$

$$\overline{\Delta\lambda} + \Delta v - k_1 s_{\overline{\Delta\lambda}} \leq \Delta y \leq \overline{\Delta\lambda} + \Delta v + k_1 s_{\overline{\Delta\lambda}}$$

However, $(\Delta u, \Delta v)$ is the true bias of the Target Array and is unknown, but approximated by $(\hat{\Delta u}, \hat{\Delta v})$. The following assumptions are now made:

(1) that $(\Delta u, \Delta v)$ consists only of the TA geodetic survey bias, and

(2) that $\hat{\Delta u}$ and $\hat{\Delta v}$ are uncorrelated, normally distributed, with estimated variances s_ϕ^2 and s_λ^2, respectively, and zero means.

The s_ϕ^2, s_λ^2 and zero covariance, mentioned in the last assumption, make up what is referred to as the geodetic survey covariance matrix for the Target Array.

Therefore, with properly chosen k_2, there is a probability, P, that

$$-k_2 s_\phi \leq \Delta u \leq k_2 s_\phi$$

and, likewise

$$-k_2 s_\lambda \leq \Delta v \leq k_2 s_\lambda$$

Using these limits on Δu and Δv, the limits previously placed on Δx and Δy can now be put into more usable form, namely,

$$\overline{\Delta\phi} - k_3\left(s_\phi^2 + s_{\overline{\Delta\phi}}^2\right)^{\frac{1}{2}} \leq \Delta x \leq \overline{\Delta\phi} + k_3\left(s_\phi^2 + s_{\overline{\Delta\lambda}}^2\right)^{\frac{1}{2}}$$

and (7.2.1-8)

$$\overline{\Delta\lambda} - k_3\left(s_\lambda^2 + s_{\overline{\Delta\lambda}}^2\right)^{\frac{1}{2}} \leq \Delta y \leq \overline{\Delta\lambda} + k_3\left(s_\lambda^2 + s_{\overline{\Delta\lambda}}^2\right)^{\frac{1}{2}}$$

where k_3 is chosen to yield confidence limits of probability P. Suppose that in the foregoing discussion, the probability P is 95%. Then the limits placed on Δx and Δy in equations (7.2.1-8) are at least 95%. They are actually somewhat better than 95%, since in going from equations (7.2.1-7) to equations (7.2.1-8), the limits on Δx and Δu were increased due to the fact that Δu and Δv were unknown, only estimated.

From equations (7.2.1-8) the true bias (Δx, Δy) of the BOA solutions can be estimated by ($\overline{\Delta\phi}$, $\overline{\Delta\lambda}$), which is a biased estimate. It is biased by an amount (Δu, Δv), as shown in equations (7.2.1-6). This fact is, however, accounted for, in equations (7.2.1-8) when placing the limits on Δx and Δy.

It also can be concluded from equations (7.2.1-8) that a confidence ellipse can be constructed from a covariance matrix, (T), such that there is at least a 95% probability that the true BOA bias (Δx, Δy), lies within the ellipse, where

$$(T) = \begin{pmatrix} s^2_{\overline{\Delta\phi}} & s_{\overline{\Delta\phi}\,\overline{\Delta\lambda}} \\ s_{\overline{\Delta\phi}\,\overline{\Delta\lambda}} & s^2_{\overline{\Delta\lambda}} \end{pmatrix} + \begin{pmatrix} s^2_{\phi} & 0 \\ 0 & s^2_{\lambda} \end{pmatrix} \qquad (7.2.1\text{-}9)$$

The first matrix on the right hand side of equation (7.2.1-9) is simply the covariance matrix of the mean of the sample (the plotted differences), and the second matrix is just the geodetic survey covariance matrix for the Antigua Target Array.

To determine the significance of the bias estimated by ($\overline{\Delta\phi}$, $\overline{\Delta\lambda}$), Hotteling's T^2 test is used. If this test indicates that the estimated bias is significant at the 5% level, then a true bias is considered to exist and is estimated to be located at ($\overline{\Delta\phi}$, $\overline{\Delta\lambda}$) and at an azimuth

given by

$$\text{Bias Azimuth} = \begin{cases} \delta + 270^{\circ}, & \overline{\Delta\lambda} > 0 \\ \delta + 90^{\circ}, & \overline{\Delta\lambda} < 0 \end{cases}$$

$$\text{where } \delta = \tan^{-1}\left\{\frac{\overline{\Delta\phi}}{\overline{\Delta\lambda}}\right\}$$

A confidence ellipse is then constructed from the covariance matrix, (T), given in equation (7.2.1-9).

If the T^2 test indicates that the estimated bias is not significant at the 5% level, it is considered that no BOA bias exists, and the true mean of the population is considered to be at the origin (0,0) of the aforementioned coordinate system. In this case, of course, no confidence ellipse is computed.

The third "measure" of BOA accuracy in the Antigua Target Array area, viz., the precision of the BOA solutions, can now be determined through the use of a tolerance ellipse, computed from the estimated covariance matrix of the sample.

In the case at hand, the true values of the mean, variances, and covariance for the sample are not known, only estimated. Techniques are being developed for the case of unknown mean and variance. Present practice is to use the equations for the tolerance ellipse of known mean and variance [Burington and May, 1958], being careful to interpret it

correctly.

That is, if a 95% tolerance ellipse is computed, using the estimated mean of a sample, and using the development in the above reference, then the percentage of the population contained within the ellipse differs somewhat from 95%. However, this difference is slight and from the standpoint of practicality, can be considered to be 95%.

It might be well to point out that the measure of BOA precision as obtained in the above discussed method, necessarily includes the precision of the Target Array. That is, the dispersion of the plotted differences is due in part to the dispersion of the TA solutions. However, the dispersion of the TA solutions is very much smaller than that of the BOA solutions, to the extent that it can safely be ignored. The resulting measure of precision therefore can be considered to be solely of the BOA system.

7.2.1.4 Method of Obtaining Pooled Accuracies - MILS/BOA and Target Array Systems

In order to determine the "pooled accuracy" achieved, e.g., by the BOA system over a series of missile tests in one of the surveyed areas, the following method has been developed. The method involves the placing of confidence limits on the means of the terms of the geodetic accuracy covariance matrices of an infinite population of tests, the limits being determined from sample statistics.

First assume that the terms, s_{ϕ}^2, s_{λ}^2, and $s_{\phi\lambda}$ of the geodetic accuracy covariance matrices of N missile tests in a BOA surveyed area compose a random sample of size N

of a trivariate population. Thus, the sample is:

$$\begin{array}{lll} S^2_{\phi_1} & S^2_{\lambda_1} & S_{\phi\lambda_1} \\ \vdots & \vdots & \vdots \\ S^2_{\phi_i} & S_{\lambda_i} & S_{\phi\lambda_i} \\ \vdots & \vdots & \vdots \\ S^2_{\phi_N} & S^2_{\lambda_N} & S_{\phi\lambda_N} \end{array}$$

where $S^2_{\phi_i}$, $S^2_{\lambda_i}$, $S_{\phi\lambda_i}$ are the terms of the geodetic accuracy covariance matrix of the i^{th} test in the surveyed area.

Then, the components $\mu_{s^2_\phi}$, $\mu_{s^2_\lambda}$, $\mu_{s_{\phi\lambda}}$, of the mean vector $\underline{\mu}$ of the population, to which the above sample belongs, can be estimated by:

$$\hat{\mu}_{s^2_\phi} = \frac{1}{N}\sum_1^N s^2_{\phi_i} = \overline{s^2_\phi}$$

$$\hat{\mu}_{s^2_\lambda} = \frac{1}{N}\sum_1^N s^2_{\lambda_i} = \overline{s^2_\lambda}$$

$$\hat{\mu}_{s_{\phi\lambda}} = \frac{1}{N}\sum_1^N s_{\phi\lambda} = \overline{s_{\phi\lambda}}$$

where, for computational convenience, the simplifying assumption is made that the degrees of freedom per sample variance are equal. (This is a good approximation for the data in most cases).

Confidence limits can now be placed on the components, $\mu_{s_\phi^2}$, $\mu_{s_\lambda^2}$, $\mu_{s_{\phi\lambda}}$, of the population mean vector $\underline{\mu}$. Thus, it can be said that if there were an infinite number of BOA missile tests in the area under consideration, there is a probability, P, that a given confidence interval encloses the mean of the (1,1) terms of the matrices of all the tests; likewise, for the mean of the (2,2) terms and the mean of the (1,2) terms.

Assuming that the distribution of the sample means approximates closely the normal distribution (by appealing to the Central Limit Theorem), then there is a 95% probability that

$$\mu_{s_\phi^2} \leq \overline{s_\phi^2} + k_\gamma \hat{\sigma}_{\overline{s_\phi^2}} \qquad (7.2.1\text{-}10)$$

where $\gamma = N-1$ degrees of freedom, k_γ is obtained from "Student's" t-distribution tables at the 95% "one-sided" level, and $\hat{\sigma}_{\overline{s_\phi^2}}$ is the estimate of the standard deviation of the mean $\overline{s_\phi^2}$.

Likewise, there is a 95% probability that

$$\mu_{s_\lambda^2} \leq \overline{s_\lambda^2} + k_\gamma \hat{\sigma}_{\overline{s_\lambda^2}} \qquad (7.2.1\text{-}11)$$

The limits placed on $\mu_{s_\phi^2}$ and $\mu_{s_\lambda^2}$ above, are 95% upper bounds.

In placing limits on $\mu_{s_{\phi\lambda}}$, however, it is more meaningful to consider both upper and lower bounds, i.e., there is a 95% probability that $\mu_{s_{\phi\lambda}}$ is in the range given by

$$\overline{s_{\phi\lambda}} - k'_\gamma \hat{\sigma}_{\overline{s_{\phi\lambda}}} \leq \mu_{s_{\phi\lambda}} \leq \overline{s_{\phi\lambda}} + k'_\gamma \hat{\sigma}_{\overline{s_{\phi\lambda}}} \qquad (7.2.1\text{-}12)$$

where k'_γ is obtained from "Student's" t-distribution tables, in this case, at the 95% "two sided" level.

Equations (7.2.1-10, -11, and -12) are thus utilized to give the confidence limits on the true means of the terms of the geodetic accuracy covariance matrices of tests, e.g., in a given BOA surveyed area.

This method is also utilized for the MILS Target Arrays. However, instead of pooling all tests in a given Target Array, it is necessary to pool all "Splash I" events together, all "Splash II"

events together, and all bomb events together, for a given Target Array. The reasons for this are (1) completely different parameters are used in the impact solutions of bomb events and splash events, and (2) "Splash I" events have always appeared to be from a different population from that of the "Splash II" events.

7.2.2 System Description

The Missile Impact Locating System (MILS) is an underwater sound detection and source location system used to determine the geodetic position and time of the impact of a missile nose cone or data capsule on the ocean surface.

The system is based on the acquisition of data in the following manner (refer to Figure 7.2.2-1).

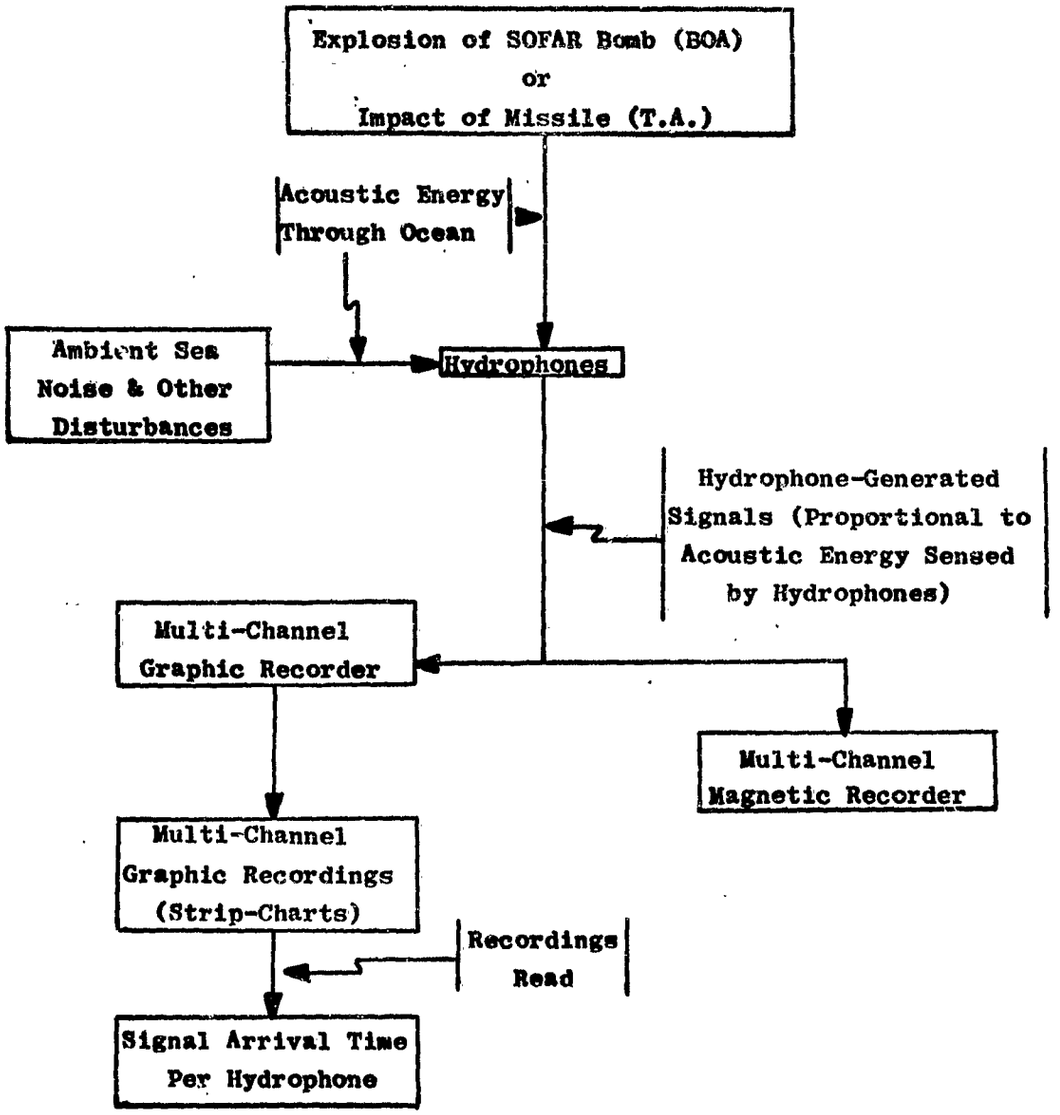
(1) Acoustic energy is produced in the ocean by one of the following sound sources:

(a) the impact of a nose cone on the ocean surface (detectable only by a MILS Target Array); or

(b) the explosion in the ocean of a SOFAR bomb(s) carried by the portion(s) of the missile for which an impact location is desired (detectable by either a Target Array or the BOA system).

(2) The acoustic energy produced is propagated through the ocean to a number of MILS hydrophones (specially designed underwater microphones). The hydrophone converts the acoustic energy into electrical energy by generating a small current proportional in time to the sound intensity sensed by the hydrophone.

FIGURE 7.2.2-1
Acquisition of
MILS Missile Test
Data



(3) The signals generated by the hydrophones are propagated through underwater cables to terminal recording stations where they are recorded on multi-channel magnetic tapes and graphic strip charts.

(4) Either WWV, or some other timing signal referenced to WWV, is also recorded on the magnetic tapes and graphic strip-charts. Thus the time of arrival of the acoustic energy at each of the hydrophones can be read from the graphic recordings.

(5) From a knowledge of the hydrophone positions, the velocity of propagation of sound in the ocean, and the hydrophone arrival times, the location and time of the source can be computed.

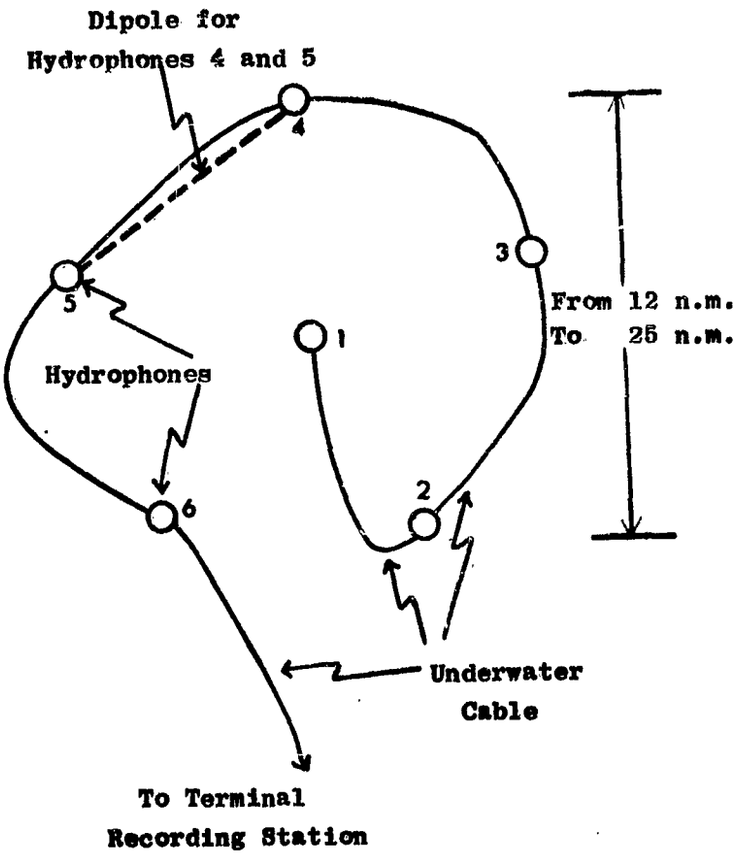
The MILS consists of two separate types of systems: the Target Array (also called the pentagon array or splash array), and the Broad Ocean Area, or BOA System. Although the above general description of data acquisition holds for both systems, there are distinct differences between the two systems in design and operation.

7.2.2.1 Target Arrays, MILS

There are three Target Arrays in the MILS at the Air Force Eastern Test Range (AFETR). They are shore-terminated at Antigua, Ascension and Grand Turk Islands, respectively (see Figure 7.2.2-7). Each of these arrays consists of six hydrophones placed on the ocean floor, five at the apexes of a regular pentagon, and the sixth in the center (see Figure 7.2.2-2). The target area for a Target Array is the water surface outlined above the pentagon. The

FIGURE 7.2.2-2

Typical Target Array
(Showing Typical Hydrophone
Position, and Underwater
Cable)



diameter of the target area is from 12 n.m. to 25 n.m. depending on the Target Array. The pentagon configuration ensures that for any point of impact within the target area, there will always be at least two hydrophone baselines (or dipoles) suitably oriented (optimum geometry) for an accurate solution. Due to the relatively short (compared to the BOA) travel-path for the sound from the impact point to any of the hydrophones in the Target Array, the sound energy produced by the nose cone impacting on the ocean surface in the target area can be detected and recorded.

If the propagation of the sound from the impact point is considered as an infinite number of rays (perpendicular to the sound wavefront), it will be seen from Figure (7.2.2-3) the direct arrival is the first to arrive at the hydrophone, the first order arrival next, then the second order arrival, etc., due to the travel path lengths. The direct arrival undergoes no reflections, the first order arrival one surface and one bottom reflection, the second order two surface and bottom reflections, etc. Due to these reflections and to the fact that the path lengths of these arrivals are respectively longer, it is obvious that each arrival is attenuated more than the preceding one, with the direct arrival being attenuated least. Figure (7.2.2-4) depicts a typical Target Array hydrophone signal showing the direct arrival received first with largest amplitude. It is this portion ("point-to-time") of the signal that is read to determine the arrival time for the hydrophone.

7.2.2.1.1 Target Array Solution, Missile Tests

The observations (arrival times) are adjusted by the least squares method, the least squares solution being the maximum likelihood location and time of impact.

FIGURE 7.2.2-3

Typical Ray Paths from Impact Point to Hydrophone (Target Array)

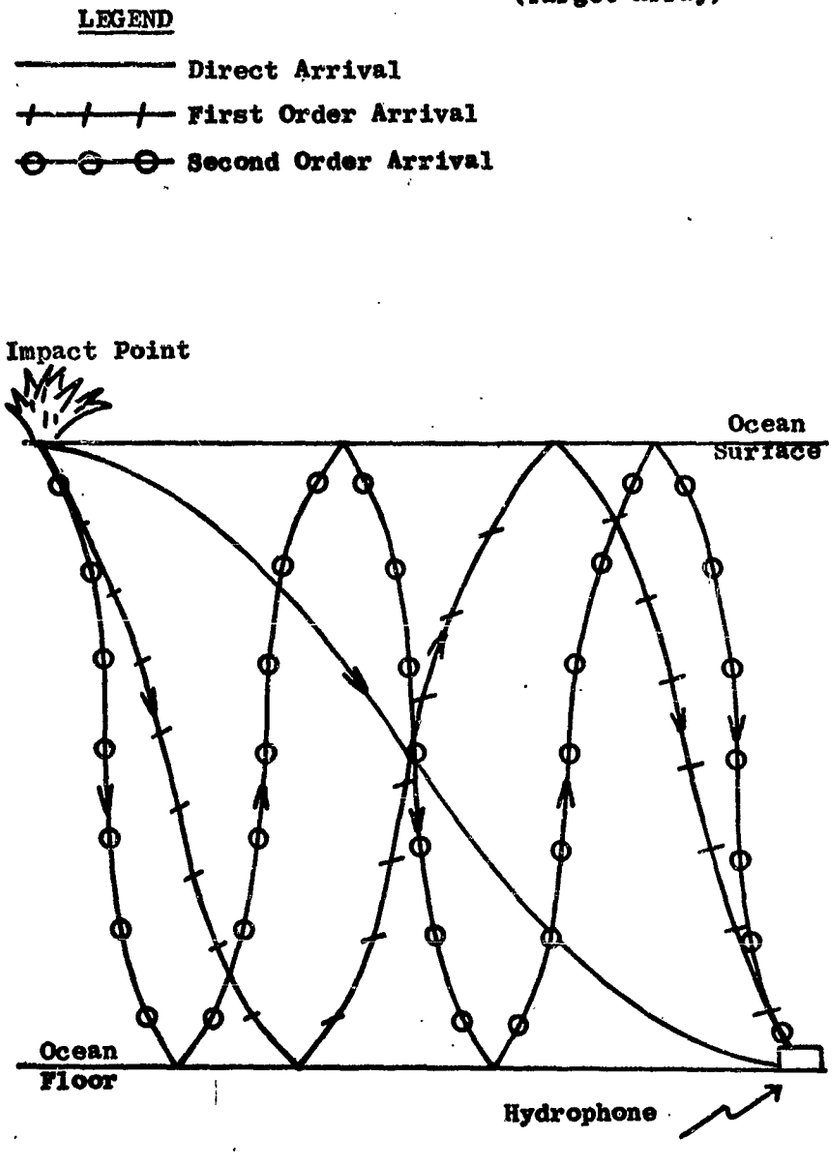
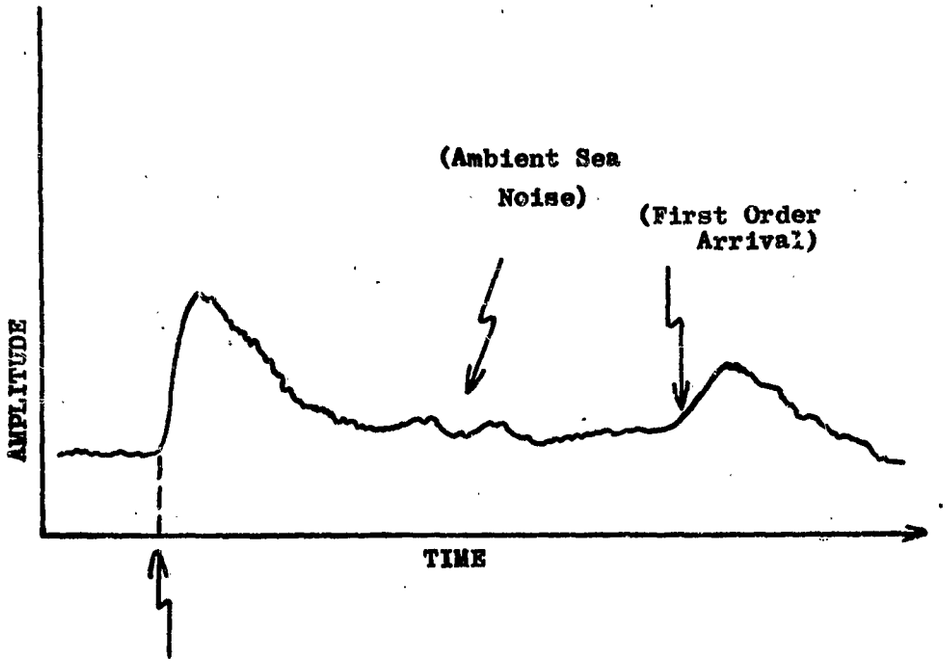


FIGURE 7.2.2-4

Typical Hydrophone
Signal (Target Array)



$$\left\{\begin{matrix}\text{Time of Direct}\\ \text{Arrival}\end{matrix}\right\} - \left\{\begin{matrix}\text{Hydrophone Arrival Time}\\ \text{to be Used in the Solution}\end{matrix}\right\}$$

Full-Wave Rectified - Logarithmic Presentation

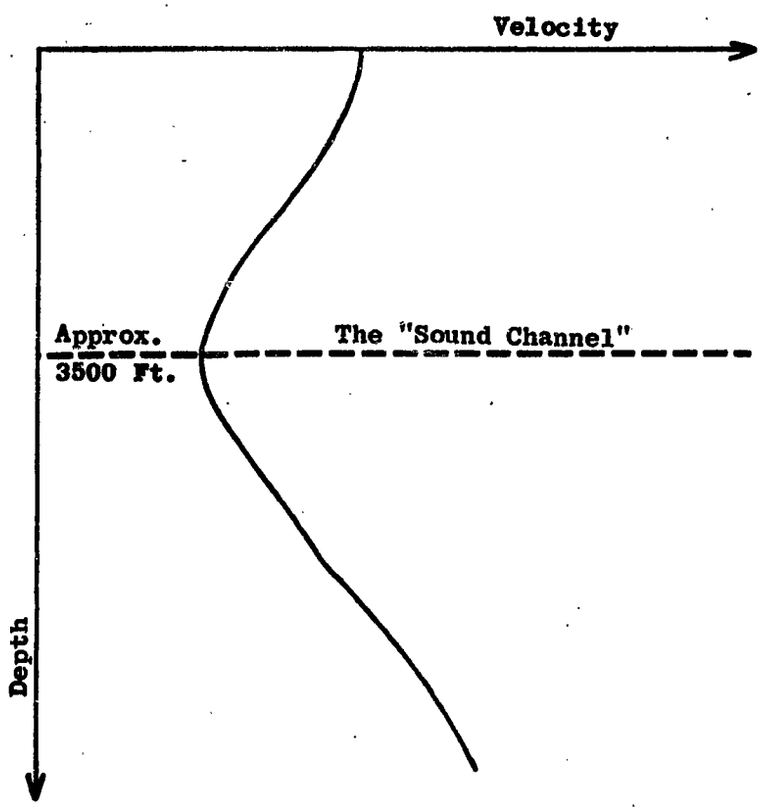
The solution covariance due to observational (timing) errors is a by-product of the least squares adjustment, and is called the "timing covariance matrix." Velocity errors and hydrophone survey (relative to local coordinate system, see Paragraph 7.2.3.2.2) errors are propagated to obtain a "hydrophone survey and velocity covariance matrix." These two matrices and the "geodetic survey covariance matrix" (geodetic survey of the local coordinate system) are summed to yield a geodetic accuracy covariance matrix. From this matrix, a geodetic confidence ellipse is computed utilizing equation (7.2.1-2) through equation (7.2.1-5).

7.2.2.2 BOA, MILS

The physical property upon which the Broad Ocean Area (BOA) is based is the velocity profile of the ocean, see Figure (7.2.2-5). Velocity of sound in the ocean decreases with depth for about the first 3500 feet, decreasing temperature having the most effect on velocity in this layer. Below about 3500 feet, velocity increases with depth, pressure affecting velocity the greatest in the deep-water layer. The depth of minimum velocity is called the "sound channel," (also referred to as the "SOFAR axis"). Attenuation of acoustic energy traveling along the sound channel is nearly proportional to the distance, rather than to the square of the distance. This, plus the fact that the sound paths (rays) are refracted toward the minimum velocity region, provides for the propagation of even relatively small sounds over extreme distances. The BOA system takes advantage of this depth of minimum velocity by placing the sound source and the hydrophones as close as possible to the "sound channel."

FIGURE 7.2.2-5

Typical Velocity Profile
Depicting the "Sound Channel"



Four of the eleven BOA hydrophones, unlike those of the Target Array, are suspended on a cable from a sub-surface float as shown in Figure (7.2.2-6), so that they are close to the depth of the sound channel. The remaining hydrophones are installed on the ocean bottom but still close to the depth of the sound channel. The unclassified geographic locations of the BOA hydrophones are approximated in Figure (7.2.2-7). Each of the hydrophones (or sets of one or more phones) is linked by underwater cable to its own terminal recording station.

The sound source for the BOA is a SOFAR (Sound Fixing and Ranging) bomb containing from 1/2 lb. to 4 lbs. of TNT and a pressure-activated detonation control, set for the pressure at the sound channel. The SOFAR bomb is carried by the portion of the missile for which a location is desired. (Due to the ranges involved between source and hydrophones and to the distance from the ocean surface to the sound channel, surface impacts cannot be detected by the BOA system.) If the location of more than one portion of the missile is desired, a SOFAR bomb is placed in each, the charge-weight of each of these bombs being made different (over-all weight identical) for identification purposes.

Concerning the sound propagation from the source (in the sound channel) to a hydrophone, (also in the sound channel) the sound traveling along a path, the majority of which is in the higher velocity layers, is the first to arrive at the hydrophone. But since this sound ray has undergone a higher number of reflections (from the surface and floor of the ocean) it has been attenuated more. A sound ray (leaving the source at a different angle) and spending less time in the higher velocity layers arrives later, suffers

FIGURE 7.2.2-6

Suspended BOA Hydrophone

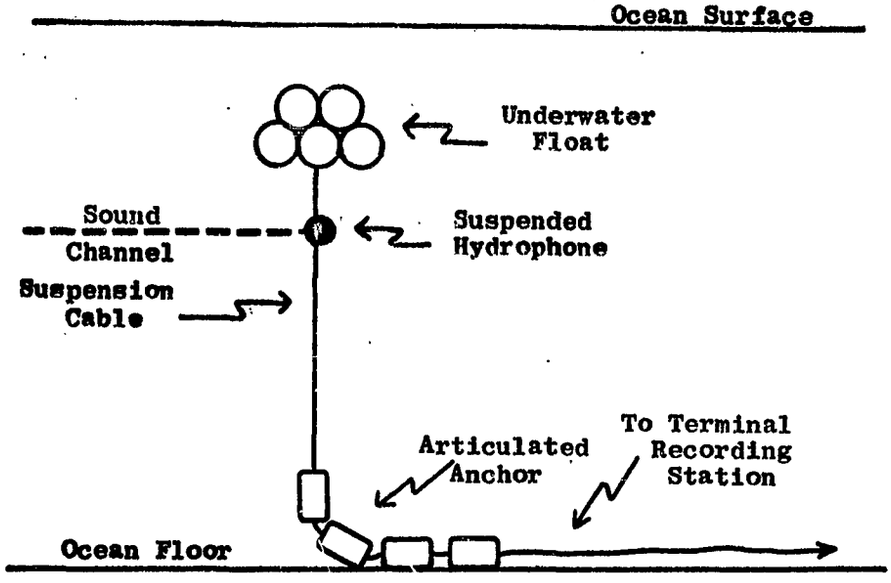
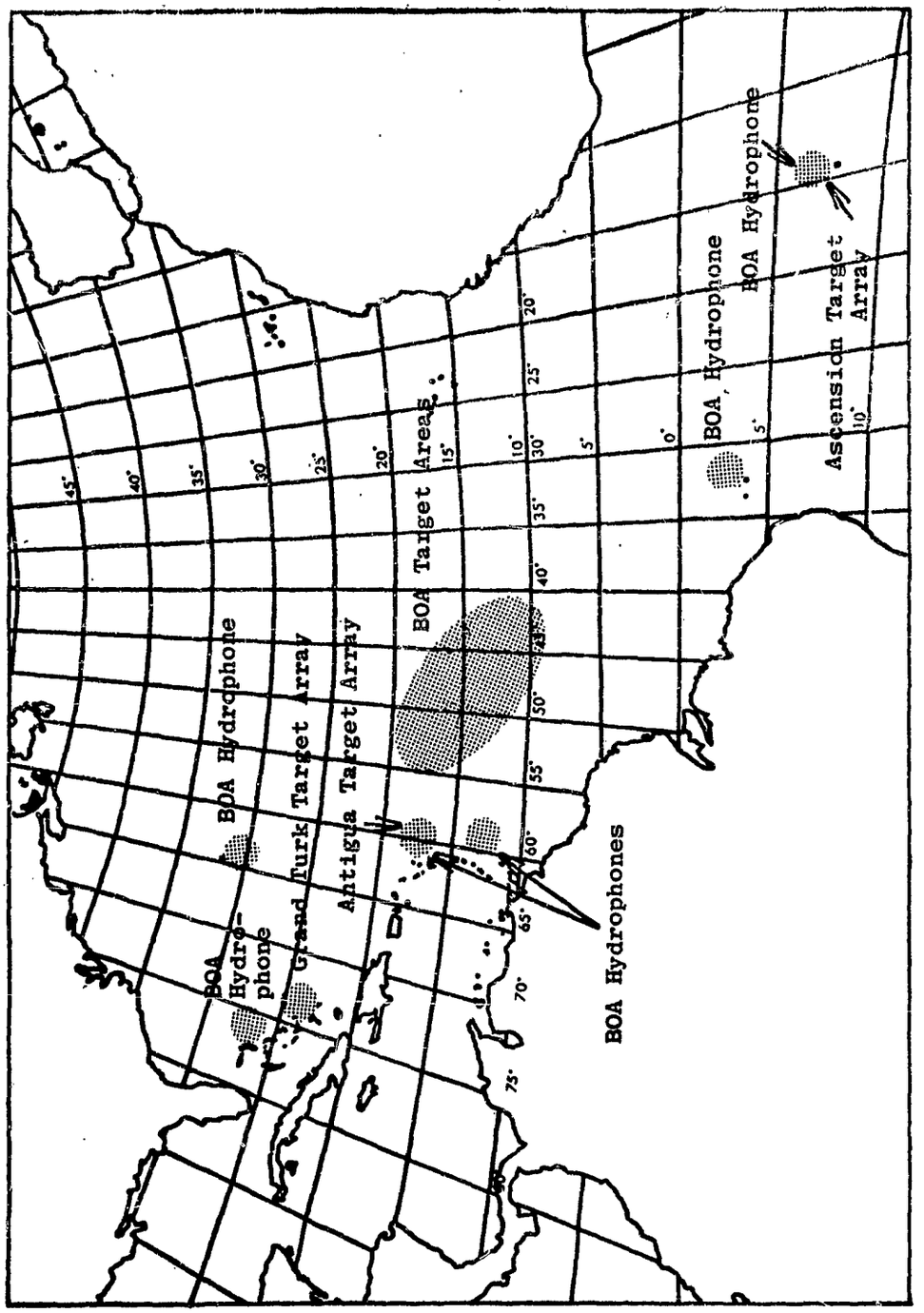


FIGURE 7.2.2-7

BOA Hydrophone Locations



fewer reflections, and is attenuated less. The last "bundle of energy" to arrive has traveled along the sound channel, undergone no reflections, and less attenuation. This process produces an arrival signal at a BOA hydrophone that appears like that in Figure (7.2.2-8). The point of signal decay back to ambient noise is the point that is read ("point-to-time") to obtain the hydrophone arrival time. This is a typical, good arrival shown with no masking (by another signal) nor has the signal been degraded due to either the source or the hydrophone (or both) being off the sound channel.

7.2.2.2.1 BOA Solution, Missile Tests

The observations (arrival times) are adjusted by the least squares method, the least squares solution being the maximum likelihood location and time of source.

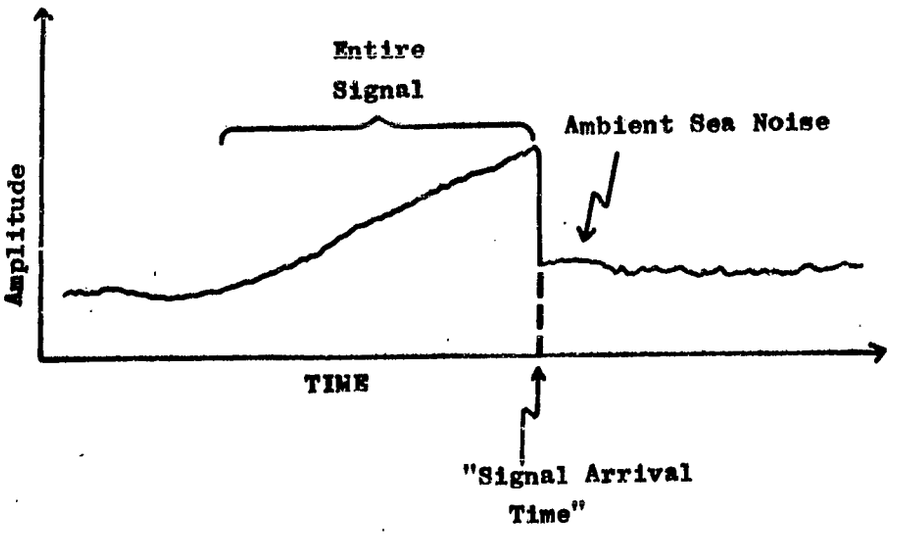
A geodetic accuracy covariance matrix and a geodetic confidence ellipse for the test are computed in the manner outlined in Paragraph (7.2.1.2).

7.2.2.2.2 Pre- and Post-Test Calibrations, BOA Surveyed Areas

The BOA system can obtain an estimated position of a SOFAR bomb exploding anywhere along the flight-path of the AFETR, but for increased accuracy, certain areas (sometimes referred to as calibrated areas, but more correctly surveyed areas) are set up as the target areas for the BOA missile tests. These surveyed areas consist of usually three underwater transponders located on the ocean floor in essentially an equilateral triangle configuration. The transponders are self-contained, battery-powered, transceivers. They are designed to respond to a common-frequency interrogate signal

FIGURE 7.2.2-8

Typical (Good) BOA
Hydrophone Signal



Full-Wave Rectified - Logarithmic Presentation

(16 kc) from a ship-towed, underwater transducer. Each of the transponders responds or replies to the interrogate signal by transmitting on separate frequencies (10 kc, 11 kc, and 12 kc) to facilitate identification of the signals. Thus a ship equipped with an underwater transducer and Precision Depth Recording (PDR) equipment, can accurately position itself geodetically in the BOA, once the geodetic position of the transponders is known. (The determination of the transponder locations is just the reverse of this process, with the ship being positioned by some navigational aid system.) The purpose for such a "surveyed area" is to provide a method for pre- and post-test calibrations for missile tests, a discussion of which follows. The necessity for calibration is due to acoustic velocity changes in the ocean which are not only uncontrollable, but, at the present time, unpredictable. These fluctuations are due to seasonal and even daily and hourly variation in temperature, pressure, and salinity of the ocean. Thus, the purposes of the pre- and post-test calibrations are as follows:

(1) to obtain a "best" estimate of the average velocity between the surveyed area and each of the hydrophones;

(2) to determine an a priori estimate of the standard deviation in timing for each hydrophone;

(3) to accomplish these as close in time to the missile test as possible.

The pre-test and the post-test calibrations are performed by dropping SOFAR bombs from a calibration ship into the surveyed area at known times and locations. The signals received at each of the BOA hydrophones are recorded and the arrival times

determined. Thus, ranges and travel times for each of the calibration bombs are calculated, from which an average velocity is computed for each hydrophone.

7.2.3 Error Sources

7.2.3.1 BOA Sources of Error

The errors affecting the MILS in support of a BOA missile test are categorized into random and systematic errors and discussed individually (see Figure 7.2.3-1).

7.2.3.1.1 BOA System Random Error Sources

There are five groups of random errors affecting the BOA System, all of which can be expressed in terms of, or handled as, either an acoustic velocity error, or a signal timing error (the latter is presently the case) due to the manner in which the BOA system is calibrated and the missile-impact position data processed.

(1) Hydrophone Movement

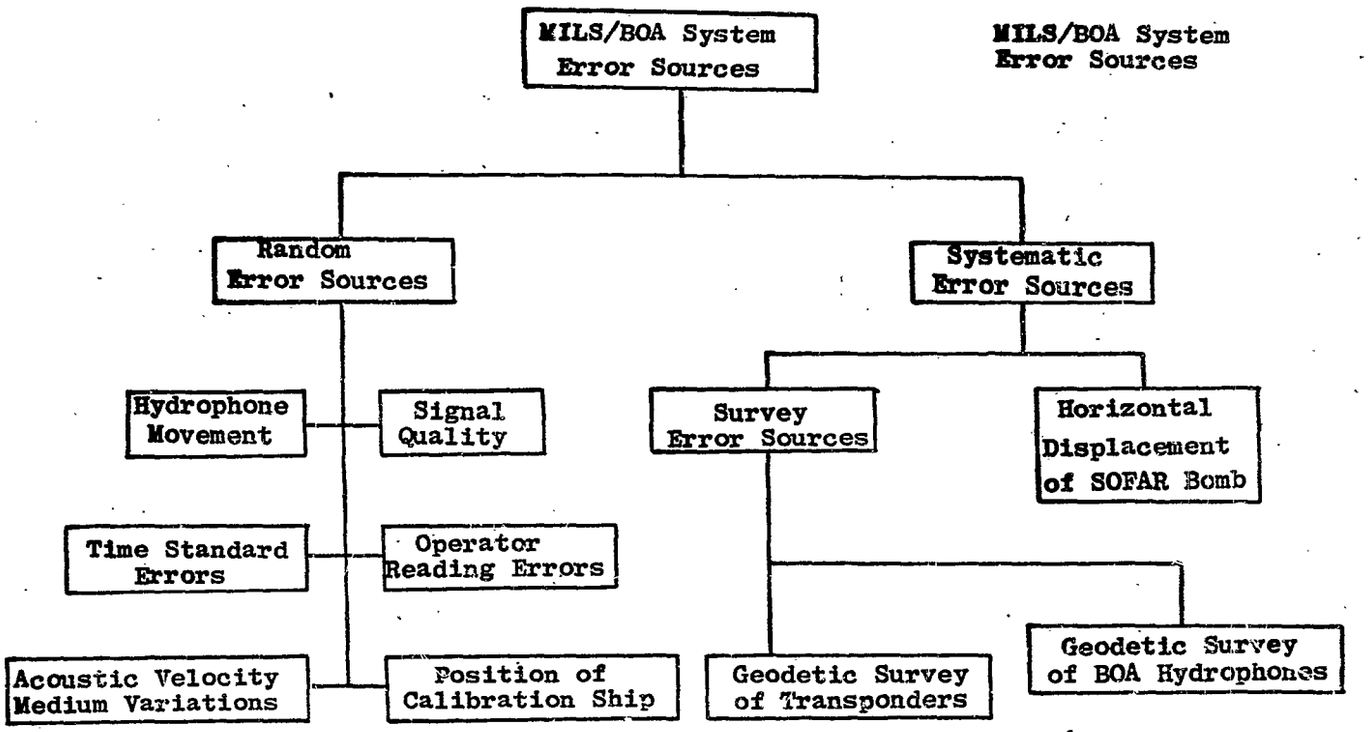
One source of error in hydrophone position is a limited movement of BOA suspended hydrophones due to ocean currents and tides. Four of the eleven hydrophones utilized in the BOA system are so affected. The remaining hydrophones are bottom-mounted and undergo no movement.

(2) Acoustic Velocity Medium Variation

The velocity of propagation of sound through the ocean (different for each hydrophone) is not constant in time per hydrophone, and the variations due to changes in ocean temperature, pressure, and salinity are

FIGURE 7.2.3-1

MILS/BOA System Error Sources



unpredictable. It is impossible to separate the changes in velocity due to variations in the medium from those due to other random system changes since all errors experienced during calibration are reflected in the velocity determination.

(3) Operator Reading Errors

The recorded MILS data are read manually, the readings being subject to human error. This is due to the inability of the individual to select consistent "points-to-time" from one arrival signal to the next. The effect of this inconsistency is a random error in the BOA missile test solution. Variation in signal quality is another cause of inconsistent reading of the recorded data.

(4) Errors in Time Standard

A majority of the MILS BOA stations have independently operating time standards which must be synchronized to WWV and have WWV propagation error corrections applied. These standards also experience some drift due to random errors in the stations' electronic equipment. These errors will introduce a random error in the estimated time and position of the SOFAR bomb explosion.

(5) Position Determination of Calibration Ship

The position of the calibration ship relative to the acoustic transponders must be determined at the time of each calibration bomb-drop (see paragraph 7.2.2.2.2).

Over the entire series of calibration bombs, the error in positioning the ship will have the effect of random error on the velocity determinations.

7.2.3.1.2 BOA Systematic Errors

Due to the calibration and operation techniques employed in the BOA system there are three systematic error sources as follows:

(1) Geodetic Survey of the Transponders.

The calibration technique employed (see paragraph 7.2.2.2.2) requires that the target areas in the BOA be surveyed geodetically. Any systematic error in these surveys will be reflected in the computed missile impact position.

(2) Horizontal Displacement of SOFAR Bomb

The MILS solution, in actuality, estimates the position of the SOFAR bomb explosion, rather than the impact point. As the bomb (and its carrier - some portion of the missile) sinks from impact to pre-set explosion depth, there is some horizontal drift that occurs due to ocean currents and vehicle configuration. Thus, the impact point is not simply vertically above the explosion point of the bomb, so that the estimated impact point is biased by the amount of horizontal displacement of the SOFAR bomb. This systematic error will exhibit random behavior over a number of tests.

(3) Geodetic Survey of the BOA Hydrophones

For missile impacts which occur in the BOA surveyed area, any error in the survey of the hydrophones is automatically compensated for. For impacts which

occur very near the surveyed area, the hydrophone position errors are considered as secondary error sources. For impacts which occur in non-surveyed areas, the hydrophone survey errors are considered as primary error sources.

7.2.3.2 MILS Target Array Error Sources

The Target Arrays are subjected more to systematic error sources than to random error sources. Both types of errors are discussed as follows, the discussions being applicable to the location of both missile impacts (splashes) and SOFAR bomb explosions. Refer to Figure (7.2.3-2).

7.2.3.2.1 Target Array Random Errors

There are only two errors in the Target Array which fall into the category of random errors.

(1) Signal Timing

Consistent timing of the signal arrivals at all hydrophones is influenced by:

(a) variations in signal quality from hydrophone to hydrophone; and,

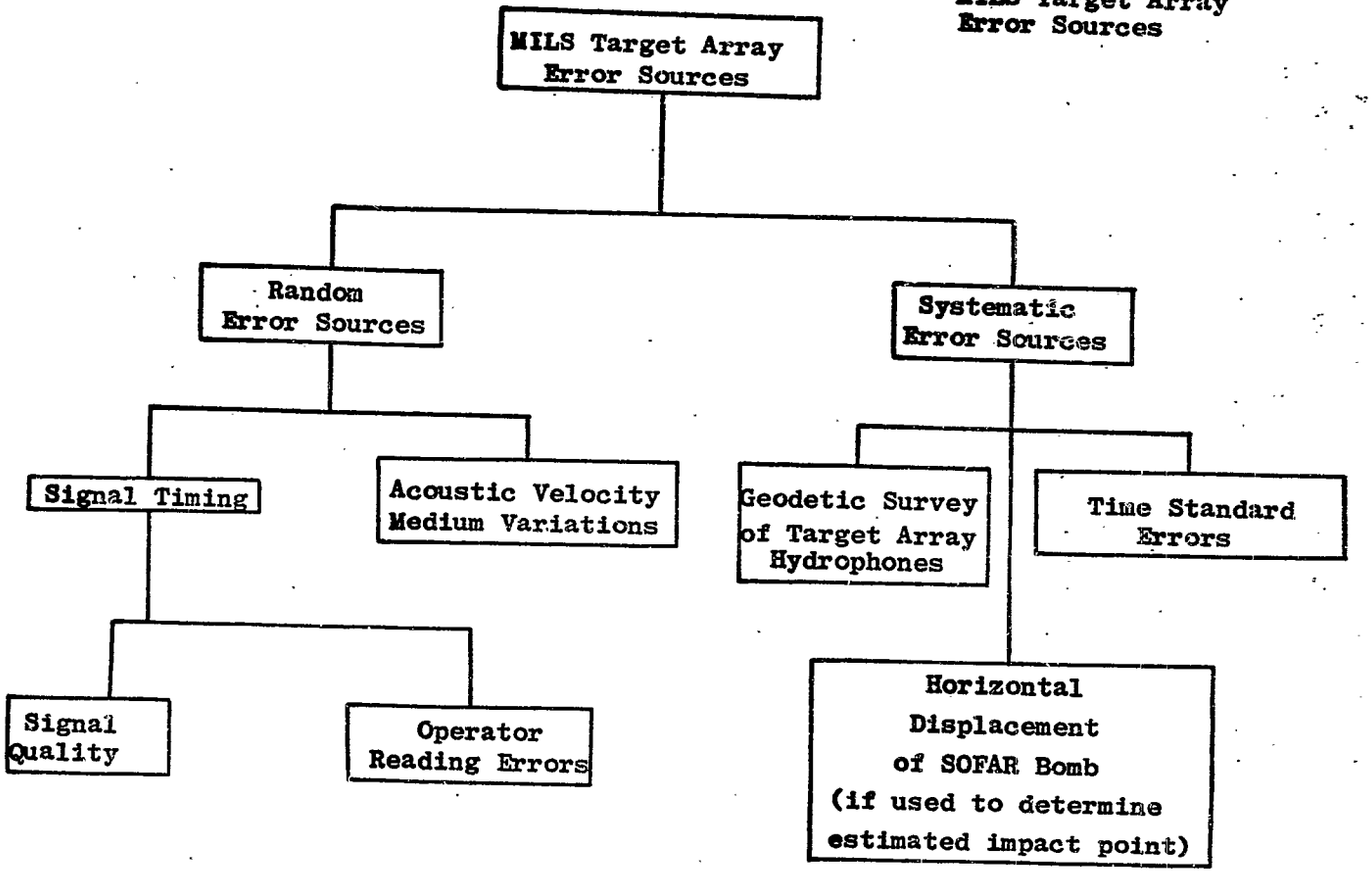
(b) the system analyst's ability to select consistent "points-to-time."

(2) Acoustic Velocity Medium Variations

Variations in the medium (ocean temperature, pressure, and salinity) cause random velocity errors in the Target Array, similar to the BOA System, except that the Target Array velocity random variations have considerably less effect on the solution than those of the BOA system.

FIGURE 7.2.3-2

MILS Target Array Error Sources



7.2.3.2.2 Target Array Systematic Errors

There are two sources of systematic errors affecting the estimated position of a missile impact as determined by the Target Array System, and one additional source which affects the estimated impact position when determined from data from a SOFAR bomb explosion in the Target Array.

(1) Geodetic Survey of Target Array Hydrophones

There are two types of surveys conducted for the Target Array hydrophones which are sources of systematic error in the TA missile impact solutions. The first is the positioning of the hydrophones in a local coordinate system (origin at center hydrophones, x-axis positive east, and y-axis positive north). The second is the geodetic positioning of the local coordinate system by positioning geodetically the center hydrophone. Due to this technique of surveying the TA hydrophones, one of the following will apply;

(a) if the missile impacts near the center of the array (i.e., within approximately 2 n.m. of the center) the errors due to the first type survey (above) are compensated for, and only the geodetic survey error (second type, above) affects the solution;

(b) if the missile impacts away from the center (but still inside the array) the first type error source is propagated in the solution, being handled as a bias uncertainty. Geodetic survey errors will also affect the solution in this case. If over a number of tests, the missile impact positions are randomly distributed

in the Target Array area away from the center, the systematic error due to the first type of survey above exhibits a random behavior over these tests.

Regardless of the impact position within the TA, the geodetic survey is always a systematic error source affecting the solution.

(2) Errors in Time Standard

An error in synchronization of the timer at the recording station with WWV will introduce a systematic error in the computed time of impact, but will have no effect on the computed impact positions. This systematic error will exhibit random behavior over a number of tests.

(3) Horizontal Displacement of SOFAR Bomb

If for some reason the impact position is not determined from the spash signals, but, instead, from the SOFAR bomb signals, then the horizontal displacement of the SOFAR bomb during sink will produce a systematic error in the estimated impact position. This systematic error will exhibit random behavior over a number of tests.

7.2.4 System Accuracies

The data from MILS calibrations and missile tests are classified SECRET.

8.0 NAVIGATION SYSTEMS

8.1 INTRODUCTION

In order to obtain position data accuracies comparable to those obtained from land based radars the location and attitude of the tracking ships need to be well defined. The Navigation and Stabilization subsystems are designed to accurately determine those quantities.

The position of a ship is determined in an Earth fixed coordinate system and its attitude is measured with respect to the plane tangent to the Earth's surface at the given location. Five quantities are obtained and are: latitude, longitude, roll, pitch and heading.

The main component of the NAV/STAB system is an inertial platform MK-I SINS on the General Arnold, MK-IV SINS on the General Vandenberg and N7C on the Twin Falls Victory. All other equipment is used as back up in the event of an Inertial Guidance System failure or to provide information to stabilize the platform and compute SINS errors.

Position and heading fixes necessary to update the SINS are obtained from the Star Tracker or the sonar bench mark interrogation. An Electromagnetic (E-M) log provides a rough estimate of the ship's velocity which is used to damp the inertial platforms. It is also used in connection with a MK-19 gyro-compass to provide position (at a reduced accuracy) by dead reckoning and ship's attitude.

Another method of determining ship's position is available. It is the LORAC Navigation net which uses four land based stations (three transmitters and a reference station with both receiver and transmitter). The ship has LORAC receivers which compare phases from combination of the signals received from the various transmitters.

8.2 LORAC

8.2.1 System Description

The LORAC (LOng Range ACcuracy) networks on the Eastern Test Range (ETR) are the type B LORAC which is a hyperbolic, multi-user CW radio navigation system. It requires two baselines, when used in the hyperbolic configuration, with one designated green and the other red. Three CW transmitters are utilized on the baselines with the end stations differing from the center station by audio frequencies. A fourth transmitter, called the reference transmitter, modulates its carrier frequency with the audio signals derived from heterodyning the green and the red baseline frequencies. Figure 8.2-1 illustrates a typical type B network and its utilization by a mobile receiver to obtain a navigational fix. At the mobile receiver, the frequencies f_2 and f_1 are heterodyned to produce the red position signal for the first family of hyperbolas. Frequencies f_2 and f_3 are also received at the mobile receiver and are heterodyned to produce the green position signal for the second family of hyperbolas. This color coding aids in distinguishing between the halves of the system with the green base line between T_2 and T_3 and the red baseline between T_1 and T_2. Heterodyning is also accomplished at the reference station, T_4, to produce frequencies $(f_2 - f_1)$ and $(f_3 - f_2)$ which are used as modulation on the transmitted frequency f_4. This rebroadcast system is phase compared at the mobile receiver to the red and green position signals to locate the receiver with respect to the positions of T_1, T_2 and T_3.

The ETR has two of the type B systems which are designated LORAC "A" and LORAC "B" networks, the "B" network being farther

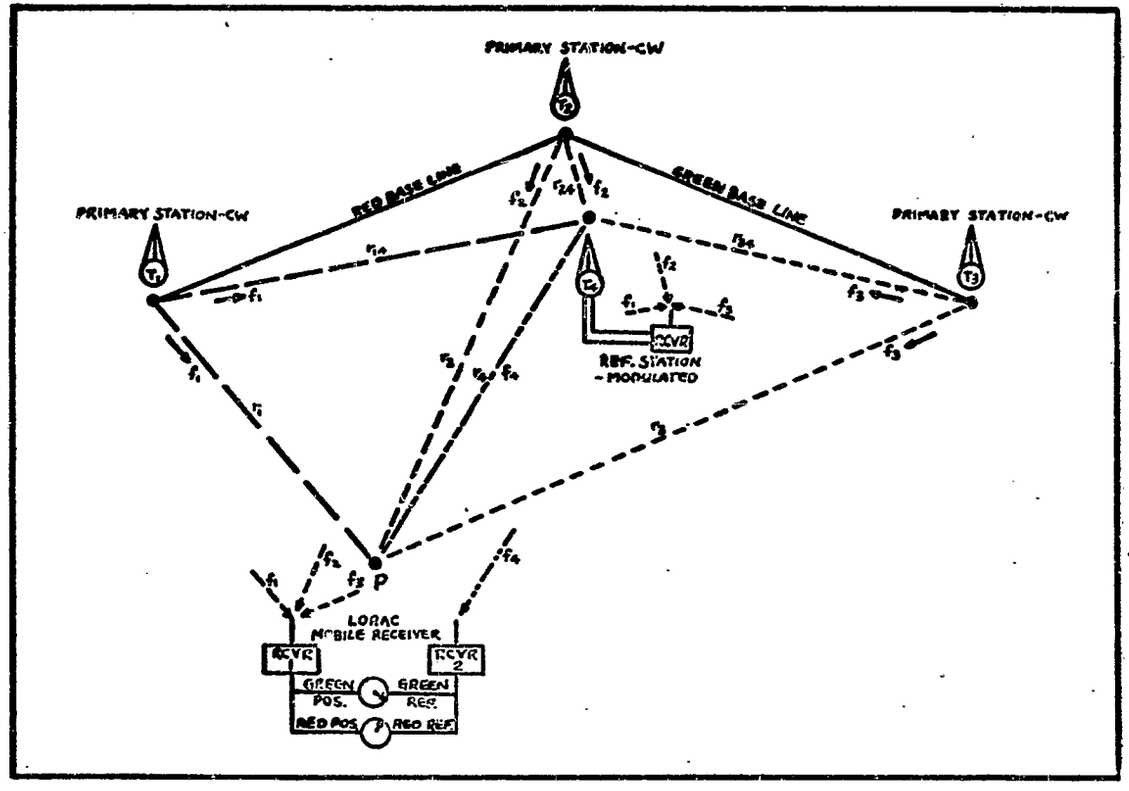


Figure 8.2-1. LORAC B TYPE NETWORK

downrange from Cape Kennedy. Figure 8.2-2 shows the location of the two networks and designates the component parts as outlined above. In the case of the ETR networks, a second mobile receiver has been permanently installed at a known point in the network and is used to monitor the LORAC pattern and indicate the system stability. It is designated the pattern monitor station. Tables 8.2-1 and 8.2-2 give the ETR locations of both networks and other network information.

The LORAC system is ambiguous only in the whole number of cycles of phase. The phase measuring equipment can determine the fractional part of the lane count. Thus, the whole lane count must be inserted into the phasemeters at the calibration point, and the equipment will then keep up with the cycles of phase change as long as the signal is not lost.

The basic equations for the computation of the lane counts at any point in either network are given below. It should be understood that the equations are based on lane number zero being located at the center station and all lane numbers extending out to the end stations being positive. The LORAC lane width, W, is then determined from the center station frequency.

$$W = \frac{V}{2f_m} = \frac{c}{2f_m n_o} \qquad (8.2\text{-}1)$$

$$L_g = \beta_g = \left[(r_3 - r_2)f_m + (r_3 - r_4)n_g\right]\frac{n_o}{c} \qquad (8.2\text{-}2)$$

$$L_r = \beta_r = \left[(r_1 - r_2)f_m + (r_4 - r_1)n_r\right]\frac{n_o}{c} \qquad (8.2\text{-}3)$$

$$L_{g_p} = \beta_g = \left[(r_{3p} - r_{2p})f_m + (r_{3p} - r_{4p})n_g\right]\frac{n_o}{c} \qquad (8.2\text{-}4)$$

(Text continued on page 8-9)

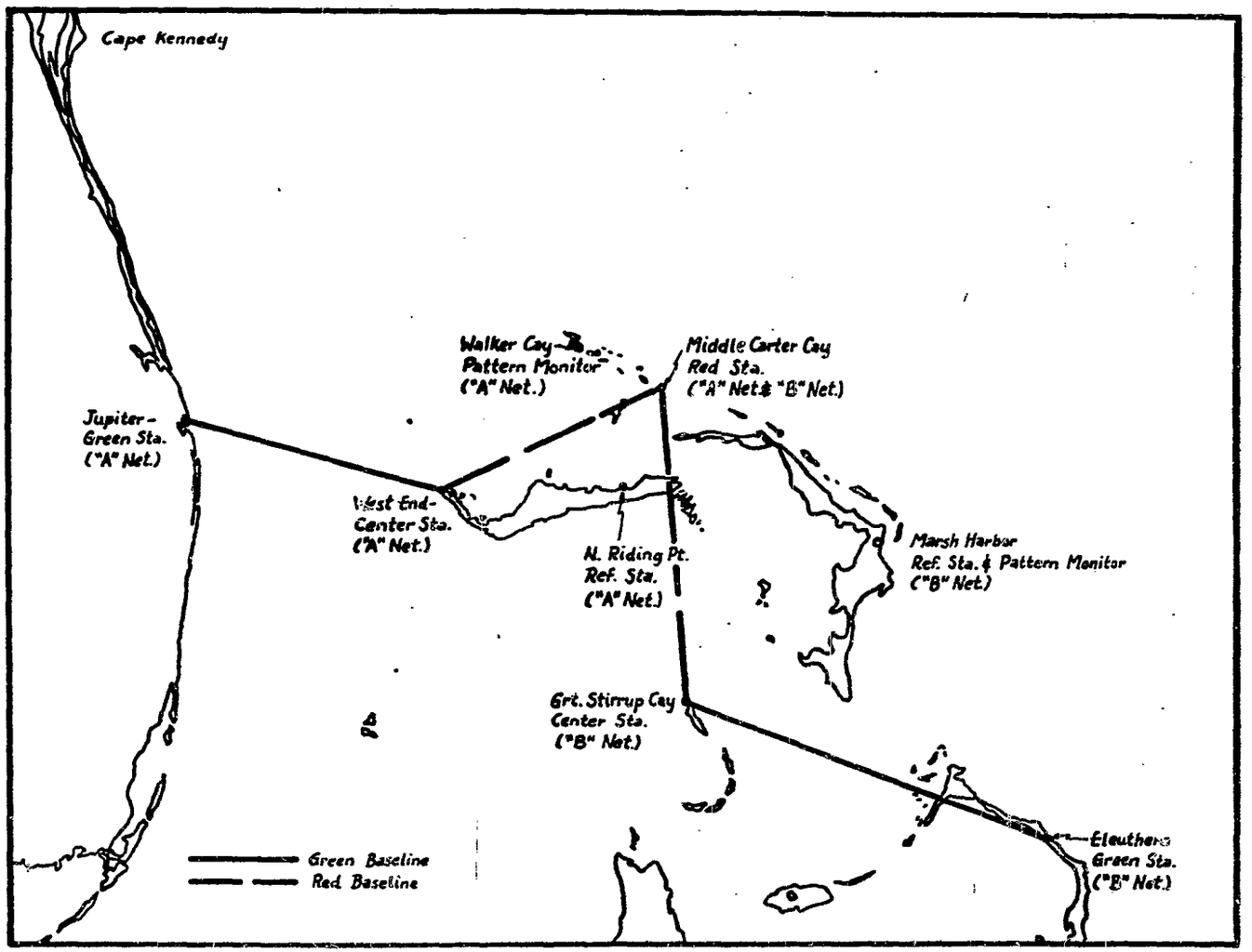


Figure 8.2-2 LOCATION OF THE LORAC A AND B NETWORKS

Table 8.2-1

LORAC "A" NETWORK CONSTANTS

(CCD - 1964 Adjustment, Clarke 1866 Spheroid)

	ϕ	λ
Green Station: Jupiter, Fla.	26°57'12".0711	80°04'49".2509
Center Station: West End, GBI	26°39'39".92460	78°55'40".98982
Red Station: Middle Carter Cay	27°05'15".16028	78°00'44".76373
Reference Sta.: N. Riding Pt., GBI	26°42'44".28141	78°09'27".27086
Pattern Monitor: Walker Cay	27°15'28".02550	78°23'38".74780

Baseline Length, Center to Green	(r_3)	119,055.0690 m.
Baseline Length, Center to Red	(r_1)	102,519.2063 m.
Distance, Center to Reference	(r_4)	76,895.3482 m.
*Forward Azimuth, Center to Green	(α_g)	106°02'30".6077
*Forward Azimuth, Center to Red	(α_r)	242°20'57".6002
Angle between Baselines	(β)	136°18'26".9925
Beat Frequency, Green	(n_g)	135 cps
Beat Frequency, Red	(n_r)	315 cps
Green Station Frequency	(f_g)	2,440,315 cps
Center Station Frequency	(f_m)	2,440,180 cps
Red Station Frequency	(f_r)	2,439,865 cps
Free Space Velocity	(c)	$2.997925 \cdot 10^8$ mps
Yearly Average Index of Refraction	(n_o)	1.000363008
Green Bias Constant	(β_g)	969.427 lanes
Red Bias Constant	(β_r)	834.738 lanes
Lane Width (on baselines)	(W)	61.4060668 M.
Velocity of Propagation	(V)	299,683,712.4 mps
Pattern Monitor Corrected Computed Readings:		
Green Lane Count	(L_{gp})	270.340 lanes
Red Lane Count	(L_{rp})	1180.598 lanes

* Clockwise from South

Table 8.2-2

LORAC "B" NETWORK CONSTANTS

(CCD - 1964 Adjustment, Clarke 1866 Spheroid)

		ϕ	λ
Green Station: Eleuthera		25°15'57".74573	76°18'28".32273
Center Station: Great Stirrup Cay		25°49'32".30404	77°54'17".57420
Red Station: Middle Carter Cay		27°05'15".16028	78°00'44".76373
Reference Sta.:Marsh Harbor,Abaco		26°31'39".732	77°03'55".438
Pattern Monitor: Marsh Harbor, A.		26°31'36".660	77°03'55".399
Baseline Length, Center to Green	(r_3)		172,055.395 m.
Baseline Length, Center to Red	(r_1)		140,217.776 m.
Distance, Center to Reference	(r_4)		114,421.789 m.
*Forward Azimuth, Center to Green	(α_g)		290°46'20".130
*Forward Azimuth, Center to Red	(α_r)		175°38'11".999
Angle between Baselines	(β)		115°08'08".131
Beat Frequency, Green	(n_g)		135 cps
Beat Frequency, Red	(n_r)		315 cps
Green Station Frequency	(f_g)		2,100,135 cps
Center Station Frequency	(f_m)		2,100,000 cps
Red Station Frequency	(f_r)		2,099,685 cps
Free Space Velocity	(c)		$2.997925 \cdot 10^8$ mps
Yearly Average Index of Refraction	(n_o)		1.000363008
Green Bias Constant	(β_g)		1205.685 lanes
Red Bias Constant	(β_r)		982.533 lanes
Lane Width (on baselines)	(W)		71.3532649 m.
Velocity of Propagation	(V)		299,683,712.4 mps
Pattern Monitor Corrected Computed Readings:			
Green Lane Count	(L_{gp})		892.982 lanes
Red Lane Count	(L_{rp})		993.587 lanes

* Clockwise from South

$$L_{r_p} = \beta_r - \left[(r_{1p} - r_{2p}) f_m + (r_{4p} - r_{1p}) n_r \right] \frac{n_o}{c} \qquad (8.2\text{-}5)$$

where: $L_g = \beta_g$ is the green bias constant for the network in lanes

$L_r = \beta_r$ is the red bias constant for the network in lanes

r_1 is the distance from the red end station to the center station in meters

$r_2 = 0$

r_3 is the distance from the green end station to the center station in meters

r_4 is the distance from the reference station to the center station in meters

n_g is the green beat frequency in cps

n_r is the red beat frequency in cps

f_m is the master or center station frequency in cps

c is the free space velocity of electromagnetic radiation = 299,792,500 meters/sec.

L_{g_p} is the green lane count at a receiving point "p" in the network

L_{r_p} is the red lane count at point p in the network

r_{1p} is the distance from the red end station to point p in meters

r_{2p} is the distance from the master or center station to point p in meters

r_{3p} is the distance from the green end station to point p in meters

r_{4p} is the distance from the reference station to point p in meters (r_4 is the distance from the reference station to the center station)

As can be seen from equations (8.2-2) and (8.2-3), the green and red bias constants are directly affected by the index of refraction as the other factors are constant for a given complex configuration and set of operating frequencies. Thus, the β's should be determined for each LORAC operation based on the index of refraction of the test as obtained from the Eastern Test Range weather records. For the complete development of the LORAC equations the reader is referred to [SEISCOR, 1960],

8.2.2 Error Sources

Each of the LORAC position readings for a position fix contains some error which is composed of errors of varying magnitudes and signs introduced by propagational and instrumental parameters. The absolute value of the difference between the observed and true ground positions cannot be predicted for any given individual observation; however, the magnitude of the difference may be estimated as an expected or probable value which a certain percentage of the actual fixes do not exceed. The probable difference value is derived from many comparisons between observed and standard positions.

The velocity of propagation of electromagnetic radiation in space, $c = 2.997925 \cdot 10^8$ mps, presented in this report gives rise to an unknown constant error, since the true or absolute value of c is not known. This gives rise to a systematic distortion in the ground position fix accuracy which is small

according to the uncertainty of c, $\pm$ 200 mps, but indeterminate.

Systematic errors being the type of error whose magnitude can be calculated or measured may be either compensated out of the LORAC system or eliminated from observed data or charts by corrections and/or calibrations. In equation (8.2-4) the second term, $(r_{3p} - r_{2p})f_m$, is sometimes used to simplify computations. While the third term, $(r_{3p} - r_{4p})n_g$, is small numerically compared to the second term, its exclusion produces a systematic error between observed and computed lines of position that is a function of position. This systematic effect is called the third frequency error when neglected and the third frequency correction if it is applied.

The velocity of propagation, which appears in every term of the position equations, depends on the index of refraction which is in turn a function of air temperature, pressure, and water vapor content. Both systematic and random errors appear in the index of refraction — systematic in the sense that the parameters involved in its determination are capable of being measured and random in the sense that these parameters are a random function of time as well as a random function of position due to turbulence and other local effects in the transmission paths. Because of the finiteness with which the index of refraction measurements must be made in time and position to perfectly account for the refraction parameters, some random error exists from this source regardless of the density of the physical measurements. Fortunately, the effective velocity of propagation shows a relatively small actual variation since the index of refraction is a number very close to 1. The average value of the index of refraction, and thus the effective velocity of propagation, varies

seasonally through a well-defined cycle. From tests conducted in the "A" network it was determined that the monthly average value for the index of refraction is of sufficient accuracy where the slope of the index curve vs time is not steep. Otherwise a daily reading should be taken or the average value for that day obtained from the Eastern Test Range weather records. [SEISCOR, 1960], page 56, has a plotted curve of the index of refraction in both LORAC complexes for an average year.

The transmission of radio energy over the surface and by reflection from the earth's surface immediately involves the electrical conductivity and dielectric constant of the surface materials of the earth. The result of the nonlinear phase characteristic of the earth's atmosphere and surface with distance is that equations (8, 2-4, & 5) must be modified by a correction term called the phase distance correction. This correction accounts for the nonlinear accumulation of phase over the linear phase change along the two paths from the base line transmitters to the point of interest. If this effect is neglected, a systematic error will be experienced between observed and computed LORAC position coordinates which is relatively insensitive to time and atmospheric conditions. The computation of this correction is more involved than that for the other systematic effects, and it is also the most important correction to be made to the raw LORAC data as a first step to final position computation. The geometry of the position fix is quite important in determining the effect of this correction. The lane width which is a function of the expansion factor will determine the magnitude of the effect of the correction, since the correction is in lanes, in both lane counts. The intersection angle of the red and green

lanes at the position fix will then furnish the final information necessary to determine the diamond of error which demonstrates the error obtained should the phase distance correction be ignored. This effect can vary from a few feet to well over 100 feet, depending on the geometry of the position fix. Appendices II and III, [SEISCOR, 1960] , present the phase distance charts and field strengths and ground constants data for the "A" and "B" networks. The water and land distances traversed by the radio wave are obtained from map measurements after the azimuth and total distance between a transmitter site and the position fix have been determined by geodetic inverse computation. The scale of the maps used should not exceed 1:80,000 to obtain the best results.

The basic radio frequency of the system can be measured and thus changes in this variable may be included in the results as a systematic correction. Since the variation in the basic radio frequency is a random function of time, spot measurements of frequency only approximate the true variation and a residual random error is always present from this source. If the basic radio frequency is measured, then a good approximation to the systematic correction is usually possible, and the residual random error due to this source is reduced to a minimum. If a standard value of frequency is used, a much larger residual random error or random bias is possible.

Variation in the beat-frequency will produce systematic effects in the results; however, the error due to this source is usually quite small.

A systematic error will arise if all computation is done in one of the plane coordinate systems used to represent the

earth's surface in an area. The distances referred to in equations (8.2-2 to 5) are earth surface distances, and these distances must be used to prevent the plane coordinate system distance and true earth surface distance from emerging as a systematic error. This error has been observed to be as large as 300 feet in both of the lane counts.

Random errors arise from short-time changes in service conditions such as variable radiation parameters, variable propagation conditions, and errors in observations by the user of the system and are assumed to follow the Gaussian law of error.

Atmospheric noise falling in the selective channels of the LORAC receiver and the audio filtering channels produces momentary and random excursions of the position indicators. This particular source of random error tends to cause the magnitude of the overall system random error to increase with distance from the LORAC stations, or as the signal from the station decreases, the random error in a LORAC system tends to increase with a decreasing signal-to-noise ratio.

Another random error is the rounding off of the individual lane counts to the nearest one-hundredth of a lane. While this error is limited in magnitude, the actual magnitude and sign are random and unknown. This error, too, is dependent on the location of the position fix and thus the lane widths.

Of the error sources discussed, the third frequency, true earth surface distance versus plane coordinate distance, and the propagation of phase effects are truly systematic, and every effort should be made to eliminate their effect on the

position fix accuracy.

8.2.3 System Accuracies

8.2.3.1 "A" Network

OD040, "Evaluation of the LORAC "A" Network by the Calibration Checkpoint Method", June 1962, involved the occupying of thirteen survey points in the Little Bahama Bank by an amphibious vehicle equipped with a mobile receiver. The daytime observations coupled with weather data taken during the OD were reduced and analyzed to obtain the accuracy information shown in Table 8.2-3.

Since the deactivation of the uprange LORAC network, the "A" network is being utilized more extensively to cover LORAC demands in both the Cape and GBI areas. In March 1964 a test was conducted to determine the accuracy of the "A" network in the uprange recovery area. The results of that test are given in Table 8.2-4.

The figures in Table 8.2-3 should be utilized when operating in the Little Bahama Bank area while those in Table 8.2-4 are to be used in the vicinity of Cape Kennedy. The mean red and green lane count figures should be subtracted from the raw data before processing as they represent biases in the network. The green and red lane count σ's are to be used in the LORAC reduction routines to determine the dimensions and orientation of the error ellipse for each LORAC to geodetic conversion.

Table 8.2-3 Accuracy of the "A" Network in the Little Bahama Bank Area

	Green (lanes)	Red (lanes)	$\Delta\phi$ (ft.)	$\Delta\lambda$ (ft.)
Mean	0.000	0.022	3.41	-4.45
σ	0.025	0.052	17.55	16.14

Table 8.2-4 Accuracy of the "A" Network in the Uprange Recovery Area (Cape Kennedy Area)

	Green (lanes)	Red (lanes)	$\Delta\phi$ (ft.)	$\Delta\lambda$ (ft.)
Mean	-0.004	0.000	-7.26	-7.03
σ	0.016	0.010	38.81	35.09

8.2.3.2 "B" Network

The accuracy figures given in Table 8.2-5 were taken from [SEISCOR, 1960].

Table 8.2-5 Accuracy of the "B" Network

	Green (lanes)	Red (lanes)	R (ft.)
Mean	-0.026	-0.045	33.07
σ	0.067	0.038	16.01

where the mean R is the mean radial error of the checkpoints in the network.

8.3 INDEPENDENT SHIP NAV/STAB SYSTEMS

Although the MK-I and MK-IV SINS or the N7C can provide both position and attitude data, they are not used as an independent NAV/STAB system. Because of time dependent errors inherent to such systems, they have to be periodically updated using an external source of position and heading data. Such data are provided by star fixes from the Star Tracker or sonar fixes.

The main NAV/STAB system on the ARIS ships can be either:

MK-I (or MK-IV) and Star Tracker

MK-I (or MK-IV) and Sonar benchmark

N7C and LORAC net

A backup system will be an EM log used in conjunction with a MK-19 gyro-compass.

Whereas the three first systems mentioned are expected to yield accuracies comparable with the Range requirements and would therefore be used to process trajectory data in normal conditions, the back-up system would yield results with a much lower accuracy.

A lower accuracy yet would be obtained if, all other systems failing, the position of the ship was determined from celestial fixes made with a sextant.

A description of individual components of the NAV/STAB system follows:

8.3.1 The Sextant

8.3.1.1 System Description

The sextant is mainly listed here for completeness of the Navigation system components. It is not used for tracking data reduction.

8.3.1.2 Error Sources

The main sources of error are:

(a) Error in determining the horizontal plane

(b) Refraction errors

(c) Mechanical errors in the sextant itself and particularly index errors. (indexing of the mechanical scale)

8.3.2 Electromagnetic Log

The EM log provides the speed of the ship relative to the water and the distance traveled through the water.

8.3.2.1 System Description

The major parts of an EM log are:

(a) The rodmeter: a sensing device near its tip develops a signal voltage proportional to the speed of the ship with respect to the water. A simplified diagram of the sensing unit will be found in Figure 8.3-1.

(b) The sea valve which provides a water tight support through which the rodmeter protrudes.

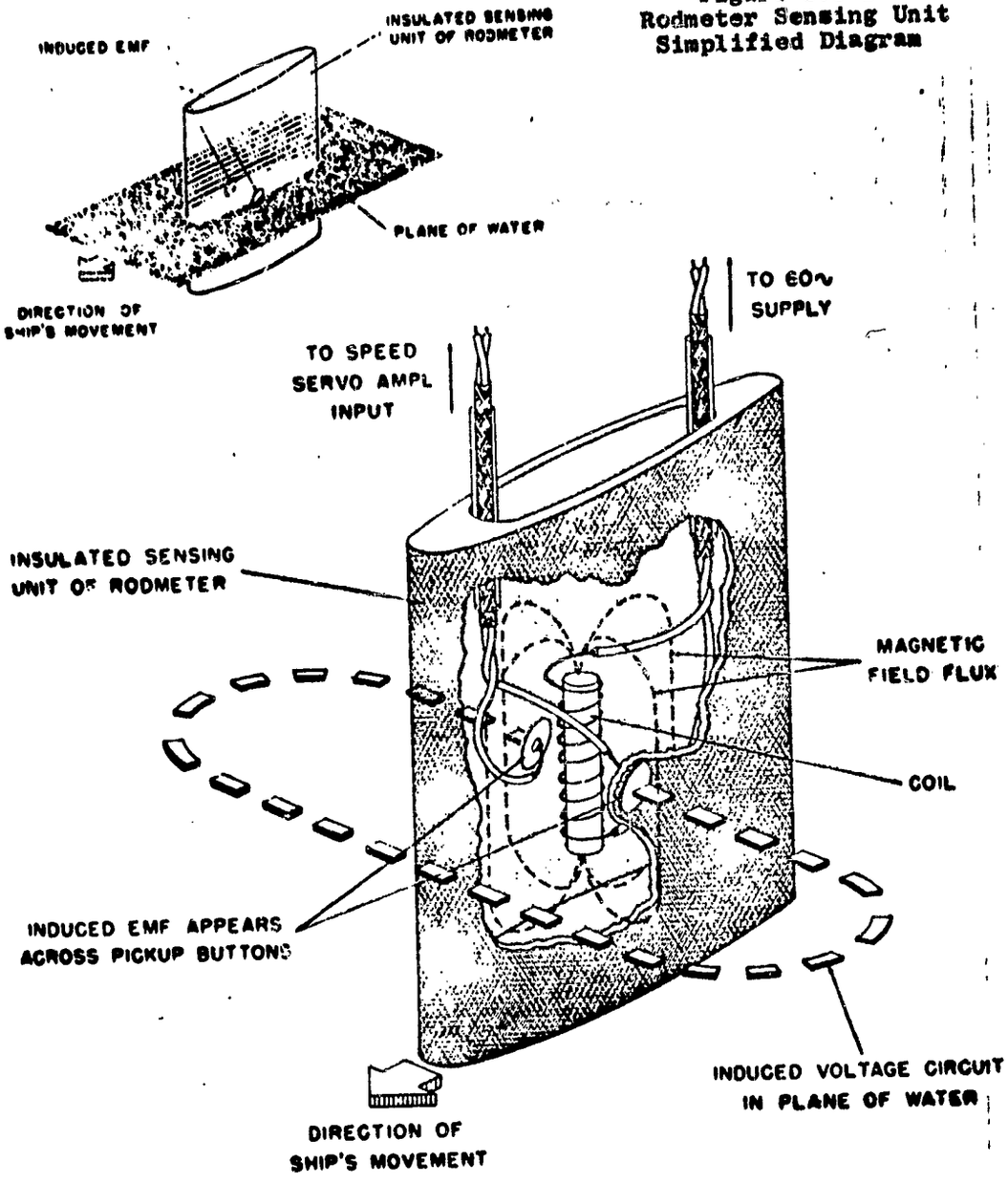


Figure 8.3-1
Rodmeter Sensing Unit
Simplified Diagram

(c) The indicator transmitter: a multistage amplifier receives the signal from the rodmeter. The output is ship's speed in knots which is displayed on a dial and, in the form of a synchro signal, is transmitted to other receivers on the ship.

8.3.2.2 Error Sources

The principle of the EM log is to measure the E.M.F. induced in a conductor (ocean saline water) by its relative motion with respect to a magnetic field created by the coil in the rodmeter. (See Figure 8.3-1).

The largest error sources are therefore

(a) The voltage induced by ship's motion is affected by the flow characteristic of the water past the rodmeter (laminar or turbulent). The flow can be modified by disturbances created by the hull.

(b) The speed which is measured is that in a plane perpendicular to the magnetic field line at the location of the pickup buttons. The actual speed measured will therefore be a combination of the translational motion of the ship and its rotational motion around its center of rotation. Unless the center of rotation of the ship and its relative distances to the attitude sensing device and the EM log are known, it is not possible to separate the various velocity components.

(c) The speed is measured with respect to the water: water current and sea state should be taken into account. If no independent measurement of such motion is available, the velocity of the ship with respect to Earth fixed coordinates cannot be obtained.

(d) Transverse velocity components are not measured since there is only one set of pickup buttons.

(e) Additional errors due to the electric circuit and mechanical integrator are of a small order of magnitude compared to the preceding.

Because most of the errors described in (a) through (d) cannot be reduced without the use of external equipment, the EM log is used only as a back-up device and provides the rough source of velocity information necessary for stabilizing the inertial platforms.

8.3.3 N7C

All information concerning the N7C inertial navigator is classified.

8.3.4 MK-19 Gyro-compass

The MK-19 gyro-compass furnishes heading, pitch and roll data. This information is available in the event of a SINS failure. Heading information is also applied to the SINS during initial alignment to insure that the SINS heading be within $\pm 6''$ of true North before the SINS gyros take control of the stable platform.

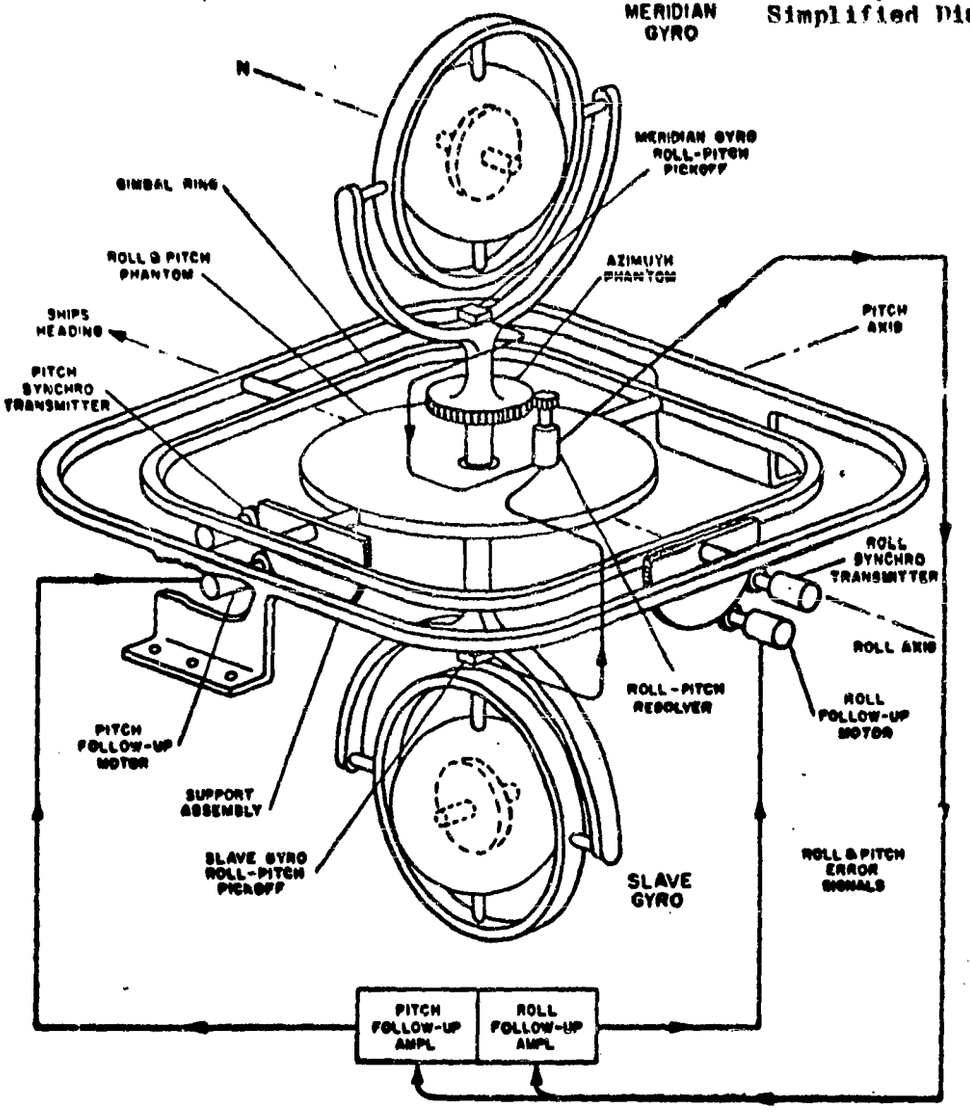
8.3.4.1 System Description

The MK-19 consists of two major units.

(a) The master compass - it contains the sensitive elements, gimbal system, gears and synchro transmitter which supply the attitude information.

A simplified diagram of the MK-19 will be found in Figure 8.3-2. It includes a North seeking Meridian gyro which furnishes azimuth data and tilts about the East West axis. A second gyro slaved

Figure 8.3-1
MK-19 Gyro Compass
Simplified Diagram



to the Meridian gyro so that their spin axes are orthogonal, measures tilts about the North South axis. Two follow up systems are incorporated in the MK-19. The azimuth follow up system keeps the azimuth phantom and the vertical ring aligned in azimuth with the gyro. The roll and pitch follow up system controls the roll and pitch phantom in a horizontal plane and enable roll and pitch data to be sensed by synchro transmitters.

(b) The control cabinet contains the electronics required for operating and indicating the condition of the gyro-compass.

8.3.4.2 Error Sources

The main source of errors for a gyro-compass is error torques. These can be produced by a number of causes such as

(a) Mass unbalance

(b) Buoyance unbalance

(c) Temperature gradients in the flotation fluid

(d) Anisoelasticity

Other possible sources of errors are:

(e) Initial azimuth error

(f) Follow up servo errors

Since the MK-I and MK-IV SINS as well as the N7C are also attitude sensing devices and are built to yield a greater accuracy then the MK-19, calibration and error analysis of the MK-19 as well as the EM log will be performed after completion of the inertial platform evaluations.

8.3.5 MK-I SINS

The MK-I SINS is a semi-geometric inertial navigator. The

outputs are latitude, longitude, roll, pitch and heading.

8.3.5.1 System Description

The system consists of a four gimbal binnac., a navigation readout console and a power supply/power amplifier console.

The gimbals in order are: latitude (inner gimbal), azimuth, pitch and roll.

Three gyros* are mounted on the latitude gimbal. Their axes are parallel to the Earth's polar axis, the intersection of the Meridian plane where the SINS is located, and the equatorial plane; the third gyro's axis is perpendicular to the two others.

The accelerometers are mounted on the azimuth gimbal and sense North-South and East-West accelerations.

Roll, pitch and heading axes are fixed with respect to the ship. The outputs of the gyros are therefore resolved about latitude and heading to transform gyro-input coordinates to ship's coordinates, and drive the gimbals so as to isolate the latitude gimbal from ship's motion.

8.3.5.2 Error Sources

Sources of errors in an inertial platform can be separated into five distinct groups:

(a) Servo loop errors:

Mechanical resonances at frequencies close to the frequency response of the servo amplifiers.

Saturation: This can produce effective lags in the servo loop if it takes place ahead of the compensation network.

*Single degree of freedom.

Saturation of the torqueing device: the result of such an occurrence is a reduction in effective loop gain which produces a reduction in stiffness and may lead to instability.

(b) Gyro errors

These were described for the MK-19.

(c) Accelerometer errors

Errors in spring constant and mass will lead to scale factor errors. Mechanical friction is reduced in a floating accelerometer but biases can appear.

(d) Integrated system errors

Disturbing torques can be applied to the system due to overall unbalance or anisoelasticity. Bearing and slip ring friction is another possible source of disturbing torques.

Non-orthogonality between the gyro output axes, platform flexibility, structural changes with time due to stress relief are other possible sources of errors.

Initial errors in platform erection and alignment are another large source of error.

(e) The last source of error which will be mentioned is the approximations in the mechanization of the system equations and the computational errors.

8.3.6 MK-IV SINS

The MK-IV is an analytical inertial navigator whose outputs are latitude, longitude, ground speed and attitude.

8.3.6.1 System Description

The system consists of a three gimbal assembly and a multi-moded computer which provides platform control, pre-navigation

platform alignment and continuous solution of the navigation problem.

The stable platform is mounted on the azimuth gimbal (inner gimbal). Three gyros and three accelerometers are mounted on the platform in an orthogonal setup. A monitor assembly containing an additional gyro and an additional accelerometer is mounted on the platform also but is free to rotate relative to it. The Z axis is parallel to the azimuth rotation axis; the X and Y axes are directed North and East respectively.

The platform is gimballed outward in the order of azimuth, pitch and roll. Gyros and gimbals operate in closed servo loops to isolate the stable platform from ship's motion. Moreover the gyros are torqued with the components of Earth's rate to maintain the platform locally level.

A simplified diagram of the MK-IV will be found in Figure 8.3-3.

8.3.6.2 Error Sources

The error sources are the same as those described for the MK-I.

8.3.7 Star Tracker

The Star Tracker is a high accuracy electro optical detection and control system which is used to update the SINS.

8.3.7.1 System Description

The Star Tracker is a two axis system: a simplified diagram will be found in Figure 8.3-4.

When designated within 15 arc minutes of a star, either manually or by computer inputs, it has the capability of

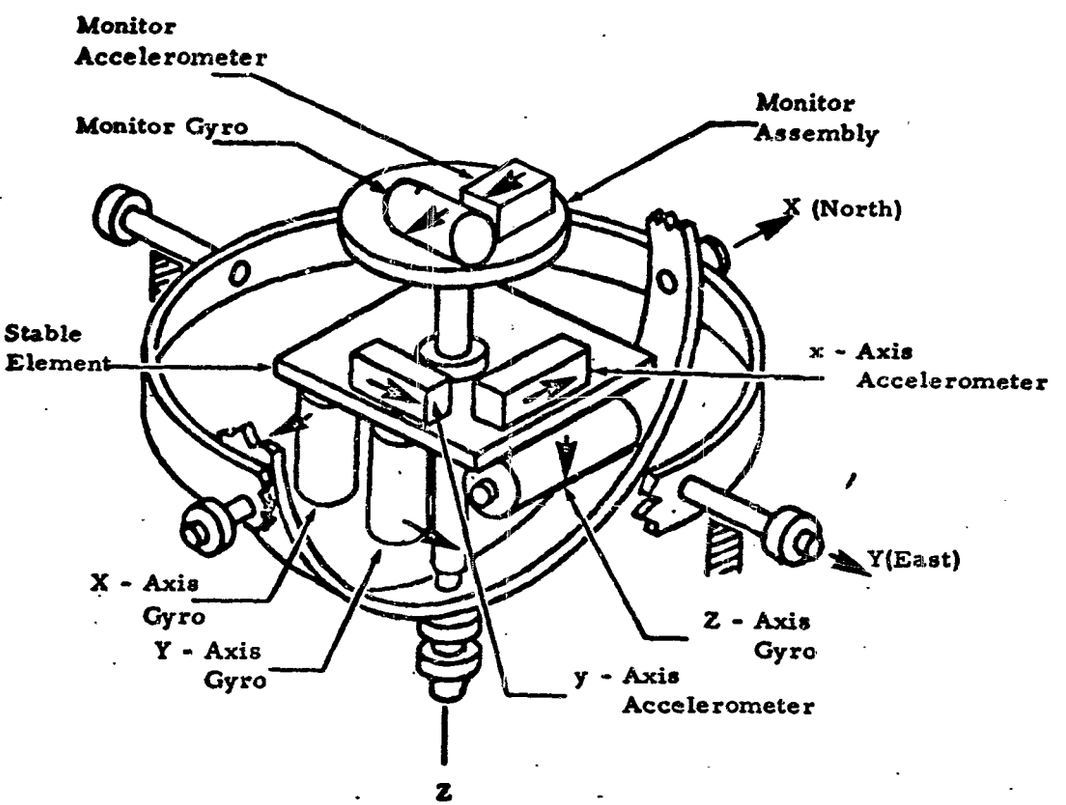
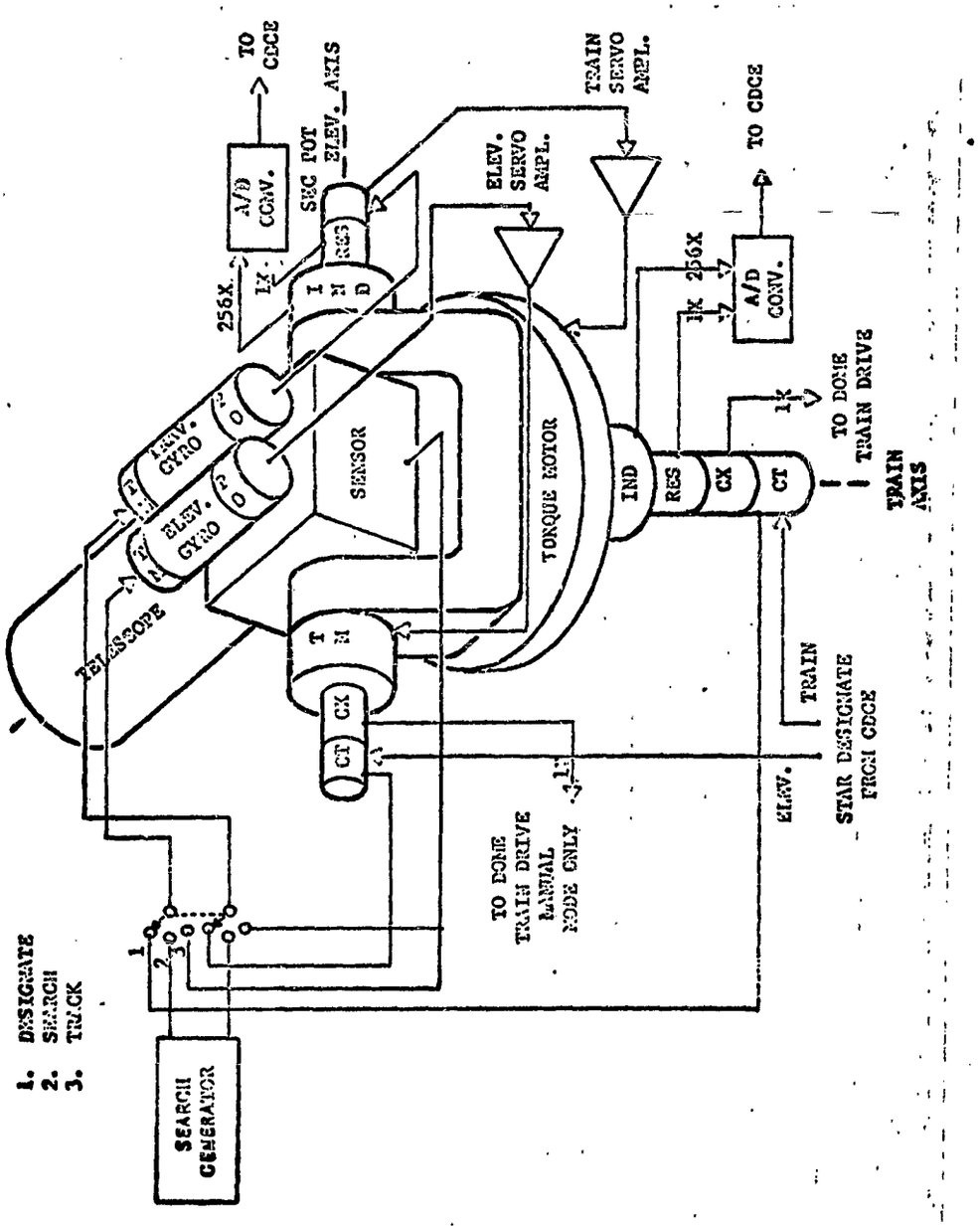


Figure 8.3-3
Stable Platform
SINS MK IV

Figure 8.3-4
Star Tracker
Diagram



automatically acquiring and tracking the star.

8.3.7.2 Error Sources

The sources of error in the Star Tracker output are:

(a) Optical: refraction, lens distortion, lens bend, collimation errors

(b) Servo errors

(c) Gyro disturbance torques

(d) Non-orthogonalities between elevation axis and optical line of sight; or between elevation and train axes

(e) Misalignment between Star Tracker axis and deck axis as defined by the SINS.

(f) Non-coincidence between the train or elevation zero and a zero output angle (zero set error).

(g) Computational errors

8.3.8 Sonar Benchmarking Equipment

8.3.8.1 System Description

This equipment includes a Precision Depth Recorder (PDR), a sonar sounding set (AN/UQN-1), and two or more bottom transponders.

The PDR and sonar sounding set are used to locate an area suitable for beacon sowing. When the beacons have been sown, the sonar set is used to record the depth range from the ship to the beacon. Using SINS-Star Tracker data a survey of the beacons is done. In sonar Fix mode, the range to the beacon is used to compute a correction to the SINS position.

8.3.8.2 Error Sources

SINS and Star Tracker errors lead to survey errors in beacon location. Since the sonar system measures a range from a transponder on the ocean floor to the sonar transducer on the ship, survey errors on the ship itself (sonar transducer to SINS position) will introduce additional errors; similarly tidal changes or variations in the ship's draft will cause changes in the vertical distance between transponder and transducer.

The system equations make use of these vertical distances as determined during the beacon survey period. Moreover a constant velocity of sound in the ocean is assumed, as well as a straight line propagation. The propagation medium characteristics are therefore another source of error (inhomogeneity of the ocean water, unstable surface, etc.)

Erroneous beacon delay time will also reflect into a position error.

8.3.9 Methods of Accuracy Determination

Until further experience is gained on the very complex total Navigation subsystem, calibration, error model terms and residual error determination have been confined to the main Navigation components.

All information on the N7C is classified. The following discussion will therefore be limited to the MK-I or MK-IV and the Star Tracker. As was explained in 8.3.8.2 the main errors in sonar navigation come from survey errors due to the SINS and/or Star Tracker.

8.3.9.1 Calibration

Typical error analysis for Inertial Guidance systems can be

found in various books on Inertial Guidance [Pitman, 1962].

Let us define the following quantities:

- $\vec{\psi}$: vectorial representation of the angular deviation between platform axes and computer axes
- $\vec{\omega}$: vectorial representation of the angular rate between platform coordinates and inertial space
- $\vec{\epsilon}$: vectorial representation of the gyros' drift rate
- ϕ: latitude (geodetic)
- λ: longitude
- H: ship's heading
- x,y,z: coordinate system with x North, y East; z forms a right handed orthogonal system with x and y (geodetic vertical)

A dot or double dot over a quantity indicates first or second time derivative.

Then:

$$\dot{\vec{\psi}} + \vec{\omega} \times \vec{\psi} = \vec{\epsilon}$$

In the case of the MK-I or MK-IV, $\vec{\omega}$ is the Earth's rotation vector $\vec{\Omega}$. The gyros' drifts are however unknown. The most commonly considered drift is a constant drift $\vec{\epsilon}$ but time varying components may exist. This precludes any calibration valid over a long period of time.

The equation shows however that the angle error will include a 24 hour oscillatory component and a linear time dependent component.

The general form of the position error equation in a tangent plane coordinate system is:

$$\ddot{\Delta R} + 2\vec{\Omega} \times \dot{\Delta R} + \vec{g}(R) - \vec{g}(R + \Delta R) = \delta\vec{A} - \vec{\psi} \times \vec{A}$$

where

$\vec{R}$	position vector
$\vec{\Delta R}$	position error vector
$\vec{A}$	acceleration vector
$\vec{g}(R)$	gravity vector
$\delta\vec{A}$	accelerometers' error vector

For the ship-borne systems the gravity term can be reduced to

$$\frac{g(R)}{R}\left[\vec{\Delta R} - \frac{\vec{\Delta R}.\vec{R}}{R^2}\vec{R}\right]$$

The above expressions show that two time constants will appear in the position error.

One is the earth's rate Ω (24 hour period), the other the Schuler frequency $\sqrt{\frac{g(R)}{R}}$ (84.4 mn period). It should be remembered that $\vec{\psi}$ has an oscillatory component of frequency $2\pi\Omega$.

For shipborne inertial platforms some simplifying hypotheses can be made [Pitman, 1962]. As an example assuming a quasi stationary position, and constant gyro drifts, the angle error equations can be integrated. The contribution of the angle error to the position error is also found. The results are as follows:

$$\psi_x = -\Delta\lambda \cos\phi = -\sin\phi\left\{\left(\frac{\epsilon_z}{\Omega}\cos\phi - \frac{\epsilon_x}{\Omega}\sin\phi\right)\sin\Omega t + \left(\psi_{zo}\cos\phi + \frac{\epsilon_y}{\Omega}\right)\cos\Omega t - \left(\psi_{zo}\cos\phi + \frac{\epsilon_y}{\Omega}\right) - \cot\psi\left(\frac{\epsilon_z}{\Omega}\sin\phi + \frac{\epsilon_x}{\Omega}\cos\phi\right)t\right\}$$

$$\psi_y = \Delta\phi = -\left\{\left(\psi_{zo}\cos\phi + \frac{\epsilon_y}{\Omega}\right)\sin\Omega t - \left(\frac{\epsilon_z}{\Omega}\cos\phi - \frac{\epsilon_z}{\Omega}\sin\phi\right)\cos\Omega t + \left(\frac{\epsilon_z}{\Omega}\cos\phi - \frac{\epsilon_x}{\Omega}\sin\phi\right)\right\}$$

$$\psi_z - \psi_x \tan\phi = \Delta H = \sec\phi\left\{\left(\psi_{zo}\cos\phi + \frac{\epsilon_y}{\Omega}\right)\cos\Omega t + \left(\frac{\epsilon_z}{\Omega}\cos\phi - \frac{\epsilon_x}{\Omega}\sin\phi\right)\sin\Omega t - \frac{\epsilon_y}{\Omega}\right\}$$

Figure 8.3-5 shows that the above equations, although derived using simplifying hypotheses, are a good approximation to the ARIS' inertial platform performance.

Figure 8.3-5
Latitude Error

Shape of the Latitude error versus time
The main component is a 24 hr. oscillation

However the position error equation shows that oscillations near the Schuler frequency and other time dependent functions, depending on the nature of the gyros' drifts and accelerometer errors, should be expected.

Since the output of the ship-borne radars are deck bearing, deck elevation and range, attitude information as well as position are necessary. The 24 hour oscillation which appears in both attitude and position error has proved to be a major contributor to trajectory data error. The main calibration consists therefore in determining the components of this oscillation. The calibration equations which are used are

$$\Delta\phi = \alpha \cos \Omega t + \beta \sin \Omega t + \mu$$

$$\Delta\lambda = -\alpha \tan\phi \sin \Omega t + \beta \tan \psi \cos \Omega t + \beta t$$

$$\Delta H = -\alpha \frac{\sin \Omega t}{\cos \phi} + \beta \frac{\cos \Omega t}{\cos \phi} + \nu$$

The coefficients are obtained by a least squares adjustment of data collected prior to a test.

8.3.9.2 Error Model

Other sources of error are amenable to long term correction. These are particularly the SINS initial vertical tilts. If $\delta\zeta$ is the North tilt and $\delta\eta$ the East tilt, the data should be corrected as follows

$$\delta(\text{Roll}) = \delta\zeta \sin H - \delta\eta \cos H$$

$$\delta(\text{Pitch}) = \delta\zeta \cos H + \delta\eta \sin H$$

$$\delta\phi = -\delta\zeta$$

$$\delta\lambda = -\delta\eta \sec\phi$$

In order to determine these tilts stabilized Star Tracker data are compared to ephemeris angles. The error model used will therefore include Star Tracker errors. Since the actual experiments are conducted in almost static conditions, all dynamic terms are suppressed from the equations. Physical misalignment and non-orthogonalities are the only quantities which are attempted to be determined. The list of error sources given with each component shows however that other terms will eventually have to be included.

The error model used at the present time is:

$$\Delta E = -\delta E_b + \delta\zeta \cos A + \delta\eta \sin A - \delta L \sin B - \delta A \cos B$$

$$\Delta A = -\delta B_b + (\delta\zeta \sin A - \delta\eta \cos A) \tan E + (\delta L \cos B - \delta A \sin B) \tan E - \delta\theta \sec E - \delta\beta \tan E$$

where

ΔE and ΔA are differences between Star Tracker stable elevation and azimuth to a star and the corresponding ephemeris angles.

δE_b and δB_b are readout devices zero errors

$\delta\zeta$ and $\delta\eta$ have been defined previously

δL and δA are misalignments between the Star Tracker and SINS

$\delta\theta$ and $\delta\beta$ are non-orthogonalities between the elevation axis and the Star Tracker line of sight, and train axis respectively.

A and E are the true star azimuth and elevation.

B is the star deck bearing (B = A - H where H is the heading).

The error model coefficients are determined by a least squares adjustment of experimental data to the equations above.

8.3.9.3 Accuracy Determination

The navigation subsystem accuracy is determined by comparing the corrected SINS position to reference data.

The reference data used are LORAC data. Estimates of the mean and standard deviation of position error in latitude, longitude are obtained.

The latitude and longitude data are assumed uncorrelated; moreover no time correlation is taken into account

If N measurements are available, the following quantities are estimated

$$\overline{\Delta\lambda} = \frac{\Sigma\Delta\lambda}{N}$$

$$\overline{\Delta\phi} = \frac{\Sigma\Delta\phi}{N}$$

$$s^2_{R\Delta\lambda} = \frac{\Sigma\Delta\lambda^2 - N\overline{\Delta\lambda}^2}{N - 1}$$

$$s^2_{R\Delta\phi} = \frac{\Sigma\Delta\phi^2 - N\overline{\Delta\phi}^2}{N - 1}$$

No independent reference data are available for attitude data accuracy computation. The procedure used at present consists in comparing SINS heading with the heading obtained from Star Tracks in the following way.

The Star Tracker tracks two stars to obtain a correction to the SINS latitude and longitude. Using this corrected position, the azimuth of one star is obtained from the ephemeris tables and the difference between this value and the star stable (pitch and roll corrected) deck bearing yields a value of ship's heading.

As can be seen the heading differences computed in this manner contain residual Star Tracker errors and include roll and pitch errors.

8.3.10 Calibration Experiments

The data used in conjunction with the error model described in 8.3.9.2 are gathered with the ship at dockside, that is, at a known location.

Prior to such a test the SINS latitude output is monitored for approximately 3 hours to obtain the coefficients of the 24 hour oscillation. This is subsequently used to correct the heading data oscillatory component.

The position of the ship being known, the azimuth and elevation of a given star can be computed using ephemeris tables.

The Star Tracker data are stabilized using the SINS pitch and roll information and the star azimuth is computed by adding the SINS heading and heading correction to the stable Star Tracker bearing. One thousand two hundred and fifty data points are gathered on each star, extrapolated back to the first datum point time and averaged.

This value is then compared to the ephemeris value.

Referring to the 24 hour oscillation equations of 8.3.9.1 it can be seen that at dockside, monitoring SINS latitude and longitude will yield the coefficients of the heading oscillation but can give no information on the heading bias. This will be included in the term δB_b of the azimuth static error model (8.3.9.2).

In at-sea conditions the error model coefficients determined from dockside tests are used to partially correct the data. Star fixes or sonar fixes where available can be used to find corrections to SINS latitude and longitude independent of the heading error. This provides the information necessary for determining the 24 hour oscillation in position. Assuming normally distributed error, a by-product of the least squares adjustment will be an estimate of the variance of SINS corrected position with respect to Star Tracker or sonar position.

During evaluation tests the ship navigates in the Lorac net. Assuming Lorac as a standard, SINS position, corrected as described above, is compared to Lorac position to yield SINS position accuracy.

8.3.11 System Accuracies

Although evaluations of all previously described Navigation System components are planned, the only systems which have been the object of extensive analysis are the MK-I and IV SINS and the Star Tracker.

Nominal (not confirmed) values for the other components are

as follows:

Sextant:	position error:	2 miles
EM log:	relative velocity error:	1.4 knots
MK-19:	heading error:	6 minutes
	pitch and roll error:	4 minutes
Sonar:	position bias error:	140 feet
	random noise:	12 feet

Star Tracker errors listed below are residual errors from the least square adjustment of the SINS - Star Tracker error model. They are therefore a combination of SINS attitude and Star Tracker error. The significance of these results will appear from the following description of trajectory data processing.

Radar data are transformed to ship's coordinate system using flexure monitor outputs and radar to Star Tracker error model. The data are then transformed to SINS stable platform using SINS attitude and Star Tracker to SINS error model. Finally SINS corrected position is used to reference the data to an Earth fixed system. Star Tracker errors and SINS attitude errors are therefore not separated in trajectory data reductions. The figures given below are a measure of the error that will influence trajectory data.

Dockside evaluation experiments have been conducted for the General Arnold in July and August 1964. The results given below reflect the results of this evaluation. However these values should only be considered as an indication of the system performance since modifications to the MK-I have been made since then. The main effort having been devoted to determining the error model coefficients, no estimate of individual test residual biases (after correction by the best estimate of the coefficients from all available data) has been made. After re-evaluation of the error model for

the modified system, a detailed analysis of errors will be made to provide values of residual bias (if any), bias uncertainty and random noise. Data from the General Vandenberg are being analyzed at the present time.

Residual errors from SINS to Star Tracker error model regression analysis were as follows

Elevation: 7 seconds of arc
Azimuth: 20.6 seconds of arc

Trajectory data will also be influenced by the SINS position error. Latitude and longitude errors were determined from tests as described in 8.3.10. The following remarks apply to the data given below:

(a) Because of the insufficient number of successful evaluation tests no estimate of the bias variation is available. The only available data are a value for the bias and the variation of the data about that bias.

(b) It is expected that the MK-I performance is better than the values given would indicate. This is due to the fact that one of the accelerometers had been changed between the dockside tests and the at-sea tests. Consequently the misalignment corrections were not applied to the data used to determine position error.

The position errors are as follows:

	Latitude Differences		Longitude Differences	
	Mean	Variance about Mean	Mean	Variance about Mean
MK-I	.5 nm	.9 nm	2.0 nm	1.0 nm
MK-IV	.16 nm	.22 nm	.05 nm	.19 nm

9.0 SIGNATURE SYSTEMS

9.1 Procedure for Determining System Accuracies

9.1.1 Introduction

Radar Signature Systems are intended for the collection and recording of echo signal strengths for determination of size and shape of a target in terms of its radar reflectivity or apparent cross section at specific frequencies. The signature data collection systems of the Eastern Test Range are the ships, General H. H. Arnold (ARIS I), General H. A. Vandenberg (ARIS II), American Mariner and land based radar at Trinidad, BWI. Each of these systems is capable of collecting pulse-by-pulse echo signal strength recordings in terms of some but not all of the following variations in mode of operation:

(a) Multiple secondary targets

(b) Transmit on vertical, horizontal and circular polarization.

(c) Receive on vertical, horizontal and circular polarization.

(d) Frequencies in C, L, X and UHF bands.

Radar cross section is the ratio of the RF energy reflected from an unknown target to the RF energy reflected from a standard target of known dimensions and reflectivity when both are illuminated by the same (or equivalent) RF field. Since the reflected energy must be measured at the radar the transmission characteristics of the intervening medium must be known and calibration of the standard target echo must be correlated for possible changes in transmitted power, receiver gain, radar range, antenna characteristics, frequency, range

and angular off-set from beam axis.

9.1.2 Radar Equation

The measurable parameters are arranged into the basic radar equation:

$$S = \overbrace{\left(\frac{P_t G}{4\pi R^2}\right)}^{(a)} \overbrace{\left(\frac{A_e}{4\pi R^2}\right)}^{(b)} \overbrace{\left(\frac{G\lambda^2}{4\pi}\right)}^{(c)}$$

where

- S = Power detected at receiver input
- R = Radar range (distance to target)
- G = Power gain ratio of transmit/receive antenna
- λ = Wavelength of transmitted signal
- P_t = Transmitted signal power
- A_e = Target cross section area*

*NOTE: Another symbol for radar cross section is σ but its use has been avoided in this document to avoid confusion with the symbol for standard deviation.

The right-hand side of the equation may be recognized as the power density at the target (a), the reflected power density at the antenna (b), and the antenna aperture (c).

Power detected by the receiver is subject to losses within the transmitter and receiver chains, and atmospheric losses

along the ray path. The expression may be rewritten to include these effects, as follows:

$$S = \underbrace{\left(\frac{P_t G}{4\pi R^2}\right) L_t L_a}_{\text{Power Density Reaching Target}} \times \underbrace{\left(\frac{A_e}{4\pi R^2}\right) L_a}_{\text{Power Density Returned to Antenna}} \times \underbrace{\left(\frac{G\lambda^2}{4\pi}\right) L_r}_{\text{Power Detected by Receiver}}$$

where L_a = one-way losses due to atmospheric attenuation,

L_t = transmitter losses, and

L_r = receiver losses.

This gives:

$$S = \frac{A_e L_a^2}{R^4} \left[\frac{P_t G^2 \lambda^2 L_t L_r}{(4\pi)^3}\right]$$

The terms within the brackets are independent of the target

being observed, and may be considered constant during a mission, or:

$$C = \left[\frac{P_{t_{ref}} G^2 \lambda^2 L_t L_r}{(4\pi)^3} \right]$$

where $P_{t_{ref}}$ = reference transmitter power at the time of calibration.

The expression for measurement of cross section of an unknown target becomes:

$$A_e = \frac{1}{C} \frac{SR^4}{L_a^2}$$

Specific radar instrumentation characteristics may introduce additional corrective terms to the equation above. For example, it may be desirable to change the transmitter power level between the time of calibration of C and time of the mission; this introduces a correction factor ρ, as follows:

$$\rho = \frac{\text{Reference transmitter power during calibration}}{\text{Transmitter power during mission}}$$

If the receiver chain includes variable attenuation to optimize the magnitude of the detected signal for tracking purposes, a term (α) must be included to correct the value of S for the attenuation factor.

Further, if the observed target departs significantly from the axis of the radar beam, the effective antenna gain will be reduced; a correction factor (θ) must be applied for this attenuation of the signal.

Incorporating these refinements yields:

$$A_e = \frac{1}{C} \frac{SR^4}{L_a^2} \quad \rho \propto \theta$$

The computations are conventionally carried out in logarithmic form to yield target cross section in db relative to a one square meter reference (dbsm), thus:

$$A_e(\text{dbsm}) = 10 \log S + 40 \log R + 10 \log \rho + 10 \log \propto + 10 \log \theta$$

$$- 10 \log C - 20 \log L_a$$

The variables in the above equation are determined by calibrating the radar against a balloon-borne standard spherical target prior to and following each data gathering mission.

9.1.3 Calibration

Measurement of R is accomplished by the conventional means in mono-pulse radars. Atmospheric losses may be computed from known attenuation characteristics when suitable meteorological observations are available. The power monitor

may be calibrated by means of a precision calorimetric water load so that ρ is determinable. The receiver response and IF attenuators are calibrated against a standard signal generator so that S becomes known in terms of IF attenuation, α, and receiver output (counts of the digitized voltage at the second detector). A balloon-borne standard target sphere and boresight camera are utilized to determine the value of C and the characteristics of θ. Figure 9.1-1 illustrates the factors influencing calibration.

The receiver response is linear-logarithmic over a dynamic range of about 50 db between noise level and saturation level. Fixed attenuation from 0 to 64 db in 8 db steps is switched in or out by the operator to keep the received signal within this dynamic range. The receiver calibration is accomplished as follows, using a standard signal generator to supply a test signal to the receiver input, the input signal level is varied through the full receiver range from the saturation to noise, noting the RF test signal attenuation level at each stop. This is repeated for each of the eight available IF attenuator settings of 8 db increments. Digitized signal strength data are recorded, and following the calibration the data may be plotted as a family of curves of receiver output versus RF input signal with IF attenuation as a parameter (see Figure 9.1-2). The data may be rearranged by plotting the receiver output versus total attenuation (RF signal attenuation + IF attenuation), as shown in Figure 9.1-3. The resultant curve permits conversion of digitized receiver output (in counts) to relative signal level in db, and further provides a check on the precision of the attenuators by comparing one with the other. If the curves of Figure 9.1-2 do not exactly superpose when rearranged as in Figure 9.1-3 one of the two attenuators would be suspect and equipment troubleshooting would be

Figure 9.1-1

BALLOON-BORNE STANDARD TARGET SPHERE CALIBRATION

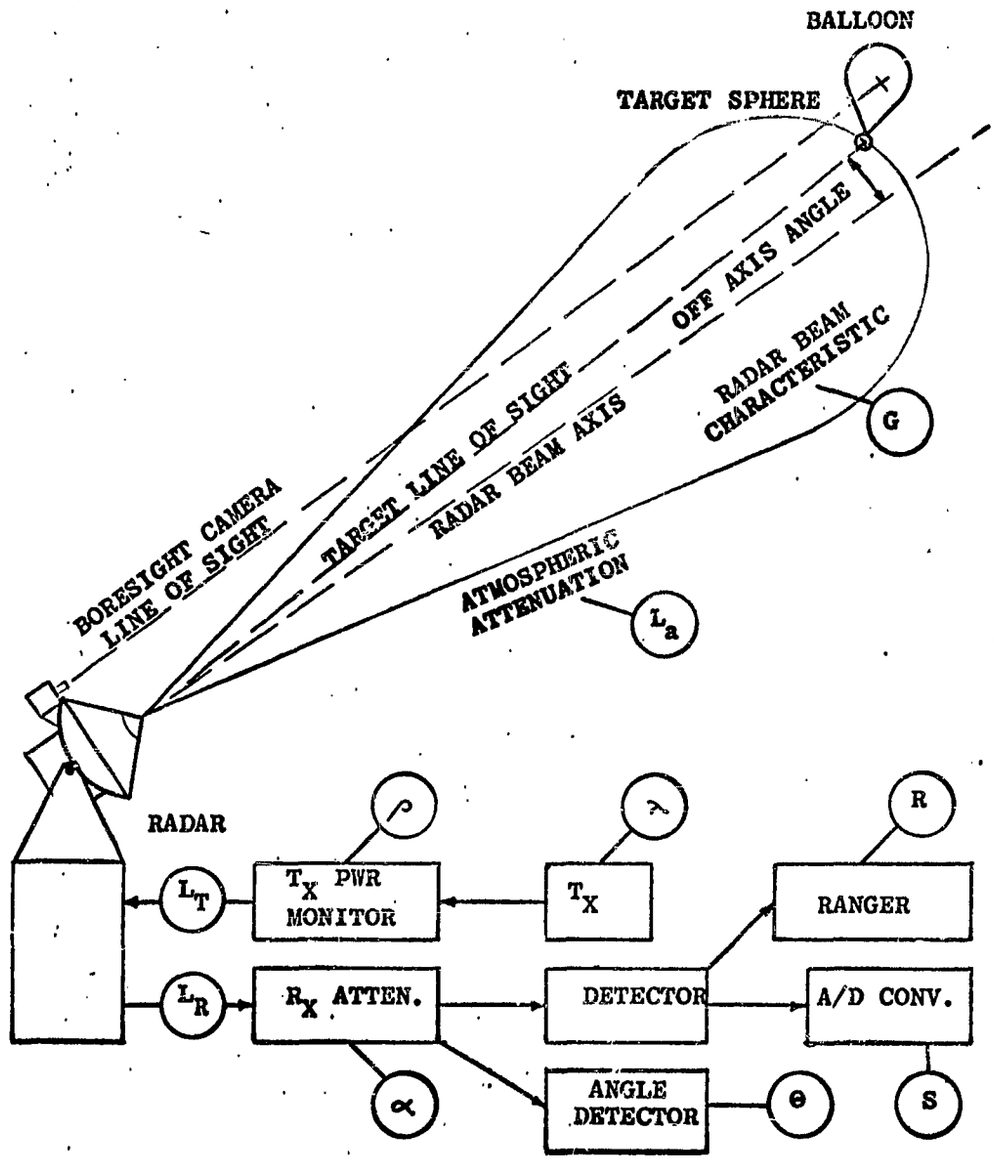


Figure 9.1-2

RECEIVER GAIN/ATTENUATION CHARACTERISTIC

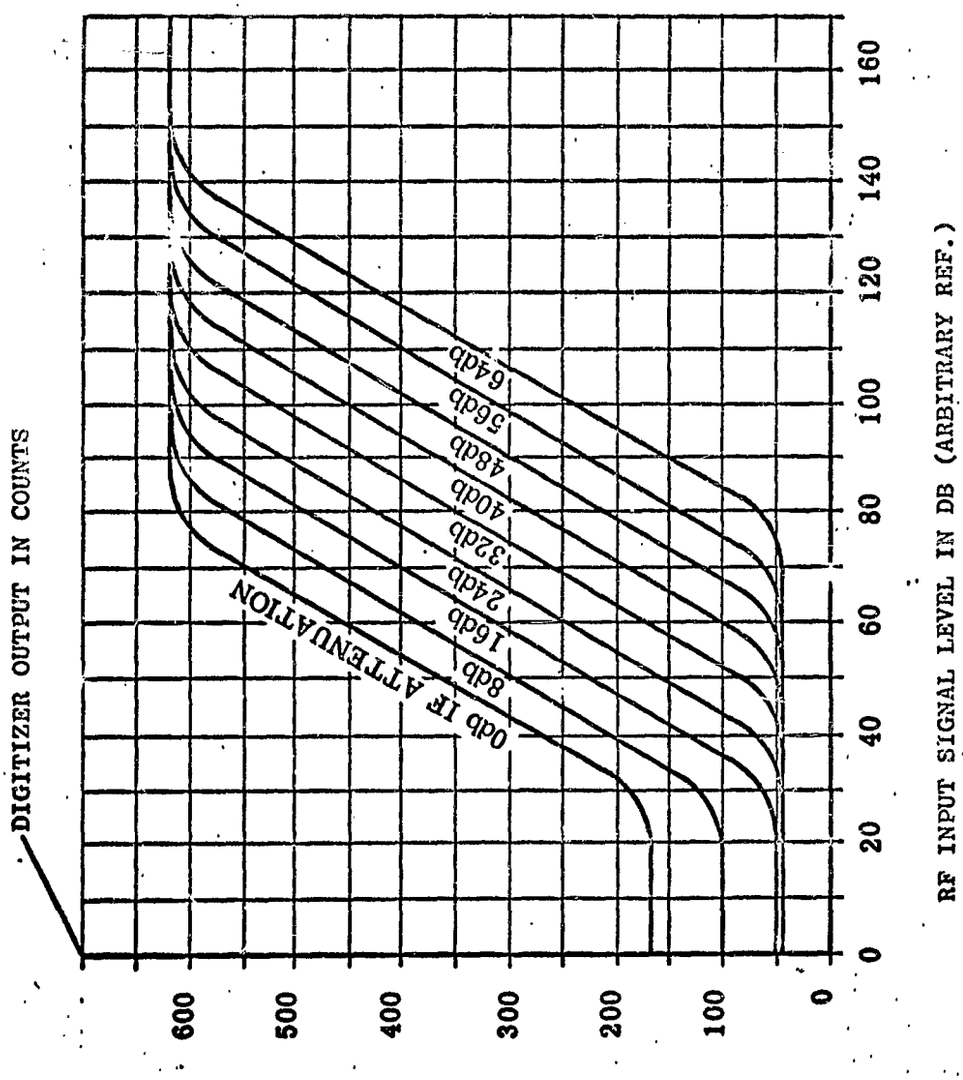
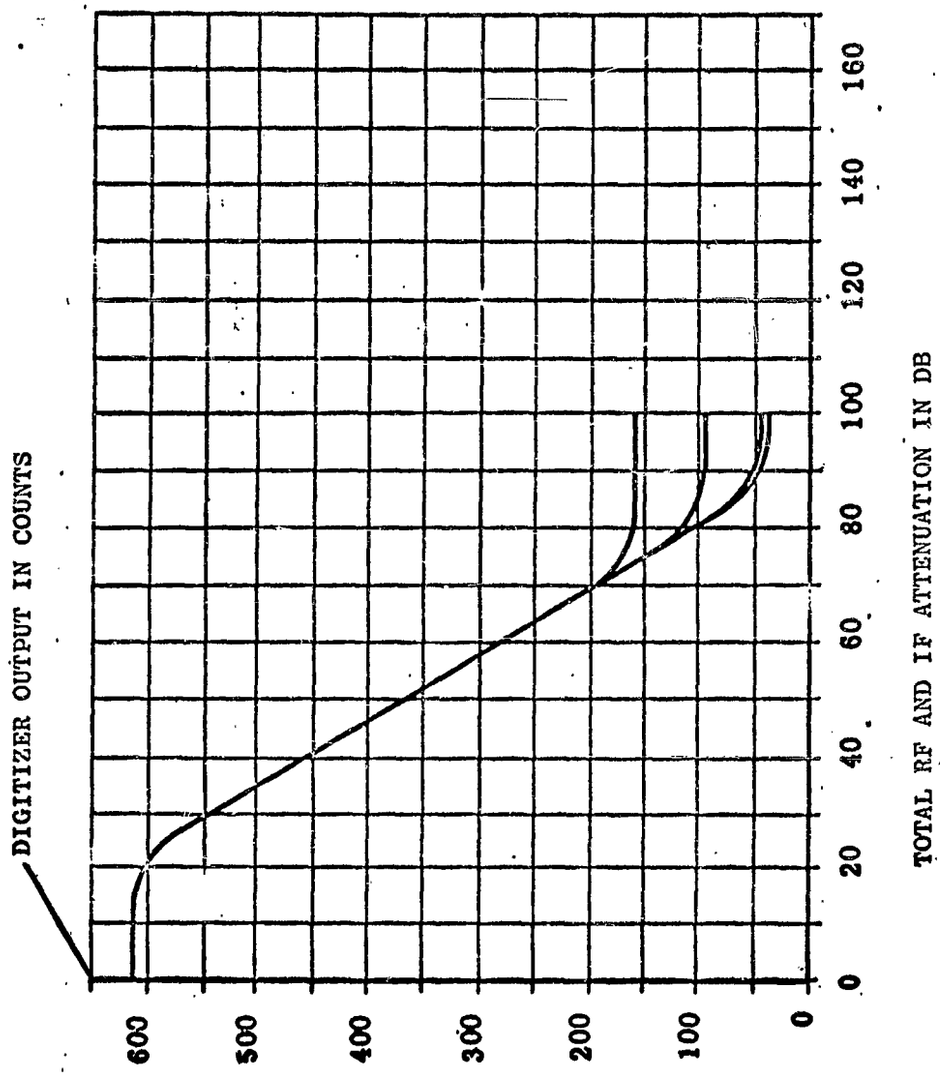


Figure 9.1-3

COMPOSITE SIGNAL STRENGTH
CALIBRATION CURVE



initiated. The curve of Figure 9.1-3 is used as the calibration for processing of signal strength data into cross section data by fitting a third-degree polynomial to the data.

The curve is represented by the equation:

$$T = A_0 + A_1E + A_2E^2 + A_3E^3$$

where T = total attenuation (RF + IF) in db.
E = receiver signal strength in counts.

A_0, A_1, A_2 and A_3 are coefficients which are determined by regression analysis and can be fitted to the data within 1 db RMS.

Having calibrated the receivers in logarithmic units, calibration of the system in absolute units of radar cross section may now be accomplished. A metal sphere of six inch diameter (A_e = -17.39 dbsm at C-Band), supported by a radar-transparent weather balloon, is tracked by the radar. The signal returns are recorded, and used in the radar equation to define C, as follows:

$$C(db) = -(A_e)_o(dbsm)+S(db)+4R(db)+\rho(db)+\alpha(db)+\theta(db)-2L_a(db)$$

where $(A_e)_o(dbsm)$ = cross section of calibration sphere in db referenced to a standard target of one square meter cross section
= -17.39 dbsm

If the transmitter power at the time of this calibration is taken as the reference level, and the target does not deviate from the radar beam axis, then

$$\rho = 0db \text{ and } \theta = 0db$$

and the equation becomes

$$C(db) = 17.39+S(db)+4R(db)+\alpha(db)-2L_a(db)$$

where S = observed receiver output in db

R = effective range attenuation in db

α = IF attenuator setting in db

L_a = calculated atmospheric loss (one way) in db.

It is interesting to note that this calibration of C is the only absolute calibration involved in preparation for the signature data gathering mission (except, of course, for the calibration of the radar ranger).

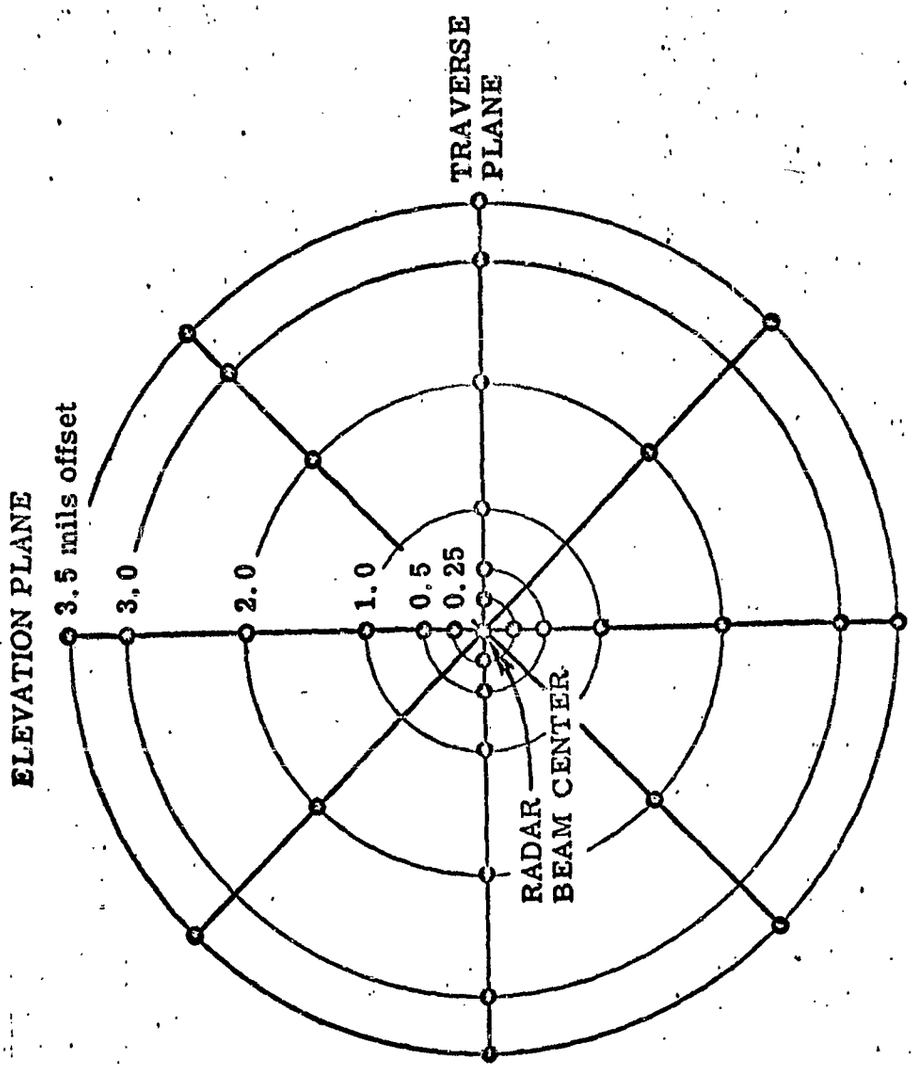
Returns from targets not on the electrical axis of the antenna require calibration of the function, θ, in terms of signal reduction vs angle off-set, ϕ_x and ϕ_y.

Calibration of the characteristic of θ is twofold; i.e., the error channel must be calibrated to measure the position of the target with respect to the radar beam axis, and the sum channel must be calibrated to yield the relative signal loss accruing to this angular displacement of the target. Both these calibrations are carried out using the same target as was used in determination of the constant, C.

The beam center is displaced from the target in discrete steps by introducing a forcing voltage in the servo system in both traverse and elevation, to produce the pattern shown in Figure 9.1-4. Offsets up to 3.5 milliradians, the one-way

Figure 9.1-4

SERVO OFFSET PATTERN FOR CALIBRATION OF ANGLE ERROR CHANNELS



half power beam width of the tracking radar, are obtained in this calibration.

The error channel calibration data thus obtained are compared with angular measurements from the boresight camera film to yield a voltage versus angle relationship such as that shown in Figure 9.1-5. As may be seen from the figure, the error channel calibration displays a strong nonlinear dependency on signal strength. The data may be fitted to a polynomial as follows:

$$\phi_x = \left(a_o + a_1 E_s + a_2 E_s^2 + a_3 E_s^3\right) + \left(b_o + b_1 E_s + b_2 E_s^2\right) V_x + \left(c_o + c_1 E_s\right) V_x^3 + d_o V_y$$

where ϕ_x = traverse error angle from boresight film,

E_s = signal strength from sum channel,

V_x = traverse channel error voltage,

V_y = elevation channel error voltage, and

a_o, a_1, a_2, a_3, b_o, b_1, b_2, c_o, c_1, & d_o = constants to be evaluated by regression, as were the receiver gain coefficients.

Figure 9.1-5

ANGLE ERROR CHANNEL CALIBRATION

A similar expression describes the elevation error calibration. The constant d_o represents the cross-coupling, and has been found to be negligible.

The signal strength data may be plotted against the angular displacement to derive the relative signal loss (θ) in db as a function of angle off axis measured from the boresight film, as shown in Figure 9.1-6. The calibration is obtained by fitting the data with a function:

$$\theta = b \left[\frac{\sin a(\phi_x + c)}{a(\phi_x + c)} \right]^2$$

where a, b, and c are constants to be evaluated by regression.

The RF power monitor used to provide the measurement of ρ is a detector coupled to the output of the klystron power amplifier through a proportional coupler. The RF signal is converted to DC through a detector and DC amplifier circuit. The DC output is calibrated in absolute units of power by comparison with a precision calorimetric water load into which the transmitter output radiates. The calibrated DC output is then used to monitor transmitter power when the output is switched to the antenna. Only changes in transmitter power are used in processing the signal strength data, however, so that a fixed scale factor error in the power monitor calibration does not influence the accuracy of the power correction ρ.

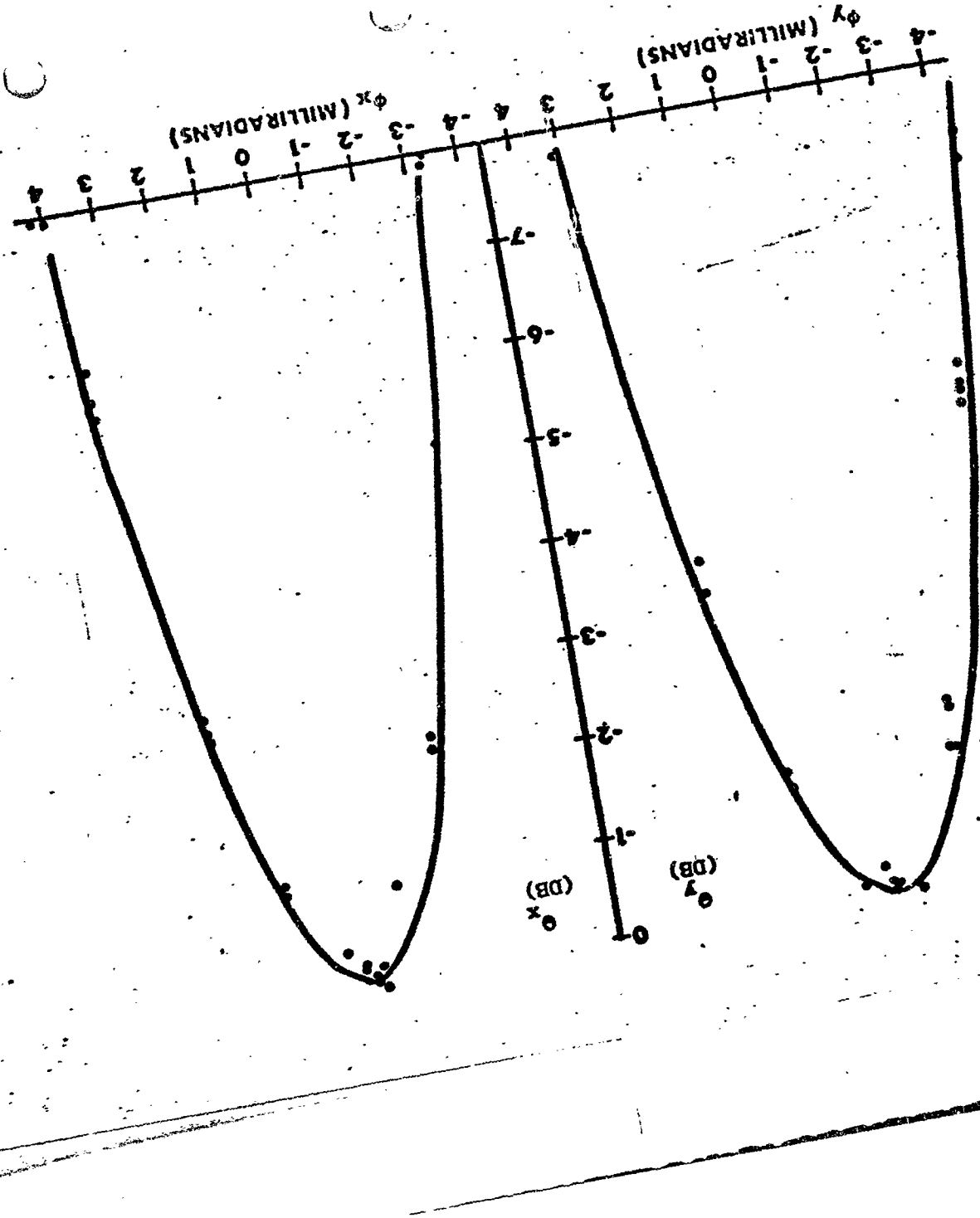


Figure 9.1-6 BEAM PATTERN CALIBRATION

9.1.4 Accuracy Determination

The accuracy of the cross section measurement is determined by the degree to which the systematic variations can be calibrated for correction and by the uncertainties due to noise.

During a balloon-borne standard target sphere calibration, signal strength data are collected at 33 discrete angular positions in the antenna beam and at 8 discrete IF attenuator settings for each calibration point in the beam pattern. Approximately five seconds of data are collected, at a data rate of 160 samples per second, at each position and at each attenuator setting. The pulse-by-pulse signal strengths are corrected for R, ρ, θ, α, L_a and C to yield a measure of A_e in db with respect to a sphere of one square meter cross section which is used as a standard of reference (0dbsm).

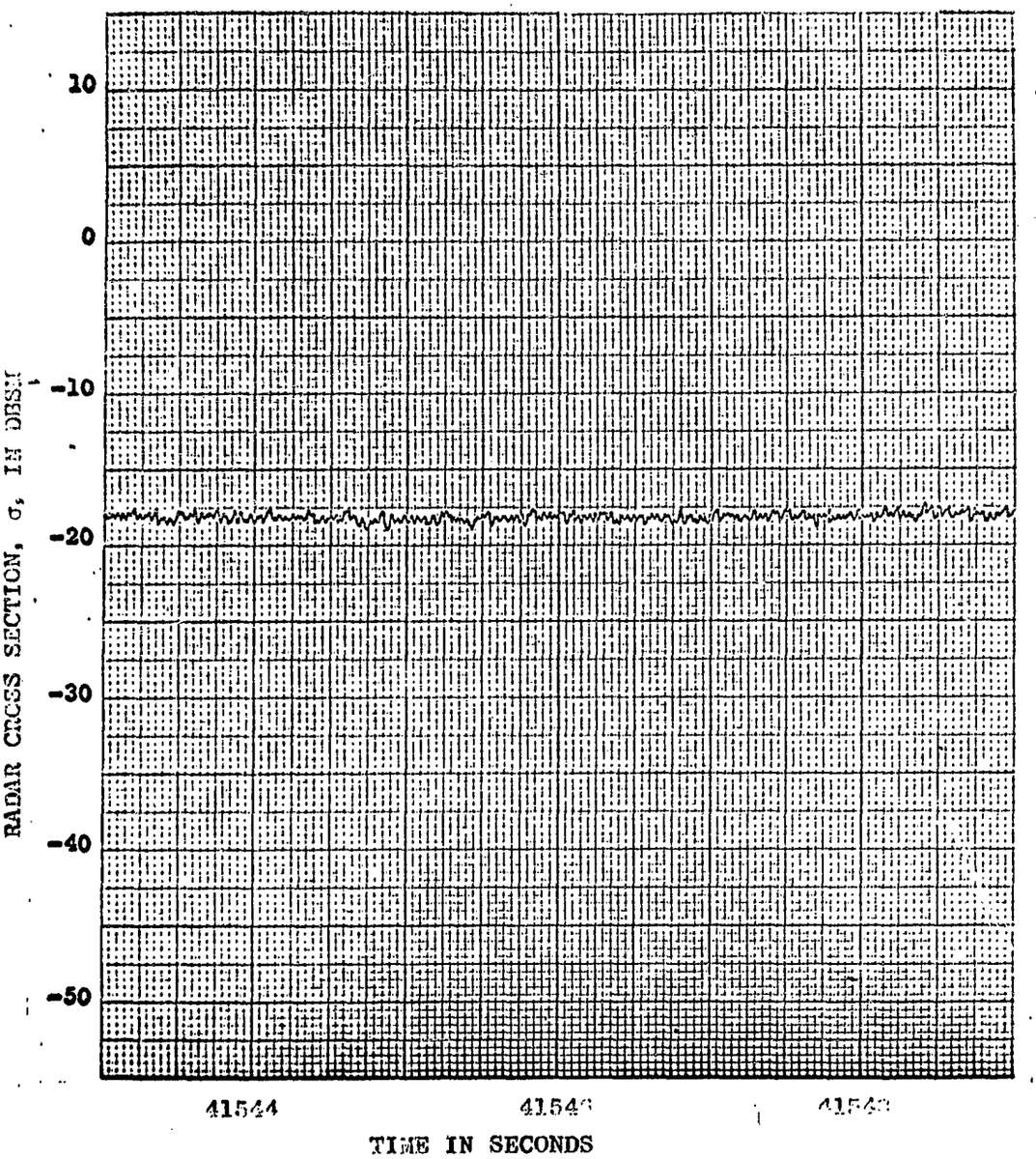
Figure 9.1-7 shows the plot of a typical span of corrected signal strength return from a 6-inch sphere at one particular range, IF attenuator setting, and beam off-set angle. The error remaining after correction for all known systematic parameter variations may be assumed to be random in nature and the best estimate of the standard deviation of the residual error is:

$$S_{A_e} = \left[\frac{\sum_{i=1}^{M} \left[(A_e)_i - (\overline{A_e}) \right]^2}{M} \right]^{\frac{1}{2}}$$

Figure 9.1-7

CROSS SECTION MEASUREMENT OF SIX-INCH SPHERE

(ARIS RADAR)



where S_{A_e} = standard deviation of random residual error

$(A_e)_i$ = measured and corrected cross section of standard target sphere

$(\overline{A_e})$ = true value of cross section of standard target sphere

M = total number of useable calibration points

The value of $(\overline{A_e})$ is unknown and unknowable. It would be equal to $(A_e)_i$ if the standard test sphere were perfect in size and shape, not subject to measurement errors due to imperfect calibration and not subject to interfering reflections from the supporting balloon or other sources of error. Previous RCA experience has indicated that the standard deviation of actual cross section is approximately 0.5 db due to variations in size and shape alone.

A reasonable approximation of the total calibration and measurement error (uncertainty) may be obtained by allowing the unknown true value of the target sphere cross section to be represented by the grand mean of the measured values over the whole range of the calibration run. The data are partitioned into 5-second samples and only the middle 3-second range is utilized. Further, each sample which includes measurements outside the dynamic range of the receiver response is discarded.

The standard deviation estimate of total error is then obtained by pooling the means and variances of each 3-second span with the 0.5 db (standard deviation) uncertainty of the standard target sphere, thus:

$$S'_{A_e} = \left[\frac{\sum_{i=1}^{k} (N_i - 1) S_i^2}{\sum_{i=1}^{k} N_i - 1} + \frac{\sum_{i=1}^{k} N_i \left[(\overline{A_e})_i - (\overline{A_e}) \right]^2}{\sum_{i=1}^{k} N_i - 1} + (0.5)^2 \right]^{\frac{1}{2}}$$

where N_i = the number of data points in the i th span

K = the number of edited spans

S_i = the estimated standard deviation of the i th span

$(\overline{A_e})_i$ = the mean of the i th span

$(\overline{A_e})$ = the grand mean of all data spans

S'_{A_e} = the standard deviation estimates of total error

9.2 Advanced Range Instrumentation Ships (ARIS)

9.2.1 System Description

The ARIS ships, General H. H. Arnold and General H. A. Vandenberg are composed of an integrated radar system of C-band tracking radars with L-band and X-band or UHF-band radars slaved to follow the tracking radar so that signature data can be collected on

several frequencies simultaneously. Figure 9.2-1 shows the physical arrangement of the ARIS equipment and a block diagram of the data flow between sub-systems. The two ships are essentially identical except that the slaved secondary dual radars on the Arnold operate on L and X frequencies while the secondary dual radars on the Vandenberg operate on L and UHF frequencies. All three C, L and X-band radars of the Arnold are capable of transmitting horizontal and vertical polarizations sequentially interleaved, and receiving horizontal, vertical or cross polarizations. The Vandenberg C-band radar can operate on the same polarization modes as the Arnold but its L-band and UHF-band radars transmit and receive only horizontal and vertical polarizations respectively. All radars can accommodate a primary target and two secondary targets if within $\pm$3.5 milliradians beam angle and within $\pm$32K yards range but not less than 250 yards separated from the primary target. The range, elevation angle and traverse angle of the primary target and the increments of range, elevation angle and traverse angle for each secondary target are recorded along with received signal strength for each target for each transmitted pulse.

The C-band master designate radar is capable of tracking in either skin or beacon mode without interference with its signature data collecting capabilities.

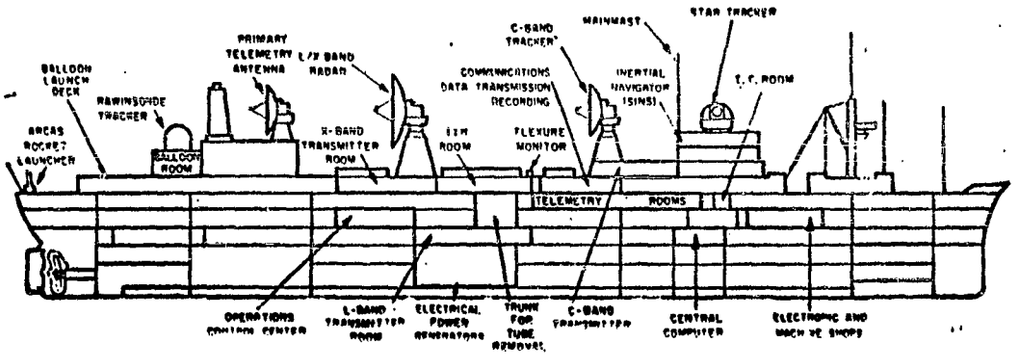
9.2.2 Error Sources

From the basic radar equation it has been shown that the apparent cross section of a target, as measured in terms of signal strength at the radar receiver output, is a complex function of transmitted power, antenna gain, range, receiver gain, wavelength, transmission line losses, transmission medium losses and angular off-set from the axis of the antenna beam. Instabilities or random variations in any of

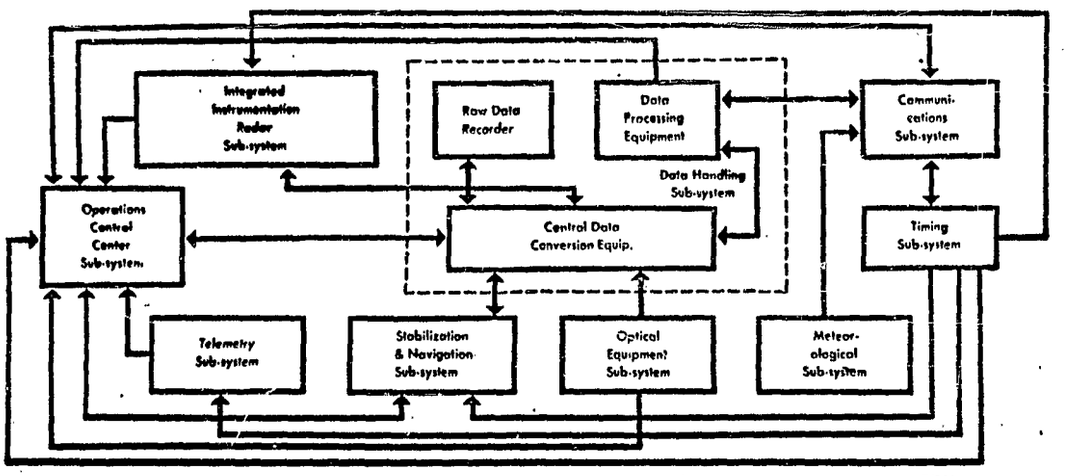
Figure 9.2-1

ARIS SHIP EQUIPMENT CONFIGURATION

PHYSICAL ARRANGEMENT



SIGNAL FLOW BLOCK DIAGRAM



these parameters could invalidate the system calibration and produce a bias error. Noise components, particularly of frequencies below the data sampling rate, can expand the uncertainty of determining the cross section on a pulse-by-pulse record. The error sources may be categorized as systematic (controllable and uncontrollable) and random (internal system and external system). The sources of error are listed in the block diagram of Figure 9.2-2.

9.2.3 System Accuracies

The ARIS signature system accuracy estimates were computed from data collected during four balloon-borne target calibration tests on the Arnold and two tests on the Vandenberg. The pooled standard deviation estimates in db are tabulated in Table 9.2-3: Blank spaces in the table indicates insufficient data are available for determination of significant error estimates for that mode.

Figure 9.2-2
Sources of Error

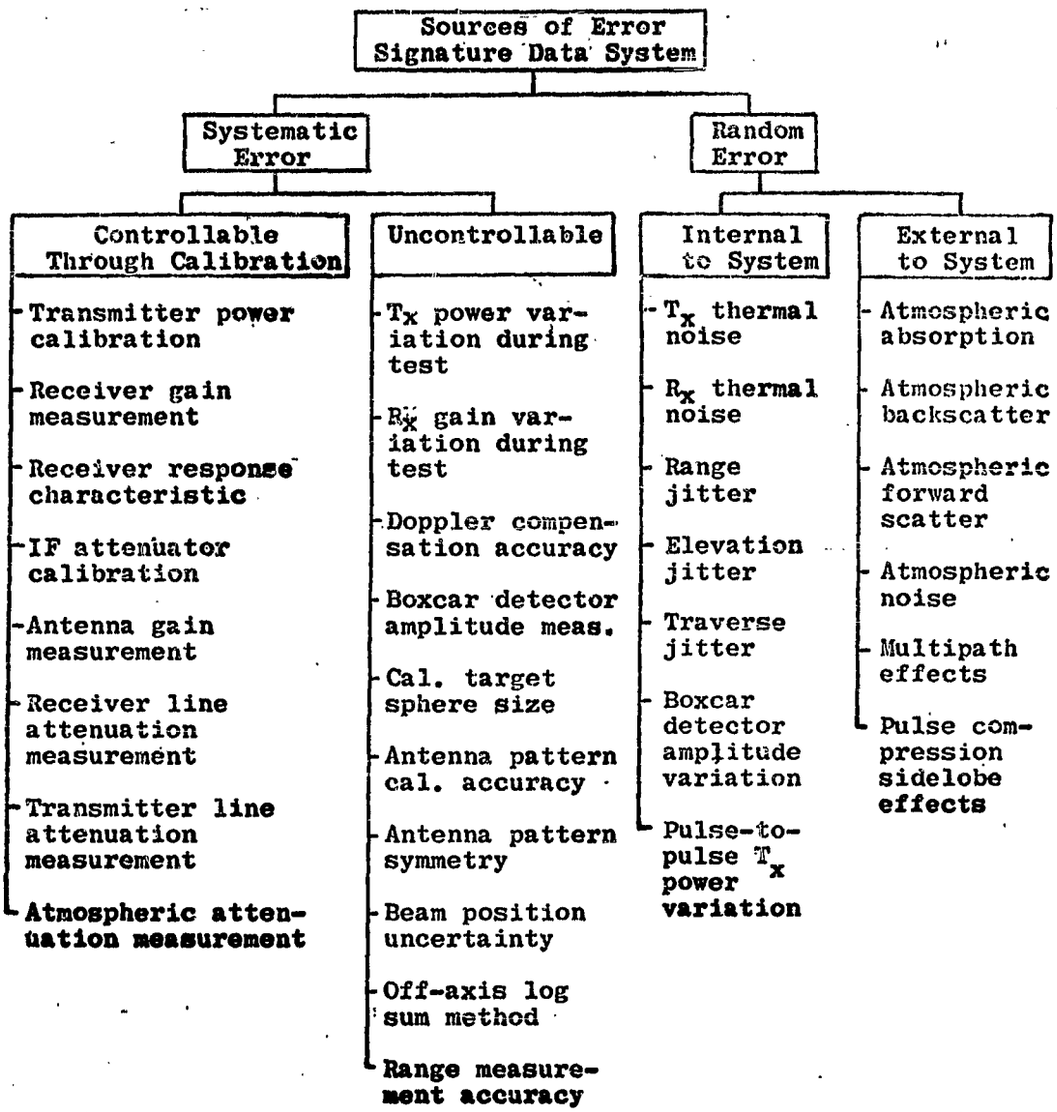


Table 9.2-3
ARIA Signature Data Accuracy

	Arnold (4 tests)			Vandenberg (2 tests)		
MODE	PT	ST1	ST2	PT	ST1	ST2
CHH	2.0	2.5	2.5	1.0	2.5	
CVV	1.9			2.0	1.8	
LHH	1.8	1.4	1.3	2.7	1.4	
LVV	1.7	1.3	1.6	NA	NA	NA
XHH	3.0	3.0		NA	NA	NA
XVV	2.3	2.3		NA	NA	NA
UVV	NA	NA	NA	1.6		

NOTE: Errors are standard deviation estimates in db. The three letter MODE code indicates:

(1) frequency band (C, L, X or UHF);
(2) the transmitter polarization (H or V)*; and
(3) the receiver polarization (H or V)*.

NA means that mode of operation is not available in that equipment.

PT = Primary target
ST1 = Secondary Target No. 1
ST2 = Secondary Target No. 2

*H = Horizontal polarization, V = Vertical polarization.

10.0 SURVEY

10.1 Terminology

In order that the tables presented in section 10.2 may be understood better a brief explanation of certain survey terms is advisable.

The computation of the geodetic coordinates is performed on an ellipsoid which closely approximates the size and shape of the earth in the area. The actual measurements made on the surface of the earth are referred to the geoid. The ellipsoid is a mathematically defined regular surface with specific dimensions. The surveys of North America and Eastern Test Range are based on the dimensions of the earth according to Clark's spheriod of reference (1866) unless otherwise stated. This spheroid is an ellipsoid of revolution and is defined by the lengths of the semi-axes. The equatorial semi-axis of Clark's (1866) spheroid is 6,378,206.4 meters and the polar semi-axis is 6,356,583.8 meters. The geoid coincides with that surface to which the oceans would conform over the entire earth if free to adjust to the combined effect of the earth's mass attraction and the centrifugal force of the earth's rotation.

Since the ellipsoid is a regular surface and the geoid is an irregular surface it is evident that the two surfaces will not coincide. The perpendicular to the ellipsoid and the geoid plumb line form an angle which is known as the deflection of the vertical. The deflection of the vertical is expressed in two components. In a north and south direction it is expressed as the deflection in the meridian and as equal to the astronomic latitude minus the geodetic latitude. The second component is in the east and west direction and is expressed as the deflection in the prime vertical and is equal to the astronomic longitude

minus the geodetic longitude times the cosine of the geodetic latitude. Positive sign indicates a north or west direction and a negative sign indicates a south or east direction.

The separations between the geoid and the spheroid are called geoid heights and are designated as N. The size of the geoid heights reveals the extent to which an ellipsoid fits the geoid and thus helps to determine the best fitting ellipsoid.

Mean sea level is the average height of the sea for all stages of the tide. It is obtained by averaging observed hourly heights of the sea on the open coast or in adjacent waters having free access to the sea, the average being taken over a period of time. A period of 19 years is generally considered as constituting a full tidal cycle, for during this period of time the more important of the tide variations will have gone through complete cycles. Hence sea level derived from 19 years of observations may be taken to constitute a primary determination and as giving accurately the datum of mean sea level. In general it may be taken that mean sea level determined from a year of observations, when compared with simultaneous observation at a suitable primary tide station will give a value correct within 0.05 foot.

The mass surplus of the mountains and the mass deficiency of the oceans cause the deflections of the vertical and the undulations of the geoid. The observed elements of the gravimetric method are the gravity anomalies, that is the difference between the observed gravity value properly reduced to sea level, and the theoretical gravity obtained from the gravity formula. Excessive mass "pulls" and deficient mass "pushes" the plumb line causing the deflection which depends on the disturbing mass anomalies. If the observed gravity is

greater than the theoretical value, the anomalies are positive.

With the advent of the space age, a new geodetic tool was discovered: the artifical earth satellite. By photographing an illuminated satellite against a star background from two or three positions on a known base line the spatial position of the light image can be determined. A camera at an unknown point by simultaneous observations can determine its camera orientation to the spatial point and thereby the camera's geodetic position. The great advantage of this technique is that directions from ground stations to the satellite are free of the local gravity vector. A world wide satellite survey to form a world geodetic datum is planned.

Precision base lines are usually measured with a geodimeter. This instrument projects a modulated beam of light to a passive reflector which is placed at the other end of the distance to be measured. The reflector, acting as a mirror, sends the light beam back to the geodimeter. By phase comparison the instrument indirectly measures the time required for the light to travel to the reflector and back. Distances can be measured with accuracies of 10mm $\pm$ one millionth of the distance.

10.2 Accuracies

Current survey accuracies are presented in the following tables.

10.2.1 Deflection of the Vertical

TABLE 10.2-1
DEFLECTION DATA
(ASCENSION ISLAND)

	MERIDIAN COMPONENT		PRIME VERTICAL COMPONENT		
LOCATION	$(\phi_A - \phi_G)$	σ	$(\lambda_A - \lambda_G)\ \mathrm{Cos}\ \phi_G$	σ	REMARKS
7° - 56'S 14° - 29'W	+ 3".3	*	+29".2	*	Offshore
7° - 53'S 14° - 26'W	+20".0	*	+13".4	*	Offshore
7° - 56'S 14° - 24'W	+ 3".2	3".7	+ 6".6	3".7	On Island
7° - 58'S 14° - 24'W	- 2".3	3".7	+ 4".2	3".7	On Island

* Not available

TABLE 10.2-2

DEFLECTION DATA

(North of Great Abaco Island)

LOCATION	DEFLECTION	
	MERIDIAN	PRIME VERTICAL
Center	+5".4	-6".3
N.W. Corner	+4".7	-9".9
N.E. Corner	+6".7	-3".2
S.E. Corner	+5".1	-2".7
S.W. Corner	+3".5	-8".8

The deflections of the vertical are available for an area of 20 nautical miles square centered at 26° N latitude and 76° W longitude.

In this area, the meridian components are positive and the prime vertical components negative. Thus the astronomic zenith is Northeast of the geodetic zenith.

Deflections at a selected point can be interpolated to 1 second of arc from the above five points. The intervals are deemed close enough for interpolation and accuracy requirements.

TABLE 10.2-3
DEFLECTION OF THE VERTICAL
C-BAND RADARS

RADAR	MERIDIAN COMPONENT $(\phi_A - \phi_G)$	PRIME VERTICAL COMPONENT $(\lambda_A - \lambda_G) \cos \phi_G$
0.18	+ 1".7	- 1".4
3.18	- 6".5	- 7".4
91.18	+ 6".0	-12".0
7.18	+13".3	- 8".3
12.18	- 2".3	+ 4".2
19.18	+ 0".8	- 1".5
1.16	+ 1".0	- 1".6
3.16	- 9".0	- 6".0
12.16	+ 3".2	+ 6".6
Bermuda	-10".5	-19".2

TABLE 10.2-4
GEODETIC UNCERTAINTIES

DEFLECTION OF VERTICAL	
Name	Standard Error (seconds of arc)
Pad No. 40	0.3
Pad No. 41	0.3
Meade's Ranch, Kan.	1.5

POSITION	
Name	Standard Error (seconds of arc)
Meade's Ranch to Cape Kennedy	0.4

GRAVITY	
Name	Standard Error
Cape Kennedy	4.5×10^{-4} cm per sec^2 (0.45 milligal)

10.2.2 Geoid Heights

TABLE 10.2-5
GEOID HEIGHTS (N)
VICINITY OF GRAND BAHAMA ISLAND

The values for the geoid heights are referred to the Clarke 1866 spheroid, North American 1927 datum, with the adopted value of 0.0 meter at station HUB at Cape Kennedy. Values for other near-by stations may be obtained by interpolation.

Station	Latitude			Longitude			(N) Meters	σ Meters
	o	'	"	o	'	"		
HUB (Cape Kennedy)	28	29	29	80	33	36	0.0	0.0
SCP-FF	26	57	02	79	06	15	+1.0	0.86
SET	26	41	40	78	59	44	+1.1	0.86
MANGROVE CAY	26	55	08	78	37	05	+1.4	0.86
WALKER	27	15	26	78	24	17	-0.5	0.86
STEWART	26	43	44	78	29	38	+1.2	0.86
ASKANIA No. 1	26	36	14	78	22	21	+0.4	0.86
ASKANIA No. 2	26	36	59	78	14	48	+0.1	0.86
ASKANIA No. 3	26	38	32	78	06	49	-0.2	0.86
SCP-DD	27	05	02	78	00	09	-2.2	0.86
ALLEN	26	59	24	77	41	11	-3.4	0.86
SCP A-7	26	57	22	77	33	16	-3.5	0.86
CAR	26	39	12	77	58	33	-0.6	0.86
TURTLE	26	45	23	77	19	34	-2.8	0.86
MORES	26	19	40	77	34	45	-1.4	0.86
MARSH HARBOR	26	32	22	77	03	36	-3.9	0.86
SCP-A	26	07	26	77	10	57	-5.6	0.86

TABLE 10.2-6

GEOID HEIGHTS (N)

PRECISE BASE LINE - VERO BEACH TO HOMESTEAD, FLORIDA

Station	Latitude			Longitude			(N) Meters	σ Meters
	o	'	"	o	'	"		
EGGS 2(Vero Beach)	27	40	29.5	80	21	45.2	+0.83	0.09
EMERSON	27	31	21.4	80	24	52.6	+1.27	0.09
BOUFFORD	27	24	42.0	80	24	15.8	+1.46	0.09
OWEN	27	09	40.9	80	19	08.4	+1.80	0.18
HAWK 2	26	56	32.2	80	13	54.4	+2.35	0.19
JUPITER INLET	26	56	53.7	80	04	56.2	+1.69	0.21
FERGAN	26	40	48.0	80	12	05.3	+3.37	0.24
CONVICT	26	32	56.4	80	12	19.5	+3.79	0.27
CLINT	26	24	31.5	80	12	13.9	+4.08	0.28
HAMMOND 2	26	15	53.1	80	12	08.5	+4.31	0.30
HAWKINS 2	26	09	51.2	80	12	10.2	+4.47	0.30
RED TOP 2	25	56	21.9	80	16	40.3	+4.99	0.31
HECTOR 2	25	45	41.3	80	20	25.0	+5.30	0.33
WALDIN(HOMESTEAD)	25	30	25.2	80	23	17.6	+5.60	0.36

TABLE 10.2-7

STANDARD ERROR OF WORLD WIDE

GEOID HEIGHTS

LATITUDE (deg.)	LONGITUDE (deg.)	GEOIDAL HTS. S_{meters}	LATITUDE (deg.)	LONGITUDE (deg.)	GEOIDAL HTS. S_{meters}
+15	5.5	11	-15	5.5	15
+15	37.5	11	-15	37.5	14
+15	69.0	13	-15	69.0	17
+15	101.0	12	-15	101.0	16
+15	132.5	15	-15	132.5	15
+15	164.5	16	-15	164.5	20
+15	196.0	14	-15	196.0	18
+15	228.0	14	-15	228.0	20
+15	259.5	12	-15	259.5	18
+15	291.5	11	-15	291.5	14
+15	323.5	12	-15	323.5	14
+45	7.0	7	-45	7.0	16
+45	50.0	8	-45	50.0	16
+45	93.0	9	-45	93.0	18
+45	136.5	11	-45	136.5	16
+45	179.5	11	-45	179.5	16
+45	223.0	10	-45	223.0	16
+45	266.0	7	-45	266.0	16
+45	309.0	10	-45	309.0	14
+75	20.0	7	-75	20.0	12
+75	140.0	7	-75	140.0	12
+75	260.0	7	-75	260.0	12

Based on: Flattening, 1/298.24 ± 0.01

: equatorial radius, 6,378,163 ± 21 meters

10.2.3 Mean Sea Level Planes

TABLE 10.2-8

ACCURACY OF MEAN SEA LEVEL PLANES

LOCATION	STANDARD ERROR
1. Grand Bahama Island	0.89 inches
2. Eleuthera Island	1.62 inches
3. San Salvador Island	0.89 inches
4. Mayaguana Island	1.69 inches
5. Antigua Island	1.69 inches
6. Ascension Island	0.96 inches

There is no record of this type of work for Grand Turk

10.2.4 Survey Accuracies

TABLE 10.2-9

STANDARD ERRORS ELEUTHERA-VALKARIA MISTRAM

POINT	TO POINT	QUANTITY	STANDARD ERRORS
Central PMSS (Eleuthera)	Central PMSS (Valkaria)	Length	1:1,110,000*
		Azimuth	0.3"
		GEOID HT	1:510,000

*The distance from Central PMSS (Eleuthera) to Central PMSS (Valkaria) is 518,193.166 meters.

TABLE 10.2-10

SPECIAL PRECISION BASE

Point Williams, Florida to Homestead, Florida

(approximate distance 215 statute miles)

QUANTITY	PROBABLE ERROR	σ (FEET)
Position	1:1,670,000*	0.55
Geodetic Distance	1:3,360,000	0.47
Geodetic Azimuth	0.2"	-

*Position of Homestead with respect to Point Williams (Cape Area), circular probable error.

TABLE 10.2-11

SURVEY ACCURACIES

(Based on USC&GS Data)

Referred to Pad No. 3, Cape Kennedy, Clarke 1866 Spheroid, North American 1927 Datum

Station	PE^*_x FT	PE_y FT	PE_z FT	σ_x FT	σ_y FT	σ_z FT	CPE** (x & y) FT
Antigua	72.0	72.0	22	106.7	106.7	33	125.6
Ascension Is.	220.0	220.0	47	326.0	326.0	69	385.0
AZUSA MK II	0.3	0.3	0	0.4	0.4	0	0.4
Bermuda	11.0	11.0	34	16.0	16.0	26	19.2
Cherry Point	15.0	15.0	4	22.0	22.0	6	26.0
Eleuthera	1.9	1.9	2.6	2.9	2.9	3.9	3.4
Grand Bahama Is.	1.8	1.8	2	2.7	2.7	3	3.2
Grand Turk	49.0	49.0	16	72.6	72.6	24	85.5
Mayaguana	42.6	42.6	14	63.2	63.2	21	74.4
Merritt Is.	0.3	0.3	0	0.5	0.5	0	0.6
1.16	0.1	0.1	0	0.1	0.1	0	0.1
IP.16	0.1	0.1	0	0.1	0.1	0	0.1
Puerto Rico	68.9	68.9	20	102.2	102.2	30	120.3
San Salvador	36.0	36.0	13	53.4	53.4	19	62.9
Savannah, Ga.	1.4	1.4	0.3	2.1	2.1	0.4	2.5

* PE - linear probable error with 50% probability

** CPE- circular probable error with 50% probability

TABLE 10.2-12

SURVEY ACCURACIES

(Based on Best Available Data)

Referred to Pad No.3, Cape Kennedy, Clarke 1866 Spheroid

North American 1927 Datum

Station	PE_x FT	PE_y FT	PE_z FT	σ_x FT	σ_y FT	σ_z FT	CPE (x&y)
ABERDEEN,MD	21	21	10	31	31	15	36
BARBADOS	80	80	29	119	119	43	140
EDWARDS AFB	43	43	15	64	64	22	75
EGLIN	16	16	12	24	24	18	28
FAIRCHILD	52	52	7	77	77	11	91
Ft.HUACHUCA	39	39	14	58	58	21	68
PMR	46	46	15	68	68	22	80
ST. HELENA	572	572	33	849	849	49	1040
TFV 86.16 (28^{o}N, 48^{o}W)	3437	3437	22	5096	5096	33	6000
TRINIDAD	83	83	18	123	123	26	145
WHITE SANDS	36	36	15	53	53	22	62

TABLE 10.2-13

ETR C-BAND RADARS

RADAR	TYPE	LATITUDE	LONGITUDE	ELEV. (MSL) ft.	σ_x ft.	σ_y ft.	σ_z ft.
0.18	AN/FPQ-6	28° 13' 33".9867	80° 35' 58".2277	48.93	0.1	0.1	0
91.18	AN/FPQ-6	17 08 34.1470	61 47 35.5176	138.79	106.7	106.7	33
7.18	AN/TPQ-18	21 27 43.7398	71 07 56.7032	118.87	72.6	72.6	24
12.18	AN/TPQ-18	-07 58 30.5315	14 24 09.7447	411.34	326.0	326.0	69
19.18	AN/TPQ-18	28 25 27.9287	80 39 52.6253	36.91	0.5	0.5	0
1.16	AN/FPS-16	28 28 52.7926	80 34 36.2309	44.76	0.1	0.1	0
3.16	AN/FPS-16	26 36 54.9493	78 20 53.1153	45.52	2.7	2.7	3
12.16	AN/FPS-16	-07 57 14.0399	14 24 49.0168	302.96	326.0	326.0	69
Bermuda	AN/FPS-16	32 20 51.132	64 39 15.046	65.36	16.0	16.0	26

TABLE 10.2-14

ACCURACIES OF LENGTHS

BETWEEN UDOP INSTALLATIONS AT GRAND BAHAMA ISLAND

(Based on USC & GS Accuracy Figures of July 1964)

UDOP INSTALLATIONS	LENGTH σ (Feet)	AZIMUTH σ (Arc Sec.)
Bassett Cove - Sale	0.21	0.74
Bassett Cove - Carter	0.24	0.40
Bassett Cove - Walker	0.34	0.46
Bassett Cove - Allans Cay	0.28	0.36
Sale - Carter	0.18	0.55
Sale - Walker	0.24	0.61
Sale - Allans Cay	0.27	0.40
Carter - Allans Cay	0.21	0.44
Carter - Walker	0.31	0.56
Walker - Allans Cay	0.38	0.44

APPENDIX I

GRAPHS FOR THE DETERMINATION OF VELOCITY AND ACCELERATION ERROR ESTIMATES

The goal in filtering is to reproduce the useful information in a signal and to reject the remainder. To accomplish this, we must know something about both the useful and the undesired part of the measurement. The useful portion of the observation will represent range, or range rate, or elevation angle, etc., of a missile with respect to a specific tracking system. The unwanted portion of the observation is composed of noise originating from such phenomena as atmospheric turbulence, electronic jitter, multipath, read out truncations, etc.

Since the missile is a massive object traveling through space, it seems logical that we should be able to represent its physical path f(t), during a small segment of its path, by some initial position, velocity, acceleration, and jerk, or in other words, by the first few terms of a Taylor series. Without loss of generality, we can assign the time origin to the center of the span of interest. Its position at time t, with respect to the center point of the span, is then represented as:

$$f(t) = f(0) + f'(0)t + \frac{f''(0)}{2} t^2 + \frac{f'''(0)}{6} t^3 \qquad (1)$$

where terms of order higher than the third have been dropped, or simply as a polynomial in t, i.e.,

$$f(t) = \sum_{\nu=0}^{3} b_\nu t^\nu \qquad (2)$$

where

b_o = f(0) (position at the center point (c.p.) of the span)

b_1 = f'(0) (velocity at c.p.)

.
.
.

If we measure not position, but, say, elevation angle, we will still assume that the useful measured signal can be represented by a low order polynomial. Since we have no such physical basis for the noise portion of the signal, we will simply assume it is random and uncorrelated in time.

The following steps are followed to filter a set of data:

1. Choose the degree of polynomial, say, n.

2. Choose the time span over which we can adequately represent the data by a polynomial of degree n. Since we have sampled data, this gives M data points in the approximating span. We prefer to have M odd so as to have a center point, and we thus let $M = 2N + 1$ and have N points on each side of the center point.

3. By a least squares technique, we determine the coefficients b_i in (2).

4. From these coefficients we can determine the position, velocity, etc., at any point in our span, say at time t_q with respect to the center point of our approximating span.

5. Using the same n, and N, we shift our approximating span of $2N + 1$ points by one sample point and determine a new set of coefficients b_i. We evaluate this newly found polynomial at t_q with respect to the center point of the shifted span.

6. This is repeated until all the desired data are processed. This technique is called moving arc polynomial filtering.

Mathematically, we accomplish this as follows: Suppose we desire to fit an n^{th} degree polynomial to $2N + 1$ data points, equally spaced in time, $f(t_i)$, $i = -N, -N + 1, \ldots, N$. The polynomial, assumed to represent the deterministic portion of the input signal, is:

$$p(t_i) = \sum_{\nu=0}^{n} a_\nu t_i^\nu \qquad \text{[step 1]} \qquad (3)$$

where the a's are adjusted to minimize the sum:

$$S = \sum_{i=-N}^{N} \left\{ f(t_i) - \sum_{\nu=0}^{n} a_\nu t_i^\nu \right\}^2 \qquad \text{[steps 1 \& 2]} \qquad (4)$$

In (4) we assume that the error portion of f(t) is uncorrelated from time point to time point. The adjusted a's may be written as:

$$a_\mu = \sum_{i=-N}^{N} h_{i,\mu}\, f(t_i), \qquad \mu = 0, 1, \ldots, n$$

where the h's are determined by minimizing equation (4) and are independent of f(t). These h's are the filter weights needed to produce the desired coefficients of the polynomial. The polynomial of degree n best fitting the span of data, in the least squares sense, at any time point t_q can be written in terms of the weights $h_{i,j}$ as follows:

1. For position

$$p(t_q) = a_0 + a_1 t_q + \ldots a_n t_q^n \qquad \text{[step 4]}$$

$$= \sum_{i=-N}^{N} \left\{ h_{i,0} + t_q h_{i,1} + \ldots + t_q^n h_{i,n} \right\} f(t_i)$$

$$= \sum_{i=-N}^{N} \left\{ H^0_{i,q,N} \right\} f(t_i)$$

The H's are a new set of filter weights used to produce the smoothed data at position q in a moving arc filter, and are a linear combination of the coefficients' filter weights. At center point $t_q = 0$, so $H^0_{i,0,N} = h_{i,0}$.

2. For velocity

$$p'(t_q) = a_1 + 2a_2 t_q + \ldots + n a_n t_q^{n-1}$$

$$= \sum_{i=-N}^{N} \left\{ h_{i,1} + 2t_q h_{i,2} + \ldots n t_q^{n-1} h_{i,n} \right\} f(t_i)$$

$$= \sum_{i=-N}^{N} \left\{ H^1_{i,q,N} \right\} f(t_i)$$

At center point $H^1_{i,0,N} = h_{i,1}$

3. For acceleration

$$p''(t_q) = 2a_2 + 6a_3 t_q + \ldots n(n-1) a_n t_q^{n-2}$$

$$= \sum_{i=-N}^{N} \left\{ 2h_{i,2} + 6t_q h_{i,3} + \ldots n(n-1) t_q^{n-2} h_{i,n} \right\} f(t_i)$$

$$= \sum_{i=-N}^{N} \left\{ H^2_{i,q,N} \right\} f(t_i)$$

At center point $H^2_{i,0,N} = h_{i,2} \times 2$.

In general, for the m^{th} derivative, we write

$$p^m(t_q) = \sum_{i=-N}^{N} \left\{ H^m_{i,q,N} \right\} f(t_i) \qquad (5)$$

At center point $H^m_{i,0,N} = h_{i,m} \times m!$.

We have assumed that the deterministic portion of the signal is of degree n and that our polynomial chosen to represent this portion of the data is also of degree n. This is, of course, not always true, since sometimes we may be wrong in our ideas as to the polynomial content of the signal. This problem is considered in Nesline [1961].

For the case in which we have chosen the proper polynomial, we represent the data as:

$$f(t_i) = \sum_{\nu=0}^{n} b_\nu t_i^\nu + e_i \qquad (6)$$

where the b_ν is the unknown coefficient in the data, which we estimate in (4), and e_i is the random error signal, stationary in time, i.e., we have

$$E(e_i e_j) = \delta_{ij} \sigma^2_{in}$$

where E is the expectation operator, δ_{ij} is the Kronecker delta, and σ^2_{in} is the variance of the random error signal.

Using equations (5) and (6), we find that the error component in the m^{th} derivative, after the polynomial fit, is given as:

$$(\text{error at } t_q) = \sum_{i=-N}^{N} H^m_{i,q,N}\, e_i.$$

We now define

$$\sigma^2_{out,q,m} = E\,(\text{error at time } t_q)^2.$$

Therefore

$$\sigma^2_{out,q,m} = \sum_{i=-N}^{N} (H^m_{i,q,N})^2\, \sigma^2_{in}$$

or

$$\frac{\sigma^2_{out,q,m}}{\sigma^2_{in}} = \sum_{i=-N}^{N} (H^m_{i,q,N})^2 \qquad (7)$$

Equation (7) gives the variance reduction factor between the input and output data.

In figures A1-1, A1-2, A1-3, we have set m = 1, and let M (=2N+1) assume the values 11, 21, 37, 51, and 75. For each value of M, we then plot the square root of

$$\frac{\sigma^2_{out,q,m}}{\sigma^2_{in}} = \sum_{i=-N}^{N} (H^1_{i,q,N})^2 \text{ vs. time point } t_q.$$

We thus plot the velocity error standard deviation reduction factor as a function of position in the filter. In figures A1-4, A1-5, A1-6, m = 2, and we plot the acceleration error standard deviation reduction factor in a similar manner. The assumptions used in the construction of the graphs may be summarized as follows:

1. The errors are uncorrelated and stationary.

2. The signal is composed of a deterministic element plus a random component.

3. The deterministic portion of the signal is a polynomial of degree n.

4. The polynomial used to represent this signal is also of degree n.

To demonstrate the use of these figures, let us assume that we choose a third order polynomial (n = 3) to represent the data, f(t), over a 21 point span of data (N = 10, M = 21). Furthermore, let us assume that the standard deviation of the data is two feet (i.e., σ_{in} = 2 feet), and that the time between sampled data points Δt is 0.5 sec (sampling rate = 2 per second). If we let F represent the ordinate read from Figure A1-2 and K represent the sampling rate, we find for the velocity standard deviation (σ_{out}), center point smoothing:

$$\sigma_{out} = \sigma_{in} F_{c.p.} K = (2)(.091)(2) = 0.364 \text{ ft/sec.}$$

For acceleration standard deviation, we use figure A1-5 and find

$$\sigma_{out} = \sigma_{in} F_{c.p.} K^2 = (2)(.013)(2)^2 = .104 \text{ ft/sec}^2.$$

For end point filtering, we use the same two figures and find, for velocity

$$\sigma_{out} = \sigma_{in} F_{e.p.} K = (2)(.32)(2) = 1.28 \text{ ft/sec},$$

and for acceleration

$$\sigma_{out} = \sigma_{in} F_{e.p.} K^2 = (2)(.078)(2)^2 = .62 \text{ ft/sec}.$$

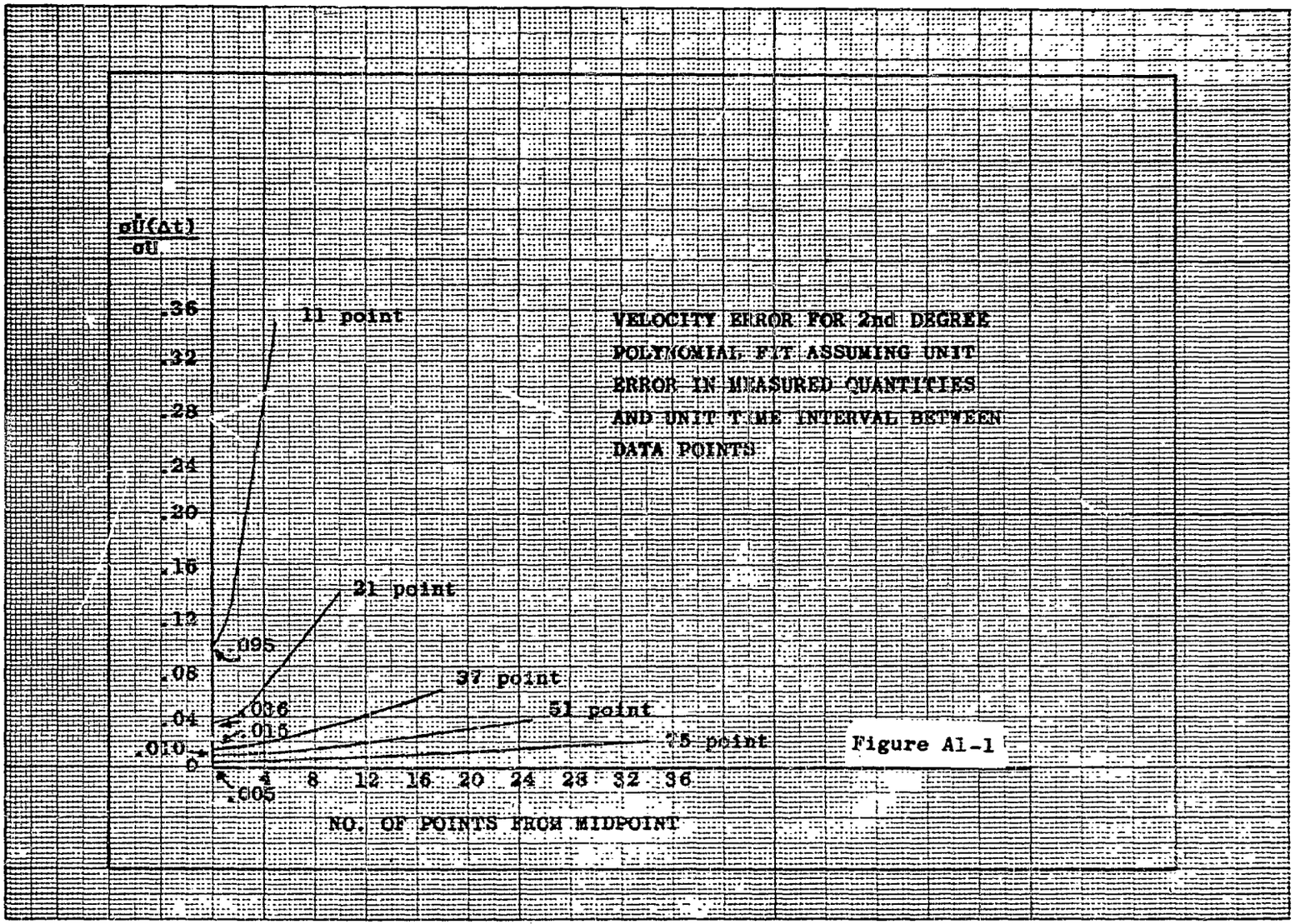

σU(Δt)/σU
.36
.32
.28
.24
.20
.16
.12
.08
.04
.010
0
11 point
21 point
37 point
51 point
75 point
.095
.036
.016
.005
4
8
12
16
20
24
28
32
36
NO. OF POINTS FROM MIDPOINT
VELOCITY ERROR FOR 2nd DEGREE POLYNOMIAL FIT ASSUMING UNIT ERROR IN MEASURED QUANTITIES AND UNIT TIME INTERVAL BETWEEN DATA POINTS

Figure A1-1

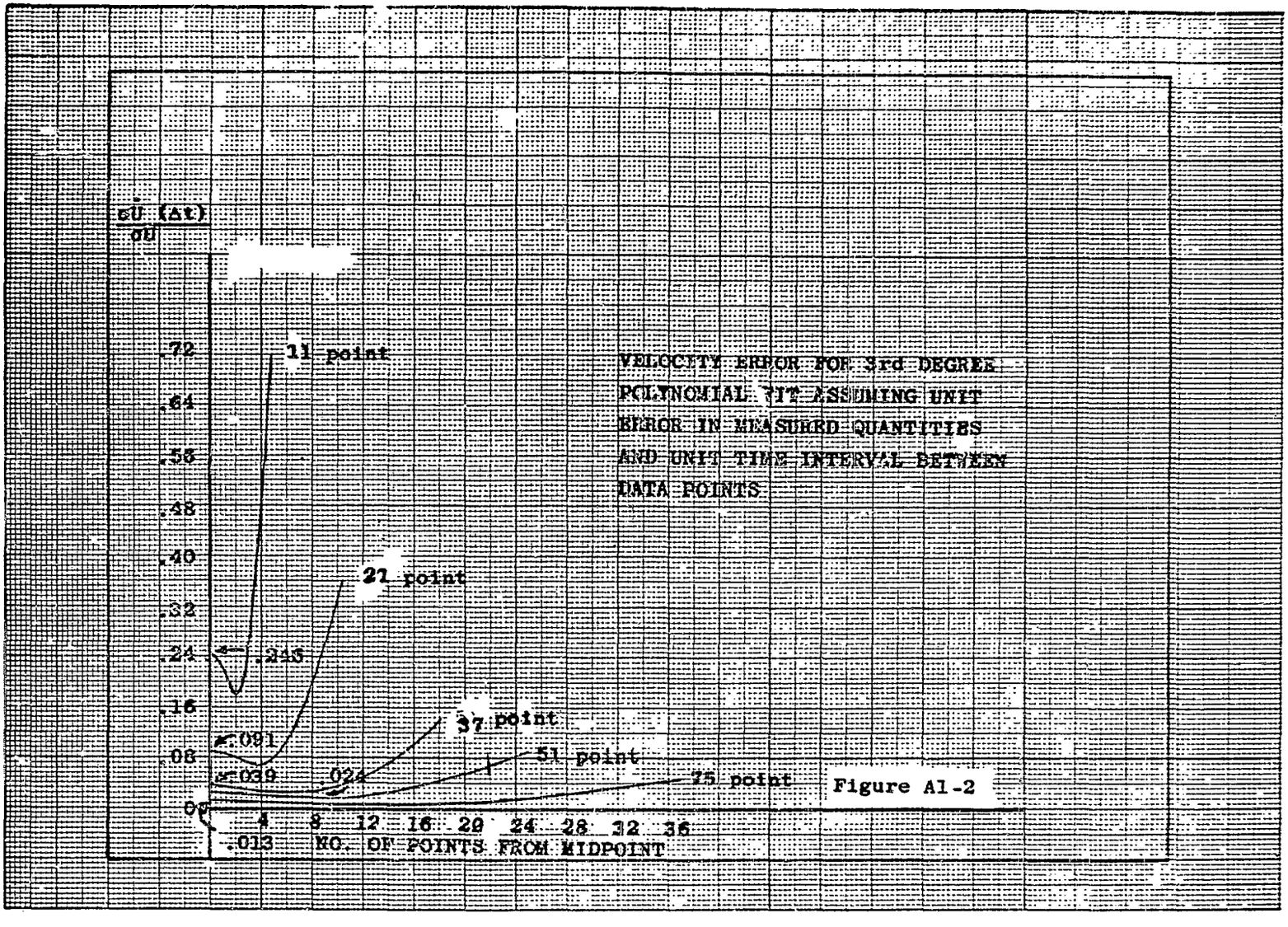

δU (Δt)
δU
.72
.64
.56
.48
.40
.32
.24
.16
.08
0
11 point
21 point
37 point
51 point
75 point
-.245
-.091
-.039
.024
4 8 12 16 20 24 28 32 36
.013
NO. OF POINTS FROM MIDPOINT
VELOCITY ERROR FOR 3rd DEGREE POLYNOMIAL FIT ASSUMING UNIT ERROR IN MEASURED QUANTITIES AND UNIT TIME INTERVAL BETWEEN DATA POINTS

Figure A1-2

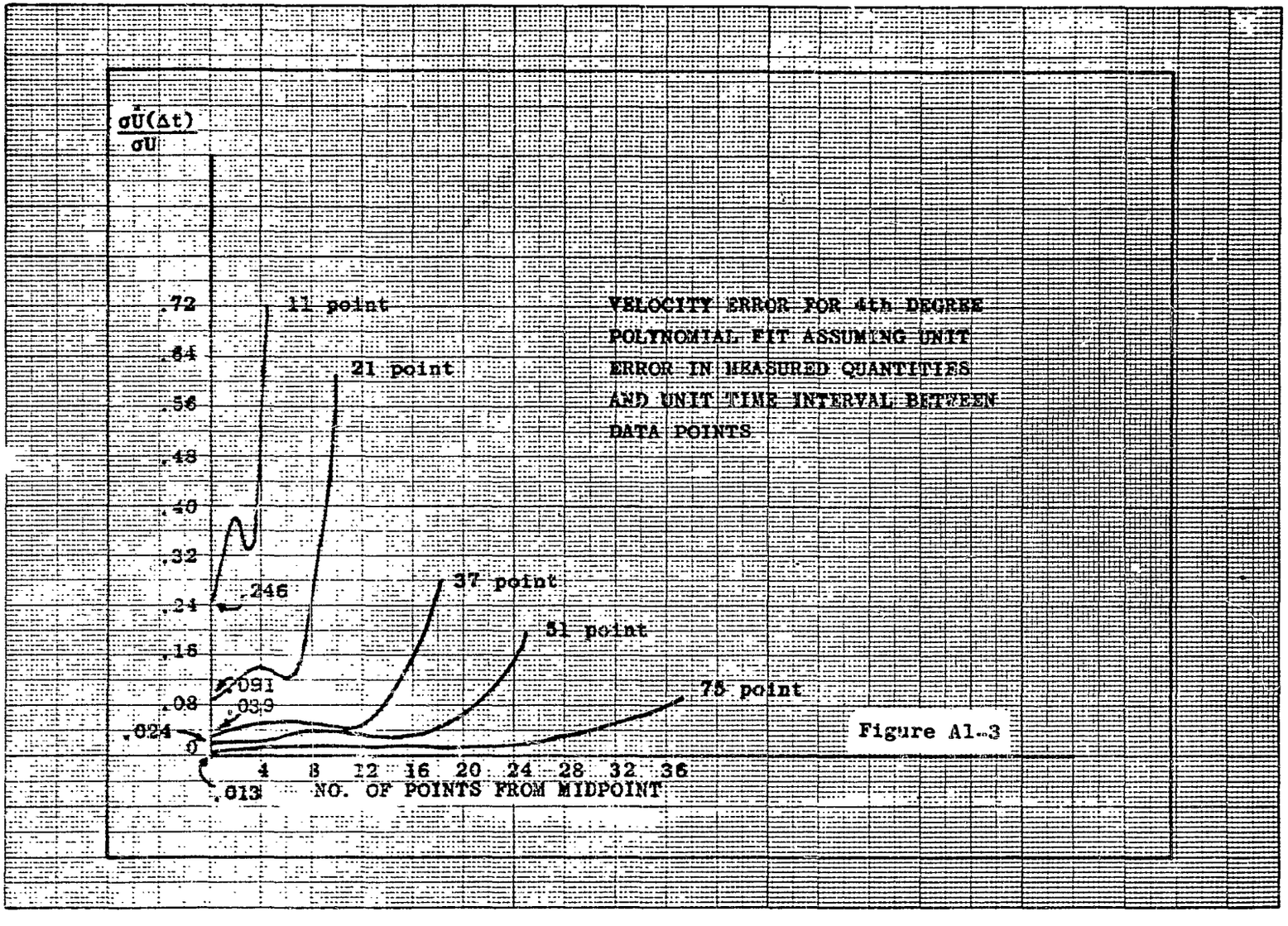

σŪ(Δt)
σU
.72
.64
.56
.48
.40
.32
.24
.16
.08
.024
0
.013
.246
.091
.039
11 point
21 point
37 point
51 point
75 point
4
8
12
16
20
24
28
32
36
NO. OF POINTS FROM MIDPOINT
VELOCITY ERROR FOR 4th DEGREE POLYNOMIAL FIT ASSUMING UNIT ERROR IN MEASURED QUANTITIES AND UNIT TIME INTERVAL BETWEEN DATA POINTS

Figure A1-3

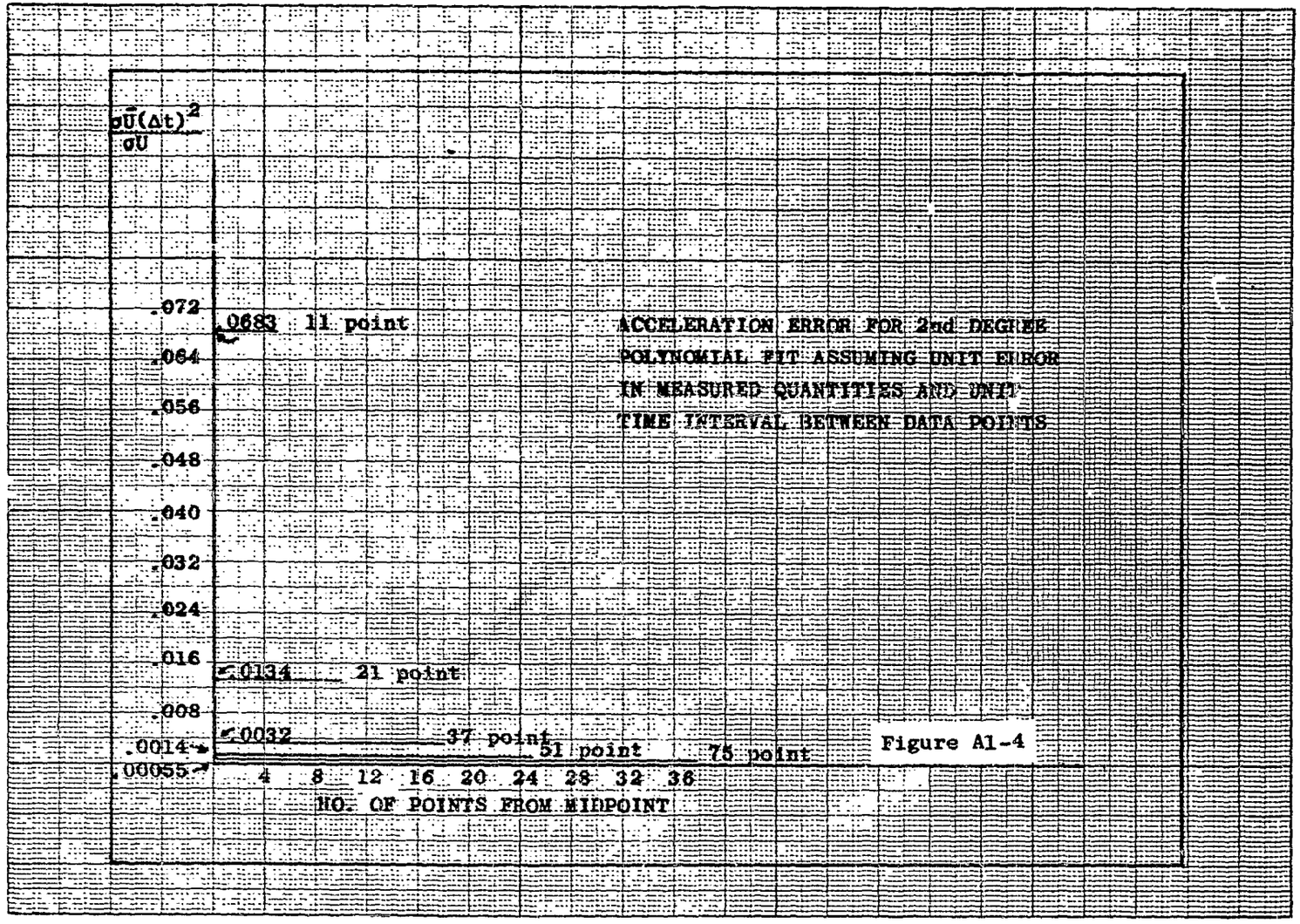

$\frac{\partial \bar{U}(\Delta t)^2}{\partial U}$
.072
.064
.056
.048
.040
.032
.024
.016
.008
.0014
.00055
.0683 11 point
.0134 21 point
.0032 37 point
51 point
75 point
4 8 12 16 20 24 28 32 36
NO. OF POINTS FROM MIDPOINT
ACCELERATION ERROR FOR 2nd DEGREE POLYNOMIAL FIT ASSUMING UNIT ERROR IN MEASURED QUANTITIES AND UNIT TIME INTERVAL BETWEEN DATA POINTS

Figure A1-4

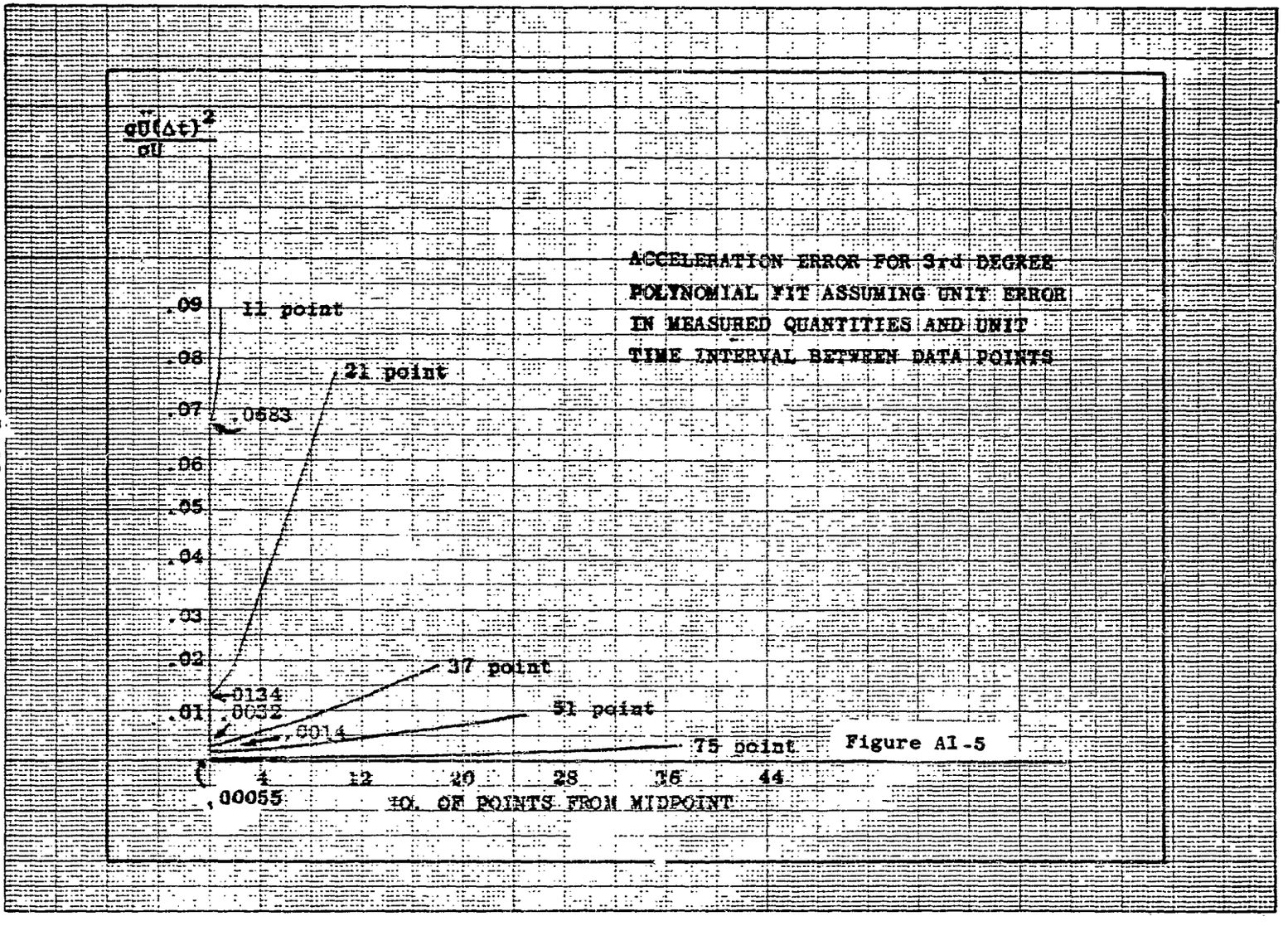

$\frac{q\ddot{U}(\Delta t)^2}{\sigma U}$
ACCELERATION ERROR FOR 3rd DEGREE POLYNOMIAL FIT ASSUMING UNIT ERROR IN MEASURED QUANTITIES AND UNIT TIME INTERVAL BETWEEN DATA POINTS
.09
.08
.07
.06
.05
.04
.03
.02
.01
11 point
21 point
37 point
51 point
75 point
.0683
.0134
.0032
.0014
.00055
4
12
20
28
36
44
NO. OF POINTS FROM MIDPOINT

Figure A1-5

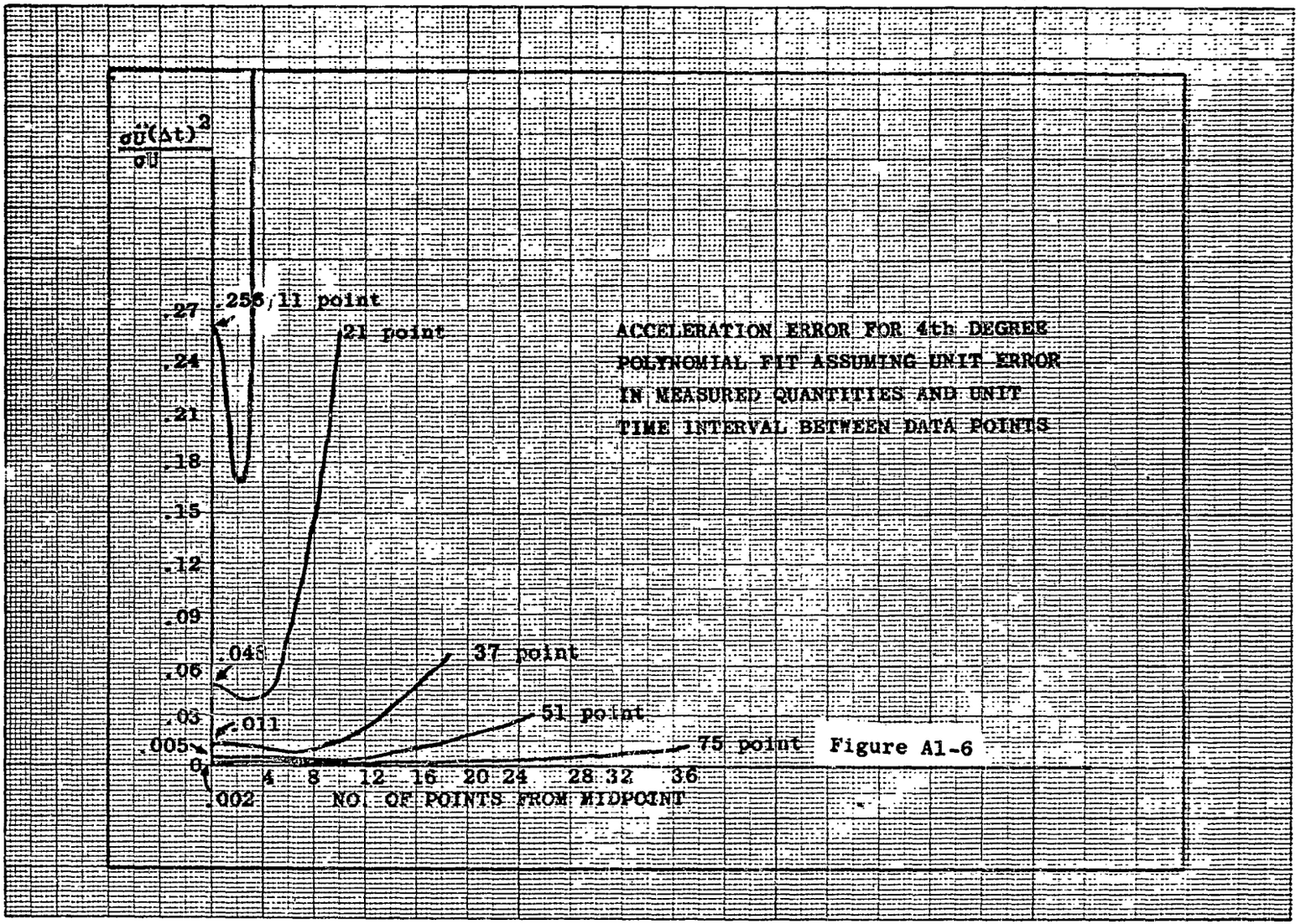

$\frac{\sigma\ddot{u}(\Delta t)^2}{\sigma u}$
.27
.24
.21
.18
.15
.12
.09
.06
.03
.005
0
.002
.256
.048
.011
11 point
21 point
37 point
51 point
75 point
4 8 12 16 20 24 28 32 36
NO. OF POINTS FROM MIDPOINT
ACCELERATION ERROR FOR 4th DEGREE POLYNOMIAL FIT ASSUMING UNIT ERROR IN MEASURED QUANTITIES AND UNIT TIME INTERVAL BETWEEN DATA POINTS

Figure A1-6

REFERENCES

Anderson, T. W., An Introduction to Multivariate Statistical Analysis, John Wiley and Sons, Inc., New York, 1958.

Arabadjis, G., General Electric Technical Information Series Report No. R62D5D7, Maximum Likelihood Estimation and Error Analysis, 27 December 1961.

Bowker, A. H. and Lieberman, G. J., Engineering Statistics, Prentice-Hall, Inc., Englewood Cliffs, N. J., 1961.

Brown, D., RCA Data Reduction Technical Report No. 39, ASTIA Document No. 124144, "A Treatment of Analytical Photogrammetry with Emphasis on Ballistic Camera Applications," August 1957.

Brown, D., RCA Data Reduction Technical Report No. 43, ASTIA Document No. 134278, "A Solution to the General Problem of Multiple Station Analytical Stereotriangulation," February 1958.

Brown, D. C., Joint AFMTC/RCA - Range User Data Processing Conference, Patrick AFB, Florida, "On a Solution to a Broad Class of Estimation Problems Arising in Missile Testing," 6-7 January 1960.

Burington, R. S. and May, D. C., Handbook of Probability and Statistics with Tables, McGraw-Hill Book Company, Inc., New York, 1958.

Chew, V., Experimental Designs in Industry, "Basic Experimental Designs," John Wiley and Sons, Inc., New York, 1958.

REFERENCES (Continued)

Chew, V., and Boyce, R., Technometrics, pages 138-140, "Distribution of Radial Error in the Bivariate Elliptical Normal Distribution," 1962.

Chew, V., Regression Analysis with Correlated Errors, RCA Systems Analysis Technical Memorandum No. 64-14, 3 January 1964a.

Chew, V., Maximum Likelihood Estimate of Unit Variance with Emphasis on Ballistic Camera Applications, RCA Systems Analysis Technical Memorandum No. 64-2, 16 July 1964b.

Chew, V., Confidence, Prediction & Tolerance Regions, RCA Systems Analysis Technical Memorancum No. 64-9, 31 December 1964c.

DiDonate, A. R. and Jarnagin, M. P., U. S. Naval Weapons Laboratory, Report No. 1768, Dahlgren, Va., "A Method for Computing the Generalized Circular Error Function and the Circular Coverage Function," 1962.

Duncan, D. B. and Ackerson, R. H., RCA Systems Analysis Technical Memo No. 12, "On the Estimation of β - Tolerance Ellipses," 1960.

Eisenhart, C., Journal of Research, National Bureau of Standards, "Realistic Evaluation of the Precision and Accuracy of Instrument Calibration Systems," 67C, pp. 161-187, 1963.

Grubbs, F. E., Ballistic Research Laboratories Report No. 642, "Some Methods for Estimating Precision of Measuring Instruments and Product Variability," January 2, 1948.

REFERENCES (Continued)

Grubbs, F. E., Journal of American Statistical Association, 43, pp. 243-264, "On Estimating Precision of Measuring Instruments and Product Variability," 1948.

Hader, R. J. and Grandage, A. H. E., Experimental Designs in Industry, "Simple and Multiple Regression Analyses," John Wiley and Sons, Inc., New York, 1958.

Hald, A., Statistical Theory with Engineering Applications, John Wiley and Sons, Inc., New York, 1952.

Harter, H. L., Journal of American Statistical Association, "Circular Error Probabilities," 55, pp. 723-731, 1960.

Kempthorne, O., The Design and Analysis of Experiments, John Wiley and Sons, Inc., New York, 1952.

Lasman, L. L., RCA Mathematical Services Technical Memo 62-7, BETY2, "Best Estimate of Trajectory," September 1962.

Mood, A. M. and Graybill, F. A., Introduction to the Theory of Statistics, McGraw-Hill Book Company, Inc., New York, 1963.

Nesline, F. W., Polynomial Filtering of Signals, IRE 1961, National Convention of Military Electronics, Proceedings, pp. 531-542.

O'Connor, J. J., Statistical Treatment of Impact Data, RCA Systems Analysis Technical Memorandum No. 31, January 1962.

REFERENCES (Continued)

Pavely, R. F., RCA Mathematical Services Technical Documentary Report No. MTC-TDR-10, AF Contract No. 08(606)5300, "A Unified Approach to Data Smoothing," June 1962.

Pitman, G. R., Inertial Guidance, John Wiley and Sons, Inc., New York - London, 1962.

Press. H. and Tukey, J. W., AGARD Flight Test Manual, Volume IV, Part IVC, pp. 1-41, (Also published as Bell Telephone System Monograph 2606), "Power Spectral Methods of Analysis and Application in Airplane Dynamics," 1956.

Relf, K. E., Greene, J. A. and Murdock, R. H., RCA Systems Analysis Technical Memorandum No. 63-4, "MISTRAM Evaluation Aircraft Test Report," 1963.

Rutledge, C. K., et al., Precise Long Range Radar Distance Measuring Techniques, Convair Report No. AE 61-0061, 13 February 1961.

SEISCOR - Final Technical Report, "Data Computations, and Certification for LORAC Radio Positioning Systems in the Bahamas," Contract No. AF 08(606) - 4353, November 23, 1960.

Starbird, H. A., Study of Emulsion Shift on Ballistic Camera Plates, Technical Documentary Report No. MTC-TDR-64-4, January 1964.

Thompson, W. A., Jr., Journal of American Statistical Association, Vol. 58, pp. 474-479, Precision of Simultaneous Measurement Procedures," 1963.

REFERENCES (Continued)

Tukey, J. W., Probability and Statistics, "An Introduction to the Measurement of Spectra," John Wiley and Sons, Inc., New York, 1959.

Tukey, John W., Statistical Techniques Research Group, Dept. of Mathematics, Princeton University, Princeton, New Jersey, ASTIA Document No. AD 155 082, "The Propagation of Errors, Fluctuations and Tolerances,"

Whitehead, L. R. and Beall, W. N., CONFIDENTIAL Report, 1963 Yearly Accuracy Report, Missile Impact Locating System (MILS) (U), RCA Systems Analysis Technical Memorandum No. 64-5, 12 August 1964.

UNCLASSIFIED
Security Classification

DOCUMENT CONTROL DATA - R&D

(Security classification of title, body of abstract and indexing annotation must be entered when the overall report is classified)

1. ORIGINATING ACTIVITY (Corporate author)	2a. REPORT SECURITY CLASSIFICATION
RCA Service Company Missile Test Project Patrick Air Force Base, Florida	Unclassified-does not contain restricted data 2b. GROUP NA

3. REPORT TITLE

THE ACCURACY OF ETR INSTRUMENTATION

4. DESCRIPTIVE NOTES (Type of report and inclusive dates)

Annual Report

5. AUTHOR(S) (Last name, first name, initial)

Part I:
R.A. Ackerson, Ph.D.
V. Chew
C.S. Cummings, Ph.D.
P.S. Dubbeldam, Ph.D.
J.A. Greene
M.A. King
P.N. Somerville, Ph.D.
Part II:*

6. REPORT DATE	7a. TOTAL NO. OF PAGES	7b. NO. OF REFS
May 1965	521	36

8a. CONTRACT OR GRANT NO.	9a. ORIGINATOR'S REPORT NUMBER(S)
RCA Subcontract 65-5300-01 b. PROJECT NO.	None
c. d.	9b. OTHER REPORT NO(S) (Any other numbers that may be assigned this report) ETR-TR-65-7

10. AVAILABILITY/LIMITATION NOTICES

Available from DDC and Clearinghouse for Federal Scientific and Technical Information of the U.S. Department of Commerce

11. SUPPLEMENTARY NOTES	12. SPONSORING MILITARY ACTIVITY
None	Systems Analysis Division Directorate for Data Processing

13. ABSTRACT

The annual summary statements of the accuracy of Eastern Test Range Tracking Instrumentation are presented in this report. The statements are based on studies by RCA Systems Analysis. The report also provides brief systems descriptions and a detailed discussion of methods and techniques used to estimate errors, error sources, specific ETR methodologies including data analysis flow diagrams and a discussion of the variance - covariance error propagation required to determine the accuracy of reduced position, velocity and acceleration data. Work on the determination of instrumentation accuracy is a continuing project and revisions and refinements to the estimates of accuracy are issued periodically as additional information is made available. (U)

* Part II:
A.S. Baron
W.N. Beall
R.A. Brown
H.C. Cox
W.L. Elenburg
J.E. French
D.E. Forrest
J.A. Greene
A.E. Hoffmann-Heyden
W.F. Kennedy
V.B. Kovac
N.L. Lindemann
J.P. Lushene
R.C. Manring
J.J. O'Connor
J.A. Paddock
D.H. Parks**
P.C. Ray
L.B. Rice, Ph.D.
V.C. Rupert
H.D. Yenzer

** RCA Mathematical Services

DD FORM 1 JAN 64 1473

UNCLASSIFIED
Security Classification

UNCLASSIFIED
Security Classification

14. KEY WORDS	LINK A		LINK B		LINK C	
	ROLE	WT	ROLE	WT	ROLE	WT
Instrumentation						
Statistical Methods						
Optical tracking instrumentation						
Electronic tracking instrumentation						
Impact location systems						
Ships, ETR instrumentation						
Error Propagation						
Refraction						
Guided missile tracking systems						
Guided missile trajectories						
Radar tracking						
Doppler tracking systems						
Calibration of tracking systems						
Accuracy of ETR instrumentation						
Navigation, Signature, Acoustic systems,						
Best Estimate of trajectory, Survey						

INSTRUCTIONS

1. ORIGINATING ACTIVITY: Enter the name and address of the contractor, subcontractor, grantee, Department of Defense activity or other organization *(corporate author)* issuing the report.

2a. REPORT SECURITY CLASSIFICATION: Enter the overall security classification of the report. Indicate whether "Restricted Data" is included. Marking is to be in accordance with appropriate security regulations.

2b. GROUP: Automatic downgrading is specified in DoD Directive 5200.10 and Armed Forces Industrial Manual. Enter the group number. Also, when applicable, show that optional markings have been used for Group 3 and Group 4 as authorized.

3. REPORT TITLE: Enter the complete report title in all capital letters. Titles in all cases should be unclassified. If a meaningful title cannot be selected without classification, show title classification in all capitals in parenthesis immediately following the title.

4. DESCRIPTIVE NOTES: If appropriate, enter the type of report, e.g., interim, progress, summary, annual, or final. Give the inclusive dates when a specific reporting period is covered.

5. AUTHOR(S): Enter the name(s) of author(s) as shown on or in the report. Enter last name, first name, middle initial. If military, show rank and branch of service. The name of the principal author is an absolute minimum requirement.

6. REPORT DATE: Enter the date of the report as day, month, year; or month, year. If more than one date appears on the report, use date of publication.

7a. TOTAL NUMBER OF PAGES: The total page count should follow normal pagination procedures, i.e., enter the number of pages containing information.

7b. NUMBER OF REFERENCES: Enter the total number of references cited in the report.

8a. CONTRACT OR GRANT NUMBER: If appropriate, enter the applicable number of the contract or grant under which the report was written.

8b, 8c, & 8d. PROJECT NUMBER: Enter the appropriate military department identification, such as project number, subproject number, system numbers, task number, etc.

9a. ORIGINATOR'S REPORT NUMBER(S): Enter the official report number by which the document will be identified and controlled by the originating activity. This number must be unique to this report.

9b. OTHER REPORT NUMBER(S): If the report has been assigned any other report numbers *(either by the originator or by the sponsor)*, also enter this number(s).

10. AVAILABILITY/LIMITATION NOTICES: Enter any limitations on further dissemination of the report, other than those imposed by security classification, using standard statements such as:

(1) "Qualified requesters may obtain copies of this report from DDC."

(2) "Foreign announcement and dissemination of this report by DDC is not authorized."

(3) "U. S. Government agencies may obtain copies of this report directly from DDC. Other qualified DDC users shall request through _____."

(4) "U. S. military agencies may obtain copies of this report directly from DDC. Other qualified users shall request through _____."

(5) "All distribution of this report is controlled. Qualified DDC users shall request through _____."

If the report has been furnished to the Office of Technical Services, Department of Commerce, for sale to the public, indicate this fact and enter the price, if known.

11. SUPPLEMENTARY NOTES: Use for additional explanatory notes.

12. SPONSORING MILITARY ACTIVITY: Enter the name of the departmental project office or laboratory sponsoring *(paying for)* the research and development. Include address.

13. ABSTRACT: Enter an abstract giving a brief and factual summary of the document indicative of the report, even though it may also appear elsewhere in the body of the technical report. If additional space is required, a continuation sheet shall be attached.

It is highly desirable that the abstract of classified reports be unclassified. Each paragraph of the abstract shall end with an indication of the military security classification of the information in the paragraph, represented as *(TS), (S), (C), or (U)*.

There is no limitation on the length of the abstract. However, the suggested length is from 150 to 225 words.

14. KEY WORDS: Key words are technically meaningful terms or short phrases that characterize a report and may be used as index entries for cataloging the report. Key words must be selected so that no security classification is required. Identifiers, such as equipment model designation, trade name, military project code name, geographic location, may be used as key words but will be followed by an indication of technical context. The assignment of links, rules, and weights is optional.

UNCLASSIFIED
Security Classification

SUPPLEMENTARY

INFORMATION

AD 616897

ERRATA

ETR-TR-65-7

THE ACCURACY OF ETR INSTRUMENTATION

C.S.Cummings,Ph.D., R.H.Ackerson,Ph.D.,
A.S.Baron,et al,RCA ITP

MAY 1965

Systems Analysis Division
Directorate for Data Processing
Deputy for Range Operations
Air Force Eastern Test Range
Air Force Systems Command
Patrick Air Force Base, Florida

Reverse of Front Cover: Delete paragraph 2 and insert the following amended availability statement:

"This document is subject to special export controls and each transmittal to foreign governments or foreign nationals may be made only with prior approval of Directorate of Data Processing, AFETR."

Issue date: 11/4/65